Dissertation zur Erlangung des Doktorgrades

der Fakultät für Chemie und Pharmazie

der Ludwig-Maximilians-Universität München

Freeze-drying of nanoparticles: Impact of particle properties on formulation and process development

Eduard Trenkenschuh

aus

Sadowoe, Kasachstan

2021

Erklärung

Diese Dissertation wurde im Sinne von §7 der Promotionsordnung vom 28. November 2011 von Herrn Prof. Dr. Wolfgang Frieß betreut.

Eidesstattliche Versicherung

Diese Dissertation wurde selbstständig und ohne unerlaubte Hilfe erarbeitet.

Biberach, den 27.07.2021

Eduard Trenkenschuh

Dissertation eingereicht am:	04.08.2021
1. Gutachter:	Prof. Dr. Wolfgang Frieß
2. Gutachter:	Prof. Dr. Olivia Merkel
Mündliche Prüfung:	16.09.2021

„Es steckt oft mehr Geist und Scharfsinn in einem Irrtum als in einer Entdeckung.“

Joseph Joubert

Acknowledgements

This thesis was prepared at Department of Pharmacy, Pharmaceutical Technology and Biopharmaceutics at the Ludwig-Maximilians-Universität München (LMU) under the supervision of Prof. Dr. Wolfgang Frieß.

I would like to express my deepest gratitude to my supervisor Prof. Dr. Wolfgang Frieß. I am grateful for all the advices, creative and sometimes crazy ideas, patience and also critics which immensely helped to expand my scientific mindset. I would also like to thank for the encouragement during the last years, the possibilities to attend to international scientific conferences and further training opportunities, e.g. at the APV. And of course, I am thankful for all the suggestions and advices on how to spend the best time in the Bavarian 'Oberland' (one of the most beautiful places on earth)!

Furthermore, thank you to Prof. Dr. Olivia Merkel for being the co-referee of this thesis and to Prof. Dr, Martin Biel, Prof. Dr. Stefan Zahler, Prof. Dr. Ernst Wagner, and Prof. Dr. Franz Paintner for joining the examination board.

Special thanks go to the trio Prof. Dr. Gerhard Winter, Prof. Dr. Wolfgang Frieß, and Prof. Dr. Olivia Merkel for providing the best working atmosphere one could imagine. The numerous activities besides research were that extra something making professional relationships to real friendships.

I also would like to thank Dr. Gregor Fuhrmann and Maximilian Richter from the Helmholtz Institute for Pharmaceutical Research Saarland for an excellent collaboration, valuable discussions and their scientific input.

I want to thank my lab mate Imke Leitner, not only for performing Karl-Fischer measurements, but also for her helping hand in general and many interesting discussions on numerous topics concerning life.

I especially thank the Damensauna including Christoph Marshall, Oliver Blümel, Fabian Moll and Inas El Bialy for their open ear for scientific and personal issues and of course the other AK Frieß members Ivonne Seifert, Robina Mayer, Martin Domnowski, Christian Haase and Natalie Deiringer for their support and amusing coffee breaks. Many thanks to Ula Savšek for being a great Master student and teaching me how to be a (more or less) good supervisor.

Thanks to the ‘Lyo Guys’, including Ivonne Seifert, Julian Gitter, Ute Rockinger, Sebastian Groël, and Nicole Härdter for the mutual support and discussions regarding technical and scientific lyophilization issues.

Furthermore, thanks to all the other colleagues, i.e. Tobias Keil, Dennis Krieg, Andreas Stelzl, Hristo Svilenov, Carolin Berner, Andreas Tosstorff, Michaela Breitsamer, Teresa Kraus, Simon Eisele, Katharina Geh, Lorenzo Gentiluomo, Alice Hirschmann, Lorenz Isert, Rima Kandil, Aditi Mehta, Weiwei Liu, Ruth Rieser, Bernard Haryadi, Bettina Gabold, Natascha Hartl, Christoph Zimmermann, Domizia Baldassi, Friederike Adams, Gerhard Simon, Alexandra Mösslang, Susanne Petzel, Regine Bahr, and Sabine Kohler for a great and intensive time, full of joy and legendary stories!

Finally, and most importantly, I wish to thank my parents and my beloved wife Simone for their great support and encouragement throughout this challenging, but incredibly beautiful time!

General Table of Contents

Chapter 1

Freeze-drying of nanoparticles: How to overcome colloidal instability by formulation and process optimization 1

Chapter 2

Objectives of the Thesis.....49

Chapter 3

Freeze-thaw stability of aluminum oxide nanoparticles.....51

Chapter 4

Formulation, process, and storage strategies for lyophilizates of lipophilic nanoparticulate systems established based on the two models paliperidone palmitate and solid lipid nanoparticles.....73

Chapter 5

Enhancing the stabilization potential of lyophilization for extracellular vesicles 111

Chapter 6

Final summary and outlook.....158

Chapter 1

Freeze-drying of nanoparticles: How to overcome colloidal instability by formulation and process optimization

Eduard Trenkenschuh, Wolfgang Friess

Pharmaceutical Technology and Biopharmaceutics, Department of Pharmacy, Ludwig-Maximilians-Universität München, 81377 Munich, Germany

This chapter has been published in the 'European Journal of Pharmaceutics and Biopharmaceutics' **(https://doi.org/10.1016/j.ejpb.2021.05.024)**.

Author contributions:

E.T. reviewed the literature and wrote the manuscript. W.F. supervised the work, provided conceptual guidance and corrected the manuscript.

Abstract

Lyophilization of nanoparticle (NP) suspensions is a promising technology to improve stability, especially during long-term storage, and offers new routes of administration in solid state. Although considered as a gentle drying process, freeze-drying is also known to cause several stresses leading to physical instability, e.g. aggregation, fusion, or content leakage. NPs are heterogeneous regarding their physico-chemical properties which renders them different in their sensitivity to lyophilization stress and upon storage. But still basic concepts can be deducted. We summarize basic colloidal stabilization mechanisms of NPs in the liquid and the dried state. Furthermore, we give information about stresses occurring during the freezing and the drying step of lyophilization. Subsequently, we review the most commonly investigated NP types including lipophilic, polymeric, or vesicular NPs regarding their particle properties, stabilization mechanisms in the liquid state, and important freeze-drying process, formulation and storage strategies. Finally, practical advice is provided to facilitate purposeful formulation and process development to achieve NP lyophilizates with high colloidal stability.

Keywords

Freeze-drying, Nanoparticles, Lipid, Liposomes, Polymer, Drug, Stability, Formulation, Process

Abbreviations

AAV	Adeno-associated virus
DLVO	Derjaguin-Landau-Verwey-Overbeek
DSC	Differential scanning calorimetry
EDL	Electrical double layer
EVs	Extracellular vesicles
HES	Hydroxyethyl starch
HSA	Human serum albumin
NLCs	Nanostructured lipid carriers
NPs	Nanoparticles
ODN	Oligodeoxynucleotide
P188	Poloxamer 188
PBS	Phosphate buffered saline
PCL	Polycaprolactone
PEG	Polyethylene glycol
PEI	Polyethylene imine
PEO	Polyethylene oxide
PLA	Polylactide
PLGA	Poly(lactic-co-glycolic) acid
PS20	Polysorbate 20
PS80	Polysorbate 80
PVA	Polyvinyl alcohol
PVP	Polyvinyl pyrrolidone
RT	Room temperature
SLNs	Solid lipid nanoparticles
T_g	Glass transition temperature of the freeze-dried cake
T_g'	Glass transition temperature of the freeze-concentrated solution
T_m	Bilayer phase transition temperature

Table of Contents

Abstract 2
Keywords 3
Abbreviations 3
1 Introduction 6
2 Mechanisms of nanoparticle stabilization 7
2.1 Stability in the liquid state 7
2.2 Stresses occurring during freezing 8
2.3 Stresses occurring during drying 11
2.4 Stability in the dried state 11
2.4.1 Water replacement hypothesis 11
2.4.2 Vitrification hypothesis 12
3 Freeze-drying of different nanoparticle types 13
3.1 Lipophilic nanoparticles 13
3.1.1 Drug nanosuspensions (= nanocrystals) 14
3.1.2 Solid lipid nanoparticles/ Nanostructured lipid carriers 14
3.2 Polymeric nanoparticles 16
3.2.1 Nanospheres/-capsules & Polyelectrolyte complexes 16
3.2.2 Polyplexes 18
3.3 Lipid bilayer vesicles: Liposomes and biological nanoparticles 19
3.3.1 Lipid bilayer: composition & phase transition T_m 20
3.3.2 Factors affecting leakage and release of vesicles 21
3.3.3 Strategies to avoid leakage & fusion of vesicles 23
3.3.4 Lipoplexes 25
3.3.5 Extracellular Vesicles 27
3.3.6 Enveloped Viruses 28
3.4 Other nanoparticles 29
3.4.1 Lipid nanoparticles 29
3.4.2 Non-enveloped Viruses 29
3.4.3 Inorganic nanoparticles 30
4 Summary and practical advices 30
4.1 Selection of cryo-/ lyoprotectant 31
4.2 Selection of bulking agents 32
4.3 Selection of buffer agent 32
4.4 Selection of surfactant 32

4.5 Osmolarity 33
4.6 The process 33
4.7 Particle properties affecting process and storage stability 34
5 Conclusion 35
6 References 36

1 Introduction

The significant efforts to develop nanoparticulate systems (NPs) for drug delivery (e.g. polyplexes, vaccines, liposomes) and to overcome the bioavailability hurdle of poorly water-soluble APIs lead to a growing number of NP-based medicines on the market, especially for parenteral use [1]. However, development of nanomedicine is challenging. Most NPs are produced in aqueous solution and suffer from both: chemical and physical instability. Depending on the NP type and cargo, chemical instabilities may include oxidation, hydrolysis, deamidation, browning reaction, and disulfide bond formation/exchange [2], while physical instability is mainly related to particle aggregation or uncontrolled release kinetics. Electrostatic stabilization, as described by the Derjaguin-Landau-Verwey-Overbeek (DLVO) theory, may overcome physical instability, but is formally only applicable for charged colloids [3]. Consequently, many NP preparations can only be used for a short time or have to be stored frozen. Still, NP long-term stability at room temperature (RT) is an important development goal.

Freeze-drying, also known as lyophilization, is a well-established process to improve the stability of labile drugs [4]. This gentle water removal process consists of sublimation of ice from the frozen state followed by desorption under vacuum. Freeze-drying of pharmaceutics received a boost in the 1990s with the rise of biologics, specifically proteins, which are highly sensitive and require parenteral application and convenient handling. Lyophilization enables the preparation of dry NP presentations with enhanced long-term storage, which helps to avoid cost-intensive and effortful cold-chain supply, as known for many vaccines [5–7]. As for biopharmaceuticals, the lyophilizates have to come with preservation of the original product properties, low residual moisture, elegant cake appearance, and fast reconstitution.

The lyophilization process itself comes with several stresses which can lead to colloidal instability, specifically particle aggregation. To this end, both the process itself, e.g. freezing protocol, product temperature during primary drying, and the formulation, e.g. the use of cryoprotectants to embed particles in an amorphous matrix, or addition of surfactants to reduce interaction with the ice surface, are key factors to ensure process and storage stability. Still, except of empirical principles, little is known about the mutual dependency of formulation and process design as well as particle properties when freeze-drying NPs.

Depending on the definition, the size distribution of NPs can range from 1 nm to 100 nm or up to 500 nm [8,9]. Besides their particle size, they can be differentiated into material categories based on physico-chemical properties, e.g. polymeric, crystalline, or liposomal NPs. As new materials and NP types arise, a meaningful classification of the broad spectrum becomes more and more a key challenge for researchers, industry, and regulators [1]. It

becomes obvious that NP types that differ in size, material, charge, morphological structure, and chemical stability require different formulation, process and storage considerations. Therefore, it is important to combine the knowledge and experience of the multiple studies to guide new developments and generate fundamental understanding.

Our review first briefly summarizes the mechanisms of colloidal NP stabilization in the liquid and the dried state. It subsequently elucidates stresses occurring during freezing and drying. Consequently, we provide individual information on lyophilization of different NP types regarding important formulation and process aspects. Understanding the sensitivity of different NP types towards different stress factors leads to optimized and purposeful lyophilization development.

2 Mechanisms of nanoparticle stabilization

2.1 Stability in the liquid state

Formulation design for NP lyophilizates must consider colloidal stabilization mechanisms in the liquid state since they fundamentally affect the sensitivity of the NPs to aggregate during freezing, drying, storage in the dry state, and reconstitution. The three main stabilization mechanisms leading to colloidal stability are electrostatic, steric and depletion stabilization [10–12] (Figure 1).

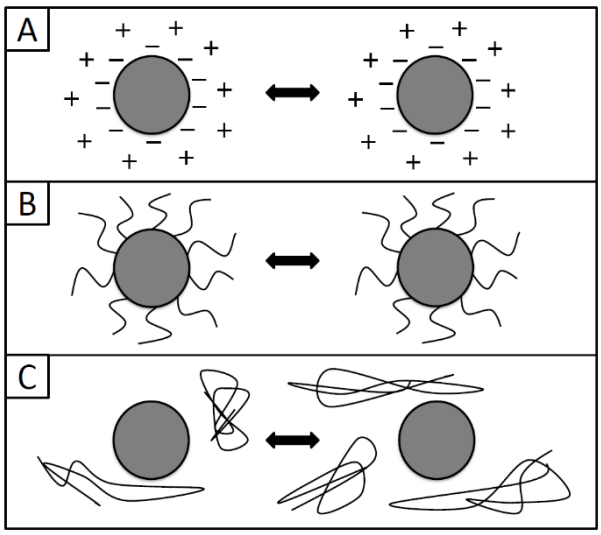

Figure 1: Stabilization mechanisms: (A) electrostatic stabilization, (B) steric stabilization and (C) depletion stabilization.

According to the DLVO theory two forces are acting on particles in aqueous medium: attractive forces (van der Waal) and repulsive forces (electrostatic) [10]. The repulsive forces originate from the overlapping of electrical double layers (EDL) surrounding the particles, and prevent agglomeration (Figure 1A). As adsorption of ions is reversible, charge stabilized NPs are sensitive to electrolyte addition and pH changes.

Steric stabilization (Figure 1B) is achieved by attachment of polymers, e.g. polyethylene glycol (PEG), poloxamer, polyvinyl alcohol (PVA), or surfactants, e.g. polysorbate, sodium dodecyl sulfate, onto the particle surface. Thereby the attractive van der Waals forces become more reduced than the repulsive electrostatic forces [13]. This mechanism depends on the polymer affinity to the respective surface, the polymer concentration and average chain length.

Depletion stabilization (Figure 1C) results from free non-adsorbing polymer in solution. The NPs may experience a depletion force originating from the excluded volume effect, for which no specific binding between the NP and polymer is required [12]. The depletion interaction is considered to have both, a short-range attractive minimum and a long-range repulsive barrier. Above a certain polymer concentration, the repulsive energy barrier becomes high enough to allow kinetical (i.e. thermodynamically metastable) stabilization [14,15]. Semenov et al. reported that the particle surface may exhibit strongly attractive sites at which polymer segments get trapped. This leads to adsorbed polymer layers which provide short-range steric repulsion. The interaction of free polymers with these fluffy layers gives rise to a depletion repulsion force between colloidal particles [16]. Still, the exact mechanism of depletion stabilization is a subject of debate.

2.2 Stresses occurring during freezing

Freezing is a widely used preservation technique to extend the shelf life of compounds suffering from poor stability. Moreover, it is the first step of freeze-drying and known to generate a variety of stresses which impact the stability of NPs, including crystal formation, interfacial effects, freeze-concentration, buffer pH change, and phase separation (Figure 2).

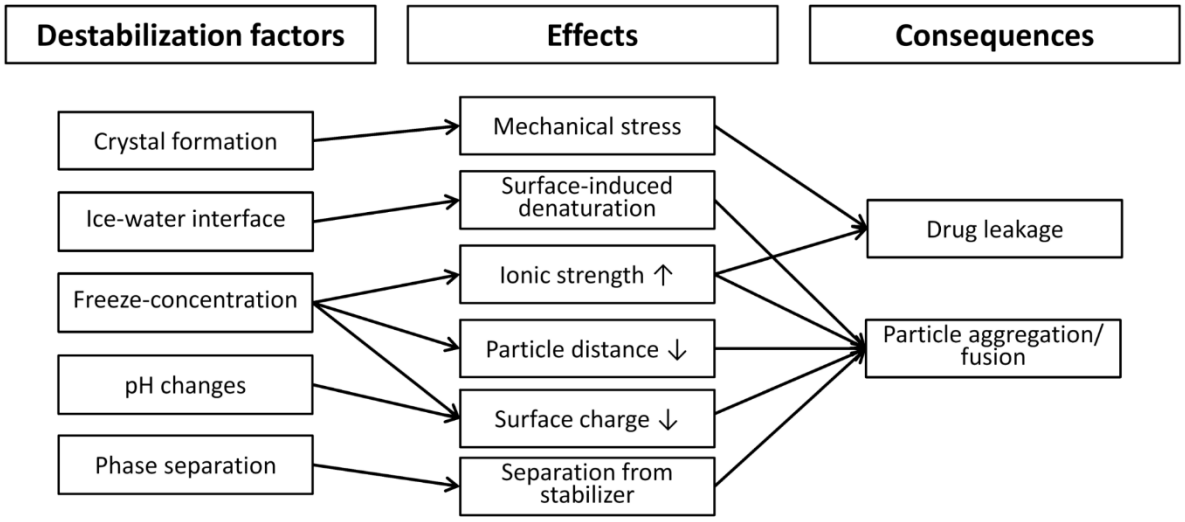

Figure 2: Destabilization factors and consequences on colloidal NP stability during freezing.

Crystal formation during freezing

Ice and also excipient, e.g. mannitol, glycine, or NaCl-eutectic crystals, can exert mechanical stress on NPs. Especially mechanically fragile types, e.g. liposomes or enveloped viruses, may be damaged [17,18]. Furthermore, these NP qualities have a liquid inner core, hence external and internal ice crystal formation creates stress [17–19]. Additionally, shear stress potentially occurring as the ice crystal matrix forms can lead to deformation and drug leakage which was reported for liposomes [20].

The higher the degree of supercooling, the higher the number of small ice crystals and the larger the interfacial area [21]. The ice-liquid interface may lead to adsorption and damage of colloidal structures as shown for proteins [22]. Surfactants can compete for adsorption on denaturing interfaces [23] which could be beneficial for surfactant-based vesicles or viruses, especially if decorated with proteins which may be negatively affected [24].

Changes during freeze-concentration

Freezing rapidly increases the concentration of all compounds in the remaining liquid fraction up to 50 times which may negatively impact particle stability [2,25]. The decreased particle distance facilitates particle-particle interactions as attractive forces can overcome repulsive forces resulting in particle aggregation. This process can be accelerated by the increased ionic strength in the freeze-concentrate shielding charges. With increasing ionic strength, the adsorbed EDL gets compressed further leading to a decreased particle distance [26]. Thus,

particle aggregation may occur due to hindered electrostatic repulsion and a higher particle concentration.

Freeze-concentration also results in an increase of the osmotic pressure on particles possessing a lipid bilayer such as liposomes, extracellular vesicles and enveloped viruses. The water flux driven by the osmotic pressure gradient imparts physical force to the membrane which can cause membrane rupture [27]. The osmotic stability during freezing highly depends on the lipid membrane composition due to selective permeability towards solutes [28,29]. After shrinkage in size, the lipid layer adapts leading to deformation into lens-shaped vesicles [30] or invagination resulting in multilamellar structured liposomes [31]. These deformation processes may lead to leakage. The osmotic pressure further impacts the release kinetics of hydrophilic and, to a minor extent, lipophilic content [32].

Buffer pH change

During freezing, buffers may undergo a significant pH change affecting the colloidal stability [33–36]. The pH shift arises from solubility limitations leading to eutectic crystallization, e.g. for sodium phosphate, succinate, and tartrate, and temperature-associated changes in the pK_a values of the buffer components, e.g. for histidine, citrate, and malate [35,37–39]. Sodium phosphate buffer is the most prominent example for this phenomenon: disodium phosphate crystallizes earlier compared to the monosodium salt which can results in a pH drop by up to 3 units [37,40]. The potassium salt of phosphate does not have this limitation [35].

Phase separation

Freeze-concentration may also lead to liquid-liquid phase separation [41] and a destabilizing effect has to be expected if NP and stabilizer separate. A characteristic of phase-separated systems are two glass transition temperatures [25]. Some polymer-polymer and polymer-salt pairs are known to cause phase separation. Many of these polymers are of interest as cryoprotectants, e.g. PEG, and polyvinyl pyrrolidon (PVP), or collapse temperature modifiers, e.g. dextran, and ficoll. Heller et al. showed that phase separation between PEG and dextran resulted in structural damage of hemoglobin during freeze-drying even after addition of 5% sucrose or trehalose [42].

2.3 Stresses occurring during drying

The drying step in lyophilization is divided into primary and secondary drying. During primary drying frozen water sublimates and during secondary drying residual adsorbed water gets desorbed. Water is an integral part of electrostatically stabilized NPs. The EDL ensures stabilization through repulsive electrostatic forces. Dehydration leads to its disruption. Especially, the loosely associated diffuse layer is prone to external influences. As a result, NP interactions may increase causing particle aggregation. Steric and depletion stabilization of NPs can also be affected by the drying step since the mobility of polymers and surfactants may be hindered in the absence of water. Therefore, the substitution of water by excipients is necessary to maintain particle properties during and after the drying step. Depending on the individual particle properties, the loss of the hydration shell could result in NP damage and aggregation; an effect, that is well known for proteins [2]. Particles possessing a lipid bilayer are furthermore affected by a shift of the phase transition temperature T_m during the drying step as a consequence of dehydration. This behavior is explained in detail in section 3.3.

2.4 Stability in the dried state

Two different stabilization mechanisms are widely discussed to explain stabilization of proteins in the dried state [43,44]. These principles, the water replacement theory and the vitrification concept, may be transferred to other colloidal systems, such as NPs.

2.4.1 Water replacement hypothesis

The water replacement theory states that sugar molecules replace the hydrogen bonds of water at the surface of a colloid maintaining the molecular structure upon drying [45]. Hydrogen bonding is assumed to be most effective when sugar molecules tightly fit the irregular colloid surface thus be in the amorphous state and not crystalline [46]. The replacement theory is supported by the fact that an increasing sugar to particle ratio usually leads to increased particle stability which is beyond a simple spacing separation effect resulting from a lower particle fraction [47–49].

Stabilization of bilayer vesicles was mainly investigated for liposomes which have the simplest structure. Crowe et al. were the first group proposing the water replacement hypothesis for liposomes (Figure 3). In the dry state, water between the phospholipid head groups is replaced by sugar molecules. As a result, the head group spacing between phospholipids can be maintained leading to reduced van der Waals interactions among the acyl chains [50,51]. Molecular simulations studies confirmed H-bonding interactions between phospholipid and

trehalose molecules supporting the water replacement hypothesis [52]. Moreover, preservation of lyophilized vesicles was improved when the cryoprotectant was also distributed inside the vesicles suggesting an additional stabilizing effect at the phospholipid inner layer [53,54].

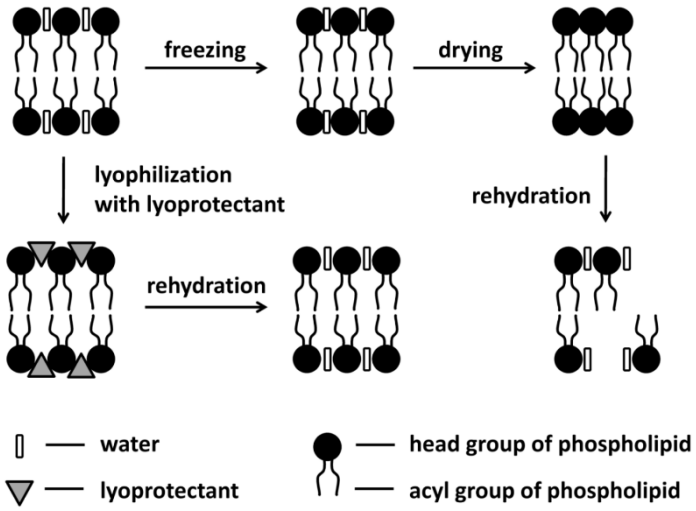

Figure 3: Mechanism of water replacement during lyophilization and rehydration of lipid bilayers (adapted from [55]).

2.4.2 Vitrification hypothesis

The vitrification theory, also called particle isolation hypothesis, describes colloidal and chemical stabilization in the dried state from a kinetic point of view. Colloids are immobilized in a rigid, amorphous glassy sugar matrix which drastically slows down diffusion, aggregation, fusion, and other degradation processes [56]. Consequently, the glass transition temperature T_g is of importance. Above T_g, the amorphous matrix is in a rubbery state where kinetic immobilization is lost. Water replacement is the predominant mechanism of stabilization when there is sufficient vitrification, i.e. T_g is at least 10 to 20 °C above the storage temperature [46]. The lack of vitrification becomes critical for stability at storage temperatures closer to or above T_g [57]. However, vitrification itself is not sufficient to preserve NPs, especially bilayer vesicles, during freezing or freeze-drying. Dextran failed to stabilize egg phosphatidylcholine-based liposomes during lyophilization compared to trehalose indicating better interaction and water replacement of the smaller disaccharide with the lipid bilayer [58]. Thus, the vitrification and water replacement theory are not mutually exclusive; instead both are required for lyophilization [51]. Both theories have their explanatory power, but leave room for further refinement [56]. Furthermore, other non-disaccharide-based mechanism are

discussed in literature. Specifically, for biological vesicles, the depression of normal metabolism, the inhibition of free radical- and enzyme-mediated membrane damage, and the accumulation of specific proteins and carbohydrates play a role in the overall stabilization [59].

3 Freeze-drying of different nanoparticle types

The colloidal stability is influenced by the surface chemistry of the NPs and affected by pH, ionic strength, buffer type, and other excipients. Additionally, the mechanical resistance against deformation triggered by ice crystals during freezing and the affinity to the ice crystal surface affect the particle stability. Thus, the set of the NP properties relevant for their stability is specific for each type. It is crucial to evaluate formulation principles within a material category first and to subsequently derive general rules. Important aspects for lyophilization of pharmaceutically relevant NP types distinguished according to their physico-chemical properties are described in the following sections (see Table 1).

Table 1: Classification of reviewed NPs.

Lipophilic nanoparticles	Polymeric nanoparticles	Vesicles	Others
• Drug nanosuspensions • Solid lipid nanoparticles	• Nanospheres /-capsules • Polyelectrolyte complexes • Polyplexes	• Liposomes • Lipoplexes • Extracellular vesicles • Enveloped Viruses	• Lipid nanoparticles • Non-enveloped Viruses • Inorganic nanoparticles

3.1 Lipophilic nanoparticles

Stabilization of lipophilic NPs, a group that comprises drug nanosuspensions or nanocrystals, solid lipid nanoparticles (SLNs), as well as nanostructured lipophilic carriers (NLCs), is usually accomplished by surfactants and/or polymers. These stabilizers affect particle-liquid and particle-particle interactions. Only a limited number of surfactants is approved for parenteral products [60] and accordingly lipophilic NPs are usually stabilized with lecithin or the non-ionic surfactants polysorbate 20 or 80 (PS20, PS80) and poloxamer 188 (P188). Steric stabilization by non-ionic surfactants leads to particles without considerable surface charge which reduces a negative impact by salt or pH change on stability. Also, the number of polymers approved for parenteral use is restricted. Therefore, usually PVP, PEG, hydroxyethyl starch (HES), gelatin, ficoll, or dextran are used as stabilizers [60–62].

3.1.1 Drug nanosuspensions (= nanocrystals)

Nanosuspensions of pure API are utilized to improve the bioavailability of poorly water-soluble compounds. The high specific surface area caused by nanonization results in an increased dissolution rate according to Noyes-Whitney and Nernst-Brunner equations [63]. However, physical stability can be problematic as small particles tend to form aggregates because of their thermodynamically unfavorable high total surface energy [3]. The aggregation tendency of a nanosuspension depends on many aspects including the stabilizers added, the API solubility, and the employed nanosizing method [64]. Freeze-drying of drug nanosuspensions is an important technique to generate a dry powder and thereby improve stability. A rapidly reconstituted lyophilizate may additionally provide more convenient handling compared to a suspension. The latter may require vigorous shaking for a longer time period to assure homogeneity which comes also with the risk of air entrapment or foaming.

Fast freezing may result in less particle aggregation [65,66]. But the effect may be limited when considering the rates possible with commercial freeze-dryers [47]. Low molecular weight sugars like sucrose and trehalose led to better stabilization of freeze-dried indomethacin nanocrystals compared to a high molecular weight sugar like maltodextrin. This is potentially due to better hydrogen bonding also with the surfactant used [67]. Beirowski et al. showed that drug nanosuspensions do not require immobilization by glass-forming excipients to inhibit aggregation unless an appropriate type of steric stabilizer is present in a suitable concentration [68]. This is in line with studies showing successful lyophilization of nanocrystals using mannitol [69] which is known to crystallize upon drying. Furthermore, polymers such as Ficoll, high molecular weight PEG, carrageen, or gelatin were able to prevent aggregation of different nanocrystal types during lyophilization [67,70,71]. Whereas Cremophor EL was inappropriate as steric stabilizer of a model drug nanosuspension, poloxamer 338 substantially inhibited aggregation during freeze-drying and long-term storage [72].

3.1.2 Solid lipid nanoparticles/ Nanostructured lipid carriers

SLNs are typically prepared by high pressure homogenization of triglycerides, monoglycerides, fatty acids, fatty alcohols, and waxes emulsified with 0.5 - 5.0% surfactant in water. SLNs have a good loading capacity for both hydrophilic and lipophilic compounds [73]. The incorporation can increase drug stability, provide controlled release, or improve bioavailability [73,74]. The focus currently shifts from small molecules to peptides, proteins, antibodies and DNA [75,76]. SLNs may suffer from a change in lipid modification upon storage. The resulting more stable modifications with less imperfections may lead to impaired drug release and drug expulsion. Therefore, NLCs composed of a blend of a solid

lipid and an oil were developed with more imperfections in the lipid matrix [77,78]. SLNs and NLCs show physical and chemical instability. Frequently, an increase in particle size will be observed within a few months [74]; lyophilization is a promising way to extend the shelf life.

Heiati et al. investigated the influence of trehalose, glucose, mannitol and lactose as cryoprotectants on process stability of zidovudine-loaded glyceryl trilaurate SLNs with lecithin as surfactant [79]. Trehalose was most effective at a sugar to lipid weight ratio of 2.6 to 3.9; the ratio depending on the phospholipid composition. A sufficiently high concentration of cryoprotectant is crucial. Cavalli et al. observed pronounced particle aggregation after lyophilization of similar SLNs with 2% trehalose for cryoprotection [48]. Using 15% trehalose provided better stabilization with a particle size of around 100 nm after freeze-drying, compared to 56.5 nm before and to 240 nm after freeze-drying with 2% trehalose. Also Schwarz et al. identified 10 to 15% glucose, mannose, maltose, and trehalose as effective protectors during freezing and thawing of SLNs [49]. After freeze-drying, they found least aggregation using 15% trehalose, but still particle size increased by a factor of 3. Loading of the SLNs with 1% tetracaine or etomidate resulted in large aggregates presumably due to an effect of free drug on the zeta potential of the particles or a change in the lipid matrix properties. Recent studies on lyophilization of progesterone-loaded SLNs showed best preservation using 20% trehalose; still, this formulation suffered from low short-term storage stability at 25 °C [80]. Other authors also reported that trehalose is not a universal solution for lyophilization of SLNs [81] concluding that further formulation parameters such as pH, surfactant type, and concentration are very important.

Ohshima et al. found that 5% glucose, fructose, maltose, or sucrose equally stabilized nifedipine-loaded SLNs during lyophilization [82]. Stabilization of SLNs can also be achieved by using mannitol which crystallizes upon lyophilization. Tiyaboonchai et al. found that 4% of mannitol is sufficient to preserve the particle size of freeze-dried curuminoids-loaded SLNs [83]. Thus, a glass forming sugar is not obligatory for freeze-drying of SLNs. Vighi et al. successfully freeze-dried cationic stearic acid SLNs without cryoprotectant [84]. However, they used a high surfactant concentration of 6%, and other lipid matrices showed irreversible particle aggregation suggesting lipid specific freeze-drying behavior.

Furthermore, it appears to play a role, when the cryoprotectant is added. Siekmann et al. found that 20% sucrose better stabilized SLNs during lyophilization, when added already before as compared to after high pressure homogenization [85]. They hypothesize that the disaccharide molecules form hydrogen bonds with the phosphodiester group of the phospholipids during homogenization which is restricted when sucrose is added after homogenization.

In none of the aforementioned publications, the surfactant/ cosurfactant composition was varied. Analogous to drug nanosuspensions, the surfactant type and concentration is assumed to be crucial for the freeze-drying success. However, in contrast to drug nanosuspensions, the surfactant/ cosurfactant types are key factors for the properties of the lipid matrices including drug loading capacity and release kinetics. Thus, interchangeability of surfactants is not straightforward in manufacturing of SLNs.

3.2 Polymeric nanoparticles

3.2.1 Nanospheres/-capsules & Polyelectrolyte complexes

Nanospheres are matrix systems in which the drug is physically and uniformly dispersed, whereas nanocapsules are vesicular systems in which the drug is located in a cavity surrounded by a polymeric layer [86]. Both types are used as drug delivery systems, mainly for controlled drug release. Commonly used synthetic polymers are poly(lactic-co-glycolic) acid (PLGA), polylactide (PLA), and polycaprolactone (PCL), whereas saccharides such as chitosan, and alginate or proteins such as human serum albumin (HSA) and gelatin are typical natural polymers used to form these NPs. Nanospheres and nanocapsules are frequently lyophilized in order to preserve their physical and chemical stability and especially in order to block payload release that can occur if stored in liquid suspension.

Disaccharides maintained the particle size of lyophilized PLGA and PCL NPs in several studies [87–91]. Additionally, release kinetics of testosterone-loaded PLGA NPs were not affected [88]. In contrast, mannitol failed to prevent aggregation concluding that vitrification is favorable. Excipients forming such an amorphous matrix are not interchangeable as shown for PLA NPs [92,93]; the smaller disaccharides were superior to the larger saccharides ficoll, and dextran as well as PVP [92]. Fonte et al. showed that co-encapsulation of lyoprotectants, e.g. trehalose, improves drug stability of insulin-loaded PLGA NPs during lyophilization [94]. Freeze-drying of cyclosporine-loaded PLGA and PCL NPs led to a 1.5-fold increase of particle size in presence of 20% sucrose as reported by Saez et al. [95] indicating further critical aspects than the choice of the cryoprotectant.

Polymeric NPs are often stabilized by polymers or surfactants, such as PVA or P188 which can bind to the NP surface. Their concentration and type strongly affect the success of lyophilization. PVA itself exhibits a cryoprotective effect as shown after freeze-thawing of PCL NPs and freeze-drying of PLGA NPs [96,97]. De Chasteigner et al. found that sodium deoxycholate instead of P188 results in complete stabilization of itraconazole-loaded PCL nanospheres after freeze-drying in presence of 10% sucrose, speculating about P188 crystallization [98]. The addition of 0.12% PS80 improved lyophilization process stability of

PLA NPs, interestingly both when added to the formulation before or to the reconstitution medium after lyophilization [99]. Thus, reconstitution appears to be a further critical step fostering aggregation. De Jaeghere et al. found that both adsorbed and covalently bound polyethylene oxide (PEO) destabilized PLA NPs during freeze-drying, which might be due to PEO crystallization [100,101]. However, this effect was minimized by increasing the amount of trehalose as cryoprotectant. Interestingly, lyophilization of insulin-loaded PLGA NPs increased drug release due to increased pore formation on the NP surface [102]. Overall, an annealing step during freezing was suitable to accelerate sublimation without negative impact on the particle size of PCL NPs [103].

HSA NPs as protein-based drug delivery vehicles can be stabilized by trehalose and sucrose during lyophilization independent of drug loading or PEGylation. The disaccharides were superior to mannitol [104,105]. Self-assembly of charged polyelectrolytes (e.g. chitosan, gelatin) with substances of opposite charge can be defined as polyelectrolyte complexes. Depending on the counterparts of the complexes, there is a smooth transition to polyplexes which are described in section 3.2.2. Disaccharides are suitable to stabilize various types of chitosan complexes [106–108]. Insulin-chitosan NPs formulated with trehalose showed comparable particles sizes before and after lyophilization [109] while freeze-drying in presence of mannitol led to a slightly decreased size [106] indicating altered particle properties. Bromelain-chitosan NPs were better stabilized using the disaccharide maltose compared to glycine as cryoprotectant [110]. Lyophilization of poly(propylacrylic acid)-peptide complexes was recently studied by Mukalel et al.. They identified sucrose, trehalose and lactosucrose as efficient stabilizers [108]. Umerska et al. furthermore observed synergistic cryoprotection of trehalose/PEG mixtures for various polyelectrolyte complexes [111].

Zillies et al. successfully lyophilized oligonucleotide-loaded gelatin NPs using sucrose or trehalose [112]. Interestingly, mannitol also showed notable process stabilization despite its crystalline nature. Based on these findings, Geh et al. further developed lyophilization of oligodeoxynucleotide (ODN)-loaded gelatin NPs investigating histidine, arginine, and glycine as alternative cryoprotectants [113]. Histidine emerged as an excellent stabilizer in contrast to arginine and glycine. Furthermore, the controlled ice nucleation technique shortened drying times of ODN-loaded gelatin NPs due the formation of larger ice crystals which accelerates sublimation.

3.2.2 Polyplexes

Nonviral vectors are a rather new class of nucleic-acid-based biopharmaceuticals used for gene delivery. These delivery systems are based on cationic polymers (= polyplexes) or cationic lipids (= lipoplexes) which form condensed complexes with the negatively charged nucleic acids [114]. Ternary complexes of cationic liposomes, polycations (cationic polymers or peptides), and nucleic acids are called lipopolyplexes [115]. Synthetic polymers such as poly(L-lysine) and polyethylene imine (PEI) are widely used cationic polymers for polyplex formation. Lipo(poly)plexes are referred to lipid bilayer structured NPs and are therefore discussed in section 3.3. The size of the complexes affects cellular uptake and should be between 70 and 90 nm [116]. Hence, aggregation of particles in aqueous solutions correlates with a loss in transfection efficiency.

Armstrong et al. observed time and temperature dependend aggregation of pDNA/PEI polyplexes in the frozen state which was inhibited at temperatures below T_g' providing complete immobilization [117]. Kasper et al. further found the initial sample viscosity and the residence time in the low-viscosity state as very important factors in pDNA/LPEI stabilization [118]. At a certain temperature and degree of freeze-concentration, particle mobility can be inhibited due to high sample viscosity even above T_g'. It is very likely that these principles also apply to other colloidal systems which degrade by aggregation. Generally, cryoprotectants forming an amorphous matrix, preferably sucrose or trehalose, proved to successfully stabilize various polyplex types (Table 2).

Table 2: Polyplexes stabilized in amorphous matrices.

Polyplex type	Reference
pDNA/ PEI	[117–119]
pDNA/ transferrin-PEI	[120]
pDNA/ poly((2-dimethylamino) ethyl methacrylate)	[121,122]
pDNA/ iodoacetic acid alkylated Cys-Typ-Lys18	[123]
pDNA/ oligopeptide end modified poly(β-aminoester)	[124]
pDNA/ chitosan	[125]
siRNA/ oligoamidoamide	[126]
siRNA/ PEG-PCL-PEI	[127]
siRNA/ chitosan	[128]
oligodeoxynucleotide/ PEI	[129]
oligonucleotide/ chitosan	[128]

Cross-linking of core-shell polyplexes improved freeze-drying process stability as shown for pDNA/PEG-poly(L-lysine) polyplexes [130]. Brus et al. found pronounced aggregation for pDNA/PEI polyplexes, while ODN/PEI polyplexes remained stable upon lyophilization independent of cryoprotectant type [129]. Similarly, the process stability of ODN/chitosan polyplexes was better compared to siRNA/chitosan polyplexes as reported by Veilleux et al. [128]. Thus, freeze-drying success does not only depend on the choice of cryoprotectant, but also on individual particle properties. Long-term stability studies of freeze-dried pDNA/LPEI polyplexes revealed successful particle size stabilization in lactosucrose, HP-β-CD/sucrose, or PVP/sucrose. However, PVP/sucrose led to a decreased metabolic activity which was already seen for freshly prepared samples and speculatively attributed to peroxide impurities [119]. Consequently, biological activity may not correlate with colloidal stability and should be assessed before lyophilization.

Polyplexes are sensitive towards buffer type and pH; ODN/chitosan polyplexes formulated at pH 6.5 were stable in histidine, Tris-maleic acid, sodium phosphate, or maleic acid, but aggregated in Tris-HCl, already before freeze-drying [128]. After lyophilization in presence of trehalose, the polyplex size furthermore increased in maleic acid and sodium phosphate, but not in histidine buffer. The particle size of pDNA/peptide condensates remained stable after lyophilization in HEPES at pH 4 to 7, but drastically increased at pH 3 which was attributed to altered surface charges [123]. Interestingly, severe aggregation of lyophilized pDNA/chitosan particles was avoided by adding 3.5 mM histidine at pH 6.5 to either sucrose, dextran, or trehalose [125]. Furthermore, it appears to be important when the buffer and cryoprotectant are added [124]. Fornaguera et al. demonstrated that polyplex precipitation was hindered in presence of sucrose and HEPES, potentially due to inhibited electrostatic interactions [124]. Lyophilization can also be used for up-concentration. Reconstitution with less volume, however, comes with increased solutes concentrations. Veilleux et al. mimicked up-concentration in liquid state and found pronounced aggregation of ODN/chitosan polyplexes with increasing buffer concentration which was attributed to partial polymer deprotonation affecting electrostatic particle interaction [128]. The effect was observed for maleic acid and phosphate buffer, but nor for histidine buffer.

3.3 Lipid bilayer vesicles: Liposomes and biological nanoparticles

Liposomes (0.05-5.0 µm) serve as drug delivery systems by entrapping drugs into their cavity or bilayer structure and form spontaneously upon hydration of certain lipids in aqueous media [131]. In this review, the term ‘vesicles’ implies the presence of a lipid bilayer. Their main constituents are amphiphilic phospholipids. Most biological NPs, such as extracellular vesicles and enveloped viruses have a similar structure. Lyophilization of these particles is

highly challenging as the lipid bilayer is both fragile and flexible. Still, it is a highly promising technique to extend storage stability of bilayer vesicles, e.g. novel liposomes tested as adjuvants, when compared to liquid formulations [132]. The complexity further increases for biological vesicles due to their heterogeneous composition. Thus, it is crucial to understand essential attributes and parameters affecting the bilayer stability. After general considerations which are applicable to most bilayer structured particles, lyophilization aspects of different types including lipoplexes, extracellular vesicles, and enveloped viruses are elucidated in more detail.

3.3.1 Lipid bilayer: composition & phase transition T_m

The lipid bilayer is a thin polar membrane composed of two layers of lipid molecules providing a barrier between intra- and extracellular components. Biological bilayers are mainly composed of amphiphilic phospholipids, but can also include cholesterol which alters properties as for example the width and packing density of the bilayer [133]. In fully hydrated state, the phospholipids are exposed to permanent fluctuations making the bilayer a fluid phase [134]. As a consequence, hydrocarbon chains of the lipid molecules are conformationally disordered.

The lipid bilayer is temperature sensitive and can undergo a gel to liquid crystalline phase transition [135]. Below the transition temperature T_m, the hydrocarbon chains are in an ordered crystalline structure, considered as the gel phase. Above T_m, the ordered structure is lost resulting in the liquid crystalline phase, also called fluid phase. Depending on the amount of water present, phospholipids can exist in one or more intermediate or mesomorphic forms [136]. The T_m depends on the hydrocarbon chain length and the degree of saturation which impact the energy necessary to overcome van der Waals interactions (see Table 3). Mixtures of phospholipids, e.g. in biological membranes, melt over a broader temperature range compared to pure lipids [137]. Furthermore, incorporation of cholesterol into the lipid bilayer leads to a broadening of T_m, both by hindering crystallization into the gel phase and by hampering bilayer mobility in the liquid crystalline phase [136]. The lipid bilayer may also be affected by the presence of surfactants; Susa et al. observed a significant reduction in size after freeze-thawing liposomes in presence of PS80 which is attributed to intercalation of the surfactant in the lipid bilayer [138].

Table 3: Bilayer phase transition temperatures of hydrated phospholipids.

Phospholipid	Acyl chains	T_m [°C]	Reference
DLPC	12:0	−1	[139]
DMPC	14:0	24	[139]
DPPC	16:0	41	[136]
POPC	16:0/18:1 cis	−3	[139]
SOPC	18:0/18:1 cis	6	[139]
DSPC	18:0	58	[136]
Egg PC	Mixed chains	−5 to −15	[136]
Soy PC	Mixed chains	−20 to −30	[136]

DLPC is dilauryl phosphatidylcholine, DMPC is dimyristoyl phosphatidylcholine, DPPC is dipalmitoyl phosphatidylcholine, POPC is 1-palmitoyl, 2-oleoyl phosphatidylcholine, SOPC is 1-steroyl, 2-oleoyl phosphatidylcholine, and DSPC is distearoyl phosphatidylcholine

The T_m of the phospholipid determines the susceptibility of payload loss and is therefore a critical process parameter. Thus, in case of artificial vesicles, lyophilization success may depend on the phospholipid selection. The importance of T_m on cooling, freezing and reconstitution of lipid bilayer vesicles is thus explained in detail in the following section.

3.3.2 Factors affecting leakage and release of vesicles

Payload retention is an important parameter to assess damage caused by lyophilization. Phospholipid packing defects and phase separation between gel and liquid crystalline domains are widely discussed to transiently increase the bilayer permeability [139,140]. In addition, phase transition and fluidity of the bilayer affect the vesicle stability by determining properties such as permeability, fusion, and aggregation [141]. Avoiding a phase transition and thereby unintended leakage is therefore a major goal to increase the payload retention during freeze-drying, subsequent storage, and upon reconstitution.

Dehydration leads to an increase in T_m of the main phase transition which is attributed to increased van der Waals forces between the phospholipids [136]. Koster et al. revealed that disaccharides diminish the increase in T_m upon dehydration [142]. They also found a relationship between T_m and the sugar glass transition temperature T_g: if $T_g > T_{m0}$ ($T_{m0} = T_m$ at full hydration), and vitrification occurs in the liquid crystalline phase, then T_m is depressed below T_{m0}; if $T_g < T_{m0}$, vitrification has no effect on T_m [143]. The T_m reduction is suggested to be driven by water replacement at the phospholipids [144]. Thus, cryoprotectant type and residual water content highly impact the bilayer phase transition during lyophilization and of the resulting product.

Specifically during freezing, dehydration, and reconstitution of lyophilizates potential leakage due to a bilayer phase transition may occur [145]. In presence of sugars, T_m is not affected until the end of ice sublimation when all of the bulk water is removed. If phase transition occurs during the dehydration step, there is no bulk water left into which the vesicle contents could be leaked. Thus, T_m depression upon dehydration in presence of a sugar can be decisive. Vesicles exhibiting a high T_m value are expected to undergo bilayer phase transition neither during lyophilization nor upon reconstitution. Vesicles with low T_m are prone for destabilization by both events. E.g. trehalose depresses the T_m of POPC liposomes from about −1 °C to −20 °C after drying [145]. Thus, both freezing (liquid → gel) and drying (gel → liquid) induce phase transitions, however not the rehydration step since the lipid is in the liquid crystalline phase after drying. In comparison, the T_m of DMPC is depressed from 26 °C to 6 °C [143] so that phase transition does not occur during lyophilization (depending on the secondary drying temperature), but during reconstitution at RT (gel → liquid). Consequently, the T_m shift in presence of sugars is crucial for leakage.

Cholesterol has a broadening effect on T_m and leads to multiple phase transitions upon dehydration [146]. Hence, longer residence in the phase transition period and thus increased drug leakage is expected. However, freeze-dried liposomes containing cholesterol showed higher retention upon rehydration [147]. Cholesterol reduces membrane fluidity by increasing membrane packing, stiffness, and thickness of the bilayer; as a result membrane permeability decreases [148]. In addition, cholesterol is able to depress T_m in the dried state [149] similarly to sugars.

Content leakage further depends on the hydrophobicity of the encapsulated substance. Hydrophilic substances ($\log P_{oct} < -0.3$) are located inside of vesicles; lipophilic substances ($\log P_{oct} > 5$) are entrapped in the acyl chains of the lipid membrane, and amphiphilic cargos ($1.7 < \log P_{oct} < 4$) can be located at either site [150]. Hence, hydrophilic or amphiphilic molecules are more prone to leakage compared to lipophilic substances. Guimarães et al. revealed that a drug located in the lipid bilayer was less susceptible to leakage after lyophilization compared to a drug present in the aqueous core [151].

Hays et al. reported that increasing cooling rates lead to a decreased residence time in the phase transition period and thus decreased leakage of liposomes [139]. The addition of defect-forming additives such as a second phospholipid or small amounts of a surfactant increased leakage during the phase transition but not above or below T_m. Moreover, payload retention of lyophilized unilamellar vesicles in presence of trehalose was higher for medium sized vesicles (50-100 nm) compared to smaller or larger ones, indicating a preferred particle size for content retention [152,153]. The size affects the length of the diffusional pathway, the surface to volume ratio, as well as the curvature which impacts packing and motion of the

phospholipids [139]. However, these observations are not generally valid since 5 µm sized multilamellar liposomes containing 5-fluorouracil were successfully freeze-dried in presence of sucrose with 80% payload retention [154].

3.3.3 Strategies to avoid leakage & fusion of vesicles

The addition of a sugar as a cryo- and lyoprotectant is considered as the most important parameter towards preservation of particle size and payload retention. Moreover, a phase transition after rehydration can be avoided by the addition of sugars since they reduce the T_m after drying. Disaccharides are preferred over monosaccharide due to higher glass transition temperatures. Polysaccharides such as HES exhibit even higher T_g values after lyophilization. However, HES did not prevent leakage from liposomes though inhibiting particle fusion which was attributed to weak interactions with the phospholipids [155]. When glucose was added to the HES matrix, the liposomes were well stabilized when kept below T_g. Thus, immobilization in an amorphous matrix and reduction of T_m may improve liposome preservation during lyophilization. Talsma et al. showed that freeze-thawing of liposomes to −50 °C in presence of trehalose (T_g'~−29 °C) resulted in carboxyfluorescein retention of 95%, while samples frozen to −25 °C lead to 50% marker retention [17] indicating leakage at temperatures above T_g'.

Trehalose is often considered to be superior to sucrose regarding its protective effects, potentially due to stronger interactions with the bilayer [156]. Crowe et al. postulated that under ideal drying and storage conditions, trehalose should act comparably to other disaccharides [145]. However, under suboptimal conditions, such as high temperatures or humidity during storage, trehalose has unique properties; it may form a dihydrate thereby shielding the vitrified matrix from further water penetration. But trehalose may also destabilize colloids during freezing due to trehalose dihydrate crystallization above T_g' [157,158]. During drying, the dihydrate dehydrates to amorphous anhydrate disguising potential previous crystallization.

Tryptophan and phenylalanine were not able to stabilize liposomes during freezing resulting in leakage and membrane fusion, although the interactions with phospholipids were similar to sugars [159,160]. Lysine, however, showed cryoprotective effects comparable to trehalose [161]. Phenylalanine is known to crystallize upon lyophilization, while lysine remains amorphous [162]. Therefore, it appears that the potential for lyoprotection depends on the ability of the amino acid to form an amorphous matrix. Antifreeze glycoproteins, especially species >13 kDa, prevented leakage of liposomes while cooled through their phase transition [163,164]. Furthermore, the phytochemical arbutin was tested for lyophilization of liposomes since it is an abundant solute in the leaves of many freezing- or

desiccation-tolerant plants [165]. Arbutin inhibits phospholipase A_2 under partially hydrated conditions and thereby prevents deesterification of membrane lipids [59]. Hincha et al. showed that the protective effect of arbutin depends on in the bilayer composition since it only prevented liposome leakage if a non-bilayer lipid such as monogalactosyldiacylglycerol was present in the membranes. Furthermore, arbutin can depress T_m upon dehydration [166].

In a recent study aiming for high-throughput screening protein-loaded liposomal formulations were successfully freeze-dried in 96 well plates [167]. Another interesting approach is the manipulation of the reconstitution medium. Zingel et al. found that rehydration of lyophilized liposomes with mannitol solution resulted in higher drug retention compared to rehydration with water or Tris buffer [168]. The rehydration step can also be used for loading as shown for reconstitution of naked liposome lyophilizates with siRNA solution [169,170].

The cryoprotectant can also affect lyophilization process stability when additionally distributed inside of vesicles. The presence of trehalose both inside and outside of vesicles decreases T_m in aqueous medium and may further maximize payload retention upon lyophilization [53,54,171]. This effect may depend on the applied freezing rate; higher freezing rates lead to higher retention during freeze-thawing of liposomes containing trehalose on both sides of the membrane [172]. In contrast, content retention was barely affected by the freezing rate when trehalose was distributed only outside the vesicles. Osmotic shrinkage during cryo-concentration is suggested to prevent mechanical damage resulting in high marker retention (see Figure 4). Formulations with cryoprotectant on both sides of the membrane do not undergo total osmotic shrinkage. Thus, the residual internal supercooled solution may either freeze or get damaged by ice penetration which depends on kinetic aspects. Van Winden et al. found that slow freezing results in higher retention rates after freeze-drying with trehalose (external) compared to fast freezing in liquid nitrogen [173]. This effect depended on the lipid composition and was observed for various DPPC liposomes, while EPC liposomes were barely affected by the freezing protocol.

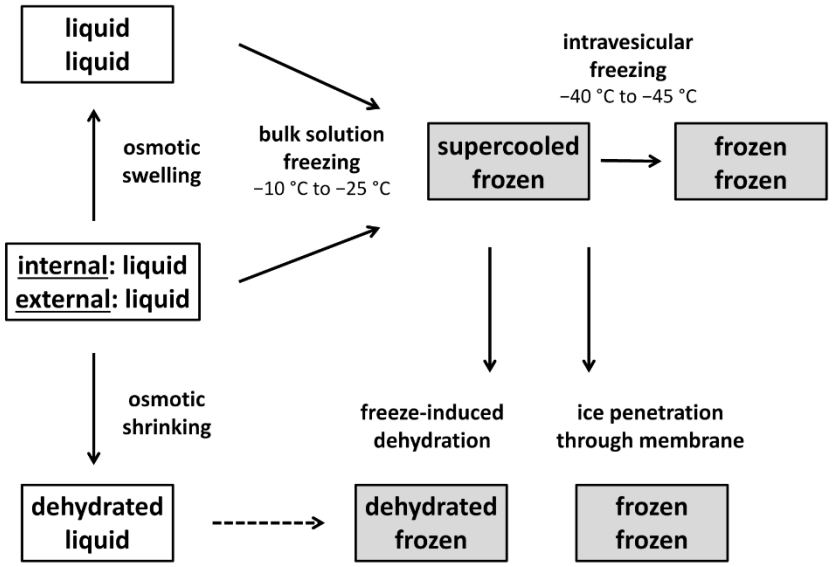

Figure 4: Schematic freezing behavior of vesicles. The physical state of internal and external water is denoted in the upper and lower rows respectively. Grey boxes indicate suggested physical states (adapted from [172]).

3.3.4 Lipoplexes

Lipoplexes are nonviral lipid-based vectors composed of cationic lipids, usually mixed with neutral co-lipids, and nucleic acids. Two types of structures were observed in plain lipoplexes: (1) a multilamellar vesicular structure, with DNA monolayers sandwiched between cationic membranes, and (2) an inverted hexagonal structure, with DNA encapsulated within cationic lipid monolayer tubes [174]. As most lipoplexes are of vesicular structure, the principles described for liposomes, should be applicable for most lipoplex types. In contrast to classical liposomes, lipoplexes are special due to their charged lipids and thus surface as well as their cargo. Therefore, the following section aims to outline studies which were conducted with lipoplexes in particular.

Molina et al. showed that not only the preservation of lipoplex size is important, but that changes in particle properties as indicated by a change in surface charge upon freezing might result in reduced transfection activity [175]. Yavada et al. reported that an activity loss of lyophilized lipoplexes is not due to siRNA damage since lyophilized siRNA when rehydrated and complexed with liposomes was still active. Instead, the change in activity correlated to the change in lipoplex size [176]. Thus, both size and surface charge are essential parameters to evaluate lyophilization success. Recent studies further suggest using disaccharides as cryoprotectants, since certain mono- or trisaccharides may induce cytotoxicity and/or off-target effects [177].

Sucrose or trehalose are suitable to protect particle size and transfection rates of lipid/DNA complexes during the lyophilization process [178,179]. More dilute samples required less excipient to prevent aggregation concluding that vitrification is not the only mechanism by which sugars protect lipoplexes during the freezing step. Instead, Allison et al. confirmed the particle isolation hypothesis by showing that the separation of individual particles within the unfrozen fraction prevents aggregation [179]. The authors also postulated that water replacement plays a significant role in lipoplex protection during lyophilization, similar as for liposomes [180]. Sucrose and trehalose are the cryoprotectants of choice as they inhibited aggregation and maintained high transfection rates of lipoplexes in several studies [178,181–191]. Sucrose was furthermore superior to other protectants including lactose, mannitol, isomaltose, isomaltotriose, and HES [179,192,193]. An appropriate amount of cryoprotectant has to be chosen as a high trehalose concentrations (>5%) can lead to slightly increased lipoplexes with decreased surface charge after freeze-drying [182]. Combinations of saccharides, such as sucrose/dextran, effectively inhibited particle aggregation upon freeze-drying [181]. Hinrichs et al. observed that both dextran and inulin were able to stabilize nonPEGylated lipoplexes while only inulin was able to protect PEGylated particles [194,195]. They hypothesized that aggregation of the PEGylated lipoplexes in dextran solutions is caused by the incompatibility between dextran and PEG. They further suggested that both oligosaccharides might be more versatile cryoprotectants than disaccharides because of their higher T_g' and T_g values which enables freezing at higher temperatures and storage at higher relative humidities respectively. Hydroxypropyl-γ-cyclodextrin was furthermore superior to several cryoprotectants including trehalose in preservation of lyophilized DNA-loaded pegylated lipoplexes decorated with covalently linked monoclonal antibodies [196]. Yu et al. showed that the addition of PS80 minimizes aggregation and loss of transfection of lyophilized lipoplexes indicating surface-induced damage, especially caused by the freezing step of lyophilization [185]. Interestingly, recovery of lipoplexes was also improved when PS80 was added to the reconstitution medium indicating that severe aggregation can also occur during the rehydration step.

The impact of the freezing rate on lipoplex stability is discussed intensively. On the one hand Li et al. reported that fast freezing caused less aggregation upon freeze-thawing [183]. On the other hand, Aso et al. observed that slow freezing led to better storage stability of lipoplex lyophilizates; they measured longer shear relaxation times for lyophilizates prepared by slow freezing indicating reduced matrix mobility [181]. The storage stability of lipoplexes is affected by multiple factors [184]. The formation of hexagonal lipid structures during storage of lyophilizates is proposed to reduce transfection efficiency over time. The rearrangement propensity depends on the lipid phase composition; hydrated lipoplexes rather adopt hexagonal structures when dioleoyl phosphatidylethanolamine is employed as helper lipid

compared to cholesterol. Furthermore, a low T_g impairs long-term stability. But cake collapse and thus increased viscous flow is not solely responsible for decreased lipoplex stability since a loss of transfection efficiency was even observed after storage temperatures at −20 °C. Trace amounts of metal ions may induce the formation of reactive oxygen species affecting the stability of lipoplexes during lyophilization and storage [187,189]; especially unsaturated lipids are prone to oxidative damage. The close proximity of DNA to the lipid component may facilitate interactions of DNA with oxidized species, e.g. peroxyl radicals and other by-products. The proceeding oxidative damage can be partly inhibited by the addition of a chelators and/or antioxidants [190]. The residual water content was elucidated as a further storage stability limiting factor [191]. Lyophilizates with a higher moisture content of 2%, demonstrated greater stability than dryer samples.

3.3.5 Extracellular Vesicles

Extracellular vesicles (EVs) are cell-derived NPs excreted by the conjugation of intermediate endocytic bodies to the plasma membrane [197,198]. EVs consist of a lipid bilayer membrane decorated with surface and membrane proteins and enable intercellular transfer of biological cargos [198,199]. Loading EVs with exogenous cargos opens up potential for controlled drug delivery [200]. However, the scope of therapeutic application is limited by effective preservation and storage which is usually accomplished by freezing EVs in phosphate buffered saline to −80 °C [201,202]. Thus, lyophilization would facilitate storage and handling and offers new possibilities for application, e.g. pulmonary drug delivery.

Trehalose improved preservation of EV size and concentration upon several freeze-thaw cycles [203]. Interestingly, EVs were able to resist one freeze-thaw cycle in absence of cryoprotectants. Lyophilization of EVs without cryoprotectant leads to marked aggregation [204,205]. Frank et al. found improved freeze-drying process stability of EVs after addition of trehalose, which was more efficient than the addition of mannitol and PEG 400. Still, a decreased particle number and activity of encapsulated enzyme after lyophilization indicated particle aggregation and cargo loss or degradation [204]. Lyophilization success also depended on the EV type; EVs derived from A549 cells were less stable compared to EVs from MSC or HUVEC cells. A recent study by Charoenviriyakul et al. revealed that the biological activity of protein and DNA-loaded EVs was preserved after lyophilization with trehalose, and storage of lyophilizates for 4 weeks at room temperature [205].

3.3.6 Enveloped Viruses

Attenuated or inactivated viruses are vaccine types which can be assigned as NPs. Their size is heterogeneous and ranges from approximately 40 to 500 nm or even 1.2 µm [206]. Most viruses exhibit a lipid bilayer as viral envelope which is decorated with proteins which enable to identify and infect host cells. Enveloped viruses can also have a protein shell between the envelope and their nucleic acid, the capsid, to further protect the viral genome. New approaches focused on the preparation of the less pathogenetic virosomes; i.e. virus-like particles, consisting of the viral envelope without encapsulated genetic material [207]. Storage and transportation at 2-8 °C is typical for stabilization. Furthermore, cold-chain is a major hurdle for supply in developing countries. But inadvertent freezing during cold-chain might also lead to a loss of efficacy. Therefore, stabilization by freeze-drying is of great interest.

A historical formulation often used for lyophilization of viruses is SPGA (**s**ucrose, potassium **p**hosphate, potassium **g**lutamate, bovine **a**lbumin) or variations thereof. SPGA was first mentioned by Bovarnick et al. in 1950 and favored survival of rickettsiae (bacteria) after freeze-thawing [208]. A second prominent stabilizer mixture is BUGS (**bu**ffered **g**elatin, **s**orbitol). In 1989, De Rizzo et al. found that a sorbitol/gelatin mixture is suitable to stabilize freeze-dried measles virus [209]. Both formulations SPGA and BUGS successfully stabilized different enveloped viruses during lyophilization and are used in many marketed products (see the comprehensive review by Hansen et al. [5]). Furthermore, sucrose and trehalose, also in combination with lactalbumin, showed good stabilization of pox virus [210], ovine rinderpest vaccine [211], ebola virus [212], herpes simplex virus [213], and parainfluenza virus [214]. Further stabilizers, such as P188 as surfactant, may additionally add to the stability of lyophilized viruses [214].

The pH and osmolarity are formulation key factors for virus stabilization in liquid state and should therefore also be considered for lyophilization. Measles virus revealed a loss of viral protein secondary structure and aggregation at acidic pH [215]. Yannarell et al. found better lyophilization process stability when influenza virus was formulated at pH 7 compared to pH 6 and pH 8 [216]. The importance of osmolarity in liquid state was described by Colwell et al.; 1000 mOsm/kg (NaCl) led to a decreased stability of marek's disease herpes virus while osmolarity below the physiological osmotic pressure merely affected stability up to 90 mOsm/kg [217]. In contrast, liquid formulations of herpes simplex virus revealed higher stability after 20 h storage in presence of 840 mOsm trehalose or Tris-HCl compared to 50 mOsm and lyophilization stability was drastically improved by increasing the amount of trehalose or sucrose up to 27% [213]. The authors hypothesized that virus shrinkage in hypertonic medium leads to an up-concentration of proteins in the tegument, the protein layer

between bilayer and capsid, which lowers the ice nucleation temperature inside the virus membrane and prevents large ice crystal growth [213]. For additional information on lyophilization of various vaccines including case studies, the authors refer to a review recently published by Preston et al. [218].

3.4 Other nanoparticles

3.4.1 Lipid nanoparticles

mRNA lipid NPs (LNPs) are a new particle type which got attention as COVID-19 vaccines. A key aspect of LNPs and the main difference from liposomes is the presence of lipids in the core [219]. Zhao et al. showed that both trehalose and sucrose were able to protect novel phospholipid-mRNA NPs only when stored in liquid nitrogen, but not during lyophilization [220]. As this particle type is a quite new modality, no comprehensive study on lyophilization is published yet.

3.4.2 Non-enveloped Viruses

Analogous to enveloped viruses, non-enveloped viruses shielded by the capsid, but no phospholipid bilayer, show a pH dependent stability profile in liquid state; enteroviruses (poliovirus, coxsackievirus) are instable at acidic pH (< 4.5) [221]. In this case, a buffer pH shift during freezing should be avoided. Sucrose was suitable to stabilize adenovirus upon freeze-drying [120]. Qi et al. showed that urea improves process and storage stability of lyophilized inactivated poliovirus vaccine (IPV) in presence of sucrose [222]. Addition of 0.4 M urea inhibited capsid denaturation during lyophilization. Potassium phosphate instead of sodium phosphate buffer better stabilized adenovirus and adeno-associated virus (AAV) after storage at −20 °C and 4 °C [223]. AAVs formulated with sucrose, mannitol and protamine showed significantly improved storage stability at −80 °C or −20 °C after addition of Span 20™ instead of P188 as surfactant. However, upon freeze-drying, titer loss was less using sucrose as cryoprotectant without further additives. Adenovirus lyophilizates revealed a narrow moisture level window of 1.5% in which viral titer was maintained. The non-enveloped infectious pancreatic necrosis virus was successfully freeze-dried using lactalbumin hydrolysate, lactose or skim milk [224], while potato virus X could be stabilized using dextran as cryoprotectant [225]. Furthermore, modified SPGA, with sorbitol and gelatine instead of sucrose and albumin, significantly improved the lyophilization process stability of duck viral hepatitis virus compared to commonly used SPGA [226].

3.4.3 Inorganic nanoparticles

Inorganic NPs, specifically functionalized silica material, gain more and more attention as mesoporous drug delivery carries [227]. But, only little literature is available on lyophilization of this NP type. Sameti et al. showed that trehalose is suitable to stabilize cationically modified silica NPs with simultaneous preservation of their DNA-binding and transfection activity [228]. Recent studies further confirmed that antibody-conjugated PEI-PEG coated mesoporous silica NPs are well stabilized by trehalose [229]. Moreover, trehalose and sucrose were superior to mannitol to stabilize freeze-dried antibody-conjugated gold nanorods [230]. Au NPs were furthermore successfully lyophilized using sucrose combined with sucrose monopalmitate as surfactant [231]. Overall, these studies highlight the prerequisite of an amorphous stabilizing matrix.

4 Summary and practical advices

The success of NP lyophilization mainly depends on the type of NP and formulation factors; nonetheless process factors should not be neglected. This review aims to summarize the current knowledge on the colloidal stability of NPs in this regard to give practical advice. In general, formulations of lyophilized NP products should include one or more of the following formulation excipients: a cryo-/ lyoprotectant, a bulking agent, a buffering agent, a surfactant. Table 4 gives a summary of commonly used excipients in freeze-drying.

Table 4: Commonly used excipients in lyophilization classified according to their function (modified from [232]).

Stabilizers	Function	Examples
Cryoprotectant	Protection during freezing	Sugars (e.g. sucrose, trehalose) Amino acids (e.g. arginine)
Lyoprotectant	Protection during drying and/or storage	Sugars (e.g. sucrose, trehalose) Polymers (e.g. PVP, HES) Amino acids (e.g. proline, arginine)
Bulking agent	Provide cake stability (amorphous) Provide elegant cake structure (crystalline)	Sugars (e.g. sucrose, trehalose) Sugar alcohol (mannitol) Amino acids (e.g. glycine, phenylalanine)
Buffering agent	pH stabilization	Histidine, citrate, phosphate, Tris
Surfactant	Prevention of adsorption and aggregation at surfaces and the liquid–ice interface	PS20, PS80, P188
Tonicity agent	Providing isotonicity for tolerability of injectables; often the cryo-/lyoprotectant, bulking agent	Sugars/ polyols (sucrose, trehalose, mannitol) Amino acids (glycine) Caution: salts, e.g. NaCl, are not recommended due to potential interference with charge interactions and poor freeze-drying performance

4.1 Selection of cryo-/ lyoprotectant

The selection of a suitable cryo- and lyoprotectant is highly important since it affects i) the NP process stability, ii) the specific process parameters, i.e. the critical temperature T_g' that the product temperature shall not exceed during primary drying, and iii) storage conditions since the storage temperature should be 10-20 °C above T_g. Table 5 provides information about T_g' and T_g of commonly used sugars for lyophilization of NPs.

Sucrose and trehalose proved to stabilize various NP types and they are the cryoprotectants of choice. Their stabilization mechanisms are well described by the water replacement and vitrification/ particle isolation theories [45–58]. Furthermore, it was demonstrated that disaccharides better stabilize lyophilized colloids compared to polysaccharides (e.g. dextran) [233]. Smaller and molecularly more flexible sugars are less affected by steric hindrance and thus better cover colloidal surface. However, at same osmolarity, oligo- and polysaccharides come with higher mass-based concentration providing better particle

isolation. Mixtures of a disaccharide and an oligo-/polysaccharide might benefit from good cryoprotection and water replacement as well as high T_g and particle isolation.

Table 5: Glass transition temperatures of commonly used sugars for lyophilization.

Sugar	T_g' [°C]	T_g [°C]	Reference
Glucose	−43	39	[2]
Sucrose	−31	77	[194]
Trehalose	−29	121	[194]
HES	−12	>110	[2]
Dextran 5 kDa	−17	175	[194]
Dextran 40 kDa	−12	227	[194]
HP-β-CD	−11	201	[234]

4.2 Selection of bulking agents

Bulking agents are added to provide mechanical strength and an attractive product appearance of the final cake [235]. Usually crystallizing agents are used for this purpose as they are also able to prevent macroscopic product collapse. Mannitol and glycine are the most frequently used bulking agents. Crystallizing agents do not contribute to vitrification and water replacement, but are able to provide particle isolation within the lyophilizate.

4.3 Selection of buffer agent

The colloidal stability of NPs is particularly sensitive to the zeta-potential, especially if strong charge-based repulsion is necessary for colloidal stabilization or if the NPs are assembled due to electrostatic interactions. Therefore, the buffer selection has to consider pH shifts upon cooling and freezing as known for sodium phosphate. Buffers without considerable pH shift are potassium phosphate, citrate and Tris buffers. In general, high buffer concentrations should be avoided since an increased ionic strength in the cryo-concentrate may destabilize NPs due to charge shielding. Furthermore, buffers may impact T_g' during freezing, and T_g of the dried formulation [236].

4.4 Selection of surfactant

Surfactants are essential for colloidal stability of lipophilic NPs, i.e. drug nanosuspensions and SLNs. The type of surfactant highly impacts their lyophilization process stability [47]. The selection of surfactant type and concentration is at present an empirical process. Surfactants also add to the stability of lyophilized viruses [214,223] and may improve NP stability when

added to the reconstitution medium [99,185]. Most commonly, lecithin and the non-ionic surfactant PS20, PS80, and P188 are utilized; all approved for parenteral use [60]. Nonetheless surfactants may come with the risk of lipid bilayer disruption and lysis. Furthermore, high surfactant concentrations may lower the T_g of lyophilizates due to a plasticizing effect which impairs storage stability.

4.5 Osmolarity

Osmolarity is an important aspect for bilayer structured NPs, including viruses. Due to freeze-concentration, vesicles are prone to damage caused by the increased osmotic pressure. Rapid water flux through the bilayer can be responsible for physical forces leading to ruptures [27]. A high osmotic pressure during cryo-concentration may also lead to osmotic shrinkage which decreases mechanical damage caused by ice crystals [172]. Overall, the osmotic stability and payload retention highly depends on the lipid membrane composition and selective permeability towards solutes [28,29]. The osmotic agent should be selected cautiously; e.g. NaCl is known to destabilize colloids during freezing and shows a poor freeze-drying performance due to its eutectic crystallization at −21 °C and low T_g at < 60 °C [2,237]. Furthermore, an increased ionic strength may shield particle surface charges and thus destabilize NPs.

4.6 The process

The lyophilization process is overall less important compared to formulation aspects, but should not be neglected during development. For basic principles, the readers are referred to a comprehensive review on the freeze-drying process itself (see [4]). It is important that the product temperature is kept below T_g' during primary drying. The secondary drying step can be used to adjust the residual moisture which was a critical process stability factor for lipoplex [191] and adenovirus [223] lyophilizates. The liquid crystalline to gel phase transition temperature T_m is a further critical parameter affecting the payload retention of lipid bilayer NPs. In addition, the freezing rate determines the ice crystal size, i.e. fast freezing leads to smaller ice crystals thereby affecting the extent of mechanical stress and the residence time in the cryo-concentrated phase. Large ice crystals may also be generated by applying controlled ice nucleation or by adding an annealing step to the freezing protocol. But all these variations should be applied with the limitations of the capacities of large-scale freeze-dryers in mind e.g. with respect to ramp rates and controlled nucleation.

4.7 Particle properties affecting process and storage stability

Depending on their stabilization mechanism, surface charge, ability to encapsulate drugs, or other properties, the described NP types are affected to a different degree. Mechanical stress caused by ice or excipient crystals is particularly relevant for lipid bilayer vesicles such as liposomes, lipoplexes and viruses. Moreover, most of the described NP types are sensitive to pH and/or electrolyte changes leading to altered release kinetics, surface charges, or osmotic pressure; especially SLNs, polymeric NPs, lipid bilayer vesicles, and inorganic NPs. NP types exhibiting low surface charges, e.g. lipophilic NPs stabilized with non-ionic surfactants or polymers, are expected to be less susceptible to charge shielding caused by pH or electrolyte changes. In general, the amount of added surfactant is high in case of lipophilic NPs and should be chosen carefully due to the T_g lowering effect in sugar matrices.

Finally, Figure 5 summarizes the aforementioned essential formulation parameters and provides a decision tree for the development of lyophilized NPs based on specific particle attributes.

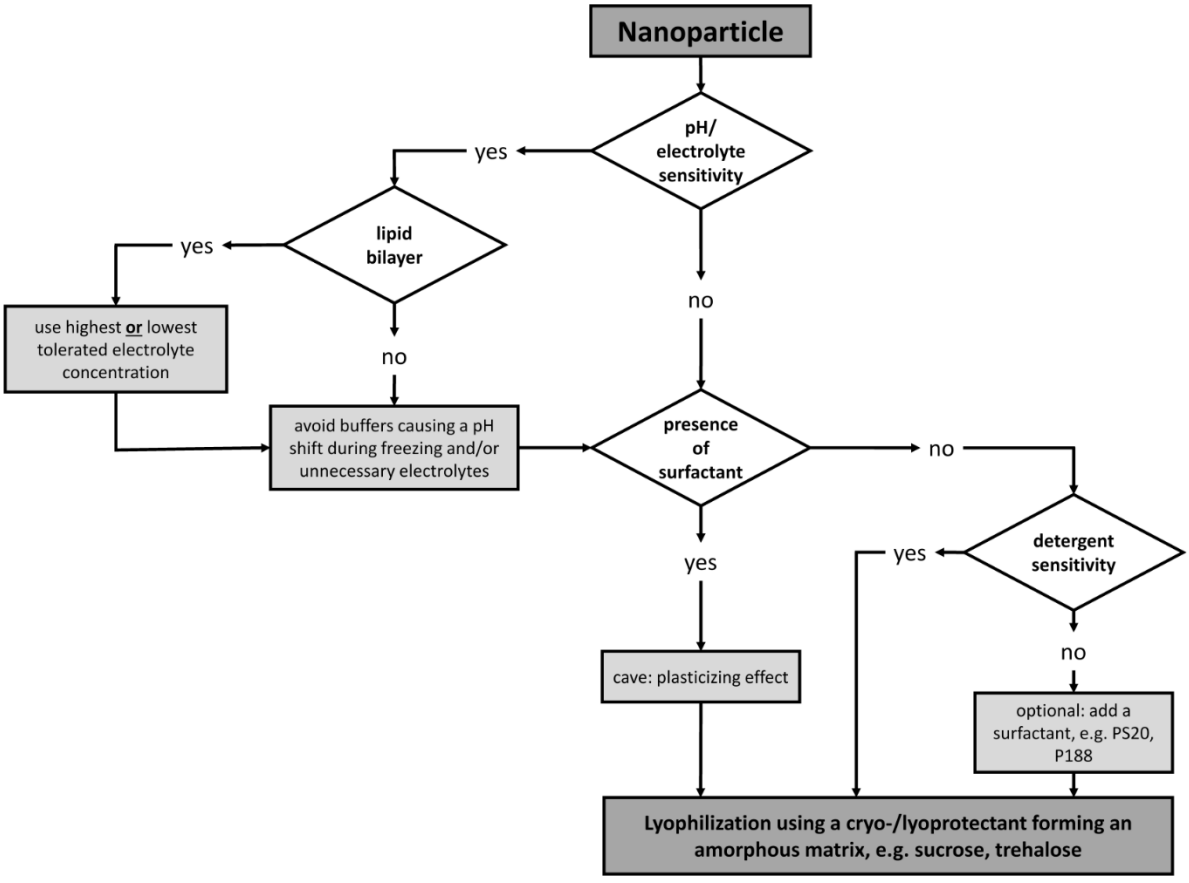

Figure 5: Suggested decision tree for the development of lyophilized NP products.

5 Conclusion

This review gives an overview of parameters affecting NP colloidal stability in the liquid state, the dried state, and during lyophilization. We further provide individual information on lyophilization of different NP types. The differentiation of NPs according to their material category brings chaos to order and allows to derive general rules; e.g. embedding NP in an amorphous matrix better stabilizes NPs compared to a crystalline matrix. The selection of appropriate excipients before freeze-drying is of vital importance as formulations factors are expected to play a key role for stabilization. Therefore, we provided practical advices concerning formulation and process development.

6 References

[1] D. Bobo, K.J. Robinson, J. Islam, K.J. Thurecht, S.R. Corrie, Nanoparticle-Based Medicines: A Review of FDA-Approved Materials and Clinical Trials to Date, Pharm. Res. 33 (2016) 2373–2387.

[2] W. Wang, Lyophilization and development of solid protein pharmaceuticals, Int. J. Pharm. 203 (2000) 1–60.

[3] L. Wu, J. Zhang, W. Watanabe, Physical and chemical stability of drug nanoparticles, Adv. Drug Deliv. Rev. 63 (2011) 456–469.

[4] X. Tang, M.J. Pikal, Design of freeze-drying processes for pharmaceuticals: practical advice, Pharm. Res. 21 (2004) 191–200.

[5] L.J.J. Hansen, R. Daoussi, C. Vervaet, J.-P. Remon, T.R.M. de Beer, Freeze-drying of live virus vaccines: A review, Vaccine 33 (2015) 5507–5519.

[6] P. Fonte, S. Reis, B. Sarmento, Facts and evidences on the lyophilization of polymeric nanoparticles for drug delivery, J. Control. Release 225 (2016) 75–86.

[7] K. Park, Prevention of nanoparticle aggregation during freeze-drying, J. Control. Release 248 (2017) 153.

[8] W. de Jong, J. Bridges, K. Dawson, T. Jung, A. Proykova, Scientific Basis for the Definition of the Term “nanomaterial”, European Commission, Brussels, 2010. pp. 1–43.

[9] Food and Drug Administration, Guidance for Industry: Considering Whether an FDA-Regulated Product Involves the Application of Nanotechnology, 2014. pp. 1–14

[10] T. Tadros, Colloid stability: The role of surface forces, Wiley-VCH, Weinheim, 2007. pp. 1–22.

[11] A.R. Studart, E. Amstad, L.J. Gauckler, Colloidal stabilization of nanoparticles in concentrated suspensions, Langmuir 23 (2007) 1081–1090.

[12] X. Zhang, M.R. Servos, J. Liu, Ultrahigh nanoparticle stability against salt, pH, and solvent with retained surface accessibility via depletion stabilization, J. Am. Chem. Soc. 134 (2012) 9910–9913.

[13] D. Napper, Steric stabilization, J. Colloid Interface Sci. 58 (1977) 390–407.

[14] R.I. Feigin, D.H. Napper, Depletion stabilization and depletion flocculation, J. Colloid Interface Sci. 75 (1980) 525–541.

[15] S. Kim, K. Hyun, J.Y. Moon, C. Clasen, K.H. Ahn, Depletion stabilization in nanoparticle-polymer suspensions: multi-length-scale analysis of microstructure, Langmuir 31 (2015) 1892–1900.

[16] A.N. Semenov, A.A. Shvets, Theory of colloid depletion stabilization by unattached and adsorbed polymers, Soft Matter 11 (2015) 8863–8878.

[17] H. Talsma, M.J. van Steenbergen, D. Crommelin, The cryopreservation of liposomes: 3. Almost complete retention of a water-soluble marker in small liposomes in a cryoprotectant containing dispersion after a freezing/thawing cycle, Int. J. Pharm. 77 (1991) 119–126.

[18] J. Kristiansen, Leakage of a trapped fluorescent marker from liposomes: Effects of eutectic crystallization of NaCl and internal freezing, Cryobiology 29 (1992) 575–584.

[19] M. Kobayashi, K. Nemoto, G. Tanaka, M. Hishida, Study of the Freezing Behavior of Liposomes, J. Therm. Sci. Technol. 6 (2011) 57–68.

[20] Z. Shen, H. Ye, M. Kröger, Y. Li, Self-assembled core-polyethylene glycol-lipid shell nanoparticles demonstrate high stability in shear flow, Phys. Chem. Chem. Phys. 19 (2017) 13294–13306.

[21] J.C. Kasper, W. Friess, The freezing step in lyophilization: physico-chemical fundamentals, freezing methods and consequences on process performance and quality attributes of biopharmaceuticals, Eur. J. Pharm. Biopharm. 78 (2011) 248–263.

[22] B.S. Chang, B.S. Kendrick, J.F. Carpenter, Surface-induced denaturation of proteins during freezing and its inhibition by surfactants, J. Pharm. Sci. 85 (1996) 1325–1330.

[23] L. Krielgaard, L.S. Jones, T.W. Randolph, S. Frokjaer, J.M. Flink, M.C. Manning, J.F. Carpenter, Effect of tween 20 on freeze-thawing- and agitation-induced aggregation of recombinant human factor XIII, J. Pharm. Sci. 87 (1998) 1597–1603.

[24] L. Shi, G. Sanyal, A. Ni, Z. Luo, S. Doshna, B. Wang, T.L. Graham, N. Wang, D.B. Volkin, Stabilization of human papillomavirus virus-like particles by non-ionic surfactants, J. Pharm. Sci. 94 (2005) 1538–1551.

[25] T.W. Randolph, Phase separation of excipients during lyophilization: effects on protein stability, J. Pharm. Sci. 86 (1997) 1198–1203.

[26] S. Bhattacharjee, DLS and zeta potential - What they are and what they are not?, J. Control. Release 235 (2016) 337–351.

[27] K. Muldrew, L.E. McGann, The osmotic rupture hypothesis of intracellular freezing injury, Biophys. J. 66 (1994) 532–541.

[28] E. Nagamachi, Y. Hirai, K. Tomochika, Y. Kanemasa, Studies on osmotic stability of liposomes prepared with bacterial membrane lipids by carboxyfluorescein release, Microbiol. Immunol. 36 (1992) 231–234.

[29] J. de Gier, Osmotic behaviour and permeability properties of liposomes, Chem. Phys. Lipids 64 (1993) 187–196.

[30] Z. Varga, A. Wacha, A. Bóta, Osmotic shrinkage of sterically stabilized liposomes as revealed by time-resolved small-angle X-ray scattering, J. Appl. Crystallogr. 47 (2014) 35–40.

[31] P. Wessman, K. Edwards, D. Mahlin, Structural effects caused by spray- and freeze-drying of liposomes and bilayer disks, J. Pharm. Sci. 99 (2010) 2032–2048.

[32] I.Y. Wu, N. Škalko-Basnet, M.P. Di Cagno, Influence of the environmental tonicity perturbations on the release of model compounds from large unilamellar vesicles (LUVs): A mechanistic investigation, Colloids Surf. B 157 (2017) 65–71.

[33] K.A. Pikal-Cleland, J.L. Cleland, T.J. Anchordoquy, J.F. Carpenter, Effect of glycine on pH changes and protein stability during freeze-thawing in phosphate buffer systems, J. Pharm. Sci. 91 (2002) 1969–1979.

[34] K.A. Pikal-Cleland, N. Rodríguez-Hornedo, G.L. Amidon, J.F. Carpenter, Protein denaturation during freezing and thawing in phosphate buffer systems: monomeric and tetrameric beta-galactosidase, Arch. Biochem. Biophys. 384 (2000) 398–406.

[35] P. Kolhe, E. Amend, S.K. Singh, Impact of freezing on pH of buffered solutions and consequences for monoclonal antibody aggregation, Biotechnol. Prog. 26 (2010) 727–733.

[36] M.S. Salnikova, H. Davis, C. Mensch, L. Celano, D.S. Thiriot, Influence of formulation pH and suspension state on freezing-induced agglomeration of aluminum adjuvants, J. Pharm. Sci. 101 (2012) 1050–1062.

[37] N. Murase, F. Franks, Salt precipitation during the freeze-concentration of phosphate buffer solutions, Biophys. Chem. 34 (1989) 293–300.

[38] E.Y. Shalaev, T.D. Johnson-Elton, L. Chang, M.J. Pikal, Thermophysical properties of pharmaceutically compatible buffers at sub-zero temperatures: implications for freeze-drying, Pharm. Res. 19 (2002) 195–201.

[39] P. Sundaramurthi, R. Suryanarayanan, The effect of crystallizing and non-crystallizing cosolutes on succinate buffer crystallization and the consequent pH shift in frozen solutions, Pharm. Res. 28 (2011) 374–385.

[40] L. van den Berg, D. Rose, Effect of freezing on the pH and composition of sodium and potassium phosphate solutions: the reciprocal system KH2PO4 · Na2HPO4 · H2O, Arch. Biochem. Biophys. 81 (1959) 319–329.

[41] B.S. Bhatnagar, R.H. Bogner, M.J. Pikal, Protein stability during freezing: separation of stresses and mechanisms of protein stabilization, Pharm. Dev. Technol. 12 (2007) 505–523.

[42] M.C. Heller, J.F. Carpenter, T.W. Randolph, Protein formulation and lyophilization cycle design: Prevention of damage due to freeze-concentration induced phase separation, Biotechnol. Bioeng. 63 (1999) 166–174.

[43] L.L. Chang, D. Shepherd, J. Sun, D. Ouellette, K.L. Grant, X.C. Tang, M.J. Pikal, Mechanism of protein stabilization by sugars during freeze-drying and storage: native structure preservation, specific interaction, and/or immobilization in a glassy matrix?, J. Pharm. Sci. 94 (2005) 1427–1444.

[44] M.T. Cicerone, M.J. Pikal, K.K. Qian, Stabilization of proteins in solid form, Adv. Drug. Deliv. Rev. 93 (2015) 14–24.

[45] J.F. Carpenter, J.H. Crowe, An infrared spectroscopic study of the interactions of carbohydrates with dried proteins, Biochemistry 28 (1989) 3916–3922.

[46] N. Grasmeijer, M. Stankovic, H. de Waard, H.W. Frijlink, W.L.J. Hinrichs, Unraveling protein stabilization mechanisms: vitrification and water replacement in a glass transition temperature controlled system, Biochim. Biophys. Acta Proteins Proteomics. 1834 (2013) 763–769.

[47] J. Beirowski, S. Inghelbrecht, A. Arien, H. Gieseler, Freeze-drying of nanosuspensions, 1: freezing rate versus formulation design as critical factors to preserve the original particle size distribution, J. Pharm. Sci. 100 (2011) 1958–1968.

[48] R. Cavalli, Sterilization and freeze-drying of drug-free and drug-loaded solid lipid nanoparticles, Int. J. Pharm. 148 (1997) 47–54.

[49] C. Schwarz, W. Mehnert, Freeze-drying of drug-free and drug-loaded solid lipid nanoparticles (SLN), Int. J. Pharm. 157 (1997) 171–179.

[50] L.M. Crowe, J.H. Crowe, Trehalose and dry dipalmitoylphosphatidylcholine revisited, Biochim. Biophys. Acta Biomembr. 946 (1988) 193–201.

[51] J.H. Crowe, F.A. Hoekstra, K.H. Nguyen, L.M. Crowe, Is vitrification involved in depression of the phase transition temperature in dry phospholipids?, Biochim. Biophys. Acta Biomembr. 1280 (1996) 187–196.

[52] C.S. Pereira, R.D. Lins, I. Chandrasekhar, L.C.G. Freitas, P.H. Hünenberger, Interaction of the Disaccharide Trehalose with a Phospholipid Bilayer: A Molecular Dynamics Study, Biophys. J. 86 (2004) 2273–2285.

[53] L.M. Crowe, J.H. Crowe, A. Rudolph, C. Womersley, L. Appel, Preservation of freeze-dried liposomes by trehalose, Arch. Biochem. Biophys. 242 (1985) 240–247.

[54] R.D. Jangle, B.N. Thorat, Effect of Freeze-Thawing Study on Curcumin Liposome for Obtaining Better Freeze-Dried Product, Dry. Technol. 31 (2013) 966–974.

[55] C. Chen, D. Han, C. Cai, X. Tang, An overview of liposome lyophilization and its future potential, J. Control. Release 142 (2010) 299–311.

[56] M.A. Mensink, H.W. Frijlink, K. van der Voort Maarschalk, W.L.J. Hinrichs, How sugars protect proteins in the solid state and during drying (review): Mechanisms of stabilization in relation to stress conditions, Eur. J. Pharm. Biopharm. 114 (2017) 288–295.

[57] W.Q. Sun, A.C. Leopold, L.M. Crowe, J.H. Crowe, Stability of dry liposomes in sugar glasses, Biophys. J. 70 (1996) 1769–1776.

[58] J.H. Crowe, S.B. Leslie, L.M. Crowe, Is vitrification sufficient to preserve liposomes during freeze-drying?, Cryobiology 31 (1994) 355–366.

[59] A.E. Oliver, O. Leprince, W.F. Wolkers, D.K. Hincha, A.G. Heyer, J.H. Crowe, Non-disaccharide-based mechanisms of protection during drying, Cryobiology 43 (2001) 151–167.

[60] V. Gervasi, R. Dall Agnol, S. Cullen, T. McCoy, S. Vucen, A. Crean, Parenteral protein formulations: An overview of approved products within the European Union, Eur. J. Pharm. Biopharm. 131 (2018) 8–24.

[61] M. Bjelošević, A. Zvonar Pobirk, O. Planinšek, P. Ahlin Grabnar, Excipients in freeze-dried biopharmaceuticals: Contributions toward formulation stability and lyophilisation cycle optimisation, Int. J. Pharm. 576 (2020) 119029.

[62] B.M. Rayaprolu, J.J. Strawser, G. Anyarambhatla, Excipients in parenteral formulations: selection considerations and effective utilization with small molecules and biologics, Drug Dev. Ind. Pharm. 44 (2018) 1565–1571.

[63] K. Göke, T. Lorenz, A. Repanas, F. Schneider, D. Steiner, K. Baumann, H. Bunjes, A. Dietzel, J.H. Finke, B. Glasmacher, A. Kwade, Novel strategies for the formulation and processing of poorly water-soluble drugs, Eur. J. Pharm. Biopharm. 126 (2018) 40–56.

[64] J.P. Möschwitzer, Drug nanocrystals in the commercial pharmaceutical development process, Int. J. Pharm. 453 (2013) 142–156.

[65] J. Lee, Y. Cheng, Critical freezing rate in freeze drying nanocrystal dispersions, J. Control. Release 111 (2006) 185–192.

[66] M.K. Lee, M.Y. Kim, S. Kim, J. Lee, Cryoprotectants for freeze drying of drug nano-suspensions: effect of freezing rate, J. Pharm. Sci. 98 (2009) 4808–4817.

[67] S. Kumar, R. Gokhale, D.J. Burgess, Sugars as bulking agents to prevent nano-crystal aggregation during spray or freeze-drying, Int. J. Pharm. 471 (2014) 303–311.

[68] J. Beirowski, S. Inghelbrecht, A. Arien, H. Gieseler, Freeze drying of nanosuspensions, 2: the role of the critical formulation temperature on stability of drug nanosuspensions and its practical implication on process design, J. Pharm. Sci. 100 (2011) 4471–4481.

[69] L. Wang, Y. Ma, Y. Gu, Y. Liu, J. Zhao, B. Yan, Y. Wang, Cryoprotectant choice and analyses of freeze-drying drug suspension of nanoparticles with functional stabilisers, J. Microencapsul. 35 (2018) 241–248.

[70] N.-O. Chung, M.K. Lee, J. Lee, Mechanism of freeze-drying drug nanosuspensions, Int. J. Pharm. 437 (2012) 42–50.

[71] S. Kim, J. Lee, Effective polymeric dispersants for vacuum, convection and freeze drying of drug nanosuspensions, Int. J. Pharm. 397 (2010) 218–224.

[72] J. Beirowski, S. Inghelbrecht, A. Arien, H. Gieseler, Freeze-drying of nanosuspensions, part 3: investigation of factors compromising storage stability of highly concentrated drug nanosuspensions, J. Pharm. Sci. 101 (2012) 354–362.

[73] A. Gordillo-Galeano, C.E. Mora-Huertas, Solid lipid nanoparticles and nanostructured lipid carriers: A review emphasizing on particle structure and drug release, Eur. J. Pharm. Biopharm. 133 (2018) 285–308.

[74] W. Mehnert, K. Mäder, Solid lipid nanoparticles, Adv. Drug. Deliv. Rev. 64 (2012) 83–101.

[75] N. Kathe, B. Henriksen, H. Chauhan, Physicochemical characterization techniques for solid lipid nanoparticles: principles and limitations, Drug Dev. Ind. Pharm. 40 (2014) 1565–1575.

[76] A. del Pozo-Rodríguez, M.A. Solinís, A.R. Gascón, J.L. Pedraz, Short- and long-term stability study of lyophilized solid lipid nanoparticles for gene therapy, Eur. J. Pharm. Biopharm. 71 (2009) 181–189.

[77] S. Weber, A. Zimmer, J. Pardeike, Solid Lipid Nanoparticles (SLN) and Nanostructured Lipid Carriers (NLC) for pulmonary application: a review of the state of the art, Eur. J. Pharm. Biopharm. 86 (2014) 7–22.

[78] S. Das, W.K. Ng, R.B.H. Tan, Are nanostructured lipid carriers (NLCs) better than solid lipid nanoparticles (SLNs): development, characterizations and comparative evaluations of clotrimazole-loaded SLNs and NLCs?, Eur. J. Pharm. Sci. 47 (2012) 139–151.

[79] H. Heiati, R. Tawashi, N.C. Phillips, Drug retention and stability of solid lipid nanoparticles containing azidothymidine palmitate after autoclaving, storage and lyophilization, J. Microencapsul. 15 (1998) 173–184.

[80] T.M. Amis, J. Renukuntla, P.K. Bolla, B.A. Clark, Selection of Cryoprotectant in Lyophilization of Progesterone-Loaded Stearic Acid Solid Lipid Nanoparticles, Pharmaceutics 12 (2020).

[81] S. Doktorovova, R. Shegokar, L. Fernandes, P. Martins-Lopes, A.M. Silva, R.H. Müller, E.B. Souto, Trehalose is not a universal solution for solid lipid nanoparticles freeze-drying, Pharm. Dev. Technol. 19 (2014) 922–929.

[82] H. Ohshima, A. Miyagishima, T. Kurita, Y. Makino, Y. Iwao, T. Sonobe, S. Itai, Freeze-dried nifedipine-lipid nanoparticles with long-term nano-dispersion stability after reconstitution, Int. J. Pharm. 377 (2009) 180–184.

[83] W. Tiyaboonchai, W. Tungpradit, P. Plianbangchang, Formulation and characterization of curcuminoids loaded solid lipid nanoparticles, Int. J. Pharm. 337 (2007) 299–306.

[84] E. Vighi, B. Ruozi, M. Montanari, R. Battini, E. Leo, Re-dispersible cationic solid lipid nanoparticles (SLNs) freeze-dried without cryoprotectors: characterization and ability to bind the pEGFP-plasmid, Eur. J. Pharm. Biopharm. 67 (2007) 320–328.

[85] B. Siekmann, Westesen K., Melt-homogenized solid lipid nanoparticles stabilized by the nonionic surfactant tyloxapol, Pharm. Pharmacol. Lett (1994) 225–228.

[86] K.S. Soppimath, T.M. Aminabhavi, A.R. Kulkarni, W.E. Rudzinski, Biodegradable polymeric nanoparticles as drug delivery devices, J. Control. Release 70 (2001) 1–20.

[87] M. Holzer, V. Vogel, W. Mäntele, D. Schwartz, W. Haase, K. Langer, Physico-chemical characterisation of PLGA nanoparticles after freeze-drying and storage, Eur. J. Pharm. Biopharm. 72 (2009) 428–437.

[88] Y.-I. Jeong, Y.-H. Shim, C. Kim, G.-T. Lim, K.-C. Choi, C. Yoon, Effect of cryoprotectants on the reconstitution of surfactant-free nanoparticles of poly(DL-lactide-co-glycolide), J. Microencapsul. 22 (2005) 593–601.

[89] W. Abdelwahed, G. Degobert, H. Fessi, Investigation of nanocapsules stabilization by amorphous excipients during freeze-drying and storage, Eur. J. Pharm. Biopharm. 63 (2006) 87–94.

[90] W.S. Cheow, M.L.L. Ng, K. Kho, K. Hadinoto, Spray-freeze-drying production of thermally sensitive polymeric nanoparticle aggregates for inhaled drug delivery: effect of freeze-drying adjuvants, Int. J. Pharm. 404 (2011) 289–300.

[91] T. Zelenková, D. Fissore, D.L. Marchisio, A.A. Barresi, Size control in production and freeze-drying of poly-ε-caprolactone nanoparticles, J. Pharm. Sci. 103 (2014) 1839–1850.

[92] D. Quintanar-Guerrero, A. Ganem-Quintanar, E. Allémann, H. Fessi, E. Doelker, Influence of the stabilizer coating layer on the purification and freeze-drying of poly(D,L-lactic acid) nanoparticles prepared by an emulsion-diffusion technique, J. Microencapsul. 15 (1998) 107–119.

[93] S. Hirsjärvi, L. Peltonen, J. Hirvonen, Effect of sugars, surfactant, and tangential flow filtration on the freeze-drying of poly(lactic acid) nanoparticles, AAPS PharmSciTech 10 (2009) 488–494.

[94] P. Fonte, F. Araújo, V. Seabra, S. Reis, M. van de Weert, B. Sarmento, Co-encapsulation of lyoprotectants improves the stability of protein-loaded PLGA nanoparticles upon lyophilization, Int. J. Pharm. 496 (2015) 850–862.

[95] A. Saez, M. Guzmán, J. Molpeceres, M. Aberturas, Freeze-drying of polycaprolactone and poly(d,l -lactic-glycolic) nanoparticles induce minor particle size changes affecting the oral pharmacokinetics of loaded drugs, Eur. J. Pharm. Biopharm. 50 (2000) 379–387.

[96] W. Abdelwahed, G. Degobert, H. Fessi, A pilot study of freeze drying of poly(epsilon-caprolactone) nanocapsules stabilized by poly(vinyl alcohol): formulation and process optimization, Int. J. Pharm. 309 (2006) 178–188.

[97] J. Wendorf, M. Singh, J. Chesko, J. Kazzaz, E. Soewanan, M. Ugozzoli, D. O'Hagan, A practical approach to the use of nanoparticles for vaccine delivery, J. Pharm. Sci. 95 (2006) 2738–2750.

[98] S. de Chasteigner, G. Cav, H. Fessi, J.-P. Devissaguet, F. Puisieux, Freeze-drying of itraconazole-loaded nanosphere suspensions: a feasibility study, Drug Dev. Res. 38 (1996) 116–124.

[99] S. Hirsjärvi, L. Peltonen, L. Kainu, J. Hirvonen, Freeze-drying of low molecular weight poly(L-lactic acid) nanoparticles: effect of cryo- and lyoprotectants, J. Nanosci. Nanotechnol. 6 (2006) 3110–3117.

[100] F. de Jaeghere, E. Allémann, J. Feijen, T. Kissel, E. Doelker, R. Gurny, Freeze-drying and lyopreservation of diblock and triblock poly(lactic acid)-poly(ethylene oxide) (PLA-PEO) copolymer nanoparticles, Pharm. Dev. Technol. 5 (2000) 473–483.

[101] F. de Jaeghere, E. Allémann, J.C. Leroux, W. Stevels, J. Feijen, E. Doelker, R. Gurny, Formulation and lyoprotection of poly(lactic acid-co-ethylene oxide) nanoparticles: influence on physical stability and in vitro cell uptake, Pharm. Res. 16 (1999) 859–866.

[102] P. Fonte, S. Soares, A. Costa, J.C. Andrade, V. Seabra, S. Reis, B. Sarmento, Effect of cryoprotectants on the porosity and stability of insulin-loaded PLGA nanoparticles after freeze-drying, Biomatter 2 (2012) 329–339.

[103] W. Abdelwahed, G. Degobert, H. Fessi, Freeze-drying of nanocapsules: impact of annealing on the drying process, Int. J. Pharm. 324 (2006) 74–82.

[104] M.G. Anhorn, H.-C. Mahler, K. Langer, Freeze drying of human serum albumin (HSA) nanoparticles with different excipients, Int. J. Pharm. 363 (2008) 162–169.

[105] M. Dadparvar, S. Wagner, S. Wien, F. Worek, H. von Briesen, J. Kreuter, Freeze-drying of HI-6-loaded recombinant human serum albumin nanoparticles for improved storage stability, Eur. J. Pharm. Biopharm. 88 (2014) 510–517.

[106] M. Diop, N. Auberval, A. Viciglio, A. Langlois, W. Bietiger, C. Mura, C. Peronet, A. Bekel, D. Julien David, M. Zhao, M. Pinget, N. Jeandidier, C. Vauthier, E. Marchioni, Y. Frere, S. Sigrist, Design, characterisation, and bioefficiency of insulin-chitosan nanoparticles after stabilisation by freeze-drying or cross-linking, Int. J. Pharm. 491 (2015) 402–408.

[107] M.V. Lozano, H. Esteban, J. Brea, M.I. Loza, D. Torres, M.J. Alonso, Intracellular delivery of docetaxel using freeze-dried polysaccharide nanocapsules, J. Microencapsul. 30 (2013) 181–188.

[108] S. Eliyahu, A. Almeida, M.H. Macedo, J. das Neves, B. Sarmento, H. Bianco-Peled, The effect of freeze-drying on mucoadhesion and transport of acrylated chitosan nanoparticles, Int. J. Pharm. 573 (2020) 118739.

[109] K. Sonaje, Y.-J. Chen, H.-L. Chen, S.-P. Wey, J.-H. Juang, H.-N. Nguyen, C.-W. Hsu, K.-J. Lin, H.-W. Sung, Enteric-coated capsules filled with freeze-dried chitosan/poly(gamma-glutamic acid) nanoparticles for oral insulin delivery, Biomaterials 31 (2010) 3384–3394.

[110] J.A. Ataide, D.C. Geraldes, E.F. Gérios, F.M. Bissaco, L.C. Cefali, L. Oliveira-Nascimento, P.G. Mazzola, Freeze-dried chitosan nanoparticles to stabilize and deliver bromelain, J. Drug Deliv. Sci. Techn. 61 (2021) 102225.

[111] A. Umerska, K.J. Paluch, M.J. Santos-Martinez, O.I. Corrigan, C. Medina, L. Tajber, Freeze drying of polyelectrolyte complex nanoparticles: Effect of nanoparticle composition and cryoprotectant selection, Int. J. Pharm. 552 (2018) 27–38.

[112] J.C. Zillies, K. Zwiorek, F. Hoffmann, A. Vollmar, T.J. Anchordoquy, G. Winter, C. Coester, Formulation development of freeze-dried oligonucleotide-loaded gelatin nanoparticles, Eur. J. Pharm. Biopharm. 70 (2008) 514–521.

[113] K.J. Geh, M. Hubert, G. Winter, Progress in formulation development and sterilisation of freeze-dried oligodeoxynucleotide-loaded gelatine nanoparticles, Eur. J. Pharm. Biopharm. 129 (2018) 10–20.

[114] A. Pathak, S. Patnaik, K.C. Gupta, Recent trends in non-viral vector-mediated gene delivery, Biotechnol. J 4 (2009) 1559–1572.

[115] M. Rezaee, R.K. Oskuee, H. Nassirli, B. Malaekeh-Nikouei, Progress in the development of lipopolyplexes as efficient non-viral gene delivery systems, J. Control. Release 236 (2016) 1–14.

[116] M.A. Mintzer, E.E. Simanek, Nonviral vectors for gene delivery, Chem. Rev. 109 (2009) 259–302.

[117] T.K. Armstrong, T.J. Anchordoquy, Immobilization of nonviral vectors during the freezing step of lyophilization, J. Pharm. Sci. 93 (2004) 2698–2709.

[118] J.C. Kasper, M.J. Pikal, W. Friess, Investigations on polyplex stability during the freezing step of lyophilization using controlled ice nucleation—the importance of residence time in the low-viscosity fluid state, J. Pharm. Sci. 102 (2013) 929–946.

[119] J.C. Kasper, D. Schaffert, M. Ogris, E. Wagner, W. Friess, Development of a lyophilized plasmid/LPEI polyplex formulation with long-term stability—A step closer from promising technology to application, J. Control. Release 151 (2011) 246–255.

[120] H. Talsma, J.-Y. Cherng, H. Lehrmann, M. Kursa, M. Ogris, W.E. Hennink, M. Cotten, E. Wagner, Stabilization of gene delivery systems by freeze-drying, Int. J. Pharm. 157 (1997) 233–238.

[121] J.Y. Cherng, H. Talsma, D.J. Crommelin, W.E. Hennink, Long term stability of poly((2-dimethylamino)ethyl methacrylate)-based gene delivery systems, Pharm. Res. 16 (1999) 1417–1423.

[122] J.-Y. Cherng, P. Wetering, H. Talsma, D. Crommelin, W. Hennink, Stabilization of polymer-based gene delivery systems, Int. J. Pharm. 183 (1999) 25–28.

[123] K.Y. Kwok, R.C. Adami, K.C. Hester, Y. Park, S. Thomas, K.G. Rice, Strategies for maintaining the particle size of peptide DNA condensates following freeze-drying, Int. J. Pharm. 203 (2000) 81–88.

[124] C. Fornaguera, C. Castells-Sala, M.A. Lázaro, A. Cascante, S. Borrós, Development of an optimized freeze-drying protocol for OM-PBAE nucleic acid polyplexes, Int. J. Pharm. 569 (2019) 118612.

[125] D. Veilleux, M. Nelea, K. Biniecki, M. Lavertu, M.D. Buschmann, Preparation of Concentrated Chitosan/DNA Nanoparticle Formulations by Lyophilization for Gene Delivery at Clinically Relevant Dosages, J. Pharm. Sci. 105 (2016) 88–96.

[126] J.C. Kasper, C. Troiber, S. Küchler, E. Wagner, W. Friess, Formulation development of lyophilized, long-term stable siRNA/oligoaminoamide polyplexes, Eur. J. Pharm. Biopharm. 85 (2013) 294–305.

[127] T. Endres, M. Zheng, M. Beck-Broichsitter, T. Kissel, Lyophilised ready-to-use formulations of PEG-PCL-PEI nano-carriers for siRNA delivery, Int. J. Pharm. 428 (2012) 121–124.

[128] D. Veilleux, R.K. Gopalakrishna Panicker, A. Chevrier, K. Biniecki, M. Lavertu, M.D. Buschmann, Lyophilisation and concentration of chitosan/siRNA polyplexes: Influence of buffer composition, oligonucleotide sequence, and hyaluronic acid coating, J. Colloid Interface Sci. 512 (2018) 335–345.

[129] C. Brus, E. Kleemann, A. Aigner, F. Czubayko, T. Kissel, Stabilization of oligonucleotide-polyethylenimine complexes by freeze-drying: physicochemical and biological characterization, J. Control. Release 95 (2004) 119–131.

[130] K. Miyata, Y. Kakizawa, N. Nishiyama, Y. Yamasaki, T. Watanabe, M. Kohara, K. Kataoka, Freeze-dried formulations for in vivo gene delivery of PEGylated polyplex micelles with disulfide crosslinked cores to the liver, J. Control. Release 109 (2005) 15–23.

[131] A. Sharma, Liposomes in drug delivery: Progress and limitations, Int. J. Pharm. 154 (1997) 123–140.

[132] M.T. Mabrouk, W.-C. Huang, B. Deng, N. Li-Purcell, A. Seffouh, J. Ortega, G. Ekin Atilla-Gokcumen, C.A. Long, K. Miura, J.F. Lovell, Lyophilized, antigen-bound liposomes with reduced MPLA and enhanced thermostability, Int J Pharm 589 (2020) 119843.

[133] T.J. McIntosh, The effect of cholesterol on the structure of phosphatidylcholine bilayers, Biochim. Biophys. Acta Biomembr. 513 (1978) 43–58.

[134] J.F. Nagle, S. Tristram-Nagle, Structure of lipid bilayers, Biochim. Biophys. Acta Biomembr. 1469 (2000) 159–195.

[135] J.F. Nagle, Theory of the Main Lipid Bilayer Phase Transition, Annu. Rev. Phys. Chem. 31 (1980) 157–196.

[136] K.M. Taylor, R.M. Morris, Thermal analysis of phase transition behaviour in liposomes, Thermochim. Acta 248 (1995) 289–301.

[137] S. Mabrey, J.M. Sturtevant, Investigation of phase transitions of lipids and lipid mixtures by sensitivity differential scanning calorimetry, Proc. Natl. Acad. Sci. U.S.A. 73 (1976) 3862–3866.

[138] F. Susa, G. Bucca, T. Limongi, V. Cauda, R. Pisano, Enhancing the preservation of liposomes: The role of cryoprotectants, lipid formulations and freezing approaches, Cryobiology 98 (2021) 46–56.

[139] L.M. Hays, J.H. Crowe, W. Wolkers, S. Rudenko, Factors affecting leakage of trapped solutes from phospholipid vesicles during thermotropic phase transitions, Cryobiology 42 (2001) 88–102.

[140] J.H. Crowe, L.M. Crowe, F.A. Hoekstra, Phase transitions and permeability changes in dry membranes during rehydration, J. Bioenerg. Biomembr. 21 (1989) 77–91.

[141] B. Maherani, E. Arab-Tehrany, M. R. Mozafari, C. Gaiani, M. Linder, Liposomes: A Review of Manufacturing Techniques and Targeting Strategies, Curr. Nanosci. 7 (2011) 436–452.

[142] K.L. Koster, M.S. Webb, G. Bryant, D.V. Lynch, Interactions between soluble sugars and POPC (1-palmitoyl-2-oleoylphosphatidylcholine) during dehydration: vitrification of sugars alters the phase behavior of the phospholipid, Biochim. Biophys. Acta Biomembr. 1193 (1994) 143–150.

[143] K.L. Koster, Y.P. Lei, M. Anderson, S. Martin, G. Bryant, Effects of Vitrified and Nonvitrified Sugars on Phosphatidylcholine Fluid-to-Gel Phase Transitions, Biophys. J. 78 (2000) 1932–1946.

[144] C. Cacela, D.K. Hincha, Low amounts of sucrose are sufficient to depress the phase transition temperature of dry phosphatidylcholine, but not for lyoprotection of liposomes, Biophys. J. 90 (2006) 2831–2842.

[145] J.H. Crowe, L.M. Crowe, A.E. Oliver, N. Tsvetkova, W. Wolkers, F. Tablin, The trehalose myth revisited: introduction to a symposium on stabilization of cells in the dry state, Cryobiology 43 (2001) 89–105.

[146] S. Ohtake, C. Schebor, S.P. Palecek, J.J. de Pablo, Phase behavior of freeze-dried phospholipid-cholesterol mixtures stabilized with trehalose, Biochim. Biophys. Acta Biomembr. 1713 (2005) 57–64.

[147] E.C. van Winden, D.J. Crommelin, Short term stability of freeze-dried, lyoprotected liposomes, J. Control. Release 58 (1999) 69–86. https://doi.org/10.1016/S0168-3659(98)00130-8.

[148] W. Shinoda, Permeability across lipid membranes, Biochim. Biophys. Acta Biomembr. 1858 (2016) 2254–2265. https://doi.org/10.1016/j.bbamem.2016.03.032.

[149] A.V. Popova, D.K. Hincha, Effects of cholesterol on dry bilayers: interactions between phosphatidylcholine unsaturation and glycolipid or free sugar, Biophys. J. 93 (2007) 1204–1214. https://doi.org/10.1529/biophysj.107.108886.

[150] M. Gulati, M. Grover, S. Singh, M. Singh, Lipophilic drug derivatives in liposomes, Int. J. Pharm. 165 (1998) 129–168. https://doi.org/10.1016/S0378-5173(98)00006-4.

[151] D. Guimarães, J. Noro, C. Silva, A. Cavaco-Paulo, E. Nogueira, Protective Effect of Saccharides on Freeze-Dried Liposomes Encapsulating Drugs, Front. Bioeng. Biotechnol. 7 (2019) 424. https://doi.org/10.3389/fbioe.2019.00424.

[152] E.C. van Winden, Freeze-Drying of Liposomes: Theory and Practice, Methods Enzymol. 367 (2003) 99–110. https://doi.org/10.1016/S0076-6879(03)67008-4.

[153] J.H. Crowe, L.M. Crowe, Factors affecting the stability of dry liposomes, Biochim. Biophys. Acta Biomembr. 939 (1988) 327–334. https://doi.org/10.1016/0005-2736(88)90077-6.

[154] M. Glavas-Dodov, E. Fredro-Kumbaradzi, K. Goracinova, M. Simonoska, S. Calis, S. Trajkovic-Jolevska, A.A. Hincal, The effects of lyophilization on the stability of liposomes containing 5-FU, Int. J. Pharm. 291 (2005) 79–86. https://doi.org/10.1016/j.ijpharm.2004.07.045.

[155] J.H. Crowe, A.E. Oliver, F.A. Hoekstra, L.M. Crowe, Stabilization of dry membranes by mixtures of hydroxyethyl starch and glucose: the role of vitrification, Cryobiology 35 (1997) 20–30. https://doi.org/10.1006/cryo.1997.2020.

[156] S. Franzè, F. Selmin, P. Rocco, G. Colombo, A. Casiraghi, F. Cilurzo, Preserving the Integrity of Liposomes Prepared by Ethanol Injection upon Freeze-Drying: Insights from Combined Molecular Dynamics Simulations and Experimental Data, Pharmaceutics 12 (2020). https://doi.org/10.3390/pharmaceutics12060530.

[157] P. Sundaramurthi, R. Suryanarayanan, Trehalose Crystallization During Freeze-Drying: Implications On Lyoprotection, J. Phys. Chem. Lett. 1 (2010) 510–514. https://doi.org/10.1021/jz900338m.

[158] S.K. Singh, P. Kolhe, A.P. Mehta, S.C. Chico, A.L. Lary, M. Huang, Frozen state storage instability of a monoclonal antibody: aggregation as a consequence of trehalose crystallization and protein unfolding, Pharm. Res. 28 (2011) 873–885. https://doi.org/10.1007/s11095-010-0343-z.

[159] A.V. Popova, A.G. Heyer, D.K. Hincha, Differential destabilization of membranes by tryptophan and phenylalanine during freezing: the roles of lipid composition and membrane fusion, Biochim. Biophys. Acta Biomembr. 1561 (2002) 109–118. https://doi.org/10.1016/S0005-2736(01)00462-X.

[160] A.V. Popova, D.K. Hincha, Specific interactions of tryptophan with phosphatidylcholine and digalactosyldiacylglycerol in pure and mixed bilayers in the dry and hydrated state, Chem. Phys. Lipids 132 (2004) 171–184. https://doi.org/10.1016/j.chemphyslip.2004.06.003.

[161] A.R. Mohammed, A.G.A. Coombes, Y. Perrie, Amino acids as cryoprotectants for liposomal delivery systems, Eur. J. Pharm. Sci 30 (2007) 406–413. https://doi.org/10.1016/j.ejps.2007.01.001.

[162] M. Mattern, G. Winter, U. Kohnert, G. Lee, Formulation of proteins in vacuum-dried glasses. II. Process and storage stability in sugar-free amino acid systems, Pharm. Dev. Technol. 4 (1999) 199–208. https://doi.org/10.1081/pdt-100101354.

[163] Y. Wu, Efficacy of antifreeze protein types in protecting liposome membrane integrity depends on phospholipid class, Biochim. Biophys. Acta Gen. Subj. 1524 (2000) 11–16. https://doi.org/10.1016/s0304-4165(00)00134-3.

[164] Y. Wu, J. Banoub, S.V. Goddard, M.H. Kao, G.L. Fletcher, Antifreeze glycoproteins: relationship between molecular weight, thermal hysteresis and the inhibition of leakage from liposomes during thermotropic phase transition, Comp. Biochem. Physiol. B Biochem. Mol. Biol. 128 (2001) 265–273. https://doi.org/10.1016/s1096-4959(00)00323-7.

[165] D.K. Hincha, A.E. Oliver, J.H. Crowe, Lipid Composition Determines the Effects of Arbutin on the Stability of Membranes, Biophys. J. 77 (1999) 2024–2034.

[166] A.V. Popova, D.K. Hincha, Interactions of the amphiphiles arbutin and tryptophan with phosphatidylcholine and phosphatidylethanolamine bilayers in the dry state, BMC Biophys. 6 (2013) 9.

[167] M.T. Hussain, N. Forbes, Y. Perrie, K.P. Malik, C. Duru, P. Matejtschuk, Freeze-drying cycle optimization for the rapid preservation of protein-loaded liposomal formulations, Int. J. Pharm. 573 (2020) 118722.

[168] C. Zingel, A. Sachse, G.L. Röβling, R.H. Müller, Lyophilization and rehydration of iopromide-carrying liposomes, Int. J. Pharm. 140 (1996) 13–24.

[169] J. Gao, J. Sun, H. Li, W. Liu, Y. Zhang, B. Li, W. Qian, H. Wang, J. Chen, Y. Guo, Lyophilized HER2-specific PEGylated immunoliposomes for active siRNA gene silencing, Biomaterials 31 (2010) 2655–2664.

[170] D. Peer, E.J. Park, Y. Morishita, C.V. Carman, M. Shimaoka, Systemic leukocyte-directed siRNA delivery revealing cyclin D1 as an anti-inflammatory target, Science 319 (2008) 627–630.

[171] S. Ohtake, C. Schebor, J.J. de Pablo, Effects of trehalose on the phase behavior of DPPC-cholesterol unilamellar vesicles, Biochim. Biophys. Acta Biomembr. 1758 (2006) 65–73.

[172] K. Izutsu, C. Yomota, T. Kawanishi, Stabilization of liposomes in frozen solutions through control of osmotic flow and internal solution freezing by trehalose, J. Pharm. Sci. 100 (2011) 2935–2944.

[173] E.C. van Winden, W. Zhang, D.J. Crommelin, Effect of freezing rate on the stability of liposomes during freeze-drying and rehydration, Pharm. Res. 14 (1997) 1151–1160.

[174] C. Tros de Ilarduya, Y. Sun, N. Düzgüneş, Gene delivery by lipoplexes and polyplexes, Eur. J. Pharm. Sci. 40 (2010) 159–170.

[175] M.C. Molina, S.D. Allison, T.J. Anchordoquy, Maintenance of nonviral vector particle size during the freezing step of the lyophilization process is insufficient for preservation of activity: insight from other structural indicators, J. Pharm. Sci. 90 (2001) 1445–1455.

[176] P. Yadava, M. Gibbs, C. Castro, J.A. Hughes, Effect of lyophilization and freeze-thawing on the stability of siRNA-liposome complexes, AAPS PharmSciTech 9 (2008) 335–341.

[177] M. Tang, S. Hu, Y. Hattori, Effect of pre-freezing and saccharide types in freeze-drying of siRNA lipoplexes on gene-silencing effects in the cells by reverse transfection, Mol. Med. Rep. 22 (2020) 3233–3244.

[178] T.J. Anchordoquy, J.F. Carpenter, D.J. Kroll, Maintenance of transfection rates and physical characterization of lipid/DNA complexes after freeze-drying and rehydration, Arch. Biochem. Biophys. 348 (1997) 199–206.

[179] S. Allison, M.d. Molina, T.J. Anchordoquy, Stabilization of lipid/DNA complexes during the freezing step of the lyophilization process: the particle isolation hypothesis, Biochim. Biophys. Acta Biomembr. 1468 (2000) 127–138.

[180] S.D. Allison, T.J. Anchordoquy, Mechanisms of Protection of Cationic Lipid-DNA Complexes During Lyophilization, J. Pharm. Sci. 89 (2000) 682–691.

[181] Y. Aso, S. Yoshioka, Effect of freezing rate on physical stability of lyophilized cationic liposomes, Chem. Pharm. Bull. 53 (2005) 301–304.

[182] T. Furst, G.R. Dakwar, E. Zagato, A. Lechanteur, K. Remaut, B. Evrard, K. Braeckmans, G. Piel, Freeze-dried mucoadhesive polymeric system containing pegylated lipoplexes: Towards a vaginal sustained released system for siRNA, J. Control. Release 236 (2016) 68–78.

[183] B. Li, S. Li, Y. Tan, D.B. Stolz, S.C. Watkins, L.H. Block, L. Huang, Lyophilization of Cationic Lipid–protamine–DNA (LPD) Complexes, J. Pharm. Sci. 89 (2000) 355–364.

[184] M.d.C. Molina, T.K. Armstrong, Y. Zhang, M.M. Patel, Y.K. Lentz, T.J. Anchordoquy, The stability of lyophilized lipid/DNA complexes during prolonged storage, J. Pharm. Sci. 93 (2004) 2259–2273.

[185] J. Yu, T.J. Anchordoquy, Synergistic effects of surfactants and sugars on lipoplex stability during freeze-drying and rehydration, J. Pharm. Sci. 98 (2009) 3319–3328.

[186] Y. Hattori, S. Hu, H. Onishi, Effects of cationic lipids in cationic liposomes and disaccharides in the freeze-drying of siRNA lipoplexes on gene silencing in cells by reverse transfection, J. Liposome Res. (2019) 1–11.

[187] M.d.C. Molina, T.J. Anchordoquy, Metal contaminants promote degradation of lipid/DNA complexes during lyophilization, Biochim. Biophys. Acta Biomembr. 1768 (2007) 669–677.

[188] T.K.C. Armstrong, L.G. Girouard, T.J. Anchordoquy, Effects of PEGylation on the preservation of cationic lipid/DNA complexes during freeze-thawing and lyophilization, J. Pharm. Sci. 91 (2002) 2549–2558.

[189] M.d.C. Molina, T.J. Anchordoquy, Degradation of lyophilized lipid/DNA complexes during storage: the role of lipid and reactive oxygen species, Biochim. Biophys. Acta Biomembr. 1778 (2008) 2119–2126.

[190] M.d.C. Molina, T.J. Anchordoquy, Formulation strategies to minimize oxidative damage in lyophilized lipid/DNA complexes during storage, J. Pharm. Sci. 97 (2008) 5089–5105.

[191] J. Yu, T.J. Anchordoquy, Effects of moisture content on the storage stability of dried lipoplex formulations, J. Pharm. Sci. 98 (2009) 3278–3289.

[192] N. Khatri, D. Baradia, I. Vhora, M. Rathi, A. Misra, Development and characterization of siRNA lipoplexes: Effect of different lipids, in vitro evaluation in cancerous cell lines and in vivo toxicity study, AAPS PharmSciTech 15 (2014) 1630–1643.

[193] Y. Maitani, Y. Aso, A. Yamada, S. Yoshioka, Effect of sugars on storage stability of lyophilized liposome/DNA complexes with high transfection efficiency, Int. J. Pharm. 356 (2008) 69–75.

[194] W.L.J. Hinrichs, N.N. Sanders, S.C. de Smedt, J. Demeester, H.W. Frijlink, Inulin is a promising cryo- and lyoprotectant for PEGylated lipoplexes, J. Control. Release 103 (2005) 465–479.

[195] W.L.J. Hinrichs, F.A. Manceñido, N.N. Sanders, K. Braeckmans, S.C. de Smedt, J. Demeester, H.W. Frijlink, The choice of a suitable oligosaccharide to prevent aggregation of PEGylated nanoparticles during freeze thawing and freeze drying, Int. J. Pharm. 311 (2006) 237–244.

[196] H. Lee, D. Jiang, W.M. Pardridge, Lyoprotectant Optimization for the Freeze-Drying of Receptor-Targeted Trojan Horse Liposomes for Plasmid DNA Delivery, Mol. Pharm. 17 (2020) 2165–2174.

[197] S.G. Darband, M. Mirza-Aghazadeh-Attari, M. Kaviani, A. Mihanfar, S. Sadighparvar, B. Yousefi, M. Majidinia, Exosomes: natural nanoparticles as bio shuttles for RNAi delivery, J. Control. Release 289 (2018) 158–170.

[198] P. Vader, E.A. Mol, G. Pasterkamp, R.M. Schiffelers, Extracellular vesicles for drug delivery, Adv. Drug. Deliv. Rev. 106 (2016) 148–156.

[199] G. Fuhrmann, A.L. Neuer, I.K. Herrmann, Extracellular vesicles - A promising avenue for the detection and treatment of infectious diseases?, Eur. J. Pharm. Biopharm. 118 (2017) 56–61.

[200] M. Lu, H. Xing, Z. Yang, Y. Sun, T. Yang, X. Zhao, C. Cai, D. Wang, P. Ding, Recent advances on extracellular vesicles in therapeutic delivery: Challenges, solutions, and opportunities, Eur. J. Pharm. Biopharm. 119 (2017) 381–395.

[201] A. Jeyaram, S.M. Jay, Preservation and Storage Stability of Extracellular Vesicles for Therapeutic Applications, AAPS J. 20 (2017) 1.

[202] K.W. Witwer, E.I. Buzás, L.T. Bemis, A. Bora, C. Lässer, J. Lötvall, E.N. Nolte-'t Hoen, M.G. Piper, S. Sivaraman, J. Skog, C. Théry, M.H. Wauben, F. Hochberg, Standardization of sample collection, isolation and analysis methods in extracellular vesicle research, J. Extracell. Vesicles 2 (2013).

[203] S. Bosch, L. de Beaurepaire, M. Allard, M. Mosser, C. Heichette, D. Chrétien, D. Jegou, J.-M. Bach, Trehalose prevents aggregation of exosomes and cryodamage, Sci. Rep. 6 (2016) 36162.

[204] J. Frank, M. Richter, C. de Rossi, C.-M. Lehr, K. Fuhrmann, G. Fuhrmann, Extracellular vesicles protect glucuronidase model enzymes during freeze-drying, Sci. Rep. 8 (2018) 12377.

[205] C. Charoenviriyakul, Y. Takahashi, M. Nishikawa, Y. Takakura, Preservation of exosomes at room temperature using lyophilization, Int. J. Pharm. 553 (2018) 1–7.

[206] R. Lippé, Flow Virometry: a Powerful Tool To Functionally Characterize Viruses, J. Virol. 92 (2018).

[207] J.-P. Amorij, A. Huckriede, J. Wilschut, H.W. Frijlink, W.L.J. Hinrichs, Development of stable influenza vaccine powder formulations: challenges and possibilities, Pharm. Res. 25 (2008) 1256–1273.

[208] M.R. Bovarnick, J.C. Miller, J.C. Snyder, The influence of certain salts, amino acids, sugars, and proteins on the stability of rickettsiae, J. Bacteriol. 59 (1950) 509–522.

[209] E. de Rizzo, E.C. Tenório, I.F. Mendes, F.L. Fang, M.M. Pral, C.S. Takata, C. Miyaki, N.M. Gallina, H.N. Tuchiya, O.K. Akimura, Sorbitol-gelatin and glutamic acid-lactose solutions for stabilization of reference preparations of measles virus, Bull. Pan Am. Health Organ. 23 (1989) 299–305.

[210] M. Prabhu, V. Bhanuprakash, G. Venkatesan, R. Yogisharadhya, D.P. Bora, V. Balamurugan, Evaluation of stability of live attenuated camelpox vaccine stabilized with different stabilizers and reconstituted with various diluents, Biologicals 42 (2014) 169–175.

[211] J. Sarkar, B.P. Sreenivasa, R.P. Singh, P. Dhar, S.K. Bandyopadhyay, Comparative efficacy of various chemical stabilizers on the thermostability of a live-attenuated peste des petits ruminants (PPR) vaccine, Vaccine 21 (2003) 4728–4735.

[212] C.F. Chisholm, T.J. Kang, M. Dong, K. Lewis, M. Namekar, A.T. Lehrer, T.W. Randolph, Thermostable Ebola virus vaccine formulations lyophilized in the presence of aluminum hydroxide, Eur. J. Pharm. Biopharm. 136 (2019) 213–220.

[213] S. Zhai, R.K. Hansen, R. Taylor, J.N. Skepper, R. Sanches, N.K.H. Slater, Effect of freezing rates and excipients on the infectivity of a live viral vaccine during lyophilization, Biotechnol. Prog. 20 (2004) 1113–1120.

[214] A.M. Abdul-Fattah, V. Truong-Le, L. Yee, E. Pan, Y. Ao, D.S. Kalonia, M.J. Pikal, Drying-induced variations in physico-chemical properties of amorphous pharmaceuticals and their impact on Stability II: stability of a vaccine, Pharm. Res. 24 (2007) 715–727.

[215] J. Kissmann, S.F. Ausar, A. Rudolph, C. Braun, S.P. Cape, R.E. Sievers, M.J. Federspiel, S.B. Joshi, C.R. Middaugh, Stabilization of measles virus for vaccine formulation, Hum. Vaccin 4 (2008) 350–359.

[216] D.A. Yannarell, K.M. Goldberg, R.N. Hjorth, Stabilizing cold-adapted influenza virus vaccine under various storage conditions, J. Virol. Methods 102 (2002) 15–25.

[217] W.M. Colwell, D.G. Simmons, J.R. Harris, T.G. Fulp, J.H. Carrozza, T.A. Maag, Influence of some physical factors on survival of Marek's disease vaccine virus, Avian Dis. 19 (1975) 781–790.

[218] K.B. Preston, T.W. Randolph, Stability of lyophilized and spray dried vaccine formulations, Adv. Drug Deliv. Rev. 171 (2021) 50–61.

[219] L. Schoenmaker, D. Witzigmann, J.A. Kulkarni, R. Verbeke, G. Kersten, W. Jiskoot, D.J.A. Crommelin, mRNA-lipid nanoparticle COVID-19 vaccines: Structure and stability, Int. J. Pharm. 601 (2021) 120586.

[220] P. Zhao, X. Hou, J. Yan, S. Du, Y. Xue, W. Li, G. Xiang, Y. Dong, Long-term storage of lipid-like nanoparticles for mRNA delivery, Bioact. Mater. 5 (2020) 358–363.

[221] R.J. Salo, D.O. Cliver, Effect of acid pH, salts, and temperature on the infectivity and physical integrity of enteroviruses, Arch. Virol. 52 (1976) 269–282.

[222] W. Qi, S. Orgel, A. Francon, T.W. Randolph, J.F. Carpenter, Urea Improves Stability of Inactivated Polio Vaccine Serotype 3 During Lyophilization and Storage in Dried Formulations, J. Pharm. Sci. 107 (2018) 2070–2078.

[223] M.A. Croyle, X. Cheng, J.M. Wilson, Development of formulations that enhance physical stability of viral vectors for gene therapy, Gene Ther. 8 (2001) 1281–1290.

[224] K. Wolf, M.C. Quimby, C.P. Carlson, Infectious Pancreatic Necrosis Virus: Lyophilization and Subsequent Stability in Storage at 4 C, Appl. Microbiol. 17 (1969) 623–624.

[225] E. Jermoljev, L. Albrechtová, Stabilization of purified potato virus X by dextran T-10 during lyophilization, Biol. Plant. 11 (1969) 375–380.

[226] M.S. Kang, H. Jang, M.C. Kim, M.J. Kim, S.J. Joh, J.H. Kwon, Y.K. Kwon, Development of a stabilizer for lyophilization of an attenuated duck viral hepatitis vaccine, Poult. Sci. 89 (2010) 1167–1170.

[227] I.I. Slowing, J.L. Vivero-Escoto, C.-W. Wu, V.S.-Y. Lin, Mesoporous silica nanoparticles as controlled release drug delivery and gene transfection carriers, Adv. Drug Deliv. Rev. 60 (2008) 1278–1288.

[228] M. Sameti, G. Bohr, M. Ravi Kumar, C. Kneuer, U. Bakowsky, M. Nacken, H. Schmidt, C.-M. Lehr, Stabilisation by freeze-drying of cationically modified silica nanoparticles for gene delivery, Int. J. Pharm. 266 (2003) 51–60.

[229] W. Ngamcherdtrakul, T. Sangvanich, M. Reda, S. Gu, D. Bejan, W. Yantasee, Lyophilization and stability of antibody-conjugated mesoporous silica nanoparticle with cationic polymer and PEG for siRNA delivery, Int. J. Nanomedicine 13 (2018) 4015–4027.

[230] M.A. Hamaly, S.R. Abulateefeh, K.M. Al-Qaoud, A.M. Alkilany, Freeze-drying of monoclonal antibody-conjugated gold nanorods: Colloidal stability and biological activity, Int. J. Pharm. 550 (2018) 269–277.

[231] H. Yokota, M. Kadowaki, T. Matsuura, H. Imanaka, N. Ishida, K. Imamura, The Use of a Combination of a Sugar and Surfactant to Stabilize Au Nanoparticle Dispersion against Aggregation during Freeze-Drying, Langmuir 36 (2020) 6698–6705.

[232] J.C. Kasper, S. Hedtrich, W. Friess, Lyophilization of Synthetic Gene Carriers, Methods Mol. Biol. 1943 (2019) 211–225.

[233] W.F. Tonnis, M.A. Mensink, A. de Jager, K. van der Voort Maarschalk, H.W. Frijlink, W.L.J. Hinrichs, Size and molecular flexibility of sugars determine the storage stability of freeze-dried proteins, Mol. Pharm. 12 (2015) 684–694.

[234] C. Haeuser, P. Goldbach, J. Huwyler, W. Friess, A. Allmendinger, Excipients for Room Temperature Stable Freeze-Dried Monoclonal Antibody Formulations, J. Pharm. Sci. 109 (2020) 807–817.

[235] F. Franks, Freeze-drying of bioproducts: putting principles into practice, Eur. J. Pharm. Biopharm. 45 (1998) 221–229.

[236] C. Wu, S. Shamblin, D. Varshney, E. Shalaev, Advance Understanding of Buffer Behavior during Lyophilization, in: D. Varshney, M. Singh (Eds.), Lyophilized Biologics and Vaccines, Springer New York, New York, NY, 2015, pp. 25–41.

[237] K. Izutsu, S. Yoshioka, S. Kojima, Effect of Cryoprotectants on the Eutectic Crystallization of NaCl in Frozen Solutions Studied by Differential Scanning Calorimetry (DSC) and Broad-Line Pulsed NMR, Chem. Pharm. Bull. 43 (1995) 1804–1806.

Chapter 2

Objectives of the Thesis

Stabilization of pharmaceutical NPs by freeze-drying has to consider both chemical and physical stability. Specifically, little is known about fundamental principles of colloidal stability of NP lyophilizates providing purposeful guidance for future development. This is due to the heterogeneity of NPs in their physico-chemical properties. But investigations on lyophilization of NPs are typically carried out focusing on one NP type.

The present thesis aims to provide a deeper understanding on the mutual dependency of particle properties, formulation composition and process parameters on the colloidal stability of NPs during lyophilization and upon storage of lyophilizates. Different NP types were investigated, including inorganic NPs, drug nanosuspensions, SLNs, and extracellular vesicles. Basic formulation aspects such as buffer type and pH were studied for all NP types for a good fundamental understanding.

At first, a comprehensive summary on parameters affecting colloidal stability of NPs in the liquid state, the dried state, and during lyophilization is required which is summarized in Chapter 1. Current knowledge on lyophilization of NPs is differentiated according to specific material categories bringing order to rather unstructured literature.

Subsequently, in Chapter 3, we describe studies on the impact of the buffer type, pH and further additives on initial colloidal stabilization and stability upon freeze-thawing of α-Al_2O_3 NPs. These inorganic NPs serve as a non-hydrophobic, mechanically and thermally stable model. Moreover, the pH changes of buffered solutions upon freezing and thawing are described.

As a next step, Chapter 4 summarizes investigations on lipophilic drug nanosuspensions and SLNs with respect to their lyophilization behavior. Crucial formulation, process, and storage aspects are evaluated. Specifically, the freezing step is investigated as a potentially critical process parameter considering conventional ramp freezing, including an annealing step as well as controlled nucleation. Results of subsequent storage stability studies provide further insight into critical formulation parameters and show up ways to overcome limited storage stability.

Finally, in Chapter 5, a development study for a lyophilized formulation of extracellular vesicles (EVs) with long-term stability regarding both colloidal stability and biological activity of an encapsulated protein is described. Freeze-thaw stability of EVs derived from bacterial and mammalian cells is studied and a fundamental understanding of the impact of the formulation on the critical freezing step generated. Additionally, formulation effects on EV size and concentration are analyzed. A 6 months storage stability study elucidates changes in the colloidal properties of lyophilized mammalian EV formulations as well as the stability of incorporated protein.

Chapter 6 summarizes this thesis and gives an outlook and suggestions for future attempts on lyophilization of NPs.

Chapter 3

Freeze-thaw stability of aluminum oxide nanoparticles

Eduard Trenkenschuh, Wolfgang Friess

Pharmaceutical Technology and Biopharmaceutics, Department of Pharmacy, Ludwig-Maximilians-Universität München, 81377 Munich, Germany

This chapter has been published in the 'International Journal of Pharmaceutics' **(https://doi.org/10.1016/j.ijpharm.2021.120932)**.

Author contributions:

E.T. performed the experiments, evaluated the data and wrote the manuscript. W.F. supervised the work, provided conceptual guidance and corrected the manuscript.

Abstract

The use of inorganic nanoparticles (NPs) gains interest for pharmaceutical applications, e.g. as adjuvants or drug delivery vehicles. Colloidal stability of NPs in aqueous suspensions is a major development challenge. Both frozen and lyophilized liquids are alternative presentations to liquid dispersion. To improve the basic understanding, we investigated the freeze-thawing stability of model α-Al_2O_3 NPs. Freeze-thawing was conducted in three different buffer types at pH 5 and 8 without and with additives to determine fundamental formulation principles. Before freeze-thawing, α-Al_2O_3 NPs could be stabilized in sodium citrate buffer at pH 5 and 8, and in sodium or potassium phosphate at pH 8. Particles revealed low zeta potential values in phosphate buffers at pH 5 indicating insufficient electrostatic stabilization. After freeze-thawing, an increase in NP size was strongly reduced in potassium phosphate and sodium citrate buffers. Subsequent pH measurements upon freezing revealed a drastic acidic pH shift in sodium phosphate which was further demonstrated to destabilize NPs. The ionic stabilizers gelatin A/B, Na-CMC, and SDS, were suitable to improve colloidal stability in phosphate buffers at pH 5 highlighting the importance of charge stabilization. Freeze-thawing stability was best in presence of gelatin A/B, followed by PVA, mannitol, or sucrose. Depletion and steric stabilization were insufficient using PEG and surfactants respectively. Thus, we could identify the fundamental formulation principles to preserve inorganic NPs upon freezing: i) sufficient charge stabilization, ii) a maintained pH during freezing, and iii) the addition of a suitable stabilizer, preferably gelatin, not necessarily surfactants. This forms the basis for future studies, e.g. on lyophilization.

Keywords

Aluminum oxide, Inorganic nanoparticles, Freeze-thawing, Buffer, pH, Colloidal Stability, Aggregation

Abbreviations

Al_2O_3	Aluminum oxide
Na-CMC	Sodium carboxymethyl cellulose
DLS	Dynamic light scattering
DSC	Differential scanning calorimetry
FT	Freeze-thawing
LO	Light obscuration
Man	Mannitol
MW	Molecular weight
NP	Nanoparticle
PDI	Polydispersity index
PEG	Polyethylene glycol
PS20	Polysorbate 20
PVA	Polyvinyl alcohol
RT	Room temperature
SDS	Sodium dodecyl sulfate
Suc	Sucrose
T_c	Crystallization temperature
T_g'	Glass transition temperature of the freeze-concentrated solution
w/o	Without

Table of Contents

Abstract 52
Keywords 53
Abbreviations 53
1 Introduction 55
2 Material and methods 56
2.1 Materials 56
2.2 Methods 56
2.2.1 Sample preparation 56
2.2.2 Freeze-thaw cycles 57
2.2.3 Dynamic light scattering (DLS) 57
2.2.4 Zeta potential measurement 57
2.2.5 Analysis of pH during freezing and thawing 57
2.2.6 Subvisible particle analysis by light obscuration (LO) 57
2.2.7 Differential scanning calorimetry (DSC) 58
3 Results and discussion 58
3.1 Impact of buffer type and pH 58
3.2 The pH shift during freezing and its impact on particle stability 60
3.3 Impact of various stabilizers 63
3.3.1 Colloidal stability before FT 63
3.3.2 FT stability 65
4 Conclusion 68
5 Supplementary Data 69
6 References 70

1 Introduction

Inorganic nanoparticles (NPs) are utilized for a number of biomedical applications, including cancer therapy, imaging, and drug delivery [1–4]. Specifically, aluminum containing adjuvants are used for decades in vaccines for human or veterinary immunizations [5,6]. In order to improve the colloidal and chemical stability of the aqueous dispersions they can be stored at low temperatures. Additionally, freezing and freeze-drying are widely used to overcome the limited stability of colloidal systems [7,8]. However, these processes are also known to cause stress which might lead to NP aggregation and size increase. During freezing, particle aggregation can be triggered by increased particle-particle interaction in the cryo-concentrated phase [9], by pH changes arising from crystallization of buffer salts [10], by surface induced destabilization at the ice-liquid interfaces [11], or by mechanical stress due to formation of ice crystals [7]. Braun et al. prevented freezing of vaccines containing alum by adding substantial amounts of propylene glycol, polyethylene glycol 300, and glycerol which lead to a freezing point depression [12]. Although this attempt prevents damage during freezing, it does not overcome the predominant problem of physical instability in aqueous media and is not in line with isotonicity requirements. Drying is further accompanied by the loss of the hydration shell leading to particle destabilization. NP aggregation can result in reduced therapeutic efficacy and embolism [13] and has to be avoided by adequate formulation and process design.

While fundamental concepts for freeze-drying of protein drugs have been a research focus in recent years, there is a lack of knowledge about freezing and lyophilization of inorganic NPs. Beirowski et al. emphasized the higher importance of formulation design over the freezing rate for drug nanosuspensions [8]. Yet, the formulation design depends on specific NP properties. For example, the physico-chemical properties and stability of alum NPs depends on the amount and type of bound antigen as well as the binding mechanism [14]. Nature and concentration of excipients like cryoprotectants, lyoprotectants, surfactants, and polymers will have substantial impact on the NP stability during freezing. Salnikova et al. found that the pH strongly affects the electrostatic charges and by that the extent of freeze-thaw aggregation of alum adjuvant [15]. But a systematic evaluation of e.g. the impact of buffer species and ionic strength in presence of different stabilizing excipients is still lacking.

The objective of this study was to close this gap investigating the impact of different buffer types in combination with various excipients on the stability of α-Al_2O_3 NPs during freezing. Freezing is considered to be the key stress for products stored as frozen liquids or lyophilizates [16]. Freeze-thaw (FT) experiments were conducted using sodium phosphate, potassium phosphate, and sodium citrate buffer at pH 5 and 8. We analyzed the pH during freezing and the impact of pH on particle size, PDI, and zeta potential of the NPs. We further

investigated the potential of different additives, including surfactants, polymers, and cryoprotectants, to preserve colloidal stability upon FT. This study illustrates the importance of sufficient charge stabilization, maintained pH during freezing, and the addition of a suitable stabilizer on particle size preservation of freeze-thawed α-Al_2O_3 NPs serving as a model for charge stabilized inorganic NPs.

2 Material and methods

2.1 Materials

α-Al_2O_3 NPs were obtained from IoLiTec Nanomaterials (Heilbronn, Germany). Sucrose, mannitol, sodium dodecylsulfate (SDS), gelatin type A 175, gelatin type B 225, polyvinyl alcohol (PVA; MW ~31.000-50.000 Da) (all Sigma-Aldrich, Steinheim, Germany), polyethylene glycol (PEG; MW ~20.000 Da), polysorbate 20 (PS20) (all Merck KGaA, Darmstadt, Germany), and sodium carboxymethyl cellulose (Na-CMC) (Tylopur C 300 P2, Clariant, Wiesbaden, Germany) were used without further purification. Na-, K-phosphate (all VWR International, Ismaning, Germany), and Na-citrate buffer (Merck, Darmstadt, Germany) were used to prepare 10 mM buffers at pH 5 and 8. Highly purified water (HPW) was used for the preparation of buffer and stabilizer stock solutions. 10R glass vials (Schott, Müllheim, Germany) with rubber stoppers (West, Eschweiler, Germany) were used throughout the studies.

2.2 Methods

2.2.1 Sample preparation

10 mM Na-citrate, Na phosphate, or K phosphate buffer at pH 5 or 8 without and with one of the stabilizers (Na-CMC, gelatin A, gelatin B, PVA, PEG 20.000, SDS, PS20, sucrose and mannitol [each at two concentrations]) were prepared by manual mixing with HPW and subsequent 0.2 µm filtration. 1 mg/mL α-Al_2O_3 NP suspension was obtained after addition of the respective solution to the NPs, 10 s ultrasonic homogenization (Bandelin Sonoplus HD 3100, Berlin, Germany), and filtration through a 1.2 µm cellulose acetate filter (Sartorius, Göttingen, Germany). The pH value was checked for each formulation.

2.2.2 Freeze-thaw cycles

The different formulations (3 mL in 10R vials) were freeze-thawed three times on a pilot scale freeze-drier (FTS LyoStar™ 3, SP Scientific, Stone Ridge, New York). Samples were frozen at –1 °C/min to –50 °C. After 90 min at –50 °C, the samples were thawed at 1 °C/min to 10 °C with a 90 min hold.

2.2.3 Dynamic light scattering (DLS)

Particle size and polydispersity index (PDI) were analyzed on a DLS platereader DynaPro II (Wyatt Technology, Dernbach, Germany) using 96 UV-well plates (Costar™, Corning, Glendale, Arizona). 100 µL sample (n=3) per well was measured at RT (10 acquisitions with 5 s each). DYNAMICS software (Version 7.8.0.26) was used for data evaluation. Corresponding preset refractive index parameters were used for all samples. Sample viscosities were determined on an AMVn Automated Micro Viscometer (Anton Paar, Graz, Austria).

2.2.4 Zeta potential measurement

Zeta potential measurements were conducted by electrophoretic light scattering on a Zetasizer Nano ZS (Malvern Instruments, Herrenberg, Germany). Undiluted samples were analyzed in a disposable capillary cell (DTS1070). NP titration was performed in combination with a Malvern MPT-2 Autotitrator. 12 mL sample was transferred into a stirred polypropylene tube and titrated from pH 8 to pH 2 in increments of 0.5 pH units (± 0.2 U) using 0.1 M HCl and 0.1 M NaOH. Zeta potential and z-average size were measured in a disposable zeta cell (DTS1070) with three measurements per pH value. Analysis was performed at 25 °C and at a voltage of 50 V in ‘monomodal mode’ with automatic attenuation selection.

2.2.5 Analysis of pH during freezing and thawing

Pure buffer solutions were analyzed for pH shifts during freezing. A low temperature pH electrode (Inlab®cool, Mettler Toledo GmbH, Giessen, Germany) was equipped with a thermocouple and placed in the center of the sample vial (6 mL in 10R vials). Shelves were cooled at –1 °C/min to –35 °C. After 90 min at –35 °C, the samples were thawed at 1 °C/min to RT.

2.2.6 Subvisible particle analysis by light obscuration (LO)

Subvisible particles (SVPs) were analyzed using a PAMAS SVSS-35 particle counter with a HCB-LD-25/25 sensor (PAMAS - Partikelmess- und Analysesysteme, Rutesheim, Germany).

Selected samples were measured in triplicates before and after freeze-thawing. After sample pre-rinse with 0.4 mL, each sample was analyzed three times with 0.3 mL. Data evaluation was carried out using the PAMAS PMA software.

2.2.7 Differential scanning calorimetry (DSC)

DSC measurements were performed using a Mettler Toledo DSC 822e (Mettler Toledo GmbH, Giessen, Germany) in order to determine the glass transition temperature of the maximally freeze-concentrated solution (T_g') or crystallization events (T_c). 20 µL sample was filled and sealed in 40 µL aluminum crucibles. The samples were cooled at 10 °C/min from 25 °C to –60 °C, held at –60 °C for 1 min, and reheated at 10 °C/min to 25 °C. T_g' were defined as the inflection point of the glass transition in the heating scan of the DSC experiment.

3 Results and discussion

3.1 Impact of buffer type and pH

α-Al_2O_3 NPs were formulated in 10 mM Na-citrate, Na-phosphate, or K-phosphate buffer in order to evaluate the impact of buffer type and pH on zeta potential and particle stability upon FT. The buffers were not in the center but still within their effective buffering range. pH 5 and 8 were chosen to obtain differently charged particles and thus investigate the impact of electrostatic stabilization. Particle size, PDI and zeta potential measurements were conducted before and after FT providing insight into colloidal stability. DLS measurements revealing particles >1 µm show a distinct qualitative information for insufficient NP stabilization and were thus not further investigated, e.g. by laser diffraction.

Before FT, α-Al_2O_3 NPs exhibited a mean particle size of 240 nm and a mean PDI below 0.4 in Na-citrate buffer at both pH values as well as in phosphate buffers at pH 8 (Figure 1). In contrast, the larger particle size of approximately 480 nm and PDI values >0.56 in Na- and K-phosphate buffer at pH 5 revealed a pronounced impact of buffer type and pH on initial colloidal particle stability. After three times FT, the DLS results did not change in Na-citrate buffer at pH 5 and 8. Particle size was markedly increased in phosphate buffer, except in K-phosphate at pH 8. Overall, all formulations showed a multimodal size distribution, as also indicated by the high PDI, independent of buffer type and pH, indicating a strong tendency of the NPs to aggregate. Crystal growth of NPs due to irreversible Ostwald ripening may be an additional source for increased particle diameters [17]. α-Al_2O_3 NPs are widely applied in

high performance ceramics, packing materials, paints, and catalysts and with its poor water solubility and stability it is not expected to show Ostwald ripening in the aqueous media within the short time period of the tests.

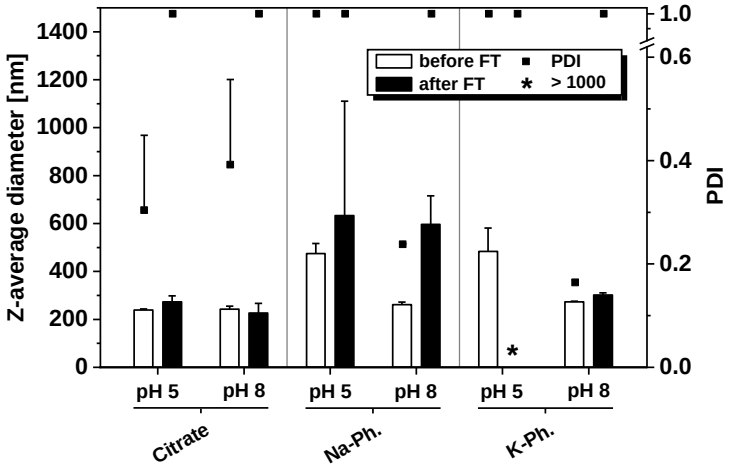

Figure 1: DLS results of α-Al_2O_3 NPs formulated in 10 mM Na-citrate, Na-phosphate, and K-phosphate buffer at pH 5 or 8 before and after 3xFT (mean ± SD; n=3). PDI values >0.56 represent a multimodal size distribution and are therefore stated as '1.0'.

The NPs showed a strong negative surface charge of ~–42 mV and ~–48 mV in Na-citrate buffer at pH 5 and 8 (Table 1). The zeta potential was significantly lower in phosphate buffers at pH 5, whereas values of ~–39 mV and ~–60 mV were obtained at pH 8 in Na- and K-phosphate buffer respectively. The NP surface charge did not change upon FT.

Table 1: ζ-Potential values of α-Al_2O_3 NPs formulated in 10 mM Na-citrate, Na-phosphate, and K-phosphate buffer at pH 5 or 8 before and after 3xFT (mean ± SD; n=3).

ζ-Potential [mV]			
Buffer	**pH**	**before FT**	**after FT**
Na-citrate	5	–42.1 ± 2.1	–40.2 ± 2.1
	8	–47.6 ± 3.3	–48.3 ± 3.7
Na-phosphate	5	–19.0 ± 0.1	–19.3 ± 0.6
	8	–38.6 ± 1.9	–34.8 ± 0.9
K-phosphate	5	–25.2 ± 1.3	–21.5 ± 0.7
	8	–60.5 ± 4.6	–58.4 ± 3.7

Salnikova et al. showed that FT induced aggregation of aluminum hydroxide and aluminum phosphate microparticles (Alhydrogel™ and Adjuphos™) can be significantly reduced at a pH far away from the point of zero charge indicating an electrostatically driven effect [15]. Thus, we assume that electrostatic particle stabilization by the polyanions citrate and phosphate is the underlying cause for α-Al_2O_3 stabilization in aqueous suspension. Adsorbed multiply charged ions and polymer coatings on NP surfaces can suppress NP agglomeration [18]. With a lower degree of protonation and consequently a higher amount of charges at higher pH an increased stabilizing effect can be seen. Two negative charges in hydrogen citrate (> 50% at pH > 4.8) and hydrogen phosphate (> 50% at pH > 7.1) and three negative charges in citrate (> 50% at pH > 6.4) appear to be preferred underlining the importance of the buffer pH and type (citric acid: pK_{a1} = 3.1, pK_{a2} = 4.8, pK_{a3} = 6.4; phosphoric acid: pK_{a1} = 2.2, pK_{a2} = 7.1, pK_{a3} = 12.3 [19]).

3.2 The pH shift during freezing and its impact on particle stability

FT of α-Al_2O_3 NPs in phosphate buffer pH 8 resulted in a smaller increase of particle size with K^+ as compared to Na^+ as counter ion (see 3.1). Since it is known that buffers might undergo a pH shift during freezing, we examined the change in pH upon freezing to –30 °C and subsequent thawing.

The pH of Na-citrate buffer slightly decreased from pH 5 to 4 and from pH 8 to 6 during freezing to approximately –30 °C (Figure 2). In contrast, a pH of 3 was measured at the lowest temperature in Na-phosphate buffer adjusted to pH 5 or 8 and in K-phosphate buffer adjusted to pH 5. The pH value of K-phosphate buffer pH 8 did not change upon freezing. In general, all buffer solutions maintained their pH until freezing started. The gradual pH shift started with ice crystallization which caused a temporarily increased solution temperature. The changes in pH were reversible upon increasing temperatures.

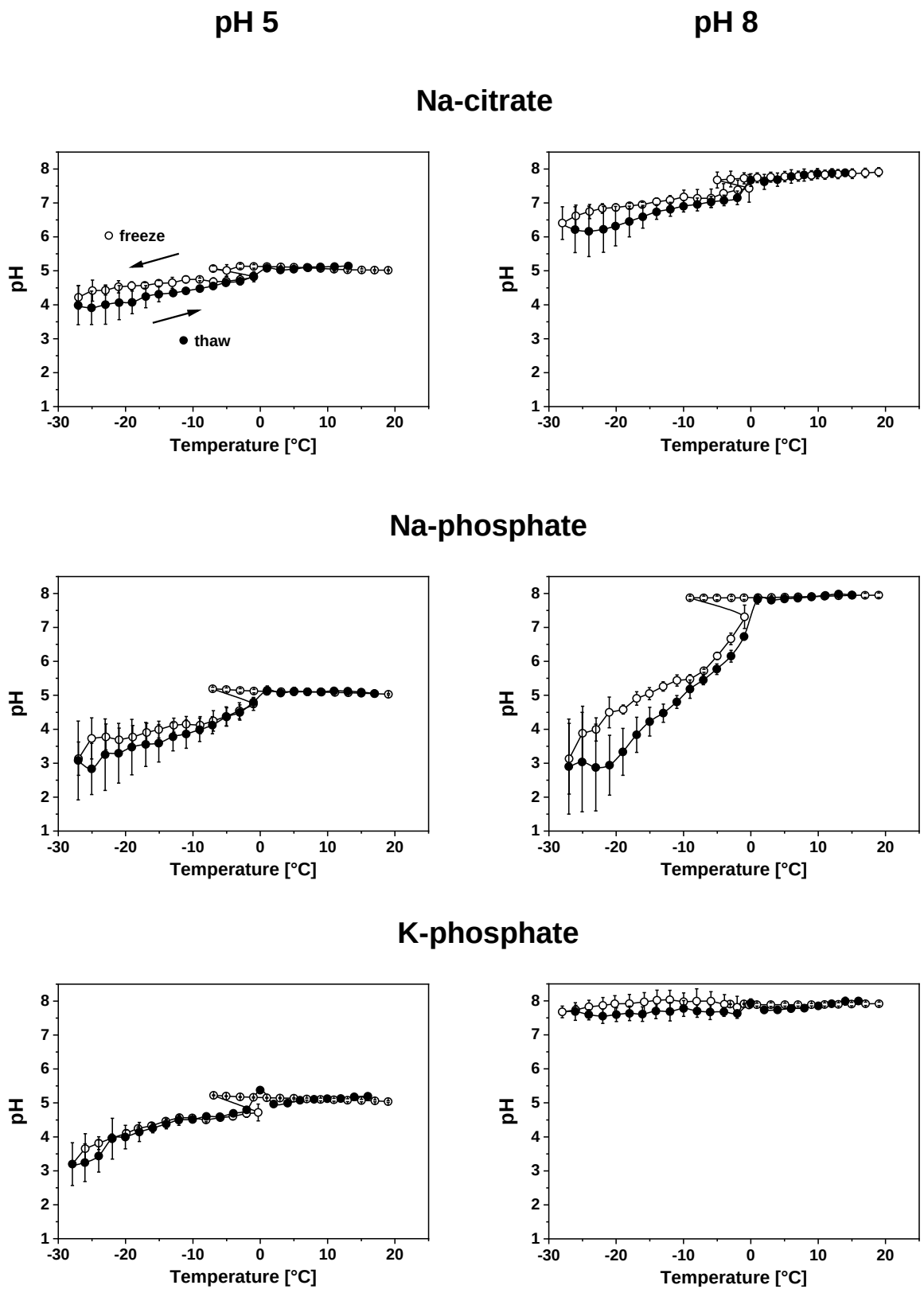

Figure 2: Change in pH as a function of temperature for 10 mM Na-citrate, Na-phosphate, and K-phosphate buffer at pH 5 or 8 during freezing to –30 °C and subsequent thawing (mean ± SD; n=3).

Our observations are in accordance to previous publications [20–22]. The pH shift during freezing of buffers depends on the (cryo-)concentration and the eutectic temperatures of the salt components relative to their solubilities [22]. The eutectic point of the acidic monosodium phosphate (T_{eut} = −9.7 °C) is lower compared to the basic disodium salt (T_{eut} = −0.5 °C) resulting in a pH decrease upon freezing. In the potassium phosphate system, the dipotassium phosphate (T_{eut} = −13.7 °C) is more soluble in water than the monopotassium salt (T_{eut} = −2.7 °C) preventing an acidic pH shift in the buffer formulated at pH 8 [20,21]. Thus, in case of phosphate buffers, the mono to di ratio of the buffer salts is crucial for the occurrence and extent of pH shift. Na-citrate buffers show only a minimal change upon freezing potentially due to partial precipitation of disodium and trisodium citrate at pH 5 and 8 respectively [22].

Additionally, we performed a pH titration to elucidate the impact of an acidic pH shift on zeta potential, particle size and PDI of α-Al_2O_3 NPs in Na-phosphate buffer pH 8. The acidic pH shift upon freezing leads to a decreasing surface charge which comes with pronounced aggregation as indicated by the increase in particle size and PDI value (Figure 3). An increased particle aggregation of α-Al_2O_3 NPs occurs as the pH approaches the point of zero charge, where van der Waals attraction forces dominate over electrostatic repulsion [23]. To the best of our knowledge, the destabilizing effect of an acidic pH shift on FT stability of inorganic NPs has not been reported yet. In contrast, it is well-known that proteins formulated in Na-phosphate buffer may denature due to the pH change during freezing leading to marked aggregation [24].

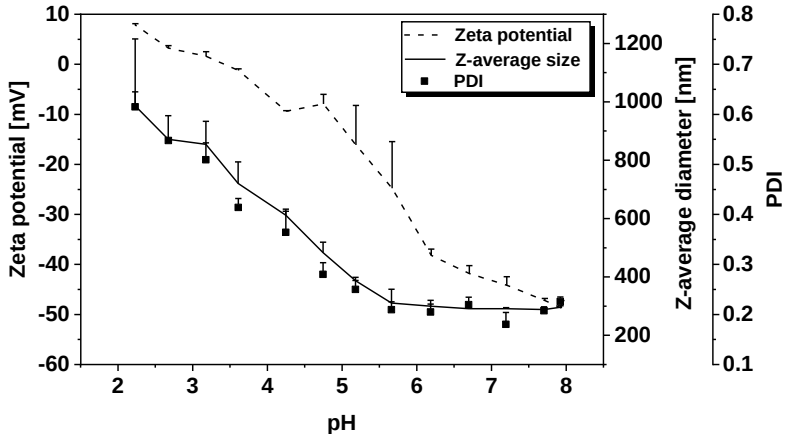

Figure 3: Change in zeta potential, particle size, and PDI of α-Al_2O_3 NPs in 10 mM Na-phosphate as a function of pH (mean ± SD; n=3).

3.3 Impact of various stabilizers

After understanding the effect of buffer and pH on the growth of α-Al_2O_3 NPs upon FT, we tested the potential of different additives to further improve FT stability as well as colloidal stability at pH 5 before FT. Na-CMC and gelatin A and B were chosen as electrostatic stabilizers and viscosity enhancers, SDS and PS20 were selected as ionic and non-ionic surfactants, and PVA and PEG 20.000 were used to test stabilization via depletion. Furthermore, mannitol and sucrose were tested as cryoprotective stabilizers and bulking agents.

3.3.1 Colloidal stability before FT

Before FT, α-Al_2O_3 NPs were well stabilized in Na-citrate independent of the buffer pH and excipient addition revealing a particle size of ~240 nm and a low PDI (Figure 4). Similarly, NPs exhibited a good colloidal stability in all samples formulated in phosphate buffer at pH 8. NP stability was critical in phosphate buffers pH 5 without the addition of further stabilizers as indicated by a large particle size and a multimodal size distribution. The uncharged stabilizers PS20, PVA, PEG 20.000, mannitol, and sucrose did not improve the initial particle stability thereby making the assessment of the FT stability obsolete. In contrast, NPs revealed a high colloidal stability in presence of gelatin independent of buffer type and pH. Additionally, Na-CMC and SDS containing formulations were able to stabilize NPs in phosphate buffers pH 5, still showing larger particle sizes compared to formulations at pH 8. The improved colloidal stability in presence of gelatin, Na-CMC, or SDS is attributed to electrostatic interactions. Likos et al. reported that gelatin adsorbs to the particle surfaces thereby providing both electrostatic and steric stabilization [25]. This effect was also described for negatively charged Na-CMC (pK_a = 4.3 [19]) and SDS [26,27]. The stabilization by gelatin appears to be independent of the net electrical charge, since gelatin exhibits an isoelectric point at pH 7.0 – 9.0 (type A) or 4.7 – 5.4 (type B) [19]. Gelatin molecules might adsorb through attractive interactions of some amino acid segments, regardless of its overall charge [28]. Interestingly, Na-CMC and SDS failed to stabilize α-Al_2O_3 NPs in K-phosphate buffer at both investigated additive concentrations. The presence of potassium ions seems to impair electrostatic interactions although sodium ions are added by Na-CMC (0.1%: 3.8 mM Na^+, 0.5%: 19.0 mM Na^+) and SDS (0.1%: 3.47 mM Na^+, 1%: 34.7 mM Na^+). We speculate that the different ion size plays a role.

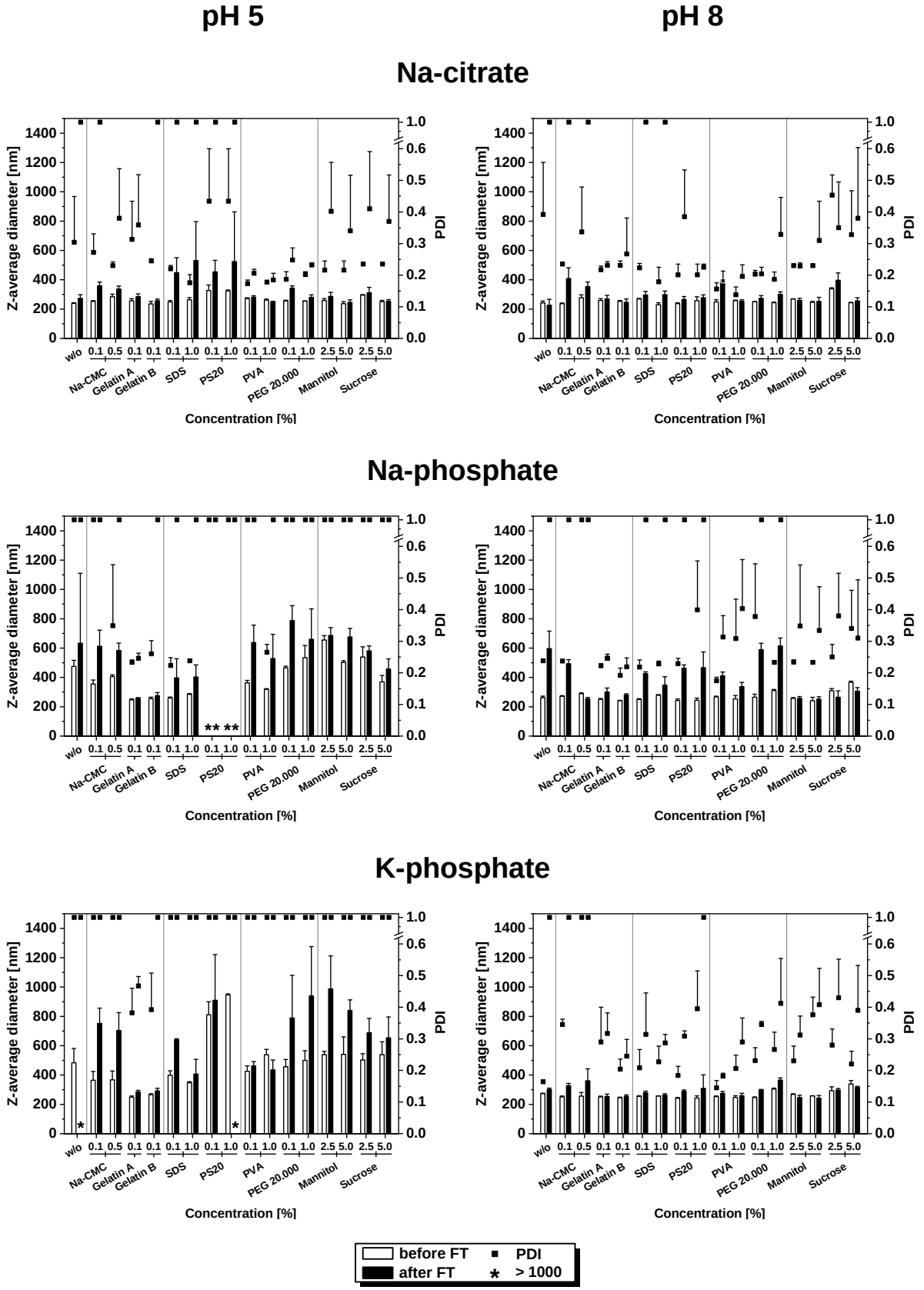

Figure 4: DLS results of α-Al_2O_3 NPs in 10 mM Na-citrate, Na phosphate, and K-phosphate buffer at pH 5 or 8 in presence of different excipients before and after 3xFT (mean ± SD; n=3). PDI values >0.56 represent a multimodal size distribution and are therefore stated as '1.0'.

The zeta potential of α-Al_2O_3 NPs was mainly determined by the buffer type and pH (Figure 5). Zeta potential measurements generally showed higher surface charges for particles prepared at pH 8 independent of the added excipient. The highest surface charge values resulted in K-phosphate pH 8. At pH 5, Na-citrate led to higher zeta potential values compared to phosphate buffers, except in Na-CMC containing samples. SDS increased while PVA and 1% PS20 decreased the surface potentials in all buffer types. Interestingly, gelatin containing formulations revealed NPs with approximately neutral surface charge independent of buffer type and pH.

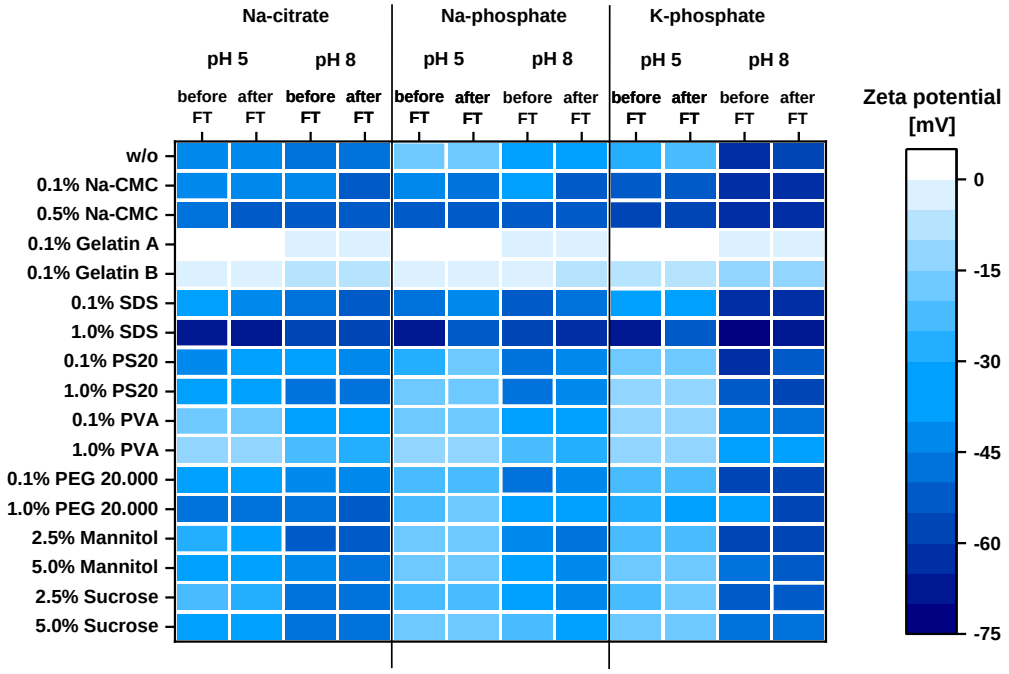

Figure 5: ζ-Potential of α-Al_2O_3 NPs in 10 mM Na-citrate, Na-phosphate, and K-phosphate at pH 5 or 8 in presence of different excipients before and after 3x FT (mean ± SD; n=3).

3.3.2 FT stability

The surface charge did not change with FT (Figure 5). In general, citrate buffer provided better stabilization than phosphate buffer highlighting the importance of electrostatic stabilization (Figure 4). The FT stability in presence of additives is discussed in more detail in the following along the line of the proposed stabilization mechanisms. Additionally, DSC measurements of aqueous excipient solutions were performed in order to assess potential glass transitions of the freeze-concentrate or solute crystallization. No thermal events were detected in samples containing Na-CMC, gelatin, PS20, PVA or PEG 20.000.

Na-CMC was not able to stabilize α-Al_2O_3 NPs except in Na-citrate pH 5. Thus, an increased initial viscosity (~7.5 mPas) is insufficient without further stabilization. In contrast, gelatin A was able to preserve NPs independent of the buffer composition. Gelatin B was beneficial at pH 8 but not around its isoelectric point of 4.7 to 5.4. The favorable cryoprotective effect of gelatin is reported for several different NP types, such as nanocapsules, viruses, and bacteriophages [29–31].

PS20 containing formulations only improved FT stability at pH 8; the pH shift in Na-phosphate seems to be critical. Furthermore, SDS only improved FT stability in K-phosphate at pH 8. During the heating scan of DSC measurements, 1% SDS revealed a thermal event in phosphate buffers at pH 8 at about –18 °C which is attributed to SDS crystallization (Figure 6). SDS crystallization is usually observed at temperatures below RT depending on its concentration [32,33]. Interestingly, in our study no crystallization event was detected in phosphate buffers at pH 5 or in Na-citrate buffer. The (partial) crystallization of SDS in K-phosphate pH 8 appears to have a cryoprotective effect upon FT speculatively by providing enhanced particle isolation during thawing.

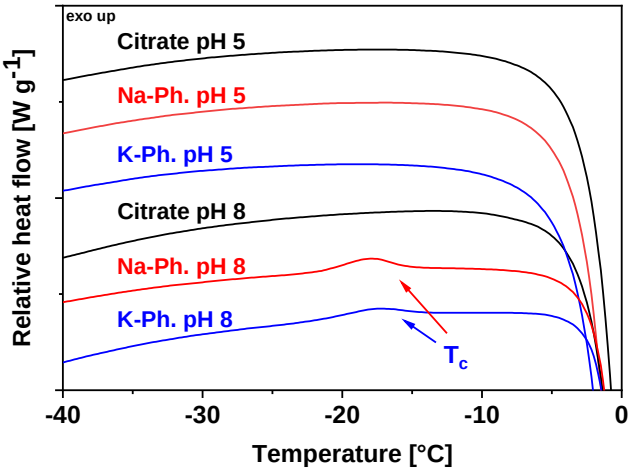

Figure 6: DSC profiles of 1% SDS in 10 mM Na-citrate, Na-phosphate, and K-phosphate buffer at pH 5 or 8.

The two polymers PVA and PEG 20.000 improved the FT stability of the NPs in Na-citrate buffer pH 5 and 8 as well as in K-phosphate at pH 8. Overall, the lowest PDI values after FT were detected in Na-citrate buffers containing PVA or PEG 20.000. PVA further improved FT stability in Na phosphate at pH 8, whereas pronounced aggregation was found in formulations containing PEG 20.000. The stabilizing effect of PVA and PEG 20.000 is related to depletion by the free polymers in solution separating particles from each other [34,35]. Furthermore, PVA is a known as an ice recrystallization inhibitor due to adsorption to the ice surface thereby

avoiding the formation of large ice crystals [36]. The anti-freezing effect of PVA was further demonstrated to slow the rate of ice crystal growth during thawing [37]. Thus, the absence of large ice crystals and recrystallization processes may reduce the mechanical stress on NPs during FT. Furthermore, lower ice nucleation temperatures might attenuate the pH shift in Na-phosphate buffer.

The small polyol mannitol and the cryoprotectant sucrose were suitable to protect α-Al_2O_3 NPs in Na-citrate at pH 5 and in all formulations prepared at pH 8 against FT stress with only a slight increase in PDI. In line with literature DSC measurements showed a T_g' of about –32 °C for sucrose in all formulations [7]. Mannitol revealed two glass transition events at ~–32 °C and ~–25 °C and an exothermic crystallization at ~–20 °C (Figure S-1) [7,38]. Thus, both excipients formed an amorphous matrix during FT which is able to stabilize the NPs. Mannitol is known to form an amorphous matrix and may crystallize upon FT depending on freezing protocol and other excipients [38,39]. Upon mannitol crystallization its beneficial effect can be lost [39]. Particle isolation, vitrification, and increased solution viscosity are used in literature to explain the cryoprotective effect of amorphous sugars and polyols on various NP types (i.e. polyplexes, lipoplexes, liposomes) during freezing [41–43]. Clausi et al. demonstrated that aggregation of aluminum hydroxide microparticles (Alhydrogel™) particles can be minimized through proper choice of buffer ions, or kinetically inhibited by rapidly forming a glassy state during freezing [44]. Furthermore, successful lyophilization of mesoporous silica and gold nanorods was reported using trehalose and sucrose [45–47]. Mannitol and sucrose furthermore successfully stabilized α-Al_2O_3 NPs in Na-phosphate buffer in spite of the earlier discussed pH shift. The amorphous sugar may completely inhibit buffer salt crystallization during freezing of phosphate buffered saline, while mannitol can at least partially suppress the crystallization thereby attenuating the pH shift [48]. Higher concentrations of stabilizers did not further substantially improve the FT stability at the investigated NP concentration. In contrast, Clausi et al. showed that high concentrations of trehalose (up to 15%) are necessary to completely prevent aggregation of aluminum hydroxide microparticles upon FT and lyophilization [44]. Our study generally shows that particle preservation of α-Al_2O_3 is more successful in formulations prepared at pH 8 highlighting the importance of electrostatic stabilization which is considered to be the predominant stabilization mechanism.

Overall, DLS measurements revealed best FT stability of α-Al_2O_3 NPs in (i) Na-citrate, (ii) at pH 8, and (iii) in presence of a suitable additive. Since DLS gives no information on the number of large particles formed after FT, we additionally performed SVP analysis. α-Al_2O_3 NPs were formulated in Na-citrate pH 8 with 0.1% gelatin A, 5% Suc, or 5% Man. Gelatin A was selected due to its ability to stabilize α-Al_2O_3 before and after FT independent of buffer

type and pH while Suc and Man might serve as potential bulking agents for lyophilization. All formulations exhibited ~10,000 particles/mL before FT (Figure 7). After three times FT, the number of SVP was increased only slightly to values between 17,000 and ~26,000 particles/mL. Surprisingly, 0.1% gelatin A showed a similar cryoprotective effect as the two matrix formers at 5%. Again, electrostatic and steric stabilization are at least as important as the formation of a glassy matrix.

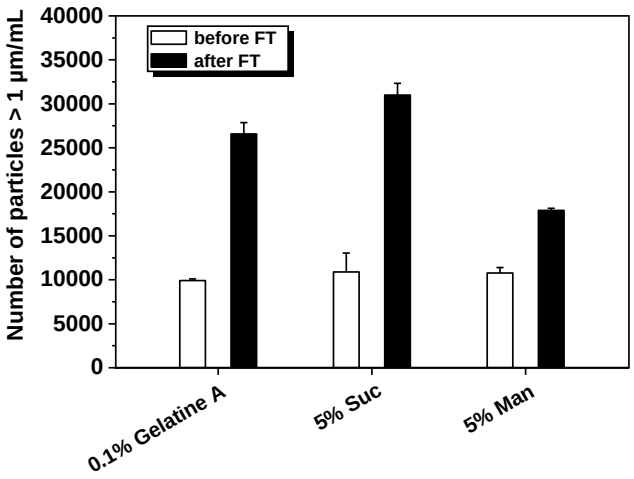

Figure 7: SVP concentrations of α-Al_2O_3 NPs in 10 mM Na-citrate pH 8 stabilized with 0.1% gelatin, 5% Suc, and 5% Man before and after 3xFT (mean ± SD; n=3).

4 Conclusion

The poor colloidal stability of inorganic NPs in aqueous suspension limits their application and is an important hurdle in development. Frozen storage and lyophilization are technologies to overcome this challenge. But a detailed and systematic investigation of the effect of pH, buffer type, and stabilizing excipients on colloidal stability is a prerequisite. We used α-Al_2O_3 NPs as a model and investigated the FT stability in presence of different buffers at pH 5 and 8, and of various excipients covering different stabilization mechanisms.

Before FT, Na- and K-phosphate buffer only provided colloidal stability at pH 8, whereas the NPs size increased at pH 5 due to the lower surface charge indicating insufficient electrostatic stabilization. Na-citrate stabilized NPs at both pH 5 and 8. The aggregation propensity upon FT was pronounced in Na-phosphate buffer at both pH 5 and 8. This is caused by the acidic pH shift in the buffers during freezing which results in a drastic decrease of the zeta potential. The colloidal stability in Na- and K-phosphate buffer pH 5 was improved by gelatin, Na-CMC, and SDS. In contrast, the uncharged stabilizers PS20, PVA, PEG, mannitol, and sucrose

were not able to increase the initial particle stability. After FT, NPs were best preserved in Na-citrate buffer pH 5 and 8 or K-phosphate buffer pH 8, still revealing larger particles in absence of further additives. The addition of gelatin, PVA, mannitol and sucrose drastically improved FT stability most likely due to enhanced particle isolation and/or the formation of a stabilizing matrix. Most remarkably, gelatin A was able to provide both colloidal and FT stability in all buffer types.

Overall, electrostatic stabilization was vital for the stabilization of α-Al_2O_3 NPs before and after FT as shown by the importance of buffer type and pH; citrate was in general superior to phosphate buffer. The addition of mannitol, sucrose and gelatin further improved FT stability and offer great potential for future studies on lyophilization which additionally involves potential stresses during drying.

5 Supplementary Data

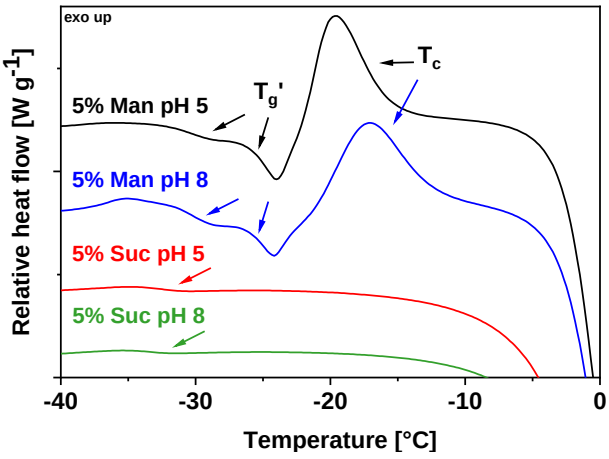

Figure S-1: Representative DSC profiles of 5% Man or 5% Suc in 10 mM K-phosphate buffer at pH 5 or 8.

6 References

[1] D. Kim, J. Kim, Y.I. Park, N. Lee, T. Hyeon, Recent Development of Inorganic Nanoparticles for Biomedical Imaging, ACS Cent. Sci. 4 (2018) 324–336.

[2] R. Ladj, A. Bitar, M.M. Eissa, H. Fessi, Y. Mugnier, R. Le Dantec, A. Elaissari, Polymer encapsulation of inorganic nanoparticles for biomedical applications, Int. J. Pharm. 458 (2013) 230–241.

[3] A. Pugazhendhi, T.N.J.I. Edison, I. Karuppusamy, B. Kathirvel, Inorganic nanoparticles: A potential cancer therapy for human welfare, Int. J. Pharm. 539 (2018) 104–111.

[4] I.I. Slowing, J.L. Vivero-Escoto, C.-W. Wu, V.S.-Y. Lin, Mesoporous silica nanoparticles as controlled release drug delivery and gene transfection carriers, Adv. Drug Deliv. Rev. 60 (2008) 1278–1288.

[5] T. Clapp, P. Siebert, D. Chen, L. Jones Braun, Vaccines with aluminum-containing adjuvants: optimizing vaccine efficacy and thermal stability, J. Pharm. Sci. 100 (2011) 388–401.

[6] R. Gupta, Aluminum compounds as vaccine adjuvants, Adv. Drug Deliv. Rev. 32 (1998) 155–172.

[7] W. Wang, Lyophilization and development of solid protein pharmaceuticals, Int. J. Pharm. 203 (2000) 1–60.

[8] J. Beirowski, S. Inghelbrecht, A. Arien, H. Gieseler, Freeze-drying of nanosuspensions, 1: freezing rate versus formulation design as critical factors to preserve the original particle size distribution, J. Pharm. Sci. 100 (2011) 1958–1968.

[9] P. Fonte, S. Reis, B. Sarmento, Facts and evidences on the lyophilization of polymeric nanoparticles for drug delivery, J. Control. Release 225 (2016) 75–86.

[10] X. Tang, M.J. Pikal, Design of Freeze-Drying Processes for Pharmaceuticals: Practical Advice, Pharm. Res. 21 (2004) 191–200.

[11] B.S. Chang, B.S. Kendrick, J.F. Carpenter, Surface-induced denaturation of proteins during freezing and its inhibition by surfactants, J. Pharm. Sci. 85 (1996) 1325–1330.

[12] L.J. Braun, A. Tyagi, S. Perkins, J. Carpenter, D. Sylvester, M. Guy, D. Kristensen, D. Chen, Development of a freeze-stable formulation for vaccines containing aluminum salt adjuvants, Vaccine 27 (2009) 72–79.

[13] K. Park, Prevention of nanoparticle aggregation during freeze-drying, J. Control. Release 248 (2017) 153.

[14] V. Jully, F. Mathot, N. Moniotte, V. Préat, D. Lemoine, Mechanisms of Antigen Adsorption Onto an Aluminum-Hydroxide Adjuvant Evaluated by High-Throughput Screening, J. Pharm. Sci. 105 (2016) 1829–1836.

[15] M.S. Salnikova, H. Davis, C. Mensch, L. Celano, D.S. Thiriot, Influence of formulation pH and suspension state on freezing-induced agglomeration of aluminum adjuvants, J. Pharm. Sci. 101 (2012) 1050–1062.

[16] P.V. Date, A. Samad, P.V. Devarajan, Freeze thaw: a simple approach for prediction of optimal cryoprotectant for freeze drying, AAPS PharmSciTech 11 (2010) 304–313.

[17] Y. Liu, K. Kathan, W. Saad, R.K. Prud'homme, Ostwald ripening of beta-carotene nanoparticles, Phys. Rev. Lett. 98 (2007) 36102.

[18] J. Jiang, G. Oberdörster, P. Biswas, Characterization of size, surface charge, and agglomeration state of nanoparticle dispersions for toxicological studies, J. Nanopart. Res. 11 (2009) 77–89.

[19] R.C. Rowe (Ed.), Handbook of pharmaceutical excipients, 6. ed. ed., APhA (PhP) Pharmaceutical Press, London, 2009.

[20] L. van den Berg, D. Rose, Effect of freezing on the pH and composition of sodium and potassium phosphate solutions: the reciprocal system KH2PO4・Na2HPO4・H2O, Arch. Biochem. Biophys. 81 (1959) 319–329.

[21] N. Murase, F. Franks, Salt precipitation during the freeze-concentration of phosphate buffer solutions, Biophys. Chem. 34 (1989) 293–300.

[22] P. Kolhe, E. Amend, S.K. Singh, Impact of freezing on pH of buffered solutions and consequences for monoclonal antibody aggregation, Biotechnol. Prog. 26 (2010) 727–733.

[23] S. Ghosh, H. Mashayekhi, B. Pan, P. Bhowmik, B. Xing, Colloidal behavior of aluminum oxide nanoparticles as affected by pH and natural organic matter, Langmuir 24 (2008) 12385–12391.

[24] K.A. Pikal-Cleland, N. Rodríguez-Hornedo, G.L. Amidon, J.F. Carpenter, Protein denaturation during freezing and thawing in phosphate buffer systems: monomeric and tetrameric beta-galactosidase, Arch. Biochem. Biophys. 384 (2000) 398–406.

[25] C.N. Likos, K.A. Vaynberg, H. Löwen, N.J. Wagner, Colloidal Stabilization by Adsorbed Gelatin, Langmuir 16 (2000) 4100–4108.

[26] G.F.S. Cabrera, M.M. Balbin, P.J.G. Eugenio, C.S. Zapanta, J.J. Monserate, J.R. Salazar, C.N. Mingala, Green synthesis of gold nanoparticles reduced and stabilized by sodium glutamate and sodium dodecyl sulfate, Biochem. Biophys. Res. Commun. 484 (2017) 774–780.

[27] J. Li, S. Bhattacharjee, S. Ghoshal, The effects of viscosity of carboxymethyl cellulose on aggregation and transport of nanoscale zerovalent iron, Colloids Surf. A Physicochem. Eng. 481 (2015) 451–459.

[28] R. Teerakapibal, Y. Gui, L. Yu, Gelatin Nano-coating for Inhibiting Surface Crystallization of Amorphous Drugs, Pharm. Res. 35 (2018) 23.

[29] P. Bejrapha, S. Surassmo, M.-J. Choi, K. Nakagawa, S.-G. Min, Studies on the role of gelatin as a cryo- and lyo-protectant in the stability of capsicum oleoresin nanocapsules in gelatin matrix, J. Food Eng. 105 (2011) 320–331.

[30] E. de Rizzo, E.C. Tenório, I.F. Mendes, F.L. Fang, M.M. Pral, C.S. Takata, C. Miyaki, N.M. Gallina, H.N. Tuchiya, O.K. Akimura, Sorbitol-gelatin and glutamic acid-lactose solutions for stabilization of reference preparations of measles virus, Bull. Pan Am. Health Organ. 23 (1989) 299–305.

[31] P. Manohar, N. Ramesh, Improved lyophilization conditions for long-term storage of bacteriophages, Sci. Rep. 9 (2019) 15242.

[32] R.M. Miller, O. Ces, N.J. Brooks, E.S.J. Robles, J.T. Cabral, Crystallization of Sodium Dodecyl Sulfate-Water Micellar Solutions under Linear Cooling, Cryst. Growth Des. 17 (2017) 2428–2437.

[33] T. Lee, K.L. Yeh, J.X. You, Y.C. Fan, Y.S. Cheng, D.E. Pratama, Reproducible Crystallization of Sodium Dodecyl Sulfate·1/8 Hydrate by Evaporation, Antisolvent Addition, and Cooling, ACS Omega 5 (2020) 1068–1079.

[34] R.I. Feigin, D.H. Napper, Depletion stabilization and depletion flocculation, J. Colloid Interface Sci. 75 (1980) 525–541.

[35] A.N. Semenov, A.A. Shvets, Theory of colloid depletion stabilization by unattached and adsorbed polymers, Soft Matter 11 (2015) 8863–8878.

[36] T. Inada, S.-S. Lu, Inhibition of Recrystallization of Ice Grains by Adsorption of Poly(Vinyl Alcohol) onto Ice Surfaces, Cryst. Growth Des. 3 (2003) 747–752.

[37] R.C. Deller, M. Vatish, D.A. Mitchell, M.I. Gibson, Synthetic polymers enable non-vitreous cellular cryopreservation by reducing ice crystal growth during thawing, Nat. Commun. 5 (2014) 3244.

[38] R.K. Cavatur, N.M. Vemuri, A. Pyne, Z. Chrzan, D. Toledo-Velasquez, R. Suryanarayanan, Crystallization Behavior of Mannitol in Frozen Aqueous Solutions, Pharm. Res. 19 (2002) 894–900.

[39] C. Telang, Effective Inhibition of Mannitol Crystallization in Frozen Solutions by Sodium Chloride, Pharm. Res. 20 (2003) 660–667.

[40] K. Izutsu, S. Yoshioka, T. Terao, Effect of Mannitol Crystallinity on the Stabilization of Enzymes during Freeze-Drying, Chem. Pharm. Bull. 42 (1994) 5–8.

[41] S. Allison, M.d. Molina, T.J. Anchordoquy, Stabilization of lipid/DNA complexes during the freezing step of the lyophilization process: the particle isolation hypothesis, Biochim. Biophys. Acta Biomembr. 1468 (2000) 127–138.

[42] T.K. Armstrong, T.J. Anchordoquy, Immobilization of Nonviral Vectors During the Freezing Step of Lyophilization, J. Pharm. Sci. 93 (2004) 2698–2709.

[43] J.C. Kasper, M.J. Pikal, W. Friess, Investigations on Polyplex Stability During the Freezing Step of Lyophilization Using Controlled Ice Nucleation—The Importance of Residence Time in the Low-Viscosity Fluid State, J. Pharm. Sci. 102 (2013) 929–946.

[44] A.L. Clausi, S.A. Merkley, J.F. Carpenter, T.W. Randolph, Inhibition of aggregation of aluminum hydroxide adjuvant during freezing and drying, J. Pharm. Sci. 97 (2008) 2049–2061.

[45] M.A. Hamaly, S.R. Abulateefeh, K.M. Al-Qaoud, A.M. Alkilany, Freeze-drying of monoclonal antibody-conjugated gold nanorods: Colloidal stability and biological activity, Int. J. Pharm. (2018) 269–277.

[46] W. Ngamcherdtrakul, T. Sangvanich, M. Reda, S. Gu, D. Bejan, W. Yantasee, Lyophilization and stability of antibody-conjugated mesoporous silica nanoparticle with cationic polymer and PEG for siRNA delivery, Int. J. Nanomedicine (2018) 4015–4027.

[47] M. Sameti, G. Bohr, M. Ravi Kumar, C. Kneuer, U. Bakowsky, M. Nacken, H. Schmidt, C.-M. Lehr, Stabilisation by freeze-drying of cationically modified silica nanoparticles for gene delivery, Int. J. Pharm. 266 (2003) 51–60.

[48] A.A. Thorat, R. Suryanarayanan, Characterization of Phosphate Buffered Saline (PBS) in Frozen State and after Freeze-Drying, Pharm. Res. 36 (2019).

Chapter 4

Formulation, process, and storage strategies for lyophilizates of lipophilic nanoparticulate systems established based on the two models paliperidone palmitate and solid lipid nanoparticles

Eduard Trenkenschuh[a], Ula Savšek[a,*], Wolfgang Friess[a]

[a] Pharmaceutical Technology and Biopharmaceutics, Department of Pharmacy, Ludwig-Maximilians-Universität München, 81377 Munich, Germany

* Current address: Department of Pharmaceutics, Friedrich-Alexander-Universität Erlangen-Nürnberg, 91058 Erlangen, Germany

This chapter has been published in the 'International Journal of Pharmaceutics' **(https://doi.org/10.1016/j.ijpharm.2021.120929)**.

Author contributions:

E.T. performed most of the experiments, evaluated the data and wrote the manuscript. U.S. performed experiments on the impact of buffer type, pH, and ionic strength on freeze-thaw stability and contributed with discussions; E.T. and W.F. conceived the presented idea and planned the experiments. W.F. supervised the work, provided conceptual guidance and corrected the manuscript.

Abstract

Lyophilization formulation and process development for lipophilic nanoparticle (NPs) products is highly challenging as the NPs have a low colloidal stability. We compared two different NP types, pure paliperidone palmitate nanocrystals and trimyristin solid lipid nanoparticles regarding formulation, process, and storage stability aspects. Freeze-thaw studies were conducted to investigate the basic formulation aspects such as buffer type, pH, and ionic strength as well as different cryoprotectants. In freeze-drying conventional ramp freezing was performed and compared to freezing with an annealing step added or with controlled ice nucleation. Different formulations were lyophilized and tested for short-term storage stability up to 6 weeks. Samples were analyzed for particle size, subvisible particle number, specific surface area, residual moisture, crystallinity, and glass transition temperature. Sucrose significantly better stabilized both NP types against freeze-thaw stress compared to mannitol demonstrating the importance of a fully amorphous matrix. While the impact of buffer type and pH was negligible, the aggregation propensity of NPs was reduced in presence of NaCl. The freezing step also impacted NP aggregation but the effect was less important than the formulation design. Surfactants did not necessarily improve the colloidal stability but resulted in a lower glass transition temperature of the lyophilizates and may cause phase separation which limits storage stability. This hurdle can be overcome by using a hydroxypropyl-β-cyclodextrin/ sucrose mixture as cryoprotectant. In general, we could show a similar freeze-drying behavior of the two NP types. Thus, we established a formulation and process approach to achieve stable lyophilizates of lipophilic NPs based on two different types of NPs. The general rules should be transferable to other NPs facilitating lyophilization development.

Keywords

Drug nanosuspension, Solid lipid nanoparticles, Freeze-thaw, Freeze-drying, Buffer type, Ionic strength, Process stability, Stability testing

Abbreviations

AN	Annealing step
CN	Controlled nucleation
DLS	Dynamic light scattering
DSC	Differential scanning calorimetry
FT	Freeze-thaw
LO	Light obscuration
Man	Mannitol
NP	Nanoparticle
PDI	Polydispersity index
P407	Poloxamer 407
PS20	Polysorbate 20
PP	Paliperidone palmitate
RM	Residual moisture
RN	Random nucleation
RT	Room temperature
SSA	Specific surface area
SLN	Solid lipid nanoparticle
Suc	Sucrose
SVP	Subvisible particle
T_c	Crystallization temperature
T_g	Glass transition temperature of the freeze-dried cake
T_g'	Glass transition temperature of the freeze-concentrated solution
w/o	Without
XRD	X-Ray powder diffraction

Table of Contents

Abstract 74
Keywords 75
Abbreviations 75
1 Introduction 77
2 Material and methods 79
2.1 Materials 79
2.2 Methods 80
2.2.1 Sample preparation 80
2.2.2 Freeze-thaw cycle 80
2.2.3 Freeze-drying 81
2.2.4 Dynamic light scattering 81
2.2.5 Zeta potential 81
2.2.6 Light obscuration 81
2.2.7 Specific surface area 82
2.2.8 Residual moisture analysis 82
2.2.9 Differential scanning calorimetry 82
2.2.10 X-ray powder diffraction 82
2.2.11 Cake appearance 83
2.2.12 Reconstitution time 83
2.2.13 Stability studies of lyophilized samples 83
3 Results 83
3.1 Impact of buffer type, pH, and ionic strength on freeze-thaw stability 83
3.2 Variation of the freezing step 87
3.2.1 Impact on process stability 87
3.2.2 Impact on macroscopic appearance and reconstitution time 89
3.3 Thermal properties of lyophilizates 91
3.4 Storage stability study 93
4 Discussion 97
4.1 Formulation aspects 97
4.2 Process aspects 99
4.3 Storage stability aspects 100
5 Conclusion 102
6 Supplementary Data 103
7 References 108

1 Introduction

The emerging field of nanomedicine combines nanotechnology with pharmaceutical and biomedical sciences and aims to develop drugs with higher efficacy and improved safety [1]. However, the development of nanoparticulate systems is challenging. Most nanoparticles (NPs) are produced and suspended in aqueous medium. They are known to have poor storage stability due to particle aggregation or other physical and chemical degradation processes. In many cases NPs can only be used for several hours or a few days. Hence, the vast majority of studies work with freshly prepared NPs [2]. This poor stability limits the experimental use and the development of drug products.

Removal of water by freeze-drying is an important technique to stabilize colloidally instable systems. The solid matrix permits long-term storage and easy transportation. Yet, freeze-drying is also known to induce NP aggregation due to freezing and drying stress. During freezing, particle aggregation can be triggered by increased particle-particle interaction in the cryo-concentrated phase [3], by pH changes arising from a temperature dependent dissociation behavior or crystallization of buffer salts [4,5], by surface induced destabilization at the ice-liquid interfaces [6] or by mechanical stress due to formation of ice crystals [7]. Consequently, stress during freezing is assumed to be a key factor during lyophilization. During drying, the removal of unfrozen water can lead to destabilization due to a loss of the stabilizing hydration shell at the NP surface [8]. These main drawbacks of lyophilization can be prevented by the addition of cryoprotectants and adjusting the lyophilization cycle. Unfortunately, except of empirical principles, there is little known about purposeful formulation and process design when freeze-drying NPs. The precise mechanisms underlying the effects of lyophilization-induced stress on nanoparticulate formulations and protection afforded by cryoprotectants are not well understood [2].

NPs can be differentiated into several material categories, e.g. polymeric NPs, crystalline NPs, and liposomal NPs. Their surface characteristics including charge, hydrophobicity, and functional groups are important for NP stability [9]. The three main mechanisms leading to colloidal stability are electrostatic, steric and depletion stabilization. A depletion force originates from the excluded volume effect in presence of free non-adsorbing polymers leading to a kinetic NP stabilization [10–12]. Consequently, during lyophilization, the diverse NP types show different colloidal instability, on top of potential chemical or other physical instability. This leads to complex formulation and process considerations due to the lack of universal rules.

Nanosized drug and solid lipid nanoparticle (SLNs) nanosuspensions are essentially stabilized by surfactants. The interaction between the steric stabilizer surrounding the NPs

and the bulking agent is crucial for NP preservation during freeze-drying [13]. In most studies, freeze-drying of NPs is conducted with one single NP type which gives limited information about general rules for lyophilization of NPs. Furthermore, variations almost exclusively focus on the freezing rate when it comes to the process or changing the cryoprotectant type or concentration with respect to the formulation. Beirowski et al. showed that the freezing rate is of minor importance compared to formulation composition when freeze-drying drug nanosuspensions [14]. Similar results were found for SLNs; type and concentration of stabilizers play a vital role for lyophilization success [15,16].

However, it is not clear, if drug nanosuspensions and SLNs can be considered as one NP type, i.e. lipophilic NPs, having fundamental lyophilization principles in common. Furthermore, formulation aspects such as buffer type and ionic strength or other modifications of the freezing step are not reported in literature. Therefore, this study aims to clarify four different aspects when freeze-drying lipophilic NPs:

1) Drug nanosuspensions are solid crystals, while SLNs are solid lipids. Although physically different, the lipophilic character and their identical stabilization mechanism in aqueous medium point to similar behavior upon freeze-drying. To the best of our knowledge, they have never been compared according to their freeze-drying behavior. Finding similarities would facilitate formulation and process development since findings from one type can be transferred to the other.

2) Buffer type and pH are known to play an important role for stabilization and freeze-drying of therapeutic proteins. For example, histidine and sodium phosphate buffers are known to cause a pH shift upon freezing affecting stability. Furthermore, the ionic strength can have a detrimental effect on freeze-thaw (FT) or freeze-drying stability due to charge shielding. However, there is a lack of experimental data in case of NPs. Therefore, we evaluated the impact of buffer type, pH, and sodium chloride (NaCl) on NP stability during freezing.

3) Besides changing the freezing rate, the freezing step can also be modified by adding an annealing step or inducing ice nucleation in a controlled fashion. These modifications have a great influence on ice crystal formation. It has been shown that the ice-liquid interfacial area leads to enrichment, association and surface-induced denaturation of colloids during lyophilization. This obstacle can be addressed by the addition of a surfactant [6]. However, to date, the impact of interfacial stress on process stability of NPs is not known. In order to investigate the impact of ice crystal

formation on particle aggregation and solid-state properties, freeze-drying was performed under three different freezing conditions.

4) Formulations of lipophilic NP formulations are characterized by their high steric stabilizer concentration; usually surfactants are used. However, surfactants can have a plasticizing effect on amorphous matrices which might impair the storage stability of lyophilizates. Thus, we investigated the impact of the surfactants polysorbate 20 and poloxamer 407 on the glass transition temperature of different formulations. Subsequently, selected samples were tested for their storage stability.

NPs were analyzed with respect to their particle size and number of subvisible particles. Lyophilizates were further characterized by Karl-Fischer titration, differential scanning calorimetry (DSC), X-ray diffraction (XRD), and BET measurements and were checked for macroscopic appearance and reconstitution time.

2 Material and methods

2.1 Materials

Sucrose (Sigma-Aldrich, Steinheim, D), D-mannitol (VWR International, Ismaning, D), hydroxypropyl-beta-cyclodextrin (Cavasol™ W7 HP, Wacker, Munich, D), poloxamer 407 (Kolliphor® P 407, BASF, Ludwigshafen am Rhein, D), polysorbate 20 (Tween 20™, Merck, Darmstadt, D), and NaCl (Merck, Darmstadt, D) were used to prepare excipient formulations at various concentrations. Na-, K-phosphate (all VWR International, Ismaning, D), and Na-citrate buffers (Merck, Darmstadt, D) were prepared at pH 5 and 8. Paliperidone palmitate (Crystal Pharma, Boecillo, Valladolid, E) and trimyristin (Dynasan® 114, Cremer Oleo, Witten, D) were used as received. Highly purified water (HPW) was used for the preparation of excipient stock solutions and buffers. Solutions were filtered using 0.2 µm polyethersulfone membrane syringe filters (VWR International, Ismaning, D). All excipients were of analytical or higher grade and were used without further purification. 2R glass vials (Schott, Müllheim, D) with according rubber stoppers (igloo, B2–TR coating, West Pharmaceutical Services, Eschweiler, D) were cleaned with HPW and dried for 8 h at 60 °C.

2.2 Methods

2.2.1 Sample preparation

Paliperidone palmitate nanosuspension

100 mg/mL of the poorly water-soluble drug paliperidone palmitate (PP) were dispersed in with 1% polysorbate 20 (PS20) or poloxamer 407 (P407). The suspensions were sonicated for 10 min at 25 °C (Ultrasonic cleaning bath, VWR International, Radnor, PA). After sonication the suspensions were comminuted using a high-pressure homogenizer (APV Micro Lab 40, Luebeck, D). Two cycles at 500 bar were applied as presteps followed by 40 cycles at 1,500 bar to obtain a nanosuspension. After homogenization, the drug nanosuspension was centrifuged at 10,000 xg on a Heraeus™ Megafuge™ 16R Centrifuge (Thermo Fisher Scientific, Waltham, MA) and filtrated with 1.2 µm filter (Minisart®, Sartorius, Goettingen, D). Centrifugation was conducted for 1 min for experiments comparing different buffer compositions while all other samples were centrifuged for 2 min. The concentration of PP was measured according to Trivedi et al. [17] using a spectrophotometer (UV-1600PC, VWR International, PA). Briefly, PP was solved after addition of THF, diluted with acetonitrile/water (60:40 v/v) and detected at 278 nm.

Solid lipid nanoparticles (SLNs)

Dynasan® 114 and 1% PS20 or P407 were separately heated in a water bath at 70 °C. After unifying the two phases, the obtained emulsion was mixed using a high-speed homogenizer at 17,000 rpm for 1 min (Euro Turrax T20b, IKA Labortechnik, Staufen im Breisgau, D). The pre-emulsion was subsequently homogenized in a 70 °C pre-heated high-pressure homogenizer (APV Micro Lab 40, Luebeck, D) conducting three cycles at 500 bar. After cooling at RT, the resulting SLNs were filtered through a 1.2 µm filter (Minisart®, Sartorius, Goettingen, D).

PP nanosuspensions and SLNs were formulated at 10 mg/mL final particle concentration and 0.5% final surfactant concentration.

2.2.2 Freeze-thaw cycle

Freeze-thaw (FT) was conducted three times using an FTS LyoStar™ 3 (SP Scientific, Stone Ridge, NY). Samples (1 mL in 2 R vials) were frozen at –1 °C/min to –50 °C followed by a 90 min hold at –50 °C, and thawed at 1 °C/min to 10 °C followed by a 90 min hold.

2.2.3 Freeze-drying

Lyophilization was performed on an FTS LyoStar™ 3 (SP Scientific, Stone Ridge, NY). 1 mL sample in 2R vials was frozen at –1 °C/min to –50 °C and held for 2 h. Primary drying was conducted at 0.08 mbar and –35 °C. The endpoint of primary drying was controlled by comparative pressure measurement between Pirani gauge and capacity manometer. Secondary drying was performed for 8 h at 25 °C and 0.08 mbar. Samples were stoppered at 600 mbar nitrogen and sealed with crimp caps. Conventional ramp freezing (RN) was modified by adding an annealing step (AN) at –15 °C for 2 h; ramp rates were set to 1 °C/min. Controlled nucleation (CN) was performed at –5 °C using an ice fog and subsequent freezing at 1 °C/min [18].

2.2.4 Dynamic light scattering

Particle size and polydispersity index (PDI) were measured using a dynamic light scattering (DLS) platereader DynaPro II (Wyatt Technology, Dernbach, D). The samples were diluted 1:1000 in corresponding formulations. 100 µL sample (n=3) per well of a 96 UV-well plate (Costar™, Corning, Glendale, AZ) was analyzed at RT using 10 acquisitions with 5 s each. DYNAMICS software (Version 7.8.0.26) was used for data evaluation. The corresponding preset refractive index parameters were used for all samples. Viscosities required for DLS measurements were determined via an AMVn Automated Micro Viscometer (Anton Paar, Graz, A).

2.2.5 Zeta potential

Zeta potential measurements were carried out by electrophoretic light scattering using a Zetasizer Nano ZS (Malvern Instruments, Worcestershire, UK). Samples without NaCl were spiked with 1M NaCl solution to obtain a 10 mM NaCl containing test sample.

2.2.6 Light obscuration

Subvisible particles (SVPs) were analyzed by light obscuration (LO) with a PAMAS SVSS-35 particle counter equipped with a HCB-LD-25/25 sensor (PAMAS - Partikelmess- und Analysesysteme, Rutesheim, D). Samples were diluted 1:1000 in the corresponding formulation and measured in triplicates. The system was cleaned with 10 mL HPW between each analysis. The rinse volume was 0.4 mL, followed by three measurements of 0.3 mL. Measurements were evaluated using the PAMAS PMA software.

2.2.7 Specific surface area

The specific surface area (SSA) analysis of freeze-dried samples was determined using Brunauer-Emmet-Teller (BET) krypton gas adsorption in a liquid nitrogen bath at 77.3 K (Autosorb 1 Quantachrome, Odelzhausen, D). Crushed lyophilizates of 80-100 mg were weighed into glass tubes and degassed under vacuum for at least 2 h at RT. An 11-point gas adsorption curve was measured from 0.05 to 0.30 relative pressure. Data evaluation was performed according to the multi-point BET method fit of the Autosorb 1 software.

2.2.8 Residual moisture analysis

The residual moisture (RM) of the lyophilizates was determined by Karl-Fischer titration. Measurements were performed using an Aqua 40.00 titrator (Analytik Jena AG, Halle, D) equipped with a headspace oven set at 100 °C. Samples of 10-20 mg crushed lyophilizates were analyzed in stoppered 2R vials.

2.2.9 Differential scanning calorimetry

The lyophilizates were analyzed using a Mettler Toledo differential scanning calorimeter (DSC) 822e (Mettler-Toledo GmbH, Giessen, D). Approximately 10 mg of the lyophilized samples was analyzed in sealed aluminum crucibles. Samples were heated from 0 to 150 °C using a scanning rate of 10 °C/min. Formulation screening studies included modulated DSC (mDSC) from 0 °C to 200 °C at 2 °C/min with an amplitude of ± 1 °C every 120 s. The glass transition of the maximally freeze-concentrated solution (T_g') up to –60 °C was measured on the Mettler instrument while freezing up to –100 °C was conducted on a Netzsch DSC 204 Phoenix (Netzsch, Selb, D). Therefore, 20 µL of the liquid samples were cooled at –10 °C/min from 20 °C to –60 °C or –100 °C, including a 1 min holding step, and reheated at 10 °C/min to 20 °C. The inflection point of the glass transition in the heat heating scan was defined as T_g and T_g'.

2.2.10 X-ray powder diffraction

The morphology of lyophilizates was measured using X-ray powder diffractometry (XRD). Analysis was carried out on an XRD 3000 TT diffractometer (Rich. Seifert & Co. GmbH & Co. KG, Ahrensburg, D). The instrument was equipped with a copper anode (40 kV, 30 mA, λ=0.154178 nm) and a scintillation detector at 1000 V. Crushed freeze-dried samples were smoothened homogenously on copper sample holders at 0.2 mm height. Samples were analyzed in steps of 0.05° using 2 s per step from 5 to 45° 2-Theta.

2.2.11 Cake appearance

Images of representative lyophilizates were taken with a Nikon D5300 camera (Nikon GmbH, Düsseldorf, D) in front of a black background.

2.2.12 Reconstitution time

The lyophilizates were dissolved by adding the required volume of HPW. The reconstitution volume was calculated based on the formulation density and solid content. The time from adding HPW to complete disappearance of a solid cake was considered as reconstitution time and visually determined. During reconstitution, the vials were gently swirled to ensure wetting of the complete lyophilizate.

2.2.13 Stability studies of lyophilized samples

For stability testing, selected lyophilizates were stored at 2-8 °C, 25 °C and 40 °C for 6 weeks.

3 Results

3.1 Impact of buffer type, pH, and ionic strength on freeze-thaw stability

Prior to lyophilization, FT studies were performed to investigate the effect of the formulation parameters buffer type, pH, cryoprotectant type, and ionic strength on the colloidal stability of PP NPs and SLNs during this initial step of freeze-drying. DLS, LO and zeta potential measurements were performed before and after FT. 10 mg/mL Nanosuspensions in 0.5% P407 were freeze-thawed three times in 10 mM Na-phosphate, K-phosphate or Na-citrate buffer at pH 5 and 8 in combination with 10% mannitol (Man) or 10% sucrose (Suc) or without a cryoprotectant.

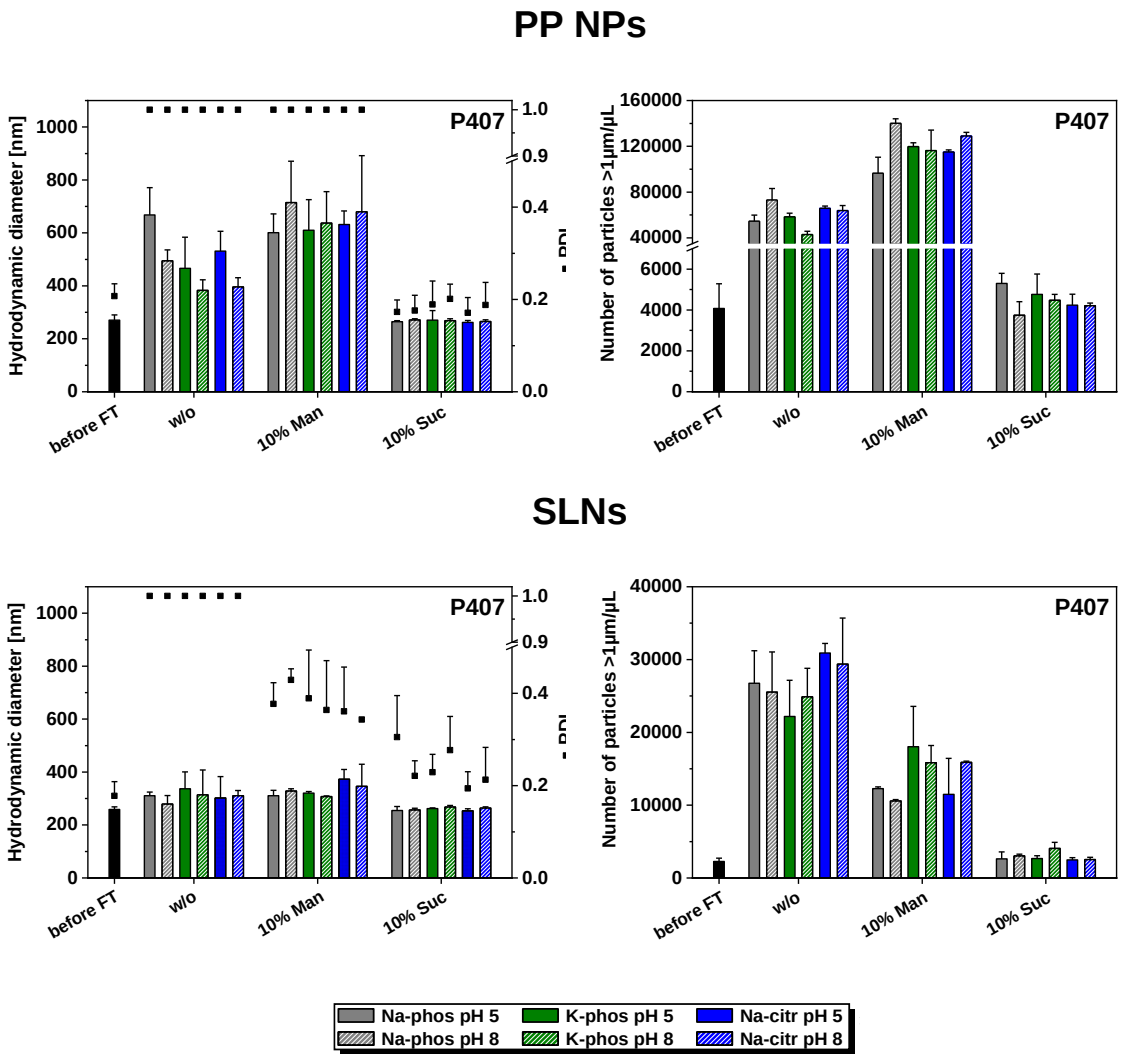

Figure 1: DLS and LO measurements of three times freeze-thawed PP NPs and SLNs stabilized with 0.5% P407 in 10 mM Na-phosphate, K-phosphate or Na-citrate buffer at pH 5 or 8 without cryoprotectant or in presence of 10% Man or 10% Suc (n=3). PDI values >0.56 represent a multimodal size distribution and are therefore stated as '1.0'.

After three times FT without a cryoprotectant and in presence of 10% Man particle size and PDI of PP NPs drastically increased up to 714 ± 156 nm and 1.0 respectively (Figure 1). A PDI of 1.0 indicates a multimodal particle size distribution and thus marked NP aggregation. In contrast, particle size and PDI remained stable in presence of 10% Suc. Similar trends were observed for SLNs. Without cryoprotectant and in presence of 10% Man the PDI increased whereas the mean particle size was not affected by freezing and thawing. SLNs formulated with 10% Suc showed comparable size and PDI before and after FT. Buffer type and pH did not impact the colloidal stability of PP NPs and SLNs.

The number of SVPs ≥1 µm was dramatically increased in samples without cryoprotectant or in presence of mannitol after FT (Figure 1). This effect was more pronounced for PP NPs

compared to SLNs. SVP numbers of PP NPs increased from ~4,000 up to ~140,000 particles/µL in 10% Man, while SLNs exhibited most SVPs when no cryoprotectant was used. In contrast, the number of SVP ≥1 µm did not increase with FT in presence of 10% Suc for all investigated buffer types. Additionally, Zeta potential measurements revealed surface charges close to neutral independent of the buffer type, pH, and cryoprotectant composition (Table 1).

Table 1: ζ-Potential values of three times freeze-thawed PP NPs and SLNs (n=3).

ζ-Potential [mV]						
			PP NPs		**SLNs**	
Cryoprotectant	Buffer	pH	before FT	after FT	before FT	after FT
w/o	Na-phos	5	0.6 ± 0.2	0.2 ± 0.1	0.8 ± 0.2	0.3 ± 0.1
		8	0.7 ± 0.1	0.4 ± 0.1	0.5 ± 0.1	1.5 ± 0.6
	K-phos	5	0.4 ± 0.1	0.8 ± 0.0	0.8 ± 0.3	0.7 ± 0.4
		8	1.0 ± 0.0	1.0 ± 0.1	1.5 ± 0.4	1.1 ± 0.4
	Na-citr	5	0.6 ± 0.1	0.2 ± 0.1	0.8 ± 0.2	1.0 ± 0.2
		8	1.7 ± 0.1	1.2 ± 0.2	1.7 ± 0.5	1.1 ± 0.3
10% Man	Na-phos	5	0.6 ± 0.1	0.6 ± 0.0	0.3 ± 0.1	0.2 ± 0.1
		8	0.9 ± 0.1	0.8 ± 0.1	0.9 ± 0.1	1.1 ± 0.2
	K-phos	5	0.8 ± 0.0	0.8 ± 0.1	0.4 ± 0.0	0.5 ± 0.1
		8	1.1 ± 0.0	1.0 ± 0.1	1.2 ± 0.1	1.2 ± 0.1
	Na-citr	5	0.4 ± 0.1	0.4 ± 0.1	0.7 ± 0.1	0.7 ± 0.1
		8	1.7 ± 0.2	1.3 ± 0.2	1.4 ± 0.0	1.6 ± 0.2
10% Suc	Na-phos	5	0.1 ± 0.0	0.4 ± 0.1	0.2 ± 0.1	0.3 ± 0.2
		8	0.8 ± 0.0	0.6 ± 0.0	0.9 ± 0.2	1.1 ± 0.2
	K-phos	5	0.3 ± 0.0	0.2 ± 0.0	0.5 ± 0.2	0.5 ± 0.1
		8	0.9 ± 0.1	1.1 ± 0.1	1.0 ± 0.1	1.2 ± 0.2
	Na-citr	5	0.4 ± 0.0	0.6 ± 0.1	0.7 ± 0.2	0.5 ± 0.0
		8	1.1 ± 0.2	1.2 ± 0.2	1.5 ± 0.1	1.5 ± 0.1

The impact of ionic strength was investigated by adding 70 or 140 mM NaCl to NPs formulated with 0, 2.5, 5 or 10% Suc in combination with 0.5% P407 or PS20. None of the PS20 containing formulations of PP NPs was negatively impacted by FT, independent of further excipient addition (Figure 2). Also P407 containing formulations showed high stability; only when no NaCl and sucrose was added the particle size slightly increased from 200.6 ± 5.1 nm to 257.1 ± 1.8 nm and the effect was less pronounced in presence of 70 or 140 mM NaCl whereas particle size and PDI were well preserved by addition of sucrose. In contrast, SLNs were less stable compared to PP NPs. Without addition of further excipients, the particle size of SLNs increased more markedly in PS20 compared to P407 containing

formulations. SLNs stabilized by PS20 exhibited a particle size of 595.6 ± 84.6 nm without the addition of NaCl and of 464.5 ± 42.1 nm and 302.2 ± 35.4 nm with addition of 70 and 140 mM NaCl respectively. The SLN size was maintained in formulations containing sucrose. Furthermore, higher sucrose concentrations led to less pronounced increase in the PDI values for SLNs stabilized by P407; the PDI did not change in PS20 based formulations with 5 or 10% sucrose and in case of NaCl containing 2.5% sucrose containing samples.

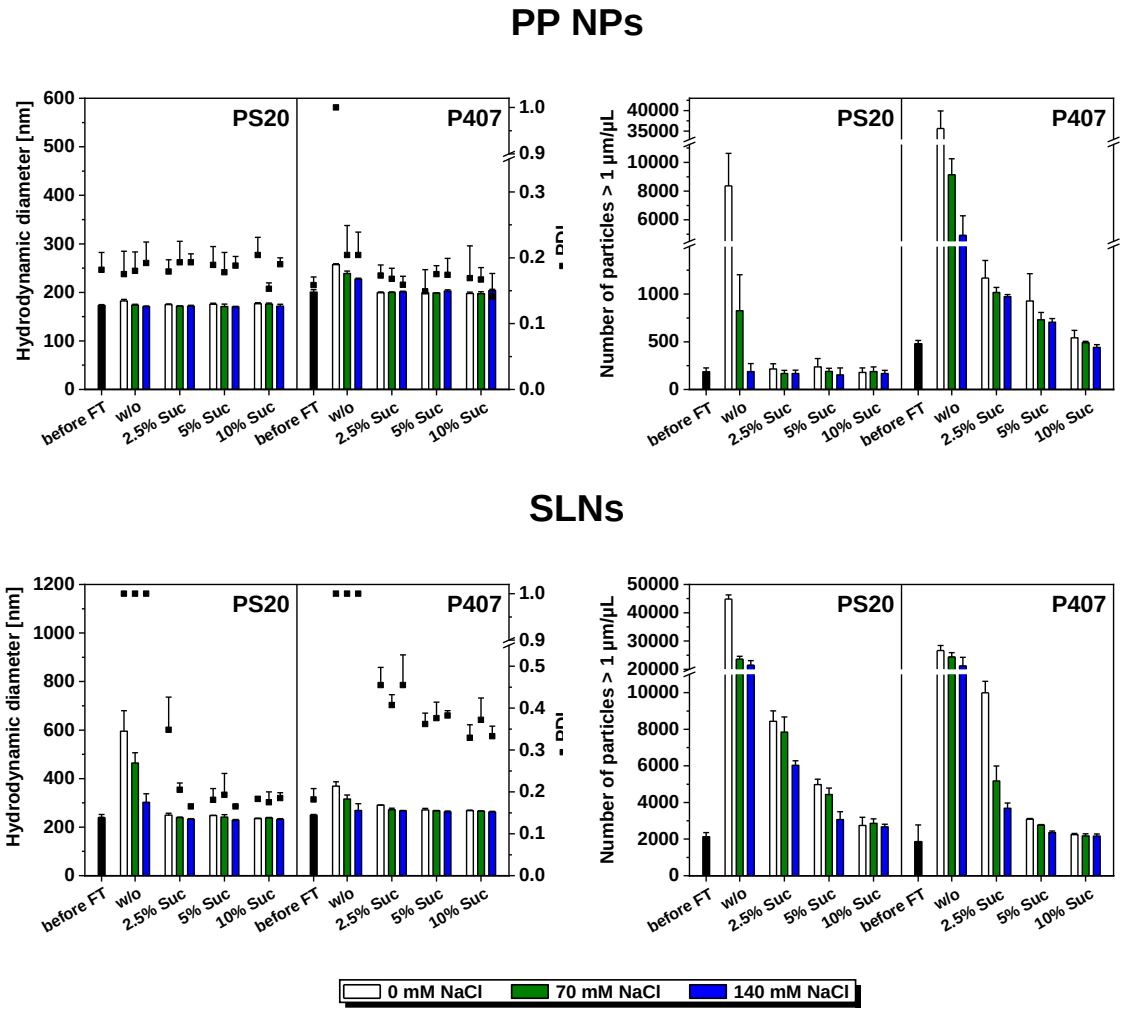

Figure 2: DLS and LO measurements of three times freeze-thawed PP NPs and SLNs stabilized with 0.5% PS20 or P407. NPs were formulated with 0, 70 or 140 mM NaCl, without cryoprotectant or in presence of 2.5, 5 or 10% Suc (n=3). PDI values >0.56 represent a multimodal size distribution and are therefore stated as '1.0'.

The formation of larger SVPs was substantially reduced in presence of NaCl and sucrose. The PP NPs were in generally less affected by FT than the SLNs. PP NPs did show SVP formation in presence of sucrose in PS20 containing formulations; only without sucrose the number of SVPs increased from ~250 particles/mL before FT to ~8,000 (0 mM NaCl) or

800 particles/mL (70 mM NaCl). In P407 containing PP NPs formulations SVPs formed upon FT with clear reduction by addition of sucrose or NaCl. SLNs similarly exhibited least SVP formation at the highest NaCl and sucrose concentrations. Overall, salt had less positive impact on SVP formation than Suc for both NP types.

Interestingly, PP NPs stabilized by PS20 did not show SVP formation at 140 mM NaCl even without a cryoprotectant. DSC measurements showed crystallization of the NaCl-water eutectic as indicated by a eutectic melting endotherm upon heating of the frozen solution (Figure S-1). This effect was not observed in presence of Suc. Moreover, increasing NaCl concentrations led to decreasing T_g' values in Suc formulations. Similar to the aforementioned buffer experiments, the NPs exhibited surface charges of ~0 mV independent of the formulation composition (Table S-1).

3.2 Variation of the freezing step

3.2.1 Impact on process stability

In the next step we evaluated the impact of the freezing process itself on NP stability. Three different freezing protocols were applied. Conventional ramp freezing (RN) was further modified by adding an annealing step at –15 °C (AN) or freezing was performed with controlled nucleation at –5 °C (CN). The NPs were lyophilized using a conservative freeze-drying cycle. Before primary drying samples were frozen to –50 °C well below T_g' in order to ensure vitrification of the sucrose matrix. Two different surfactant stabilizers (PS20, P407) in combination with three different sucrose concentrations (2.5, 5 and 10%) were evaluated.

Before freeze-drying, both NP types exhibited a particle size of approximately 200-250 nm and a PDI of ~0.2 (Figure 3). An increasing sucrose concentration led to better NP stabilization upon freeze-drying; particle size and PDI of both NP types were best preserved in presence of 10% Suc. Additionally, the type of surfactant used for initial particle stabilization had a great impact. In 2.5% Suc, PP NPs revealed a PDI < 0.5 in PS20 formulations as compared to 1.0 in P407 samples. The impact of the surfactant type became less pronounced in presence of 5% and 10% Suc. Nevertheless, a lower number of SVPs after lyophilization (RN) was achieved by using 1.0% P407 as compared to 0.5% (Figure S-2). SLNs stabilized with P407 exhibited less aggregation and a lower PDI compared to PS20 formulations at all sucrose levels. Overall, the freezing condition did not substantially affect particle size and PDI.

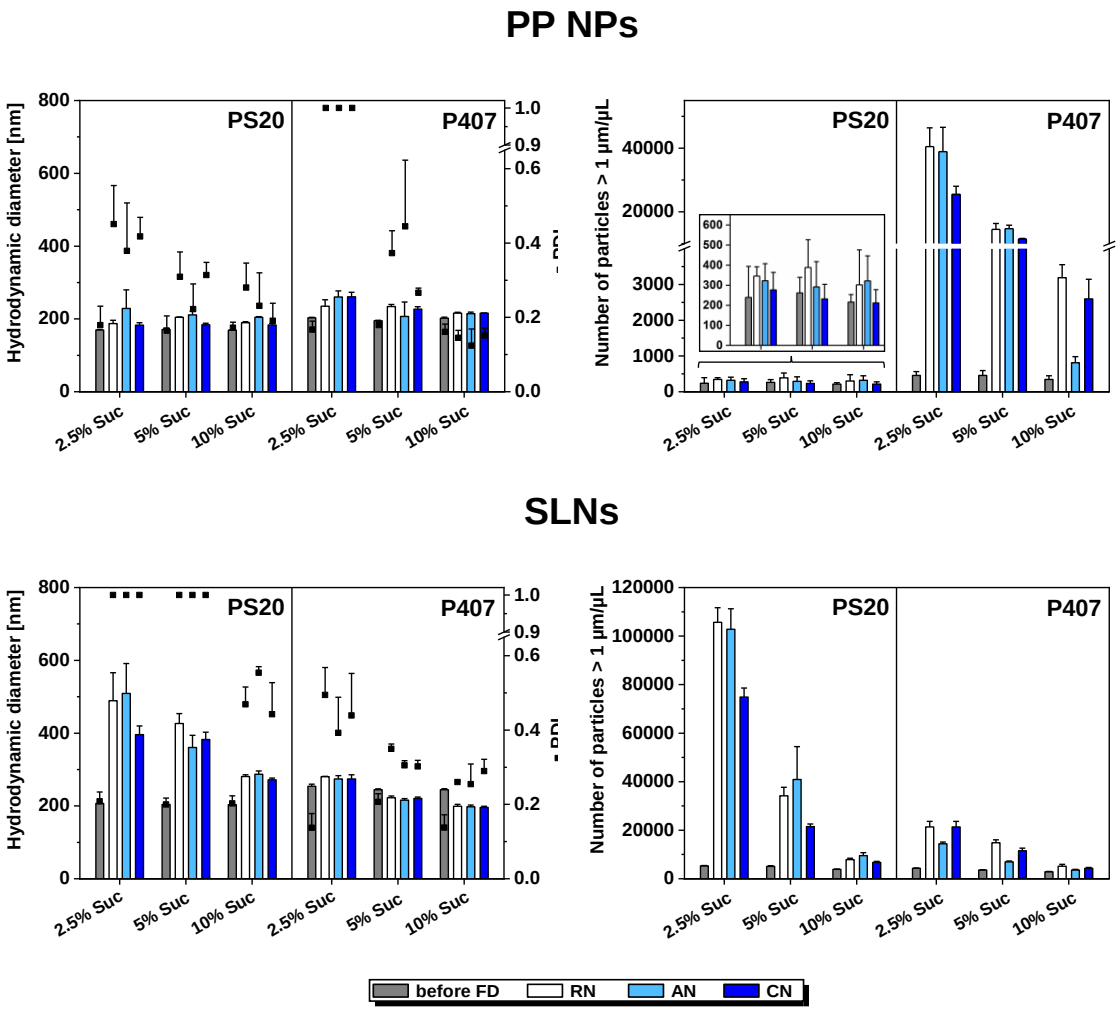

Figure 3: DLS and LO measurements of lyophilized PP NPs and SLNs stabilized with 0.5% PS20 or P407 in presence of 2.5, 5 or 10% Suc (n=3). Conventional ramp freezing (RN), including an annealing step (AN), or under controlled nucleation (CN) was applied. PDI values >0.56 represent a multimodal size distribution and are therefore stated as '1.0'.

The number of SVPs, reflecting larger NP agglomerates, increased slightly from ~250 particles/mL up to ~390 particles/mL after freeze-drying in presence of PS20 for PP. Surprisingly, the aggregation propensity was not affected by the sucrose concentration. In contrast, the number of SVPs drastically increased from ~400 particle/mL up to ~40,000 particles/mL in P407 formulations with 2.5% Suc. In contrast, SLNs showed higher SVP numbers in PS20 containing formulations compared to P407 formulations. In general, an increasing sucrose concentration led to decreasing SVP formation except for PP NPs stabilized with PS20. The SVP number was furthermore affected by the applied freezing condition. Generally, CN led to a lower number of SVPs compared to RN, while AN showed no clear trend on SVP formation.

The SSA of NP lyophilizates formulated with 10% Suc was analyzed in order to investigate the impact of the freezing step on the interfacial surface area which is potentially the site of NP agglomeration (Table 2). The lyophilizates produced via RN showed the highest, while CN samples revealed the smallest SSA. The SSA was slightly higher for PS20 compared to P407 containing samples.

Table 2: SSA of NP lyophilizates in presence of 10% Suc (n=3).

SSA [m^2/g]			
Formulation	**Freezing step**	**PP NPs**	**SLNs**
PS20	RN	0.97 ± 0.03	0.84 ± 0.04
	AN	0.78 ± 0.02	0.76 ± 0.05
	CN	0.50 ± 0.02	0.66 ± 0.04
P407	RN	0.88 ± 0.04	0.87 ± 0.03
	AN	0.67 ± 0.04	0.73 ± 0.03
	CN	0.47 ± 0.01	0.57 ± 0.02

For all freeze-dried samples the RM levels were low (≤0.6%; Figure S-3). In general, CN resulted in higher residual moisture contents compared to RN and AN. Furthermore, the higher the sugar concentration the higher were the RM levels of the lyophilizates. All samples were amorphous according to DSC and XRD measurements independent of the freezing condition.

3.2.2 Impact on macroscopic appearance and reconstitution time

Cake appearance is an important attribute of freeze-dried products [19]. The lyophilizates of both NP types showed a pharmaceutically acceptable cake appearance without macroscopic cake collapse at all Suc concentrations. Thus, the cake appearance was not affected by the investigated type and concentration of NPs and surfactant. However, CN samples showed substantial fogging which is only minor for RN and AN samples (Figure 4). Furthermore, AN samples revealed less cracking of the top skin and the most elegant cake appearance.

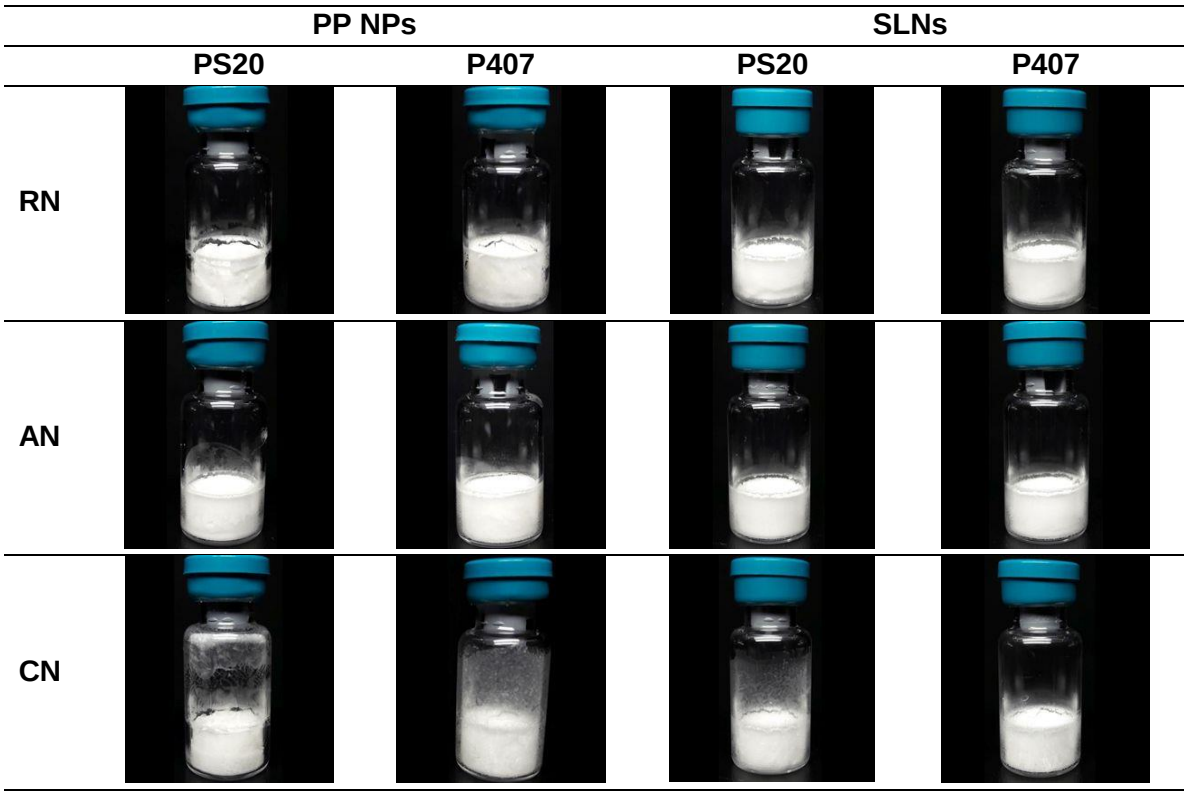

Figure 4: Macroscopic appearance of lyophilized NPs in presence of 10% Suc.

All PP lyophilizates instantly dissolved upon reconstitution. As shown in Figure 5, reconstitution of lyophilized SLNs was fast in presence of 5% (< 11 s) and 10% Suc (< 6 s). The reconstitution time was about 60 s for RN 2.5% Suc samples. Furthermore, the reconstitution time could be reduced by applying AN or CN.

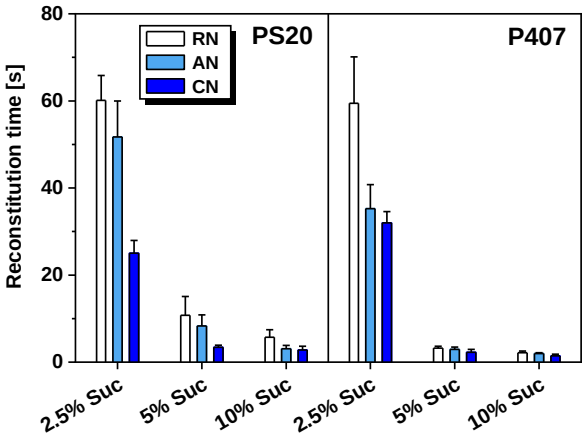

Figure 5: Reconstitution times of lyophilized SLNs stabilized with PS20 or P407 in presence of 2.5, 5 or 10% Suc (n=3). Conventional ramp freezing (RN), including an annealing step (AN), or under controlled nucleation (CN) was applied.

3.3 Thermal properties of lyophilizates

Prior to stability studies, the T_g of the lyophilizates which is an important parameter limiting the storage stability was assessed by DSC. Exemplarily, DSC thermograms of 10% Suc lyophilizates are presented in Figure 6. Two glass transition events (T_{g1}~50 °C, T_{g2}~60 °C) were detected in all formulations, except in SLNs stabilized with PS20. T_{g1} was more distinct in P407 samples compared to PS20 samples. Furthermore, an exothermic crystallization peak (T_c) was found at ~86 °C in PS20 and at ~92 °C in P407 verum and placebo samples. In contrast to placebo, SLN and PP lyophilizates exhibited a broad endothermic melting event at ~57 °C and ~110 °C respectively. The calorimetric events of the lyophilizates formulated with 2.5, 5 or 10% Suc are summarized in Table S-2. Most notably, the lower the Suc concentration and thus Suc/surfactant ratio the lower the T_g and T_c values of the lyophilizates; e.g. 2.5 and 5% Suc formulations revealed a T_{g1} at ~40-45 °C.

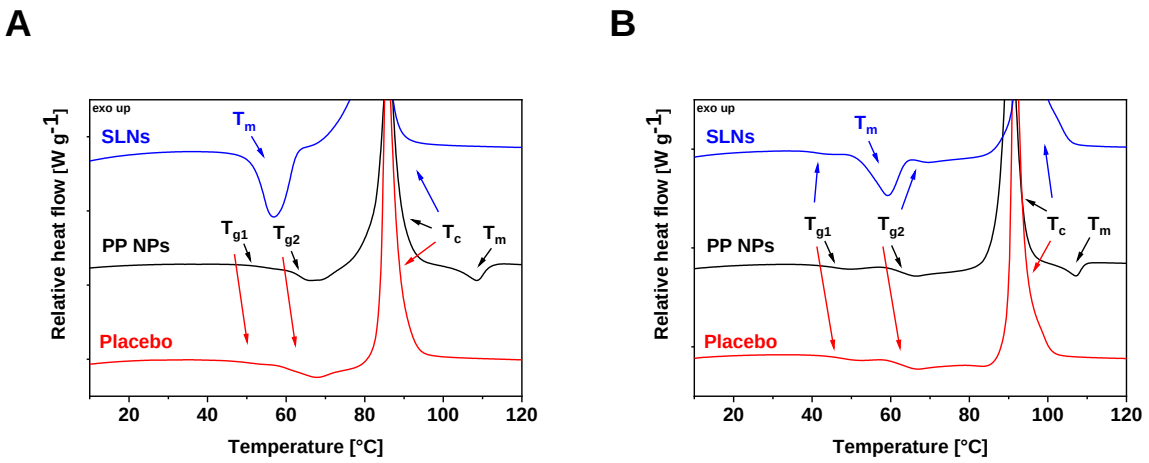

Figure 6: Representative DSC profiles of lyophilized SLNs, PP NPs, and placebo formulations in presence of 10% Suc and 0.5% PS20 (A) or P407 (B).

Additional DSC measurements of both PS20 and P407 solutions with 10% Suc revealed also two T_g' events at approximately −50 °C and −32 °C, whereas a pure PS20 solution showed one broad step in the heat capacity curve at ca. –72 °C (Figure S-4). In comparison, a pure P407 solution exhibited one T_g' at ~–68 °C followed by an exothermic crystallization at ~–44 °C and an endothermic melting event at ~–14 °C.

Since both surfactants contributed to a second glass transition event in both frozen solutions and in the lyophilizates, a more detailed screening of freeze-dried placebos by mDSC was performed. Pure sucrose lyophilizates revealed one T_g at ~66 °C followed by crystallization at ~108 °C independent of the sugar concentration (Figure 7). PS20 containing sucrose formulations showed one glass transition at 0.1% PS20 and two glass transitions at

0.5% PS20; T_g values were slightly higher in presence of 10% Suc. 1% PS20 lyophilized with 5% Suc resulted in collapsed cakes without detectable thermal events while with 10% Suc one glass transition at ~47 °C could be detected. P407 formulations revealed two glass transitions at all surfactant concentrations in presence of 10% Suc and at 0.1% P407 in 5% Suc (T_{g1}~50 °C, T_{g2}~62 °C). Interestingly, both T_g values were independent of the sucrose and surfactant concentration. An endothermic melting peak and one glass transition were detected at 0.5% P407 while no glass transition was identified at 1% P407 in 5% Suc. All products, except the collapsed 1% PS20 in 5% Suc formulations, exhibited an exothermic crystallization event. In general, an increasing sucrose concentration led to an increasing T_c value while an increasing surfactant concentration resulted in decreasing crystallization temperatures.

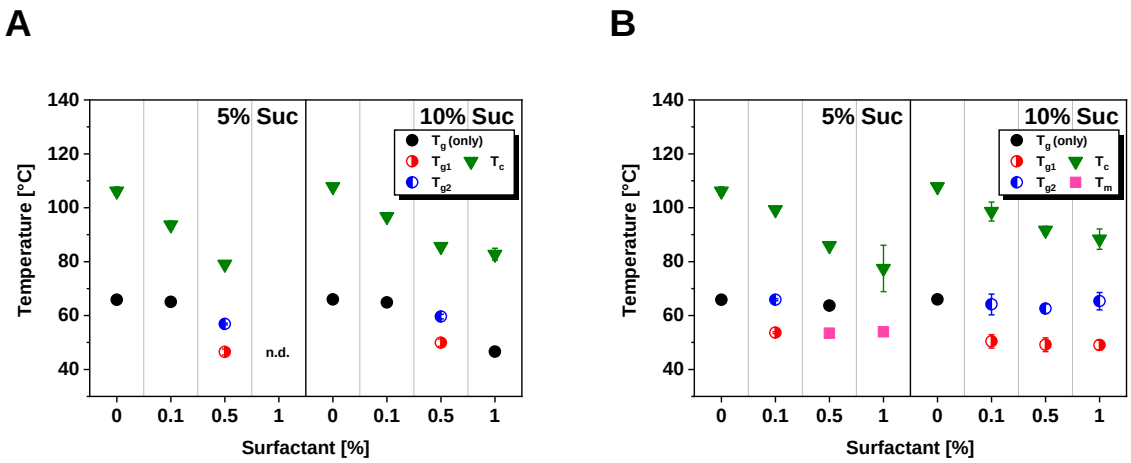

Figure 7: **G**lass transition temperatures (T_g, T_{g1}, T_{g2}), crystallization temperatures (T_c), and melting temperatures (T_m) of lyophilized placebo formulations in presence of 5 or 10% Suc and 0, 0.1, 0.5 or 1% PS20 (A) or P407 (B) (n=3). n.d. = not detectable (collapsed cake).

The glass transition at about 50 °C may be critical during storage, especially at elevated storage temperatures (e.g. 40 °C) when intending storage at room temperature. Therefore, we tested Suc/HP-β-CD mixtures with different surfactant concentrations to obtain lyophilizates with higher glass transition temperatures. Residual moisture levels were below 0.8% in all lyophilizates. The T_g values of lyophilized 1:3 and 1:2 Suc/HP-β-CD samples were substantially higher above 100 °C (Figure 8). At a 1:1 Suc/HP-β-CD ratio, the T_g values were similar to the pure Suc based formulations. With higher surfactant concentration and lower Suc/HP-β-CD ratio the tendency to two glass transition events substantiated and was more pronounced with P407 as compared to PS20. Overall, various combinations with T_g values above 100 °C and high surfactant concentration could be realized.

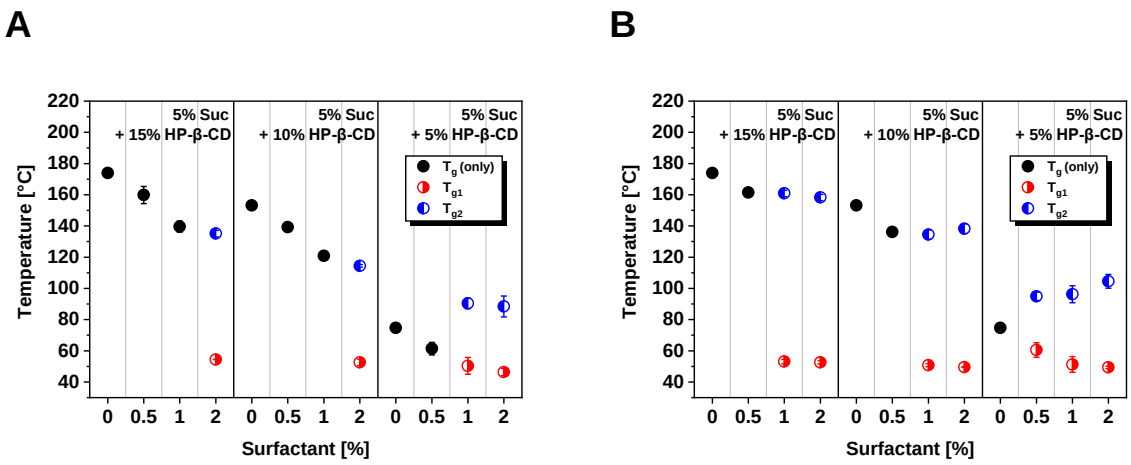

Figure 8: Glass transition temperatures (T_g, T_{g1}, T_{g2}) of lyophilized placebo formulations in presence of 5% Suc and 5, 10 or 15% HP-β-CD and 0, 0.5, 1 or 2% PS20 (A) or P407 (B) (n=3).

3.4 Storage stability study

PP NPs and SLNs formulated with 0.5% PS20 or P407 and 10% Suc, 10% HP-β-CD or '5% Suc + 10% HP-β-CD' were selected for a storage stability test at 2-8 °C, 25 °C or 40 °C for 6 weeks. After reconstitution, samples were analyzed for particle size and particles; solid state characterization included Karl-Fischer titration, DSC and XRD measurements.

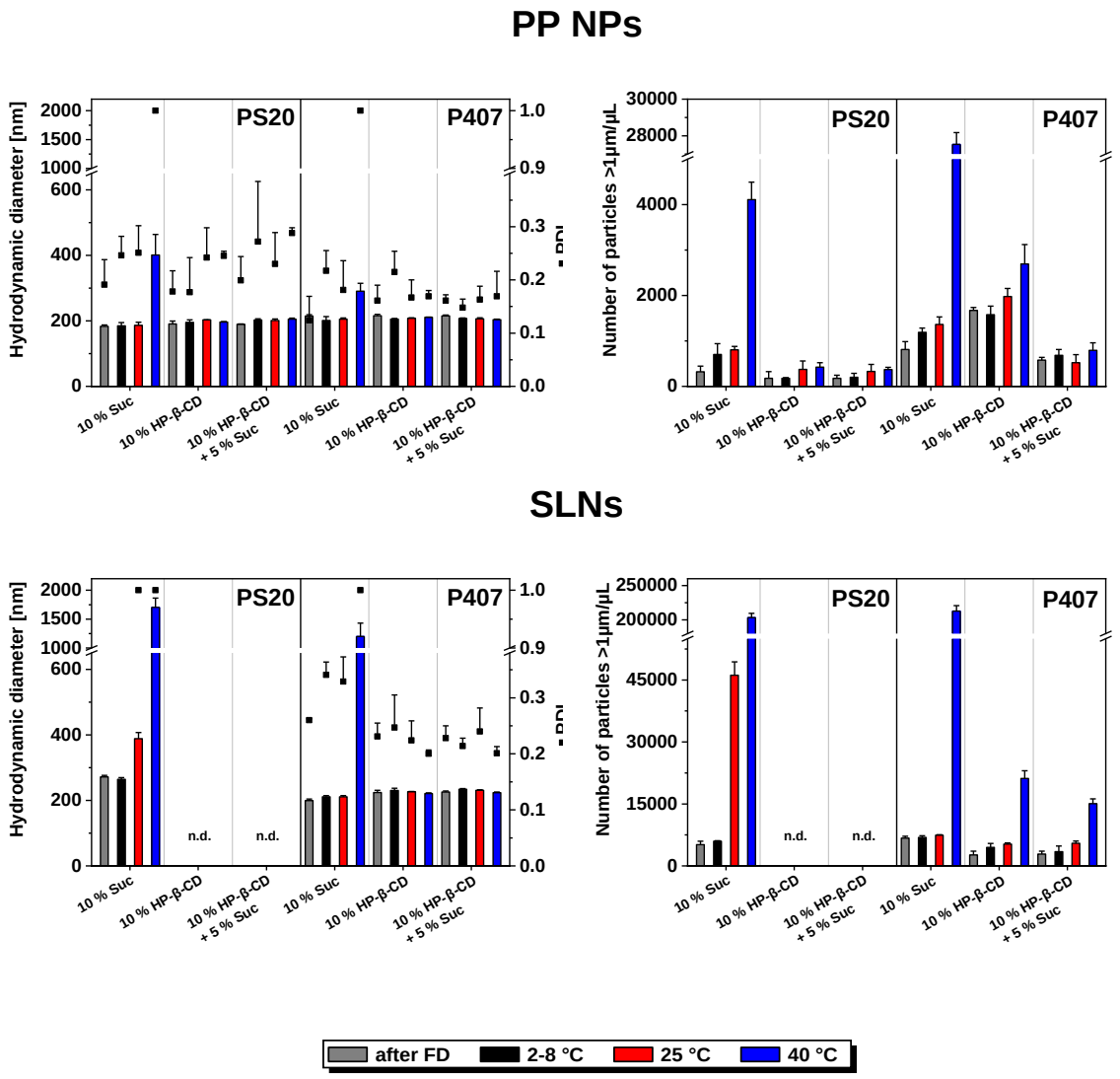

Figure 9: DLS and LO measurements of lyophilized PP NPs and SLNs stabilized with 0.5% PS20 or P407 in presence of 10% Suc, 10% HP-β-CD or '5% Suc + 10% HP-β-CD' (n=3). Samples were stored for 6 weeks at 2-8 °C, 25 °C or 40 °C. PDI values >0.56 represent a multimodal size distribution and are therefore stated as '1.0'. n.d. = not detectable (reconstitution not possible).

All lyophilizates, except PS20 containing SLNs formulated with 10% HP-β-CD or '5% Suc + 10% HP-β-CD', instantly (< 5 s) dissolved upon reconstitution. After storage at 40 °C, the particle size of PP NPs formulated with 10% Suc increased from about 200 nm to ~400 nm and to ~300 nm in presence of PS20 and P407 respectively exhibiting PDI values of 1.0 (Figure 9). Similarly, SLNs stored at 40 °C revealed drastically increased particle sizes in 10% Suc formulations independent of the surfactant type. Furthermore, PS20 containing SLNs stored at 25 °C showed an increased particle size of ~400 nm and a PDI of 1.0 in presence of 10% Suc while P407 samples remained unchanged. All other NP lyophilizates showed no significant change in particle size and PDI after 6 weeks storage.

Similar trends were observed for the number of subvisible particles. In general, the number of particles ≥1 µm did not change upon storage at 2-8 °C and 25 °C independent of NP type and formulation composition, except for PS20 containing SLNs formulated with 10% Suc and stored at 25 °C. All samples formulated with 10% Suc revealed dramatically increased SVP numbers after storage at 40 °C. Aggregation at 40 °C could be substantially reduced or even prevented in HP-β-CD containing formulations. Directly after lyophilization, P407 stabilized PP NPs showed a higher number of SVPs in 10% HP-β-CD compared to 10% Suc and '5% Suc + 10% HP-β-CD' formulations, although particle numbers were similar prior to lyophilization.

The calorimetric events of 10% Suc lyophilizates are summarized in Table 3. Thermograms of PP lyophilizates remained unchanged after storage at 2-8 °C (Figure 10). Only one glass transition at ~51 °C (PS20) or ~62 °C (P407) was observed in samples stored at 25 °C and no T_g and T_c were detected after storage at 40 °C. P407 samples revealed an endotherm at ~56 °C after storage at 25 °C and 40 °C. In general, SLN lyophilizates exhibited a broad endotherm at ~58 °C hindering the detection of further glass transitions and revealed no T_c after storage at 40 °C. Furthermore, the T_c was lower in samples stored at 25 °C compared to samples stored at 2-8 °C.

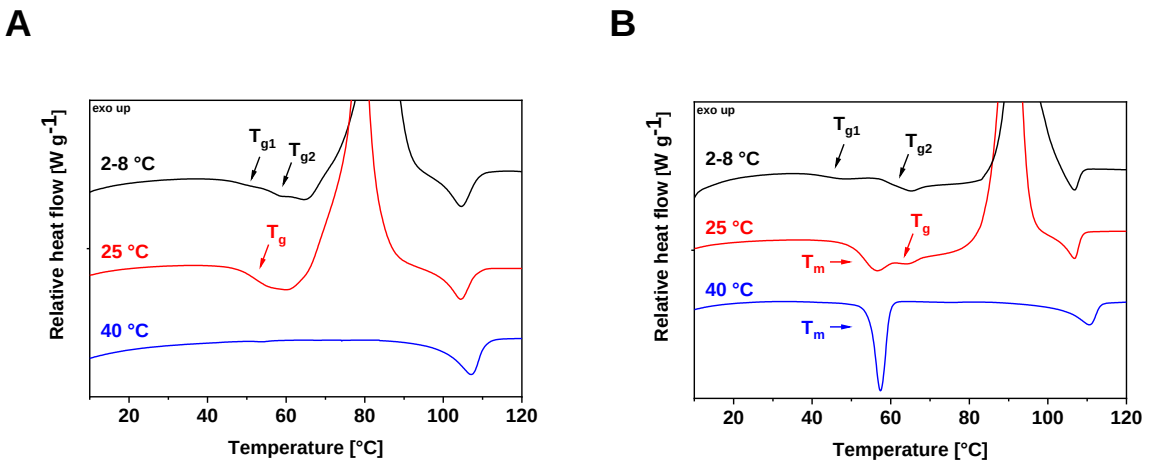

Figure 10: Representative DSC profiles of lyophilized PP NPs stored for 6 weeks at 2-8 °C, 25 °C or 40 °C in presence of 10% Suc and 0.5% PS20 (A) or P407 (B).

Table 3: Calorimetric events of NP lyophilizates formulated with 0.5% PS20 or P407 and 10% Suc after 6 weeks storage at 2-8 °C, 25 °C or 40 °C (n=3).

Formulation		Storage temp. [°C]	T_{g1} [°C]	T_m [°C]	T_{g2} [°C]	T_c [°C]	T_m [°C]
PS20	**PP NPs**	2-8	48.8 ± 0.3	-	57.1 ± 0.3	83.4 ± 0.7	104.6 ± 0.1
		25	50.7 ± 4.1	-	-	76.0 ± 3.8	104.3 ± 0.3
		40	-	-	-	-	107.1 ± 0.2
	SLNs	2-8	-	56.2 ± 0.3	-	86.9 ± 3.8	-
		25	-	56.2 ± 0.4	-	75.8 ± 5.1	-
		40	-	56.3 ± 0.5	-	-	-
P407	**PP NPs**	2-8	45.6 ± 2.5	-	61.4 ± 2.1	92.1 ± 0.9	107.0 ± 0.1
		25	-	55.9 ± 0.2	61.8 ± 0.3	90.0 ± 0.6	106.8 ± 0.1
		40	-	57.2 ± 0.2	-	-	110.4 ± 0.1
	SLNs	2-8	41.6 ± 0.5	58.3 ± 0.6	64.1 ± 1.3	90.3 ± 1.9	-
		25	41.9 ± 0.6	58.1 ± 3.1	63.5 ± 2.2	87.8 ± 1.9	-
		40	-	56.8 ± 0.6	-	-	-

Thermograms of HP-β-CD containing lyophilizates were characterized by one glass transition. After storage, PP NPs lyophilized with 10% HP-β-CD showed T_g values ≥170 °C while SLN formulations revealed T_g values ≥140 °C (Table S-3). In comparison, PP NPs and SLNs lyophilizates with '5% Suc + 10% HP-β-CD' revealed T_g values of ≥120 °C and ≥110 °C respectively. T_g values remained unchanged in samples stored at 2-8 °C and only slightly decreased after storage at 25 °C or 40 °C.

Upon storage RM levels remained ≤0.9% in '5% Suc + 10% HP-β-CD' and in 10% Suc formulations, but slightly increased up to 1.4% for 10% HP-β-CD samples, most pronounced upon 40 °C storage (Table S-4). After storage, all samples formulated with HP-β-CD remained fully amorphous according to XRD measurements (Figure S-5). Lyophilizates formulated with 10% Suc and stored at 2-8 °C or 25 °C resulted in fully amorphous solids represented by an amorphous halo (Figure 11). However, storage at 40 °C showed sucrose crystallization.

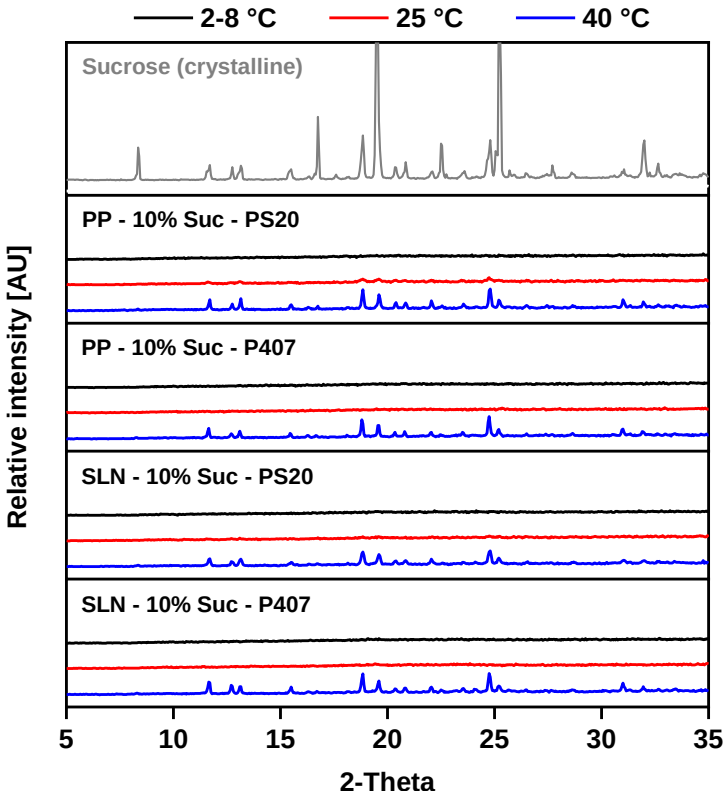

Figure 11: XRD patterns of lyophilized PP NPs and SLNs stabilized with 0.5% PS20 or P407 and formulated with 10% Suc. Samples were stored for 6 weeks at 2-8 °C, 25 °C or 40 °C.

4 Discussion

4.1 Formulation aspects

Several stresses are known to affect NP stability during freeze-drying. The freezing step is considered to be the more aggressive step of lyophilization [20] and includes mechanical stress by ice crystals, cryo-concentration resulting in increased particle-particle interactions, potential phase separation or interactions at the ice-water interface [3].

Since the formulation composition is assumed to have the greatest impact on NP stability upon freeze-drying [14], FT studies were conducted prior to lyophilization to systematically evaluate previously neglected formulation parameters still lacking from comprehensive studies including buffer type, pH and ionic strength, in combination with different cryoprotectants.

The impact of buffer type and pH was investigated using NPs stabilized with P407 which served as a model for non-ionic surfactants. Na-phosphate is known to cause an acidic pH shift upon freezing thereby destabilizing colloids [7]. Therefore, we compared Na-phosphate

with K-phosphate and Na-citrate buffers which maintain their pH during freezing [5,21]. The buffer type and pH were found to have a negligible effect on FT stability which can be attributed to the NP properties. Both, PP NPs and SLNs are stabilized by surfactants which are essentially needed for the nanonization of lipophilic compounds in liquid state. Non-ionic surfactants provide steric stabilization for lipophilic particles and result in particles with close to neutral surface charge which we confirmed by zeta-potential measurements. The surface charge was independent of the formulation pH explaining minor effects of the pH shift on particle stability in Na-phosphate buffer.

The addition of cryo- and lyoprotectants is usually necessary to accomplish sufficient stabilization of colloids during freezing and freeze-drying. We tested the impact of sucrose and mannitol on NP stability upon FT. Both NP types were well preserved in presence of 10% Suc while particle size, PDI and SVP numbers were increased in 10% Man and in formulations without a cryoprotectant. The increase in number of SVPs is mainly attributed to aggregation and/or crystal growth of NPs resulting in microparticles. These processes may be triggered by the high NP concentration in the freeze concentration and the NP enrichment the freeze-concentrate ice interface.

Sucrose forms an amorphous matrix while mannitol is known to at least partially crystallize upon freezing [7,22]. Thus, our study indicates that immobilization of particles in a fully vitrified matrix is crucial for sufficient NP stabilization. The particle isolation hypothesis, vitrification hypothesis and increased solution viscosity during freezing all explain the cryoprotective effect (i.e. polyplexes, liposomes, lipoplexes) [23–25]. The particle isolation theory states that separation of individual particles within the unfrozen fraction is crucial for NP stabilization. The vitrification theory is related to viscosity effects during freezing and states that sugar solutions become highly viscous cryo-concentrates and form a stable glassy matrix preventing aggregation through immobilization of particles.

Interestingly, the NaCl concentration significantly influenced the FT stability of PP NPs and SLNs. The addition of NaCl led to decreasing SVP numbers, especially without addition of a cryoprotectant and at low sucrose concentrations. NaCl is known to destabilize colloids due to the reduction of the surface potential facilitating attractive interactions. However, in our study, NPs exhibited a neutral surface charge making charge driven effects unlikely. DSC measurements revealed eutectic melting of NaCl in absence of sucrose indicating a preceded crystallization during freezing. Thus, salt crystals might serve as a spacer separating NPs. Addition of NaCl to sucrose solutions caused a T_g' reduction as also reported previously [26,27]. According to Her et al., NaCl leads to an increasing quantity of unfrozen water in the freeze-concentrate acting as a plasticizer [26]. But whether this

increase in cryoconcentrate volume, corresponding to a lower NP concentration and thus larger NP distance, has a positive effect on particle-particle interaction is up to speculation.

The study demonstrates that the type of surfactant used for particle stabilization has the greatest impact on the formation of SVPs upon NP lyophilization. In case of PP NPs, PS20 was superior to P407 at lower sucrose concentrations whereas SLNs were best preserved in P407 formulations. The suitability of a surfactant for NP stabilization is still not well understood and is typically determined experimentally for each NP type. In a screening study, van Eerdenbrugh et al. evaluated the efficiency of different stabilizers to produce stable nanosuspensions of nine model compounds [28]. Typical physicochemical properties such as molecular weight, melting point, log P, solubility and density of a drug substance were not able to explain stabilization mechanisms and interactions between particles and stabilizers including surfactants. However, they could show that higher stabilizer concentrations in general improved NP production and subsequent stability which was further seen in lyophilization experiments by Beirowski et al. [14]. Our results propose that an insufficient steric stabilizer concentration could be well compensated by a higher concentration of cryoprotectant. Thus, recommendations in literature have to be taken with a grain of salt; in presence of sufficient other stabilizers, e.g. much sugar as cryoprotectant, a detailed surfactant effect may not be noticeable whereas without an adequate stabilizer the effect may be drastic.

4.2 Process aspects

Three different freezing conditions were compared in order to investigate the impact of the freezing step on NP stability. AN showed no clear impact on SVP formation. In contrast, CN led to a lower number of SVPs compared to RN indicating surface-induced destabilization of NPs at the ice-water and/or solid-air interface during freezing and/or drying. During lyophilization, ice crystals are removed by sublimation, and the interface between the solid and the voids left behind contribute to the SSA of the lyophilizate [29]. BET measurements confirmed that CN led to the smallest solid-ice interface due to a low degree of supercooling which leads to large ice crystals [30]. In contrast, RN led to the formation of smaller ice crystals and thus larger SSA. Ostwald ripening by annealing fostered ice crystal growth resulting in a larger SSA compared to CN samples, but smaller than RN samples.

The ice-water interfacial area is known to destabilize colloids leading to aggregation. As shown for proteins, aggregation depends on the nucleation temperature which determines the ice surface area. Aggregation can be inhibited by the addition of surfactants mainly by replacing the protein molecules at the interface reducing protein enrichment and unfolding

[6,31]. Since unfolding is not relevant for NPs, the closer vicinity of NPs in the cryo-concentrated state at the interface appears to foster aggregation. Beirowski et al. demonstrated that higher steric stabilizer concentrations substantially improved the lyophilization success of drug nanosuspensions [14]. Concluding from our study and literature reports, the interfacial area, the steric stabilizer type and concentration and the NP aggregation propensity affect aggregation during the freezing step.

Overall all cakes were pharmaceutically elegant. Annealing resulted in a reduction of cracks as it allows the unfrozen fraction to relax resulting in a glass with lower excess free volume and decreased internal stress [32,33]. Furthermore, Ostwald ripening leads to a more uniform ice structure and favors a homogeneous ice distribution [34,35]. Interestingly, substantial vial fogging was observed which can be a critical cosmetic defect and may endanger container closure integrity [36,37]. Vial fogging is caused by Marangoni flow driven by a surface tension gradient. The high amount of the mandatory surface-active component in lipophilic NP formulations facilitates this process. Deposition and partial melting of ice crystals at the vial inner surface upon CN via an 'ice fog' technique might additionally foster creeping of unfrozen components. However, this mechanism needs to be confirmed in future studies. The most robust approach to eliminate vial fogging is by using vials with a hydrophobic inner surface [37,38].

4.3 Storage stability aspects

The T_g of lyophilizates is one of the major determinants of storage stability [7] and was therefore systematically assessed with DSC. The exothermic event observed in all formulations is attributable to sucrose crystallization while the endotherm in PP lyophilizates is related to API melting [39]. The endotherm in P407 samples is referred to P407 melting (T_m = 52-57 °C [40]). Lyophilizates of SLNs, showed an endotherm at approximately 57 °C due to melting of the triglyceride [41].

The presence of a surfactant has a substantial impact on the thermal properties of lyophilizates. Numerous formulations showed two glass transition events. The detection of two T_g's was previously reported by Abdul-Fattah et al. for 5% Suc + 0.2% Poloxamer 188 and indicates a phase separation with a surfactant-rich and a surfactant-poor phase [42]. Freezing polymer solutions may cause phase separation since the polymer solubility is altered at low temperatures [7]. This may cause destabilization of the entity in need of protection if the stabilizer gets separated [4]. DSC measurements of a sucrose solution confirmed that the investigated surfactants contribute to phase separation and a second glass transition in the frozen state. T_{g1} and $T_g'_1$ are supposed to represent the surfactant-rich

phase due to the surfactants' plasticizing effect. It is recommended that lyophilizates should have a T_g value 20 °C above the intended storage temperature to minimize mobility [43]. Referring to this recommendation, the low T_{g1} at about 50 °C is assumed to impair the storage stability of lyophilizates at room temperature.

Screening studies with placebo formulations were conducted to elucidate the impact of the sucrose and PS20/P407 concentration on the thermal behavior of lyophilizates. Surfactant concentrations up to 1.0% are used in commercial drug nanosuspensions (INVEGA SUSTENNA®: 1.2% PS20) and were therefore included in the screening study. A decreasing sucrose/surfactant mass ratio led to phase separation, and decreasing T_c and T_g values which is attributed to the plasticizing effect of the surfactants. A correlation between T_g and T_c of sucrose was already reported in previous studies [41]. As a consequence of partially overlapped calorimetric events (e.g. 5% Suc/1.0% P407), the T_c value of sucrose gains importance for the evaluation of thermograms and may be used as a surrogate for T_g.

Previously, formulations with Suc/HP-β-CD were reported to be superior to pure Suc formulations regarding the long-term storage stability of lyophilized proteins at 40 °C due to a high T_g [45]. Therefore, we evaluated Suc/HP-β-CD mixtures in presence of high PS20/P407 concentrations. Without surfactant addition, the mixture of HP-β-CD and Suc revealed one glass transition reflecting a miscible amorphous matrix. In presence of the investigated surfactants, a lower Suc/HP-β-CD mass ratio suppressed the formation of a second phase which may be highly beneficial for stability of NP products.

Overall, 10% Suc formulations showed good stability upon storage at 2-8 °C and generally acceptable stability at 25 °C. The lyophilizates, however, exhibited poor stability at 40 °C which is attributed to sucrose crystallization impairing NP protection in the amorphous matrix. We were able to overcome this limited storage stability for both NP types by the addition of HP-β-CD. In general, a Suc/HP-β-CD mixture was superior to pure HP-β-CD; the disaccharide molecules are more flexible than larger oligosaccharides (i.e. HP-β-CD) and therefore better stabilizers for lyophilization [46]. Thus, mixtures of disaccharides with oligo- or polysaccharides may benefit from sufficient stabilization and high T_g values improving storage stability. A minor increase of the SVP number after storage suggests that rather a kinetic than a thermodynamic stabilization is provided with reduced but still residual risk of aggregation and/or crystal growth over time. Based on this study, we further assume that the aggregation propensity of SLNs stored at 40 °C is related to the melting characteristics of the triglyceride. Trimyristin has a melting onset at approximately 50 °C concluding that rather T_m than T_g is the stability limiting factor for this NP type. The T_m of lipids is known to be shifted towards lower temperatures the smaller the particles size [41] potentially

contributing to the low stability at 40 °C. These aspects and means to overcome this obstacle would be of high interest for further studies.

Overall, we were able to confirm that the model drug nanosuspension and SLNs share basic formulation, process, and storage considerations leveraging purposeful lyophilization development of these lipophilic NP types.

5 Conclusion

We investigated crucial aspects for successful lyophilization of lipophilic NPs including formulation, process, and storage strategies, i.e. i) comparability of different particle types, ii) impact of buffer type, pH, and ionic strength, iii) impact of the freezing step, iv) impact of the surfactants PS20 or P407 on the glass transition temperature of lyophilizates.

PP NPs and SLNs exhibited comparable freezing and lyophilization behavior. At first detailed FT studies were performed. Sucrose better stabilized NPs compared to mannitol emphasizing the importance of a fully amorphous matrix. We further demonstrated that the buffer composition and pH are negligible when NPs are stabilized with an adequate amount of non-ionic steric stabilizer. Lyophilization studies revealed surface-induced destabilization of NPs which can be addressed by the surfactant type and concentration and the sucrose concentration. The combined view on both excipient types is important e.g. an inappropriate steric stabilizer selection can be well compensated by increasing the cryoprotectant concentration. The surfactant/cryoprotectant mass ratio highly affected the storage stability of both PP NPs and SLNs. The steric stabilizer concentration is crucial since it determines the T_g and might induce phase separation resulting in a phase of higher mobility. In that respect lower surfactant concentrations are beneficial. Suc/HP-β-CD mixtures were even more suitable to sufficiently protect NPs upon lyophilization and provide a high T_g improving long-term storage stability. Furthermore HP-β-CD can reduce the phase separation effect of high PS20/P407 concentrations.

In conclusion, we successfully lyophilized drug nanosuspensions and SLNs revealing important lyophilization principles. Lyophilization of NPs offers improved storage stability and facilitates shipping of temperature sensitive nanomedicine. The cryoprotectant and surfactant type and concentration are crucial for NP stability. Especially optimization of the surfactant concentration is highly recommended to achieve long-term stability of lyophilized lipophilic NPs.

6 Supplementary Data

Table S-1: ζ-Potential values of three times freeze-thawed PP NPs and SLNs (n=3).

ζ-Potential [mV]									
		PP NPs				**SLNs**			
		PS20		**P407**		**PS20**		**P407**	
NaCl [mM]	Suc [%]	before FT	after FT	before FT	after FT	before FT	after FT	before FT	after FT
0	0	3.2 ± 1.9	2.9 ± 0.4	-1.0 ± 1.2	-1.9 ± 0.4	-2.8 ± 0.2	-2.9 ± 0.3	-1.8 ± 0.4	-1.6 ± 0.3
	2.5	2.9 ± 0.2	2.9 ± 0.2	-0.7 ± 0.4	-0.9 ± 0.2	-1.1 ± 0.3	-1.9 ± 0.9	-2.0 ± 0.9	-1.9 ± 0.7
	5	2.3 ± 1.4	2.6 ± 0.0	-0.2 ± 0.2	-0.6 ± 0.0	-1.9 ± 0.3	-1.6 ± 0.8	-1.2 ± 0.4	-1.2 ± 0.2
	10	2.2 ± 1.2	2.2 ± 0.9	-1.1 ± 0.7	-1.2 ± 0.9	-1.3 ± 0.5	-1.6 ± 0.3	-1.7 ± 0.2	-1.2 ± 0.6
70	0	2.4 ± 0.9	2.3 ± 0.5	-1.7 ± 0.4	-1.3 ± 0.5	-1.9 ± 0.3	-2.3 ± 0.7	-1.7 ± 0.4	-1.9 ± 0.7
	2.5	2.7 ± 0.2	2.3 ± 1.1	-1.0 ± 0.5	-1.7 ± 1.1	-1.9 ± 0.5	-2.0 ± 0.7	-1.1 ± 0.2	-1.4 ± 0.8
	5	2.6 ± 0.8	2.8 ± 0.2	-1.3 ± 0.5	-1.8 ± 0.2	-1.6 ± 0.3	-1.4 ± 0.8	-1.5 ± 0.5	-1.8 ± 0.2
	10	2.5 ± 0.6	2.0 ± 0.2	-1.2 ± 0.5	-2.0 ± 0.2	-1.2 ± 0.5	-1.5 ± 0.5	-1.2 ± 0.5	-1.7 ± 0.9
140	0	2.9 ± 0.2	2.2 ± 1.0	0.0 ± 0.6	-2.2 ± 1.0	-1.6 ± 0.1	-1.9 ± 0.5	-1.0 ± 0.5	-1.4 ± 0.9
	2.5	2.5 ± 1.1	2.1 ± 0.1	-1.5 ± 1.0	-1.5 ± 0.1	-1.6 ± 0.3	-1.4 ± 0.4	-1.7 ± 0.3	-1.8 ± 0.2
	5	2.4 ± 0.6	2.2 ± 1.1	-0.1 ± 1.0	-0.1 ± 1.1	-1.1 ± 1.0	-1.8 ± 0.2	-1.8 ± 0.3	-1.4 ± 0.6
	10	2.6 ± 0.6	2.3 ± 0.3	-1.8 ± 0.7	-1.3 ± 0.3	-1.6 ± 0.2	-1.6 ± 0.4	-1.4 ± 0.9	-1.0 ± 0.5

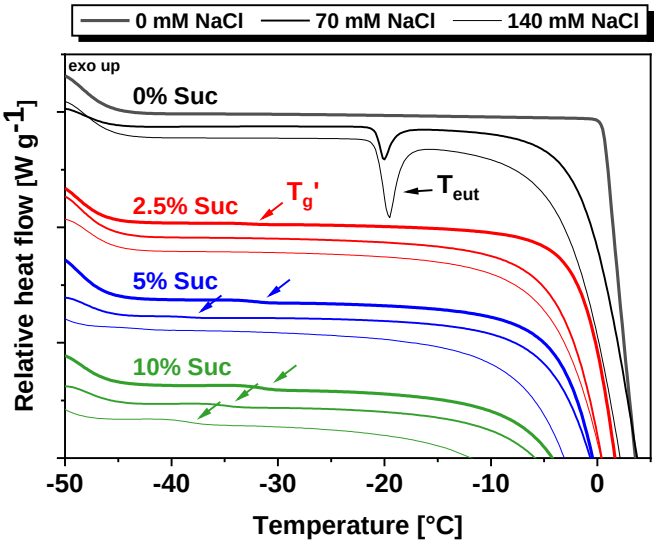

Figure S-1: Representative DSC profiles of sucrose solutions (0, 2.5, 5, or 10%) in absence or presence of 0, 70, or 140 mM NaCl.

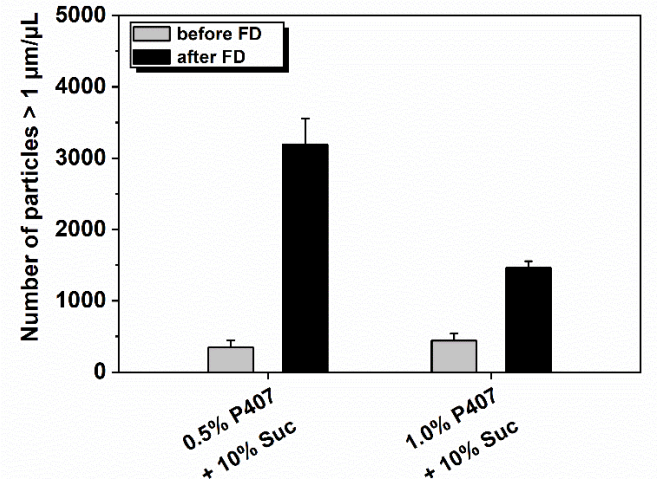

Figure S-2: LO measurements of lyophilized PP NPs stabilized with 0.5% or 1.0% P407 in presence of 10% Suc (n=3). Conventional ramp freezing was applied.

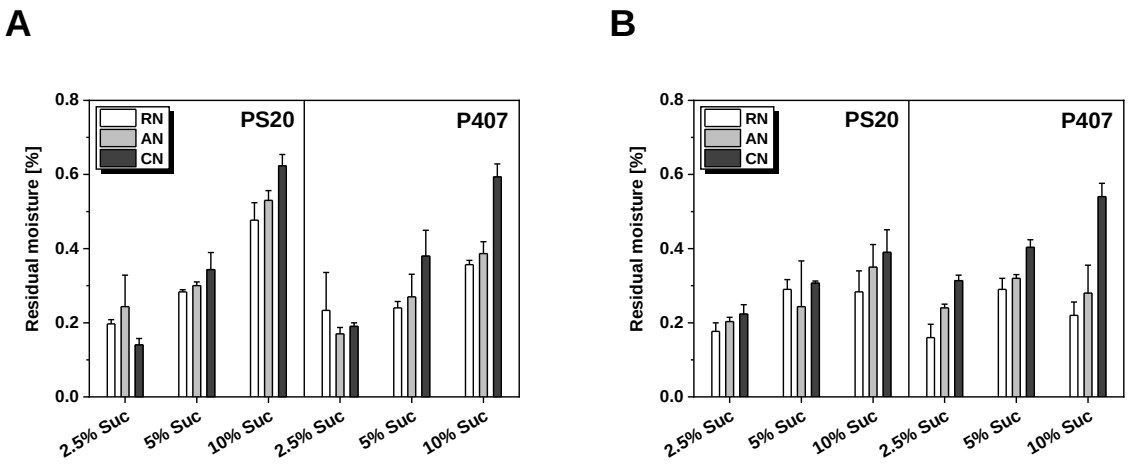

Figure S-3: Residual moisture levels of lyophilized PP NPs (A) and SLNs (B) stabilized with PS20 or P407 in presence of 2.5, 5 or 10% Suc (n=3). Conventional ramp freezing (RN), including an annealing step (AN), or under controlled nucleation (CN) was applied.

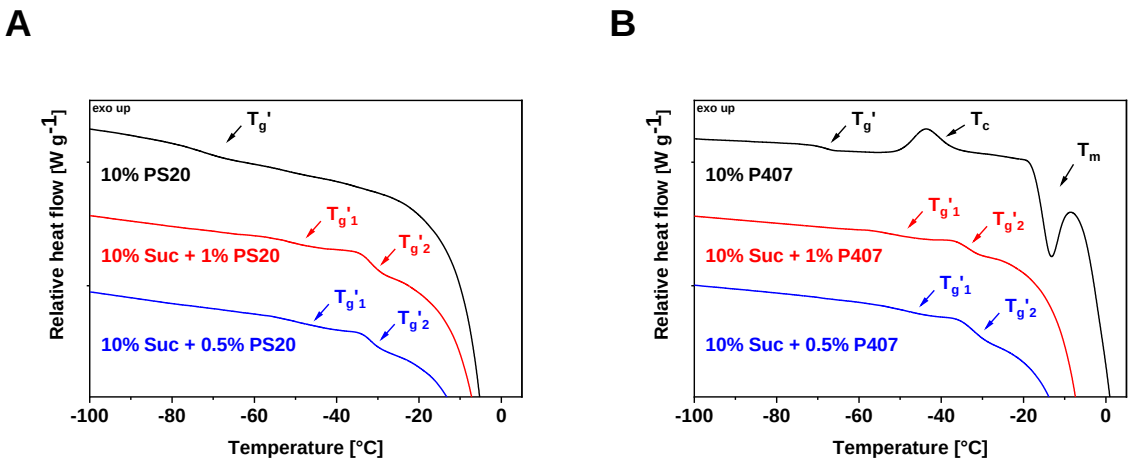

Figure S-4: Representative DSC profiles of PS20 (A) and P407 (B) solutions in absence or presence of 10% Suc.

Table S-2: Calorimetric events of NP lyophilizates formulated with 0.5% PS20 or P407 and 2.5, 5, or 10% Suc (n=3).

Formulation		Suc [%]	T_{g1} [°C]	T_m [°C]	T_{g2} [°C]	T_c [°C]	T_m [°C]
PS20	**PP NPs**	2.5	43.5 ± 1.0	-	50.6 ± 0.4	66.4 ± 1.4	108.1 ± 1.3
		5	42.8 ± 1.6	-	55.6 ± 2.2	78.3 ± 0.8	105.6 ± 0.5
		10	49.8 ± 3.8	-	60.0 ± 2.5	86.2 ± 4.5	105.1 ± 0.6
	SLNs	2.5	42.2 ± 1.9	57.3 ± 0.3	-	66.7 ± 1.4	-
		5	45.0 ± 1.8	56.7 ± 0.2	-	71.2 ± 2.9	-
		10	-	57.5 ± 1.6	-	87.5 ± 3.7	-
	Placebo	2.5	41.0 ± 3.7	-	57.3 ± 4.5	72.1 ± 2.8	-
		5	46.5 ± 1.1	-	56.9 ± 0.3	79.1 ± 0.8	-
		10	49.9 ± 1.3	-	59.6 ± 0.9	85.6 ± 0.9	-
P407	**PP NPs**	2.5	45.5 ± 1.8	54.6 ± 0.3	-	64.7 ± 1.9	111.2 ± 1.3
		5	-	53.9 ± 0.6	62.5 ± 0.1	83.9 ± 1.6	108.2 ± 0.1
		10	47.8 ± 4.3	-	64.0 ± 1.1	91.3 ± 1.4	107.3 ± 0.2
	SLNs	2.5	40.0 ± 0.8	57.4 ± 0.3	-	76.6 ± 1.0	-
		5	41.1 ± 1.3	57.6 ± 0.4	-	86.0 ± 2.6	-
		10	42.0 ± 0.6	59.3 ± 0.9	66.3 ± 3.0	94.1 ± 2.2	-
	Placebo	2.5	-	52.5 ± 1.6	-	75.8 ± 1.5	-
		5	-	53.4 ± 0.4	63.7 ± 1.1	85.9 ± 0.7	-
		10	49.2 ± 2.6	-	62.6 ± 1.8	91.6 ± 1.5	-

Table S-3: Glass transition temperatures (T_g) of HP-β-CD containing lyophilizates directly after freeze-drying (after FD) and after 6 weeks storage at 2-8 °C, 25 °C or 40 °C (n=3).

Formulation			**T_g [°C]**			
			after FD	**2-8 °C**	**25 °C**	**40 °C**
PS20	**PP NPs**	10% HP-β-CD	185.7 ± 0.8	178.4 ± 1.4	175.9 ± 0.6	171.8 ± 2.1
		5% Suc + 10% HP-β-CD	132.4 ± 5.9	130.0 ± 3.5	125.1 ± 3.1	122.6 ± 2.3
	SLNs	10% HP-β-CD	159.8 ± 2.8	157.8 ± 2.1	153.8 ± 1.5	151.9 ± 3.7
		5% Suc + 10% HP-β-CD	119.6 ± 3.8	120.1 ± 3.5	116.6 ± 5.6	114.9 ± 5.9
P407	**PP NPs**	10% HP-β-CD	180.5 ± 3.5	179.8 ± 0.7	171.3 ± 4.5	171.7 ± 5.4
		5% Suc + 10% HP-β-CD	130.8 ± 1.0	131.5 ± 2.8	126.0 ± 4.5	125.7 ± 3.2
	SLNs	10% HP-β-CD	154.2 ± 2.0	154.6 ± 2.3	145.7 ± 6.4	141.7 ± 3.6
		5% Suc + 10% HP-β-CD	117.7 ± 1.6	118.4 ± 5.5	117.7 ± 1.6	114.1 ± 1.8

Table S-4: Residual moisture levels) of lyophilizates directly after freeze-drying (after FD) and after 6 weeks storage at 2-8 °C, 25 °C or 40 °C (n=3).

RM [%]						
			after FD	**2-8 °C**	**25 °C**	**40 °C**
PS20	**PP NPs**	10% Suc	0.5 ± 0.1	0.6 ± 0.1	0.7 ± 0.1	0.0 ± 0.0
		10% HP-β-CD	0.8 ± 0.0	1.1 ± 0.1	1.1 ± 0.3	1.4 ± 0.3
		5% Suc + 10% HP-β-CD	0.6 ± 0.1	0.6 ± 0.1	0.7 ± 0.1	0.9 ± 0.2
	SLNs	10% Suc	0.4 ± 0.1	0.6 ± 0.1	0.8 ± 0.1	0.2 ± 0.0
		10% HP-β-CD	0.7 ± 0.1	0.9 ± 0.0	1.1 ± 0.3	1.3 ± 0.1
		5% Suc + 10% HP-β-CD	0.5 ± 0.0	0.5 ± 0.0	0.6 ± 0.0	0.9 ± 0.1
P407	**PP NPs**	10% Suc	0.4 ± 0.0	0.6 ± 0.1	0.6 ± 0.1	0.0 ± 0.0
		10% HP-β-CD	0.7 ± 0.1	1.2 ± 0.1	1.2 ± 0.1	1.2 ± 0.3
		5% Suc + 10% HP-β-CD	0.5 ± 0.1	0.5 ± 0.1	0.5 ± 0.2	0.8 ± 0.1
	SLNs	10% Suc	0.3 ± 0.1	0.9 ± 0.0	0.9 ± 0.1	0.0 ± 0.0
		10% HP-β-CD	0.8 ± 0.1	1.1 ± 0.4	1.1 ± 0.2	1.3 ± 0.1
		5% Suc + 10% HP-β-CD	0.5 ± 0.1	0.6 ± 0.2	0.6 ± 0.1	0.8 ± 0.1

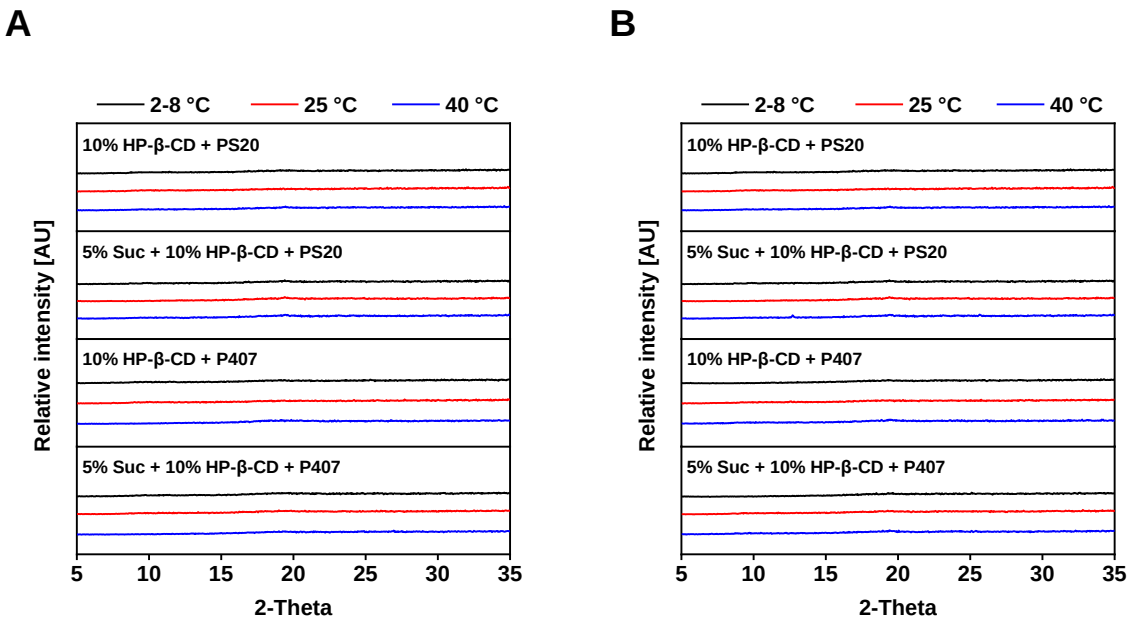

Figure S-5: XRD patterns of lyophilized PP NPs (A) and SLNs (B) stabilized with 0.5% PS20 or P407 and formulated with 10% HP-β-CD or '5% Suc + 10% HP-β-CD'. Samples were stored for 6 weeks at 2-8 °C, 25 °C or 40 °C.

7 References

[1] D. Bobo, K.J. Robinson, J. Islam, K.J. Thurecht, S.R. Corrie, Nanoparticle-Based Medicines: A Review of FDA-Approved Materials and Clinical Trials to Date, Pharm. Res. 33 (2016) 2373–2387.

[2] K. Park, Prevention of nanoparticle aggregation during freeze-drying, J. Control. Release 248 (2017) 153.

[3] P. Fonte, S. Reis, B. Sarmento, Facts and evidences on the lyophilization of polymeric nanoparticles for drug delivery, J. Control. Release 225 (2016) 75–86.

[4] X. Tang, M.J. Pikal, Design of Freeze-Drying Processes for Pharmaceuticals: Practical Advice, Pharm. Res. 21 (2004) 191–200.

[5] P. Kolhe, E. Amend, S.K. Singh, Impact of freezing on pH of buffered solutions and consequences for monoclonal antibody aggregation, Biotechnol. Prog. 26 (2010) 727–733.

[6] B.S. Chang, B.S. Kendrick, J.F. Carpenter, Surface-induced denaturation of proteins during freezing and its inhibition by surfactants, J. Pharm. Sci. 85 (1996) 1325–1330.

[7] W. Wang, Lyophilization and development of solid protein pharmaceuticals, Int. J. Pharm. 203 (2000) 1–60.

[8] W. Abdelwahed, G. Degobert, S. Stainmesse, H. Fessi, Freeze-drying of nanoparticles: formulation, process and storage considerations, Adv. Drug Deliv. Rev. 58 (2006) 1688–1713.

[9] N. Desai, Challenges in development of nanoparticle-based therapeutics, AAPS J. 14 (2012) 282–295.

[10] X. Zhang, M.R. Servos, J. Liu, Ultrahigh nanoparticle stability against salt, pH, and solvent with retained surface accessibility via depletion stabilization, J. Am. Chem. Soc. 134 (2012) 9910–9913.

[11] S. Kim, K. Hyun, J.Y. Moon, C. Clasen, K.H. Ahn, Depletion stabilization in nanoparticle-polymer suspensions: multi-length-scale analysis of microstructure, Langmuir 31 (2015) 1892–1900.

[12] R.I. Feigin, D.H. Napper, Depletion stabilization and depletion flocculation, J. Colloid Interface Sci. 75 (1980) 525–541.

[13] S. Kumar, R. Gokhale, D.J. Burgess, Sugars as bulking agents to prevent nano-crystal aggregation during spray or freeze-drying, Int. J. Pharm. 471 (2014) 303–311.

[14] J. Beirowski, S. Inghelbrecht, A. Arien, H. Gieseler, Freeze-drying of nanosuspensions, 1: freezing rate versus formulation design as critical factors to preserve the original particle size distribution, J. Pharm. Sci. 100 (2011) 1958–1968.

[15] C. Schwarz, W. Mehnert, Freeze-drying of drug-free and drug-loaded solid lipid nanoparticles (SLN), Int. J. Pharm. 157 (1997) 171–179.

[16] W. Mehnert, K. Mäder, Solid lipid nanoparticles, Adv. Drug Deliv. Rev. 64 (2012) 83–101.

[17] R.K. Trivedi, R. Jupudi, M. Patel, D. Trivedi, H. Jogia, A Validated Spectrophotometric Method for Determination of Paliperidone Palmitate in Bulk Drug and its Pharmaceutical Dosage Form, J. Pharm. Pharm. Sci. 2 (2013) 37–41.

[18] R. Geidobler, S. Mannschedel, G. Winter, A new approach to achieve controlled ice nucleation of supercooled solutions during the freezing step in freeze-drying, J. Pharm. Sci. 101 (2012) 4409–4413.

[19] S.M. Patel, S.L. Nail, M.J. Pikal, R. Geidobler, G. Winter, A. Hawe, J. Davagnino, S. Rambhatla Gupta, Lyophilized Drug Product Cake Appearance: What Is Acceptable?, J. Pharm. Sci. 106 (2017) 1706–1721.

[20] P.V. Date, A. Samad, P.V. Devarajan, Freeze thaw: a simple approach for prediction of optimal cryoprotectant for freeze drying, AAPS PharmSciTech 11 (2010) 304–313.

[21] L. van den Berg, D. Rose, Effect of freezing on the pH and composition of sodium and potassium phosphate solutions: the reciprocal system KH2PO4・Na2HPO4・H2O, Arch. Biochem. Biophys. 81 (1959) 319–329.

[22] R.K. Cavatur, N.M. Vemuri, A. Pyne, Z. Chrzan, D. Toledo-Velasquez, R. Suryanarayanan, Crystallization behavior of mannitol in frozen aqueous solutions, Pharm. Res. 19 (2002) 894–900.

[23] S. Allison, M.d. Molina, T.J. Anchordoquy, Stabilization of lipid/DNA complexes during the freezing step of the lyophilization process: the particle isolation hypothesis, Biochim. Biophys. Acta Biomembr. 1468 (2000) 127–138.

[24] T.K. Armstrong, T.J. Anchordoquy, Immobilization of nonviral vectors during the freezing step of lyophilization, J. Pharm. Sci. 93 (2004) 2698–2709.

[25] J.C. Kasper, M.J. Pikal, W. Friess, Investigations on polyplex stability during the freezing step of lyophilization using controlled ice nucleation—the importance of residence time in the low-viscosity fluid state, J. Pharm. Sci. 102 (2013) 929–946.

[26] A. Hawe, W. Friess, Impact of freezing procedure and annealing on the physico-chemical properties and the formation of mannitol hydrate in mannitol-sucrose-NaCl formulations, Eur. J. Pharm. Biopharm. 64 (2006) 316–325.

[27] L.-M. Her, M. Deras, S.L. Nail, Electrolyte-Induced Changes in Glass Transition Temperatures of Freeze-Concentrated Solutes, Pharm. Res. 12 (1995) 768–772.

[28] B. van Eerdenbrugh, J. Vermant, J.A. Martens, L. Froyen, J. van Humbeeck, P. Augustijns, G. van den Mooter, A screening study of surface stabilization during the production of drug nanocrystals, J. Pharm. Sci. 98 (2009) 2091–2103.

[29] Y. Xu, P. Grobelny, A. von Allmen, K. Knudson, M. Pikal, J.F. Carpenter, T.W. Randolph, Protein quantity on the air-solid interface determines degradation rates of human growth hormone in lyophilized samples, Journal of pharmaceutical sciences 103 (2014) 1356–1366.

[30] R. Geidobler, G. Winter, Controlled ice nucleation in the field of freeze-drying: fundamentals and technology review, Eur. J. Pharm. Biopharm. 85 (2013) 214–222.

[31] R. Fang, K. Tanaka, V. Mudhivarthi, R.H. Bogner, M.J. Pikal, Effect of Controlled Ice Nucleation on Stability of Lactate Dehydrogenase During Freeze-Drying, J. Pharm. Sci. 107 (2018) 824–830.

[32] S.D. Webb, J.L. Cleland, J.F. Carpenter, T.W. Randolph, Effects of annealing lyophilized and spray-lyophilized formulations of recombinant human interferon-gamma, J. Pharm. Sci. 92 (2003) 715–729.

[33] S. Ullrich, S. Seyferth, G. Lee, Measurement of shrinkage and cracking in lyophilized amorphous cakes. Part IV: Effects of freezing protocol, Int. J. Pharm. 495 (2015) 52–57.

[34] J.A. Searles, J.F. Carpenter, T.W. Randolph, Annealing to optimize the primary drying rate, reduce freezing-induced drying rate heterogeneity, and determine T(g)' in pharmaceutical lyophilization, J. Pharm. Sci. 90 (2001) 872–887.

[35] M. Badal Tejedor, J. Fransson, A. Millqvist-Fureby, Freeze-dried cake structural and physical heterogeneity in relation to freeze-drying cycle parameters, Int. J. Pharm. 590 (2020) 119891.

[36] C. Langer, H.-C. Mahler, A. Koulov, N. Marti, C. Grigore, A. Matter, P. Chalus, S. Singh, T. Lemazurier, S. Joerg, R. Mathaes, Method to Predict Glass Vial Fogging in Lyophilized Drug Products, J. Pharm. Sci. 109 (2020) 323–330.

[37] M. Huang, E. Childs, K. Roffi, F. Karim, J. Juneau, B. Bhatnagar, S. Tchessalov, Investigation of Fogging Behavior in a Lyophilized Drug Product, J. Pharm. Sci. 108 (2019) 1101–1109.

[38] A.M. Abdul-Fattah, R. Oeschger, H. Roehl, I. Bauer Dauphin, M. Worgull, G. Kallmeyer, H.-C. Mahler, Investigating factors leading to fogging of glass vials in lyophilized drug products, Eur. J. Pharm. Biopharm. 85 (2013) 314–326.

[39] D. Leng, H. Chen, G. Li, M. Guo, Z. Zhu, L. Xu, Y. Wang, Development and comparison of intramuscularly long-acting paliperidone palmitate nanosuspensions with different particle size, Int. J. Pharm. 472 (2014) 380–385.

[40] R.C. Rowe (Ed.), Handbook of pharmaceutical excipients, 6. ed. ed., APhA (PhP) Pharmaceutical Press, London, 2009.

[41] T. Unruh, H. Bunjes, K. Westesen, M.H.J. Koch, Observation of Size-Dependent Melting in Lipid Nanoparticles, J. Phys. Chem. B 103 (1999) 10373–10377.

[42] A.M. Abdul-Fattah, V. Truong-Le, L. Yee, E. Pan, Y. Ao, D.S. Kalonia, M.J. Pikal, Drying-induced variations in physico-chemical properties of amorphous pharmaceuticals and their impact on Stability II: stability of a vaccine, Pharm. Res. 24 (2007) 715–727.

[43] F. Franks, Long-term stabilization of biologicals, Bio/technology 12 (1994) 253–256.

[44] A. Saleki-Gerhardt, G. Zografi, Non-isothermal and isothermal crystallization of sucrose from the amorphous state, Pharm. Res. 11 (1994) 1166–1173.

[45] C. Haeuser, P. Goldbach, J. Huwyler, W. Friess, A. Allmendinger, Excipients for Room Temperature Stable Freeze-Dried Monoclonal Antibody Formulations, J. Pharm. Sci. 109 (2020) 807–817.

[46] W.F. Tonnis, M.A. Mensink, A. de Jager, K. van der Voort Maarschalk, H.W. Frijlink, W.L.J. Hinrichs, Size and molecular flexibility of sugars determine the storage stability of freeze-dried proteins, Mol. Pharm. 12 (2015) 684–694.

Chapter 5

Enhancing the stabilization potential of lyophilization for extracellular vesicles

Eduard Trenkenschuh[a], Maximilian Richter[b.c], Eilien Heinrich[b.c], Marcus Koch[d], Gregor Fuhrmann[b,c], and Wolfgang Friess[a]

[a] Pharmaceutical Technology and Biopharmaceutics, Department of Pharmacy, Ludwig-Maximilians-Universität München, 81377 Munich, Germany

[b] Helmholtz Centre for Infection Research (HZI), Biogenic Nanotherapeutics Group (BION), Helmholtz Institute for Pharmaceutical Research Saarland (HIPS), Campus E8.1, 66123 Saarbrücken, Germany

[c] Department of Pharmacy, Saarland University, Campus E8.1, 66123 Saarbrücken, Germany

[d] INM – Leibniz Institute for New Materials, Campus D2 2, 66123 Saarbrücken, Germany

This chapter has been published in the Journal 'Advanced Healthcare Materials' **(https://doi.org/10.1002/adhm.202100538)**.

Author contributions:

E.T. performed freeze-thaw and freeze-drying experiments, colloidal stability and lyophilizate analysis, and evaluated the data. M.R. and E.H. isolated extracellular vesicles, performed analysis on biological activity, and contributed with discussions. Cryo-TEM measurements were performed at the group of M.K.; E.T., M.R., G.F. and W.F. conceived the presented idea and planned the experiments. E.T. and M.R. wrote the manuscript. W.F. and G.F. supervised the work, provided conceptual guidance and corrected the manuscript.

Abstract

Extracellular vesicles (EV) are an emerging technology as immune therapeutics and drug delivery vehicles. However, EVs are usually stored at −80 °C which limits potential clinical applicability. We therefore studied freeze drying of EVs striving for long-term stable formulations. The most appropriate formulation parameters were identified in freeze-thawing studies with two different EV types. After a freeze-drying feasibility study, four lyophilized EV formulations were tested for storage stability up to 6 months. Freeze-thawing studies revealed improved EV stability in presence of sucrose or potassium phosphate buffer instead of sodium phosphate buffer or phosphate buffered saline. Less aggregation and/or vesicle fusion occurred at neutral pH compared to slightly acidic or alkaline pH. EVs could be most effectively preserved by addition of low amounts of poloxamer 188. Polyvinyl pyrrolidone failed to preserve EVs upon freeze-drying. Particle size and concentration of EVs was retained over 6 months at 40 °C in lyophilizates containing 10 mM K- or Na-phosphate buffer, 0.02% poloxamer 188 and 5% sucrose. The biological activity of encapsulated beta glucuronidase was maintained for 1 month, but decreased after 6 months. Here we present optimized parameters for lyophilization of EVs that enable to generate long-term stable EV formulations.

Keywords

extracellular vesicles, outer membrane vesicles, freeze-thawing, freeze-drying, long-term stability, particle preservation, stability testing

Abbreviations

β-Glu	Beta glucuronidase
DLS	Dynamic light scattering
DSC	Differential scanning calorimetry
EVs	Extracellular vesicles
FD	Freeze-drying
FT	Freeze-thaw
NP	Nanoparticle
OMVs	Outer membrane vesicles
PDI	Polydispersity index
P188	Poloxamer 188
PS20	Polysorbate 20
PBS	Phosphate buffered saline
RM	Residual moisture
RT	Room temperature
Suc	Sucrose
SVP	Subvisible particle
T_g	Glass transition temperature of the freeze-dried cake
T_g'	Glass transition temperature of the freeze-concentrated solution
TRPS	Tunable resistive pulse sensing
w/o	Without

Table of Contents

Abstract 112
Keywords 113
Abbreviations 113
1 Introduction 115
2 Results 117
2.1 Freeze-thawing studies 117
2.1.1 Impact of buffer type, pH and ionic strength 117
2.1.2 Impact of sucrose and surfactant 121
2.2 Lyophilization of EVs 123
2.3 Long-term stability of lyophilized EVs 125
2.3.1 Colloidal stability of lyophilized EVs 126
2.3.2 Biological activity of encapsulated β-Glu 129
3 Discussion 130
4 Conclusion 136
5 Experimental Section 137
5.1 Materials 137
5.2 Methods 138
5.2.1 Cell culture 138
5.2.2 Bacterial culture 138
5.2.3 FACS of RO EVs 139
5.2.4 Beta glucuronidase encapsulation 139
5.2.5 Size exclusion chromatography 140
5.2.6 Beta glucuronidase assay 140
5.2.7 Cryo-TEM 140
5.2.8 Formulation preparation 141
5.2.9 Freeze-thawing cycle 141
5.2.10 Freeze-drying cycle 141
5.2.11 Long-term stability testing of lyophilized samples 142
5.2.12 Dynamic light scattering 142
5.2.13 Tunable resistive pulse sensing 142
5.2.14 Subvisible particles 143
5.2.15 Nanoparticle tracking analysis 143
5.2.16 Karl-Fischer Titration 143
5.2.17 Differential scanning calorimetry 143
5.2.18 Statistical analysis 144
6 Supporting Information 144
7 References 151

1 Introduction

Lyophilization is a commonly used method to achieve stable biopharmaceutical products [1]. Substantial literature is available on freeze-drying of protein biopharmaceuticals, whereas knowledge about lyophilization of nanoparticulate biopharmaceuticals like vaccines, viruses or polyplexes is limited [2]. Due to their different particle properties, nanoparticulate systems require different colloidal and chemical stabilization mechanisms which increases lyophilization complexity.

EVs are nanoparticles produced by cells from all branches of the phylogenetic tree. They are surrounded by a lipid-membrane that contains transmembrane proteins. In their lumen EVs can contain a plethora of biomolecules, such as proteins, RNA and DNA [3]. Depending on the producing species, the mechanism of their assembly and the composition of their membrane differs. Mammalian cells produce two main variants of EVs, exosomes derived from multivesicular bodies and microvesicles produced directly by blebbing from the cell-surface [4]. EVs derived from gram-negative bacteria, the so-called outer membrane vesicles (OMVs), are produced by blebbing from the bacterial outer membrane [5]. EVs can successfully deliver functional cargo for intercellular communication [6]. This cargo is encapsulated in EVs and can be composed of proteins and nucleic acids. EVs are therefore intensely investigated as therapeutics [7,8], drug-delivery vehicles [9] and biomarkers for various diseases [10–12]. However, to be viable alternatives to established treatment-options and to allow for their broad use in clinical settings, many hurdles still need to be overcome [13,14]. Besides the reproducibility of their production and purification, storage stability is a big challenge [15,16]. EVs may be relatively stable in liquid state for a few weeks at room temperature [17,18]; still, clinical use would require extended shelf life. Since physical and biological stability is typically rather limited to a shorter time period, the International Society of Extracellular Vesicles recommends storage at –80 °C in phosphate buffered saline (PBS) [19]. However, this storage condition is unfavorable in terms of energy consumption, transportation and most importantly clinical application. In general, freezing-thawing (FT) is considered to destabilize EVs, e.g. by changing EV morphology, function, particle size and concentration [20–24]. EV stability differs by vesicle source and potentially the preparation method [25]. Pieters et al. demonstrated that milk-derived EVs are highly stable upon FT while the number of macrophage-derived vesicles was significantly reduced [26–29].

Freeze-drying of EVs could accelerate research and offers long-term stabilization which is an important step towards their application as therapeutics. Moreover, lyophilizates offer new options for administration routes, e.g. pulmonary delivery. Nevertheless, lyophilization increases stress during freezing and drying, which can result in EV damage unless appropriate stabilizers are added [30]. Freezing stress includes mechanical damage due to

crystal formation of ice or excipient, exposure to ice-liquid interfaces [31], pH shifts due to partial buffer salt precipitation [32–34], and cryo-concentration of the vesicles as well as all solutes, leading to a particle-rich phase with increased ionic strength [30,31,35]. During drying, the dehydration of the EVs affects their stability. Damage on lyophilized vesicles may also result upon rehydration e.g. with swelling of the amphiphilic molecules forming the vesicle bilayer or osmotic effects.

Frank et al. investigated the stability of different types of EVs during lyophilization [36]. Particle numbers of lyophilized EVs decreased compared to EVs stored at 4 °C or –80 °C indicating particle loss or aggregation. They also found a cell type specific freeze-drying behavior. When comparing different cryoprotective agents, trehalose was found to be superior to mannitol and polyethylene glycol 400. In earlier studies, it was already shown that trehalose is able to protect EVs from freeze-thawing stress [37]. Charoenviriyakul et al. also examined the impact of trehalose on aggregation and the biological activity of lyophilized exosomes [38]. Lyophilization with 50 mM trehalose had no impact on biological activity and polydispersity compared to samples stored at –80 °C. A possible damage already taking place during freezing to –80 °C was not considered. Although lyophilization of EVs seems to be feasible, there is no comprehensive study on their long-term stability.

Most EV formulations are based on PBS which is known to be critical upon freezing and lyophilization of biopharmaceuticals. During freezing, phosphate buffers cause an acidic pH shift which destabilizes proteins [1]. This effect might be relevant for surface and/or membrane proteins of EVs. In addition, the pH shift affects the zeta potential and thus the colloidal interactions of EVs [39]. Furthermore, the high ionic strength in PBS might foster particle aggregation shielding repulsive charge-based interactions of EVs. To the best of our knowledge, these effects have not been elucidated yet.

The aim of this study was to develop a lyophilized formulation for EVs with long-term stability of encapsulated cargo up to 6 months at 2-8 °C, including the evaluation of basic formulation components such as buffer agent and cryoprotectant. In order to provide a high number of different formulations, particle characterization was focused on methods using low vesicle concentrations thereby disregarding experiments such as cryo-EM which would have required increasing vesicle amounts by up to two orders of magnitude.

FT studies were performed to investigate the impact of PBS, various buffers and pH values, and the addition of sucrose and surfactants on EV stability. Here, OMVs derived from SBCy050 myxobacteria and EVs derived from B lymphoblastoid cells (RO cells) were evaluated. RO cells were isolated from the blood of a patient with severe combined immunodeficiency [40]. As they do not express MHC class II complexes they might be lower

in immunogenicity, as this prevents possible MHC-mismatches [41]. RO cells can be cultivated under serum-free conditions which removes the challenges associated with the use of fetal bovine serum [42]. Thus, RO cell-derived EVs are a highly interesting basis for EV-based drug delivery applications.

Based on findings from the FT studies, suitable formulations were selected for freeze-drying experiments of mammalian RO EVs. The lyophilizates were investigated for their long-term colloidal stability over 6 months at different temperatures. Vesicles were characterized with respect to their hydrodynamic diameter and polydispersity index (PDI) using dynamic light scattering (DLS). Particle number-based size distribution was examined by tunable resistive pulse sensing (TRPS), while subvisible particle (SVP) numbers were detected by flow cytometry imaging. Lyophilizates were additionally tested for their ability to preserve the biological activity of beta glucuronidase (β-Glu) encapsulated into the vesicles as a sensitive model biomacromolecule. Enzyme activity was quantified employing a simple fluorescence-based assay.

2 Results

2.1 Freeze-thawing studies

2.1.1 Impact of buffer type, pH and ionic strength

Figure 1 A-D shows cryo-TEM pictures of EVs from RO cells (mammalian) and SBCy050 OMVs (bacterial) both directly after UC and after an additional step of purification by SEC. Before SEC, the samples still contained non-vesicular material that was removed after SEC. Purified RO EVs were positive for two typical EV-markers, CD9 and CD63 (Figure 1 E and F) and negative for the endoplasmic reticulum marker calnexin (Figure S-1). The hydrodynamic particle size and PDI values before formulation preparation, i.e. before dialysis, filtration and excipient addition, were measured by DLS and are summarized in Table S-1. The conducted purification steps (i.e. ultracentrifugation, SEC and 0.2 µm filtration) help to avoid the presence of foreign particles.

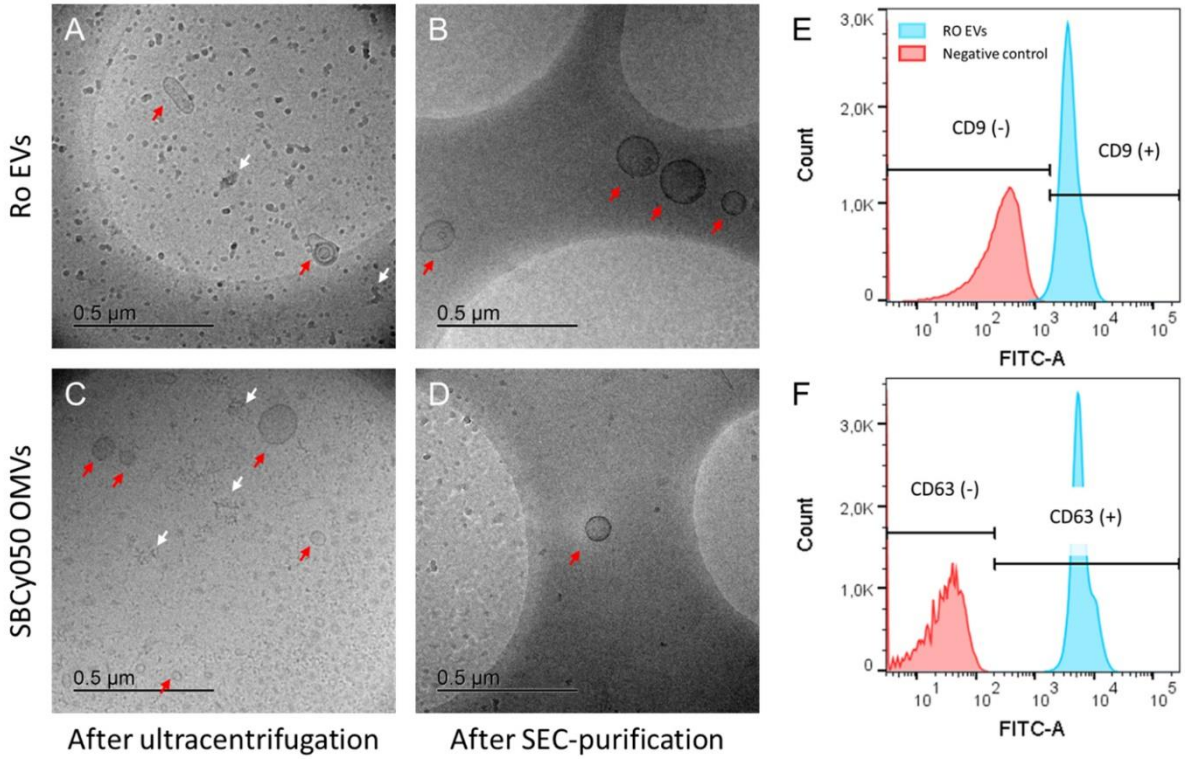

Figure 1: Characterization of RO EVs and SBCy050 OMVs by Cryo-TEM, both directly after ultracentrifugation (A and C) and after an additional step of SEC-purification (B and D). Red arrows point to vesicular structures, while white arrows indicate non-vesicular structures and cell debris. Panels E and F show the analysis of RO EVs by flow cytometry (FACS). RO EVs were positive for both CD9 (E) and CD63 (F).

Different formulation parameters (buffer type, pH, ionic strength) were initially tested in FT studies prior to EV freeze-drying and extended stability studies. FT was conducted in a freeze-dryer allowing controlled and thus reproducible ramp freezing (200 µL vial fill volume). Samples were frozen to a minimum of −50 °C since lower temperatures are not relevant for medium and larger scale pharmaceutical freeze-dryers. Buffer type and ionic strength may be critical formulation parameters affecting the stability of colloids upon FT and freeze-drying [1]. For this purpose, EVs were prepared in 10 mM Na- or K-phosphate buffer of different pH values, and in PBS. EVs are usually frozen and stored at pH 7.4 [19]. Thus, pH values of 7.4 ± ca. 1 pH unit were investigated in this study. As particle size and concentration are important quality criteria, DLS and TRPS measurements were performed before and after FT providing information about colloidal stability. In contrast to DLS, TRPS measurements provide further insight into number-based particle size distributions. Nanopores with two different size ranges were used to identify FT stable vesicles (NP100) as well as aggregates and/or fused vesicles (NP600). Before FT, SBCy050 OMVs and RO EVs

exhibited a mean particle size of 120 nm and 127 nm (NP100) respectively. DLS revealed particle sizes of 110 nm (SBCy050 OMVs) and 150 nm (RO EVs) with a polydispersity index (PDI) below 0.4 (Figure S-2).

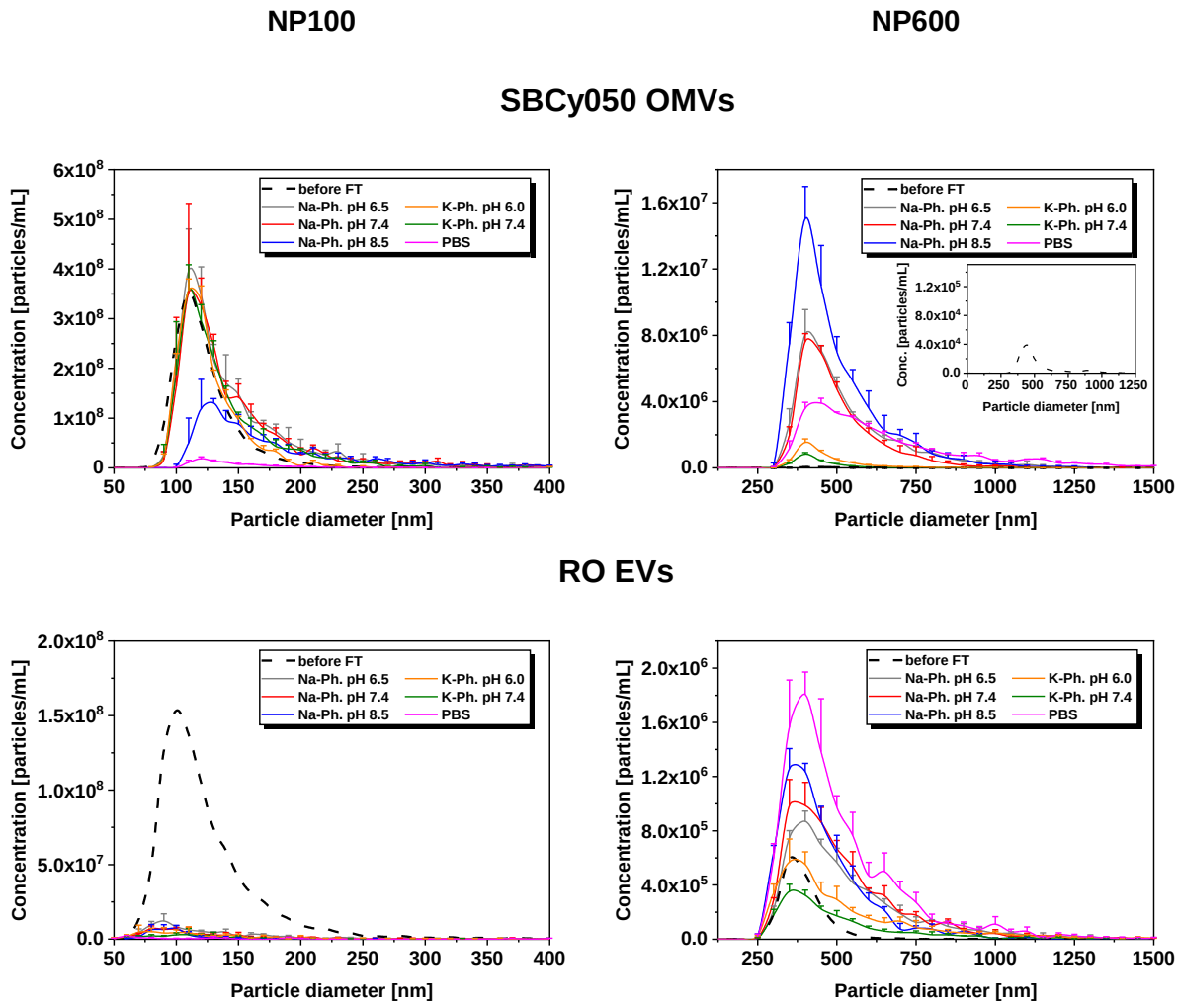

Figure 2: Number-based particle size distribution of EVs before FT (mean) or three times freeze-thaw stressed SBCy050 OMVs and RO EVs (TRPS, NP100 and NP600) formulated in 10 mM Na- or K-phosphate buffer at different pH values, and in PBS (mean ± SD; n=3).

After three FT cycles, the number of intact RO EVs decreased more drastically (total particle reduction ~96%) compared to bacterial SBCy050 OMVs (Figure 2) indicating a markedly lower FT stability of the RO EVs. For both vesicle types, the total number of larger particles increased after FT; up to 330-fold for SBCy050 OMVs formulated at pH 8.5, and up to ~4-fold for RO EVs in PBS (Figure S-3). Interestingly, the number of larger particles became markedly higher for SBCy050 OMVs compared to RO EVs. Thus, SBCy050 OMVs predominantly increased in size (e.g. due to aggregation or vesicle fusion) while RO EVs potentially got disrupted upon freezing. For both vesicle types, flow imaging measurements revealed the

highest number of subvisible particles in PBS-containing samples (Figure S-5). These results were in line with DLS (Figure S-2).

The pH value substantially affected FT stability of EVs. Both vesicle types revealed a lower number of large particles in K-phosphate buffer at pH 7.4 compared to pH 6.0; total particle reduction ~54% and ~45% for SBCy050 OMVs and RO EVs respectively. SBCy050 OMVs exhibited a low number of small particles and simultaneously a high number of large particles at pH 8.5. In case of RO EVs, an increasing pH resulted in a higher quantity of large particles (total number of particles/mL at pH 6.5: ~5.06E+06; pH 7.4: ~5.90E+06; pH 8.5: ~5.99E+06) which was also represented by an increasing particle size in DLS measurements (Figure S-2). In general, K-phosphate buffers led to a significantly lower number of large particles compared to Na-phosphate buffers. This effect was more pronounced for SBCy050 OMVs compared to RO EVs.

To further evaluate the impact of buffer pH on colloidal stability, EVs were formulated in K-phosphate at four different acidic pH values and measured by DLS over 1 h (Figure 3). At acidic pH values, larger particle sizes were already measured at T_0 indicating low particle stability, especially for bacterial SBCy050 OMVs. Over time, the particle size of SBCy050 OMVs substantially increased at pH 3, 4 and 5. RO EVs showed less particle growth which corresponded to the behavior upon FT shown before. Thus, a near-neutral pH proved to be most suitable for particle stability.

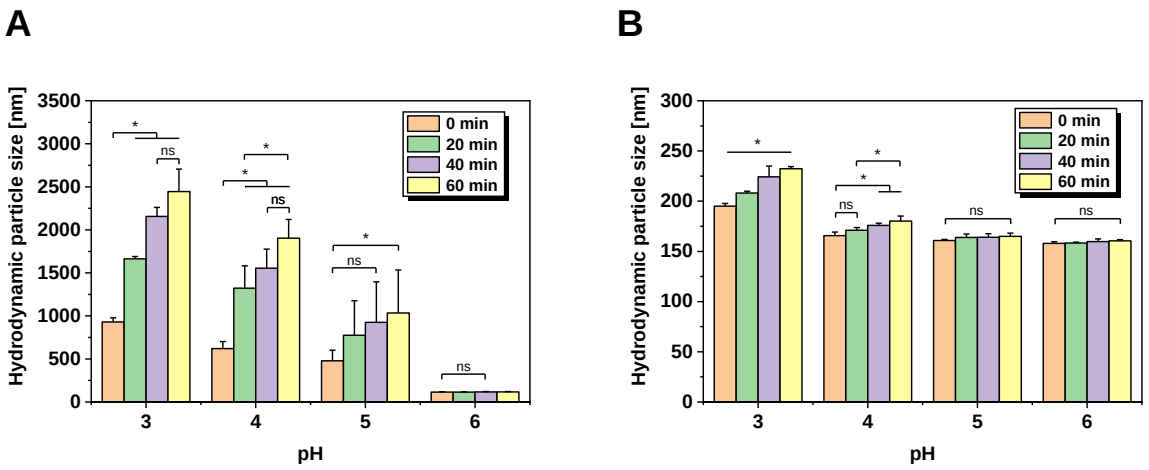

Figure 3: Hydrodynamic particle size (DLS) of SBCy050 OMVs (A) and RO EVs (B) formulated in K-phosphate buffer at different pH values over 1 h at 25 °C (n=3). Each data point represents mean ± SD, n=3. Two-way ANOVA, Bonferroni-Holm post-hoc test, *p<0.05, ns=non-significant.

2.1.2 Impact of sucrose and surfactant

Subsequently, different stabilizers were evaluated for their suitability to protect EVs upon freezing. PS20 and P188 were chosen as potential surface-active stabilizers while sucrose was tested as a cryoprotectant. Vesicles were either formulated in 10 mM Na-phosphate at pH 7.4 or in PBS, using more critical buffer conditions than K-phosphate to challenge the stabilizer capacity. K-phosphate was tested in combination with P188 in the following storage stability study providing a control for the Na-phosphate formulation. FT induced particle growth could be reduced in presence of sucrose (Figure 4, for DLS results see Figure S-2). The total number of large particles was reduced by ~11% and ~44% for SBCy050 OMVs and by ~57% and ~55% for RO EVs in samples formulated in PBS and 10 mM Na-phosphate respectively (Figure S-3). Still, a pronounced loss of intact vesicles and a high number of larger particles were found in PBS-containing samples compared to 10 mM Na-phosphate. Sucrose better stabilized SBCy050 OMVs compared to RO EVs in 10 mM Na-phosphate (measured with NP100). However, particle growth was also more pronounced for SBCy050 OMVs and confirmed for both vesicle types by DLS.

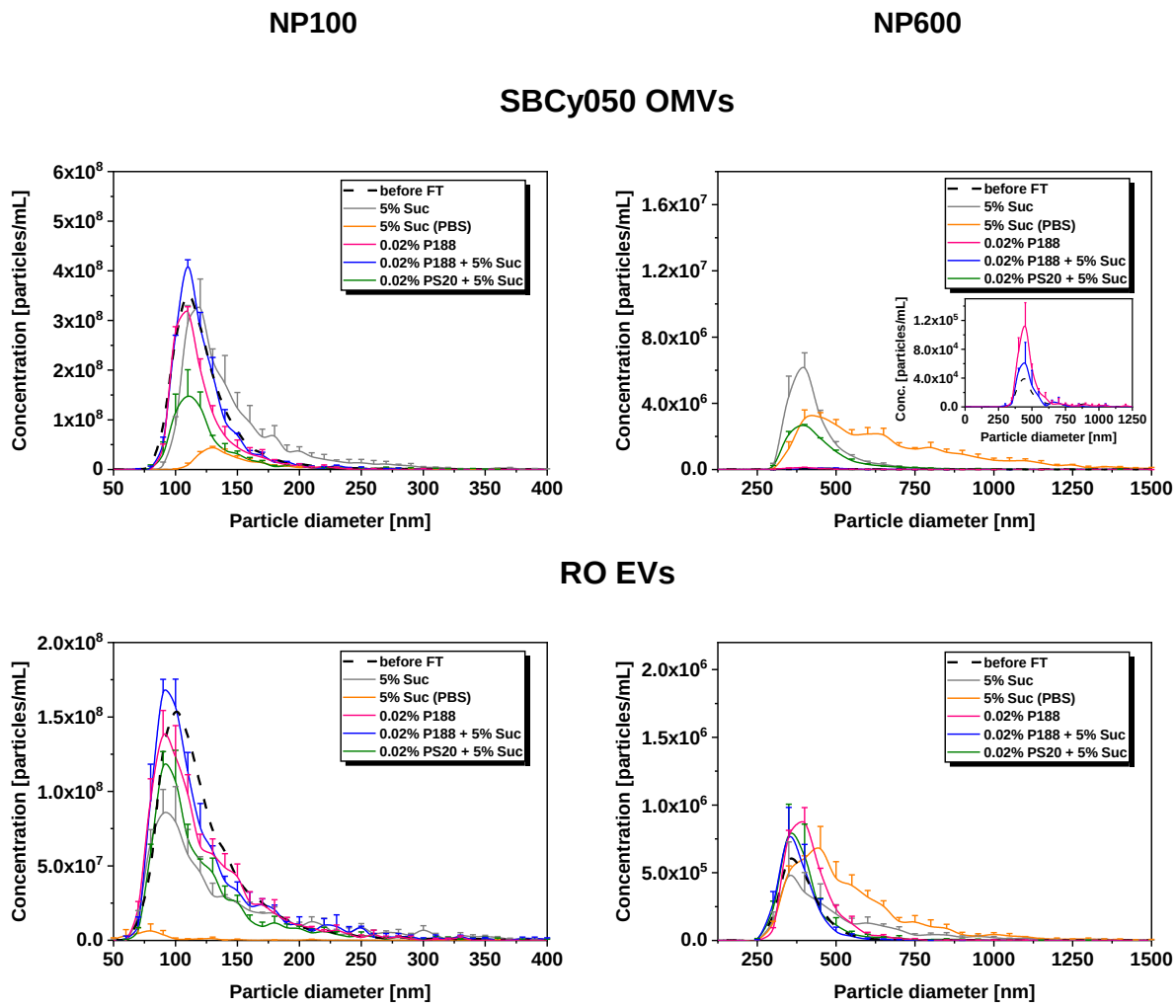

Figure 4: Number-based particle size distribution of EVs before FT (mean) or three times freeze-thaw stressed SBCy050 OMVs and RO EVs (TRPS, NP100 and NP600) formulated in 10 mM Na-phosphate pH 7.4 or PBS with sucrose and/or surfactants (mean ± SD; n=3).

The addition of P188 led to preserved EV numbers with a slight increase of larger particles (SBCy050 OMVs: ~1.8-fold; RO EVs: ~1.5-fold; Figure S-3). Moreover, P188 combined with sucrose as cryoprotectant led to the highest number of intact vesicles and the lowest number of aggregated and/or fused particles. The concentration of RO EVs could be preserved in samples containing PS20 and 5% sucrose. In contrast, SBCy050 OMVs showed a loss of approximately 60% of vesicles (6.87E+08 particles/mL instead of ~1.70E+09 particles/mL) already before FT and were thus excluded from the mean particle size distribution (data not shown). Interestingly, in spite of the initial loss, about 90% of SBCy050 OMVs were maintained after FT with an increased number of larger particles compared to P188. SBCy050 OMVs exhibited a mean particle size of 55 nm and a PDI of 1.0 according to the cumulant fit analysis in DLS measurements (Figure S-4). The more suitable regularization fit analysis for non-monomodal particle size distributions revealed two particle

populations: (i) a population with a particle size of 130 nm which corresponded to intact vesicles, and (ii) a population with a particle size of about 23 nm indicating fragments of disrupted EVs. This effect was not observed for RO EVs which indicates that this population in the 20 nm size range does not reflect PS20 micelles. In DLS, placebos of surfactant containing formulations revealed 7 nm sized particles in presence of PS20 representing micelles, while no particles were detected in presence of P188 due to a concentration below the critical micelle concentration [43] (data not shown). TRPS using NP100 was not suitable to detect micelles in placebo formulations.

Before FT, SBCy050 OMVs and RO EVs revealed a surface charge of ~−25 mV and ~−30 mV respectively, independent of buffer type, pH, sucrose or surfactant addition (Table S-2). After FT, the surface charge increased by up to 80% in formulations causing a high number of large particles. In contrast, the surface charge changed to 10-30% in surfactant or K-phosphate containing samples.

2.2 Lyophilization of EVs

Consequently, mammalian RO EVs and bacterial SBCy050 OMVs formulated in 10 mM Na-phosphate buffer in combination with 0.02% P188 and 5% sucrose were tested for their freeze-drying stability (same EV batches as for FT studies). In addition to the assessment of the colloidal stability, unfiltered RO EVs were lyophilized and analyzed for vesicle morphology by cryo-TEM and EV markers by FACS. A conservative freeze-drying cycle was applied (200 µL vial fill volume). The samples were frozen to –50 °C and the product temperature during primary drying was maintained well below the T_g' of sucrose (–32 °C) at 40 mTorr chamber pressure and –20 °C shelf temperature. The lyophilized samples showed a good cake appearance and dissolved instantly (< 5 s) upon addition of 190 µL HPW (calculation based on the solid content).

Figure 5 A and B shows cryo-TEM pictures of unfiltered RO EVs after lyophilization and subsequent reconstitution. RO EVs were positive for the two typical EV markers, CD9 and CD63 (Figure 5 C and D).

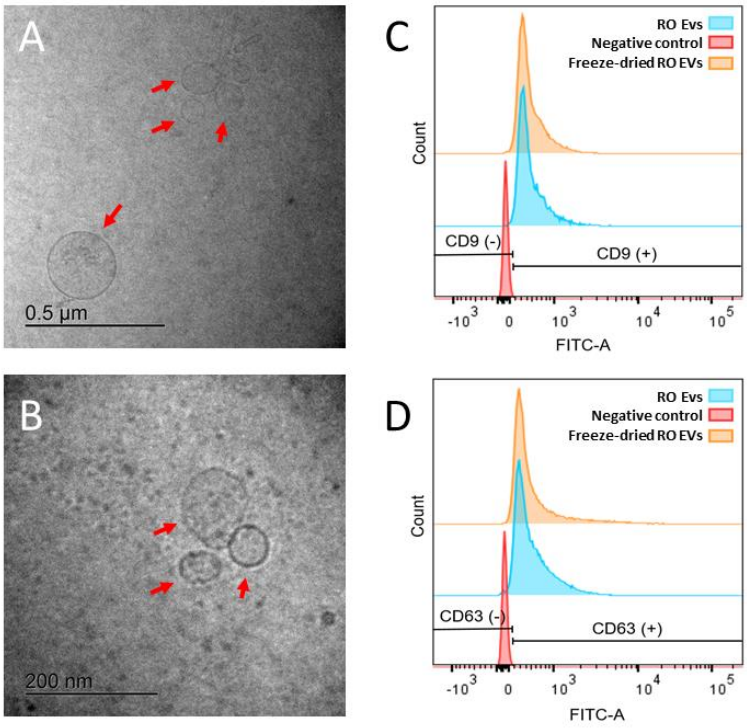

Figure 5: Characterization of unfiltered RO EVs by cryo-TEM, directly after lyophilization and reconstitution (A and B). Red arrows point to vesicular structures. RO EVs were positive for both CD9 (C) and CD63 (D) as shown by flow cytometry (FACS) analysis.

The particle concentration of 0.2 µm filtered was well preserved for both vesicle types with a slight decrease of small particles for RO EVs (Figure 6). However, lyophilization led to an increased number of larger particles compared to FT stressed vesicles; this effect was more pronounced for bacterial SBCy050 OMVs (15-fold increase of the total particle number). In DLS, the mean particle sizes and PDI did not change (Figure S-6).

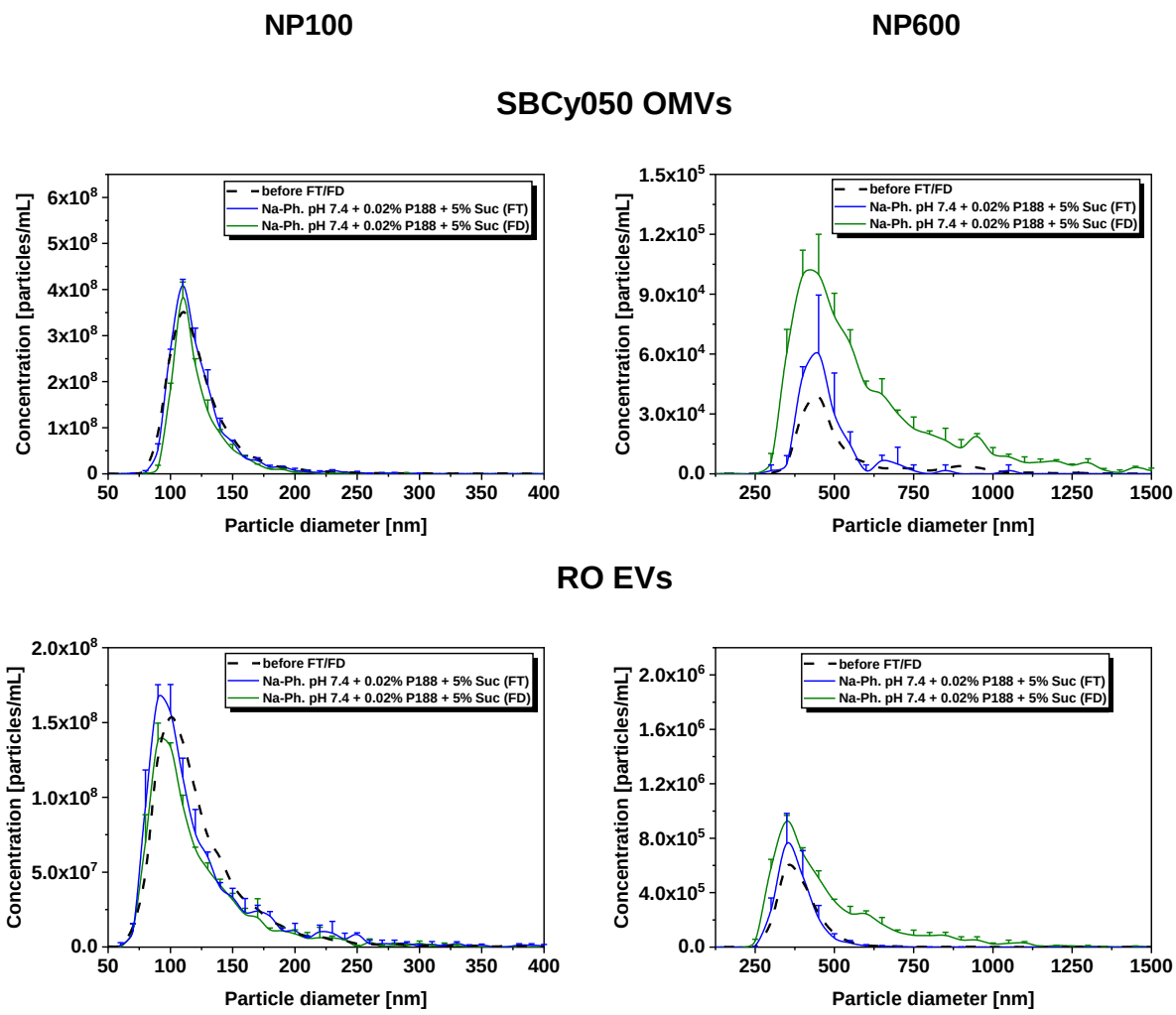

Figure 6: Number-based particle size distribution of EVs before FT/FD (mean), three times freeze-thaw stressed (FT), and freeze-dried (FD) SBCy050 OMVs and RO EVs (TRPS, NP100 and NP600) (mean ± SD; n=3).

2.3 Long-term stability of lyophilized EVs

Based on the previous results, four formulations of mammalian RO EVs loaded with β-Glu were prepared using saponin-based encapsulation, with the enzyme acting as an easily quantifiable surrogate for biologically active EV-cargoes. Samples were investigated regarding long-term colloidal stability over 6 months at 2-8 °C, 25 °C and 40 °C. After reconstitution of the lyophilizates, samples were analyzed for particle size, particle concentration, surface charge and the biological activity of the associated model enzyme β-Glu. Furthermore, solid-state properties of lyophilized placebo formulations were characterized by Karl-Fischer titration and DSC. FT experiments had shown that the addition of P188 drastically improved EV stability. Although colloidal stability issues of EVs in Na-phosphate buffer can be overcome by the addition of P188, the influence of the buffer salt

type on biological activity of the encapsulated enzyme over time was unclear. Therefore, formulations in a Na-phosphate and K-phosphate buffer were considered for the long-term stability study. Furthermore, PVP (MW ~8.000-10.000 Da) was investigated as a surface-active polymer. It is used in lyophilization due to its cryoprotective properties and the ability to form elegant lyophilizate cakes [44–46]. Thus, 0.02% PVP was tested as an alternative to P188, while 5% PVP was evaluated as a sucrose replacement.

2.3.1 Colloidal stability of lyophilized EVs

Upon lyophilization and storage, the particle size and concentration of samples containing P188 and sucrose remained stable independently of the used phosphate buffer type (Figure 7). According to TRPS NP600 measurements, large particles formed during freeze-drying. Their number slightly further increased with increasing storage temperature and time.

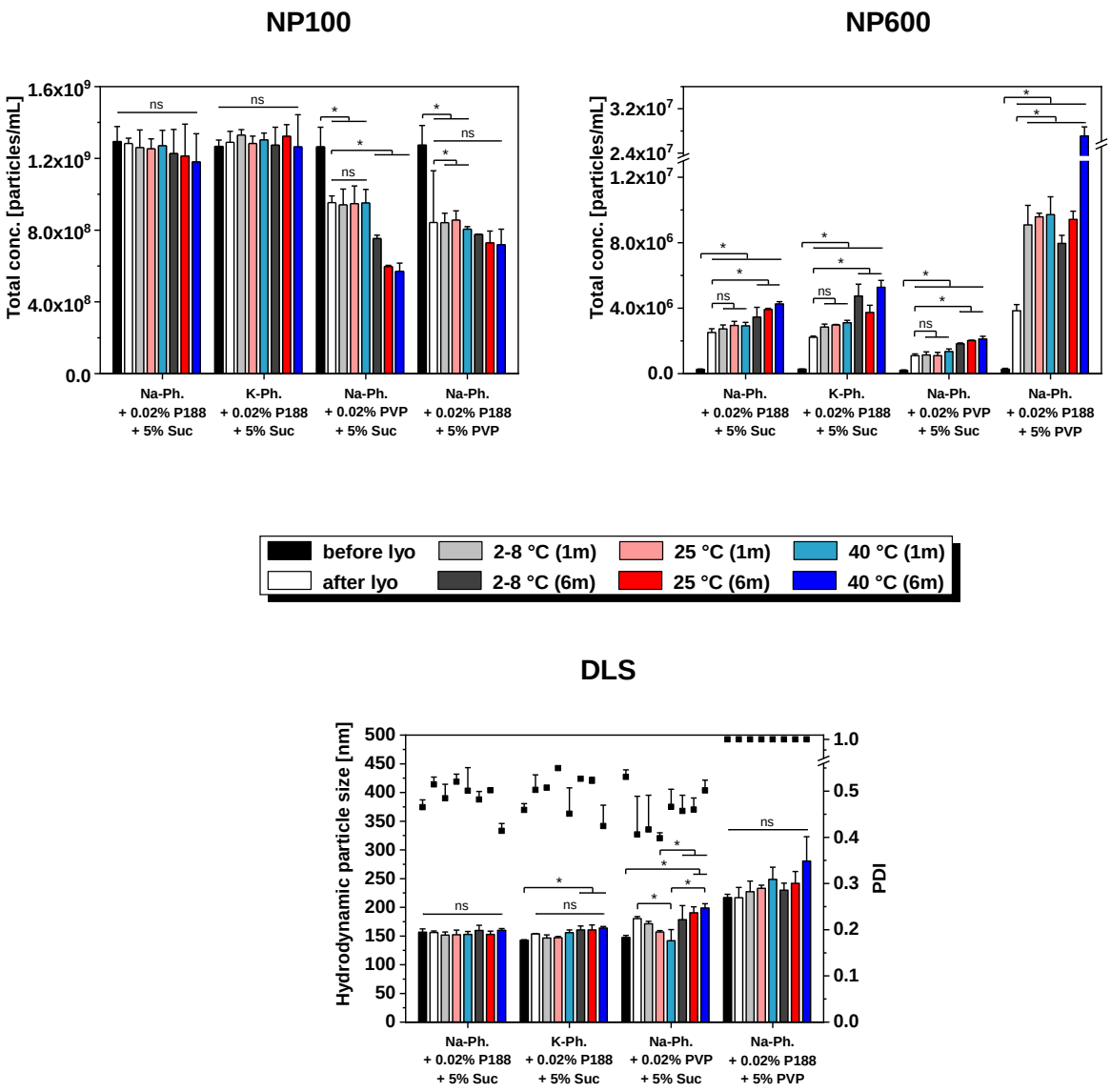

Figure 7: Particle concentration and size of beta glucuronidase encapsulated RO EVs before lyophilization, after lyophilization, and after storage for 1 month and 6 months at 2-8 °C, 25 °C, and 40 °C measured with TRPS using NP100 and NP600, and DLS. Each data point represents mean ± SD, n=3. One-way ANOVA, Bonferroni post-hoc test, *p<0.05, ns=non-significant.

Before lyophilization, DLS measurements revealed an EV particle size of about 217 nm in samples containing 5% PVP compared to about 150 nm in the other formulations. This discrepancy was not observed in TRPS measurements. Furthermore, a PDI of 1.0 for these formulations resulted from an additional peak in the low nanometer range in the intensity versus size distribution. This peak was reproducible for EVs and placebo formulations (i.e. 10 mM Na-phosphate + 0.02% P188 + 5% PVP without EVs) and no additional peaks at bigger particle diameters were detected (data not shown). The particle number measured by TRPS NP100 directly after lyophilization was decreased by 27% and 35% in 0.02% and 5% PVP samples respectively. The number of small particles remained constant over

1 month, but decreased further over 6 months storage. In parallel, a low number of larger particles was measured for 0.02% PVP samples while a distinct increase was detected in presence of 5% PVP, especially after 6 months at 40 °C. Zeta potential measurements revealed similar surface charge in all formulations (~−24 mV) which remained mostly unchanged during storage (Table S-3). To ensure that the particles measured were not related to aggregated free enzyme, non-encapsulated β-Glu formulated in phosphate buffer containing P188 and sucrose was freeze-dried. NTA measurements did not reveal enzyme aggregation (Figure S-7).

The residual moisture levels of all lyophilizates increased with increasing storage temperature and longer storage time (Table 1). 5% PVP formulations showed higher water contents (0.8 - 3.4%) compared to 5% Suc formulations (0.7 - 2.3%). The T_g values decreased corresponding to the increase in moisture. 5% PVP formulations revealed the highest T_g values between 111.9 °C and 86.0 °C.

Table 1: T_g' before lyophilization and T_g and RM directly after lyophilization and after storage for 1 month or 6 months at 2-8 °C, 25 °C, and 40 °C (mean ± SD; n=3).

	10 mM Na-Ph. 0.02% P188 + 5% Suc		**10 mM K-Ph. 0.02% P188 + 5% Suc**		**10 mM Na-Ph. 0.02% PVP + 5% Suc**		**10 mM Na-Ph. 0.02% P188 + 5% PVP**	
	T_g'/T_g [°C]	**RM [%]**	**T_g'/T_g [°C]**	**RM [%]**	**T_g'/T_g [°C]**	**RM [%]**	**T_g'/T_g [°C]**	**RM [%]**
before lyo	-31.9 ± 0.1		-32.1 ± 0.1		-31.6 ± 0.1		-24.5 ± 0.0	
after lyo	65.3 ± 0.9	0.7 ± 0.1	65.5 ± 0.5	0.7 ± 0.0	65.8 ± 1.7	0.7 ± 0.1	111.9 ± 0.7	0.8 ± 0.0
1 m 2-8 °C	65.6 ± 0.4	0.7 ± 0.1	64.0 ± 0.6	0.7 ± 0.0	65.6 ± 0.4	0.7 ± 0.0	111.1 ± 1.1	0.9 ± 0.0
1 m 25 °C	59.9 ± 0.7	1.2 ± 0.1	59.4 ± 1.1	1.2 ± 0.1	60.8 ± 0.5	1.3 ± 0.0	103.7 ± 2.3	1.5 ± 0.0
1 m 40 °C	55.6 ± 0.6	1.8 ± 0.1	54.9 ± 0.4	1.9 ± 0.1	56.1 ± 1.0	1.9 ± 0.1	98.3 ± 0.5	2.8 ± 0.1
6 m 2-8 °C	54.9 ± 1.5	1.4 ± 0.2	50.6 ± 2.2	1.3 ± 0.0	53.9 ± 1.6	1.4 ± 0.1	95.9 ± 3.5	1.6 ± 0.1
6 m 25 °C	48.3 ± 2.8	2.1 ± 0.0	46.0 ± 1.3	2.0 ± 0.0	47.9 ± 1.2	2.1 ± 0.1	88.4 ± 5.2	3.1 ± 0.1
6 m 40 °C	47.1 ± 1.5	2.2 ± 0.2	44.5 ± 3.2	2.2 ± 0.2	47.7 ± 2.5	2.3 ± 0.1	86.0 ± 4.9	3.4 ± 0.1

2.3.2 Biological activity of encapsulated β-Glu

As the assessment of the colloidal vesicle-stability already showed that formulations containing the combination of 5% Suc and 0.02% P188 best preserved EVs, they were further evaluated regarding the stability of encapsulated β-Glu. Figure 8 shows the activity of encapsulated β-Glu before and after lyophilization and storage of the formulations containing 5% Suc, 0.02% P188 and either 10 mM Na-phosphate or 10 mM K-phosphate. Samples were purified by SEC to remove non-encapsulated enzyme and the enzyme-activity in EV-containing fractions was measured by the conversion of non-fluorescent fluorescein-di-β-D-glucuronide to fluorescent fluorescein. EVs from both formulations showed a similar initial fluorescence. After lyophilization, there was a decrease in enzyme activity compared to the initial value, which was more pronounced for K-phosphate samples. After one month of storage between 66 and 100% enzyme-activity were recovered for Na-phosphate and between 52 and 67% for K-phosphate. After 6 months of storage, the recovered enzyme activity was reduced for all samples to 15-25% at 2-8 °C and 25 °C. In samples containing Na-phosphate, 26% enzyme activity remained at 2-8 °C and 18% at 25 °C, while no activity remained in samples stored at 40 °C. EV samples containing K-phosphate, stored 6 months at 2-8 °C or 40 °C showed a recovery of approx. 20% of the initial enzyme activity, while 15% remained in sample stored at 25 °C.

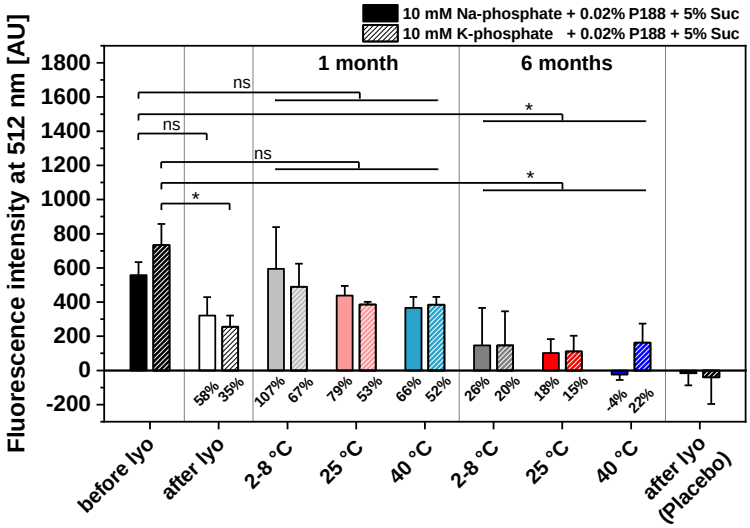

Figure 8: Comparison of the stability of beta glucuronidase encapsulated in RO EVs formulated with 5% Suc, 0.02% P188 and either 10 mM Na-phosphate or 10 mM K phosphate. Enzyme activity is expressed as the fluorescence-intensity of fluorescein generated through the enzymatic conversion of fluorescein-di-β-D-glucuronide. Percent values indicate the recovery rate of active enzyme after lyophilization and after storage for 1 and 6 months compared to samples before lyophilization. Placebo indicates samples containing only the respective buffers and cryoprotectants and no EVs. Each data point represents mean ± SD, n=3. Two-way ANOVA, Bonferroni-Holm post-hoc test, *p<0.05, ns=non-significant.

3 Discussion

We studied the stabilization of EVs derived from RO cells and SBCy050 bacteria by lyophilization. Cryo-TEM showed the typical morphology of EVs and OMVs in the size-range reported in literature [42,47,48] and the successful removal of non-vesicular structures from the samples. The appearance of fewer vesicles was attributed to the dilution of the vesicles due to SEC. The isolated and purified EVs were further processed by dialysis and filtration which may lead to vesicle loss due to adsorption processes [49] and exclusion of larger vesicles respectively. These steps, however, ensured reliable particle characterization using well-established techniques (i.e. TRPS, DLS and SVP measurements). Especially before FT, polydisperse samples do not allow comparison of PDI values (all >0.56) and hamper TRPS measurements due to nanopore clogging using NP100 as seen in preliminary studies (data not shown). TRPS was introduced as a suitable method providing an insight into number-based particle size distributions. Nonetheless, this method may not be able to discriminate between different types of particles [50], such as intact EVs, protein aggregates or vesicle fragments. Furthermore, particles much smaller than the nanopore may not be detected resulting in an underestimated particle concentration [51].

The stability of EVs can be drastically affected by freezing and drying. Both aspects of lyophilization cause several types of stresses, such as cryo-concentration, mechanical damage by ice crystals, interaction at the ice-water interfacial area, and loss of a stabilizing hydration shell [1]. The effect of freezing itself was investigated prior to lyophilization by FT studies and may be the more aggressive step [52]. Three FT cycles were conducted to evaluate the stabilizer capacity and the damage promoted by freezing. Recent studies showed a correlation of EV particle and cargo stability upon the freezing and lyophilization process [36,53]. Nevertheless, FT is also reported as a method enabling drug loading into exosomes, however, suffering from low encapsulation efficiency and the formation of large particles most likely due to aggregation [54].

Maintenance of biological activity is the most important aspect after lyophilization. A loss of vesicles or the formation of larger particles indicate inappropriate stabilization and have to be avoided, especially as the number of visible particles is restricted in injectable drug products [55]. Thus, for the sake of simplicity, FT and FD feasibility were performed using unloaded EVs, while EV loading with β-Glu was introduced in the subsequent storage stability study. The stabilizer excipients used throughout this study were carefully chosen and are approved for various administration routes, including parenteral use [56]. Furthermore, side effects due to potassium ions are not expected at the low dosing levels required for EVs.

In general, mammalian RO EVs were more prone for colloidal destabilization upon freezing compared to SBCy050 EVs. The different compositions of the lipid bilayer and surface and/or membrane proteins of EVs originating from mammalian cells and gram-negative bacteria are assumed to lead to the divergent stability profiles. The trend could be observed for different formulation parameters varying in buffer type, pH, the addition of sucrose and a surfactant. Differences in the stability profiles after lyophilization of EVs from different mammalian cell-lines were also identified by Frank et al. [36].

The formulation itself drastically affected the propensity of EV's to form larger particles. These larger particles may be formed due to aggregation of intact vesicles, or components thereof, or fusion into larger vesicles as seen for liposomes [57]. Interestingly, surface charge measurements by TRPS revealed no differences between the formulations before FT/FD; this might be due to, in fact, little surface charge variations or potential charge shielding in presence of 140 mM NaCl. A more detailed investigation of the nature of the particles was beyond the scope of the study. It could be executed by cryo-TEM which however requires up-concentration bearing a high risk of artefacts. Without other stabilizers, the number of larger particles was substantially reduced in K-phosphate compared to Na-phosphate buffer. Na-phosphate buffer systems are known to cause an acidic pH shift during freezing due to selective crystallization of buffer components while K-phosphate buffers are able to maintain the pH [34]. This pH shift appears to destabilize EVs during freezing. Therefore, the impact of acidic pH was further investigated in the liquid state. DLS measurements over time showed that an acidic pH is unfavorable for colloidal stability leading to the formation of large particles. A detrimental effect of an acidic environment was also shown by Cheng et al. when comparing EV loss upon storage at pH 4 to pH 7 and 10 [53]. A change in pH also affects the EV surface charge and thereby the electrostatic interactions [58]. In case of SBCy050 EVs, after FT a higher concentration of larger particles was found at pH 8.5 compared to pH 6.5 and pH 7.4. Thus, a pH optimum providing colloidal stability is essential and has to be maintained during the freezing process.

PBS is the most commonly used buffer for the processing of EVs. Therefore, PBS is usually used during storage at –80 °C which is the gold standard for preservation of EVs [19]. Interestingly, PBS reveals to be unfavorable for both EV types since a high number of large particles was measured after FT. This effect might be driven by the aforementioned pH shift of Na-phosphate which is part of the buffer system. Furthermore, the salt present in PBS (137 mmol NaCl, 2.7 mmol KCl) can be assumed to trigger particle aggregation. During freezing, the formation of extracellular ice leads to up-concentration of the extracellular solutes. High salt concentrations are known to negatively impact the stability of colloids by shielding repulsive forces [1,59]. Furthermore, surface and/or integral proteins of EVs might

be prone to salt denaturation. The cryo-concentration of salts also elevates the extracellular osmotic pressure and rapid water flux through the bilayer can be responsible for physical forces leading to rupture and destabilization [60].

Cryo- and lyoprotection is an important means to preserve the stability of proteins and colloids during freezing and freeze-drying. We therefore tested the effect of sucrose on the colloidal stability of EVs. Both EV types showed less particle growth in presence of sucrose, but this effect could not be avoided completely. Various mechanisms, such as the preferential exclusion theory, and increased viscosity were discussed in the past in order to explain how cryoprotectants preserve colloids during freezing. The preferential exclusion theory was originally proposed for proteins and later for liposomes [61]. The theory states that solutes are preferentially excluded from protein surfaces or membranes leading to the formation of a stabilizing solvent layer. Due to cryo-concentration, the solute concentration drastically increases intensifying this mechanism. Furthermore, the increased solution viscosity during freezing is assumed to restrict diffusion and thus colloidal interactions slowing down aggregation and degradation processes [62].

Surfactants are known to protect colloids from surface-induced damage during freezing [1]. However, the use of surfactants is generally avoided in lipid delivery vehicles due to the fear of disrupting the lipid bilayer. During freezing, this effect is even more critical due to the up-concentration of the surfactant. PS20 and P188 are approved in parenteral products and were therefore selected in this study [56]. We could demonstrate here that the type of surfactant has to be chosen carefully. In contrast to RO EVs, our SBCy050 OMVs showed a low number of intact vesicles in presence of PS20 already before FT. The small particles measured by DLS are attributed to EV fragments formed upon lysis. The phenomenon of differential detergent sensitivity was also reported by Osteikoetxea et al. showing surfactant and concentration dependent lysis of EVs [63]. Although surfactants can be detrimental to lipid bilayers, Yu et al. showed that the addition of polysorbate 80 could minimize aggregation and loss of transfection-activity of lyophilized lipoplexes [64].

Interestingly, in presence of P188, size and concentration of EVs were preserved upon FT independently of the vesicle type. Furthermore, the detrimental effect of Na-phosphate was not observed indicating protective properties of the surfactant in spite of the pH shift during freezing. A stabilizing effect of P188 on lipid membranes was reported by Sharma et al. who observed that P188 decreased the susceptibility of lipid membranes to electroporation [65]. Further studies revealed that P188 directly inserts into lipid monolayers [66]. This mechanism was confirmed by later computer simulation studies. It is suggested that hydrophobic chains of P188 get inserted into damaged lipid bilayers, ultimately closing pores [67]. A stabilizing effect of P188 was also reported for liposomes [68,69]. Surfactants protect proteins against

surface-mitigated aggregation which could be the second mechanism for EV stabilization [70]. The addition of sucrose as a cryoprotectant was not mandatory to preserve the size and concentration of RO EVs in presence of P188. The combination of P188 and 5% Suc only slightly reduced the number of larger particles for SBCy050 EVs. This finding indicates that vitrification may be less critical for EV preservation upon freezing. Freezing-induced damage is rather promoted at the ice-liquid interface or due to hydrophobic interactions which are reduced by surfactants. The differences in molecular weight and hydrophilic/lipophilic balance of P188 (MW ~8400 Da, HLB=29) and PS20 (MW ~1200 Da, HLB=16.7) are assumed to lead to different interactions with lipid bilayers and therefore different lysing properties. The gained information is furthermore helpful for current storage practice, i.e. storage at −80 °C; our studies confirm that physical stability can be maintained upon repeated FT which may avoid discarding of once thawed but unused sample.

Since sucrose was suitable to provide vesicle stability in presence of P188, it was used as a bulking agent for freeze-drying to render isotonicity and to obtain an elegant macroscopic cake appearance. Both EV types were evaluated for their lyophilization feasibility using the formulation containing P188 and sucrose in Na-phosphate buffer at pH 7.4. Particle size and concentration of EVs were well-preserved after lyophilization showing a negligible increase of larger particles compared to three times FT samples. Furthermore, the vesicle morphology and the typical markers CD9 and CD63 were maintained, as shown for RO EVs. The drying step of lyophilization appears to be less critical compared to freezing and thus FT studies prove to be an important formulation screening tool to evaluate physical stability. Storage stability studies were conducted with vesicles lyophilized in four different formulations:

i) a formulation containing P188 and sucrose in Na- phosphate buffer pH 7.4

ii) a formulation containing P188 and sucrose in K-phosphate buffer pH 7.4 to evaluate the criticality of the pH shift for the freeze-dried product with a cargo

iii) a formulation with 0.02% PVP as an alternative stabilizer to P188 with similar molecular weight (PVP ~8.000-10.000 Da)

iv) a formulation with 5% PVP as an alternative stabilizer, lyoprotectant and bulking agent since PVP is commonly used in lyophilization and known for the excellent cake appearance of lyophilizates due to the relatively high T_g' and T_g values

RO EVs were chosen for the freeze-drying storage stability studies due to the greater relevance of EVs derived from mammalian cells in current efforts for clinical translation [8]. To assess not only the colloidal stability, but also gain insight into the fate of their cargo, β-Glu was encapsulated as a surrogate. Saponin based encapsulation of hydrophilic cargoes has

been used previously without negative impact on EV-morphology [54,71]. Correspondingly, we did not observe differences in the physicochemical characterization of freshly lyophilized RO EVs with or without encapsulated β-Glu.

Before freeze-drying, the identity of EVs derived from RO cells was further confirmed by assessing typical surface-markers CD9 and CD63 and proving the absence of the endoplasmic reticulum marker calnexin by FACS [72]. RO EVs exhibited a larger particle size in 5% PVP compared to sucrose formulations. This marked size difference was detected by DLS but not in TRPS measurements. The larger size in DLS is attributed to significantly different osmolality in 5% Suc and 5% PVP solutions. In contrast, TRPS measurements are conducted in presence of 140 mM NaCl which is required to provide sufficient conductivity of the solution. Thus, the osmotic effect of the cryoprotectant may become negligible resulting in vesicles of similar particle size.

After lyophilization and storage, the particle concentration of small particles (NP100) decreased drastically in PVP containing formulations while the concentration of large particles (NP600) increased indicating insufficient particle stabilization. These results are in line with findings by El Baradie et al. who observed an EV loss after lyophilization in presence of 100 mM trehalose/ 5% PVP40 [73]. Thus, the ability of P188 to directly interact with lipid membranes is vital for freeze-drying success. Furthermore, we conclude that RO EVs are better embedded in sucrose compared to PVP due to enhanced water replacement and interactions between the lyoprotectant and vesicles. Our observation is in accordance with findings by Mensink et al. who showed that molecularly more flexible disaccharides better stabilized proteins during freeze-drying than molecularly more rigid polysaccharides [74]. The excess of PVP might furthermore lead to hampered stabilization by P188 due to competitive interactions with the vesicle lipid bilayer.

The solid-state properties of the lyophilizates showed an increase in residual moisture content over time up to 3.4% which might be due to i) transfer of moisture from stoppers to the formulation, ii) diffusion or transmission of moisture through the stopper, and iii) microleaks in the stopper-vial seal [1]. The low fill volume and thus lyophilizate mass contributes to the pronounced increase of water content upon uptake of only little absolute water amounts. The T_g of the lyophilizates was decreased by about 27% due to the plasticizing effect of water. Vitrification becomes the limiting factor for storage stability when the storage temperature is closer to or above the T_g. In order to avoid residual viscous flow of the lyophilizate, Franks proposed that the T_g value should be 20 °C above of the storage temperature [75]. This specification was kept at 2-8 °C and 25 °C storage but was exceeded at 40 °C. Still, we did not see any extreme decrease in colloidal stability at 40 °C.

Na- and K-phosphate were both suitable to maintain particle size and concentration of lyophilized and 6 months stored RO EVs. Thus, the pH shift of a Na-phosphate buffer does not affect particle stability. However, the lyophilization process and further storage led to a decrease of the enzyme activity which is in line with previous findings [76,77], as freezing and dehydration cause stress to the protein. The increased recovery of β-Glu activity after 1 month of storage compared to samples directly after lyophilization speculatively could be an indication for reversible conformational changes of the enzyme inside the EVs [78,79]. Storage for 1 month at 2-8 °C revealed no statistically significant changes in encapsulated enzyme activity in both formulations. However, the mean value for K-phosphate was reduced compared to Na-containing formulation, which is in contrast with previous findings, were K-phosphate showed better suitability for the preservation of lyophilized enzymes [80]. Pikal-Cleland et al., however, looked at free enzyme, while in our study the EV-membrane prevents the direct contact between β-Glu and buffer. After 6 months of storage, both formulations showed a pronounced reduction in enzyme activity. Storage at 2-8 °C best preserved β-Glu revealing an enzyme recovery of 20-26%. In general, Na-phosphate samples exhibited slightly higher recovery rates. Only at 40 °C the K-phosphate containing samples showed a clear improvement over their Na-phosphate counterpart. Overall, β-Glu activity did not correlate with the high colloidal stability. This points to either enzyme leakage or enzyme degradation within the vesicle as the main causes for the β-Glu activity loss. The high enzyme recovery after 1 month suggests that general leakage of the enzyme during freeze-drying or rehydration was not the reason for the activity-reduction after 6 months. Thus, we speculate that β-Glu encapsulated in the lyophilized EVs degraded over time [77]. Whether activity-reduction is related to lyophilization in general or to the specific environment and the conditions inside the EVs should be subject of detailed future studies including freeze-drying of free enzyme in different formulations with various stabilizers and concentrations.

To the best of our knowledge, there are no publications, concerning the long-term stability of lyophilizates of liposomes or EVs loaded with enzymes that could allow a closer insight. As hydrophilic molecules do not readily cross the EV-membrane [71], sucrose and P188 will not be present inside the vesicles in sufficient amounts for cryo- and lyoprotection of the encapsulated enzyme. Kannan et al. found that during the lyophilization of liposomes, luminal sucrose increased stability, by stabilizing the liposomes from the inside [81]. A similar effect might be found for EVs if sucrose could be actively encapsulated in sufficient amounts. Nonetheless, compared to previous studies, where after two weeks of storage at 4 °C in a 4% trehalose lyophilizate only 25-50% of enzyme-activity remained [36], we showed a substantial improvement in preserving the β-Glu activity in this work. β-Glu only served as a surrogate to other vesicle cargoes, such as RNA, its sensitive tertiary and quaternary

structure making it a good indicator of unfavorable storage-conditions. Its facile encapsulation into EVs and the straightforward and sensitive evaluation of its stability made it possible to screen manifold EV-formulations in parallel. With the knowledge gathered here, the next step would be to characterize the EV integrity and apply our recommended formulation parameters (see Box 1) to other biomedically relevant EVs. Ideal targets could be mesenchymal stem cell-derived EVs that have shown promising results in many applications [82], myxobacterial OMVs with antibacterial activity [83] or OMVs with protective effects in inflammatory bowel disease [84], where lyophilization could provide an ideal basis for the development of solid dosage forms.

Recommended formulation parameters for lyophilization:

- Buffer: replace PBS with 10 mM Na- or K-phosphate pH 7.4
- Cryo- and lyoprotection: 0.02% P188 and 5% sucrose
- Proposed lyophilization conditions:
  - Freezing: 1 °C/min to −50 °C
  - Primary drying: −20 °C, 40 mTorr, manometric endpoint determination (product temperature below T_g')
  - Secondary drying: 20 °C, 40 mTorr, 8h

Box 1: Collected formulation parameters for EV-lyophilization

4 Conclusion

The growing interest in EVs for various pharmaceutical applications rises the demand for long-term stable formulations without the need for storage at –80 °C. Lyophilized formulations provide easier shipping and storage, and offer new options for administration, such as pulmonary delivery. We therefore investigated the long-term stability of lyophilized RO-cell derived EVs regarding colloidal and cargo stabilization for up to 6 months stored at 2-8 °C, 25 °C, and 40 °C.

Prior to lyophilization, FT studies were performed to select the most effective buffer type and stabilizers. Most freezing-induced damage of both SBCy050 OMVs and RO EVs was seen in PBS, which is commonly used in EV isolation and preservation. This damage could be minimized by using 10 mM phosphate buffer without salts. K-phosphate instead of Na-phosphate buffer or the addition of sucrose further improved the FT stability. The colloidal stability of both vesicle types could be most effectively preserved by the addition of low amounts of the surfactant P188. PS20 was not suitable for SBCy050 EVs since it reduced the initial particle concentration. The well-established cryo-/lyoprotectant and bulking agent

sucrose was found to be appropriate for successful lyophilization. The lyophilized and stored RO EVs formulated with P188 and sucrose showed comparable particle size and concentrations in Na-phosphate and K-phosphate buffer. Colloidal stability was preserved for 6 months while *in vitro* experiments revealed that the activity of encapsulated β-Glu was maintained for at least 1 month. PVP was included in the freeze-drying study as an alternative stabilizer to either P188 or sucrose, but turned out to be not able to sufficiently preserve mammalian RO EVs after lyophilization and storage.

In conclusion, we could successfully lyophilize mammalian EVs derived from RO cells, maintaining their original particle size and concentration without cargo loss. Storage at 2-8 °C appears suitable for at least 1 month. We further demonstrated that colloidal stability can be provided for at 6 months. Since enzymes are known for their sensitivity during storage, future research might focus on more stable cargos (e.g. RNA, DNA) providing further insight into content retention. In addition, the stabilizing effect of P188 could be elucidated by testing different types of poloxamer.

5 Experimental Section

5.1 Materials

RO cells (ACC452) were obtained from DSMZ, Braunschweig, D. Strain SBCy050 of the Cystobacterineae order of myxobacteria was kindly provided by Rolf Müller, Department of Microbial Natural Products, Helmholtz Institute for Pharmaceutical Research, Saarbrücken.

RPMI medium and insulin-transferrin-selenium-ethanolamine were obtained from Thermo Fisher Scientific (Waltham, MA). 2SWC medium was prepared from Bacto Casitone, Bacto Soytone (both Becton, Dickinson, NJ, US), glucose, $MgSO_4$ heptahydrate, $CaCl_2$ dihidrate (all Sigma-Aldrich, Steinheim, D), maltose monohydrate, cellobiose (both MP Biomedicals SARL, Illkirch-Graffenstaden, FR), HEPES (Carl Roth, Karlsruhe, D) and KOH (Thermo Fisher Scientific, Waltham, MA, US). PBS was prepared from tablets (Thermo Fisher Scientific, Waltham, MA, US). 10 mM Na-phosphate (Sigma-Aldrich, Steinheim, D) at pH 7.4 was prepared for size exclusion chromatography. Both buffers were filtered through a 0.2 µm mixed cellulose ester membrane filter (GE Healthcare, Chicago, IL) prior to use. The protein content of EV-samples was measured using a QuantiPro BCA assay kit (Sigma-Aldrich, Steinheim, D). Bovine serum albumin (BSA) was obtained from Sigma-Aldrich (Steinheim, D). To adsorb EVs in FACS experiments, aldehyd/sulfate latex beads with 4 µM diameter (Thermo Fisher Scientific, Waltham, MA) were used.

Stabilizer stock solutions of sucrose (Sigma-Aldrich, Steinheim, D), poloxamer 188 (Kolliphor® P188, BASF, Ludwigshafen am Rhein, D), polysorbate 20 (Tween 20™, Merck, Darmstadt, D), and polyvinylpyrrolidone (Kollidon® 17 PF, BASF, Ludwigshafen am Rhein, D) were prepared at various concentrations. 20 mM Na-phosphate and K-phosphate buffers (VWR International, Ismaning, D) at different pH values were prepared for dialysis. Stabilizer stock solutions were filtered with 0.2 µm polyethersulfone (PES) membrane syringe filters (VWR International, Ismaning, D). For the preparation of buffers and stock solutions, HPW was used. All excipients had analytical or higher grade and were used without further purification.

Carboxylated polystyrene particle standards with a nominal mean diameter of 110 nm and 950 nm, denoted as CPC100 and CPC1000 were used for tunable resistive pulse sensing instrument calibration (Izon Science Europe, UK). 2R glass vials (Fiolax® clear, Schott, Müllheim, D) with igloo rubber stoppers (B2–TR coating, West Pharmaceutical Services, Eschweiler, D) were cleaned with HPW and dried for 8 h at 60 °C.

5.2 Methods

5.2.1 Cell culture

RO cells (DSMZ, ACC 452) were cultivated as described previously [42]. Briefly, cells were cultured in RPMI with 1% (v/v) insulin-transferrin-selinium-ethanolamine and a density of 0.75×106 cells/mL in 45 mL. 25 mL of the total volume were replaced with 50 mL new medium after 3 days. Vesicles were isolated after 7 days from cells cultured until passage 33. RO cell supernatants were centrifuged at 300 xg for 8 min to pellet cells. Subsequently, supernatants were centrifuged at 9,500 xg for 15 min and then filtered through a 0.45 µm bottletop filter with a polyvinylidene fluoride membrane (Steritop®, Merck, Darmstadt, D). Cell free conditioned medium was subjected to ultracentrifugation (UC) on the same day. UC was performed using a Type 45 Ti rotor (Beckman Coulter, Brea, CA) for 2 h at 100,000 xg with 70 mL polycarbonate tubes (Beckman Coulter, Brea, CA). The resulting EV pellet was resuspended in residual supernatant, left in the tubes after decanting. This resulted in a total volume of approx. 800 µL resuspended EV pellet obtained from one UC run with six tubes.

5.2.2 Bacterial culture

SBCy050 myxobacteria were cultured in 2SWC medium (0.5% Bacto Casitone, 0.1% Bacto Soytone, 0.2% glucose, 0.1% maltose monohydrate, 0.2% cellobiose, 0.05% CaCl2 dihydrate, 0.1% $MgSO_4$ heptahydrate, 10 mM HEPES, adjusted to pH 7.0 with KOH) for

4 days, starting with an optical density of 0.04±0.01. To obtain conditioned medium the cultures were centrifuged at 9,500 xg for 10 min and then filtered through a 0.45 µm pore size bottletop filter (see above). Cell free conditioned medium was subjected to UC on the same day. UC was performed using a SW 32 Ti rotor (Beckman Coulter, Brea, US) for 2 h at 100,000 xg using 32 mL polycarbonate tubes (Beckman Coulter, Brea, US). EV pellets were resuspended as described above.

5.2.3 FACS of RO EVs

EV evaluation by FACS was based on the protocol of Hoppstaedter et al. [85]. The protein content of RO EVs was measured using a bicinchoninic acid assay kit. Then the vesicles were mixed 1:1 with FACS beads (µg/mL protein to µL beads), incubated for 15 min at room temperature, diluted to 1 mL with PBS and incubated for 1 h applying mild shaking. Next, 1 mL of a 200 mM glycine stop solution was added to saturate the beads. After 20 min incubation, the beads were centrifuged twice at 2000 xg for 4 min and resuspended in 1% BSA in PBS, in the original volume of FACS beads employed in the initial step. Next, 10 µL of sample were mixed with 10 µL of FITC-labeled antibody, either anti CD9, anti CD63 or calnexin or the isotype control and incubated on ice for 30 min in the dark (see Table S-4 for further information on antibodies). After dilution to 1 mL using 1% BSA in PBS, samples were centrifuged twice at 2000 xg for 4 min, then measured by FACS (LRS Fortessa, BD Biosciences, NJ) using BD FACSDiva v9.0 software. Data was analyzed using FloJo (version 10.7.0). Negative controls were prepared in the same way as EV-containing samples, but EVs were replaced with the respective amount of BSA. For the positive calnexin and isotype control with RO cells, cells were centrifuged at 300 xg and resuspended in PBS. One million cells per 100 µL were fixed with 4% paraformaldehyde for 10 min, washed twice with PBS and then incubated with 0.1% saponin and 1 µl calnexin or 2.1 µL of the respective isotype for 30 min. Cells were washed once and resuspended in 400 µL PBS for FACS analysis.

5.2.4 Beta glucuronidase encapsulation

β-Glu was encapsulated in RO EVs as previously described [86]. The resuspended pellet was mixed with β-Glu and saponin to final concentrations of 1.5 and 0.1 mg/mL respectively and incubated for 10 min at ambient temperature.

5.2.5 Size exclusion chromatography

To remove impurities carried over from UC and free glucuronidase, EV samples were purified by SEC. SEC was performed using a 1.5 cm diameter glass column (Flex Column®, Kimble Chase, Vineland, NJ), filled with 35 mL of sepharose Cl 2b (Cytiva, Marlborough, MA). PBS was used as mobile phase with a flow rate of 1 mL/min. Up to 750 µL UC pellet were purified per SEC run, purified EVs were collected in 1 mL fractions. The process was automated using an ÄKTA start system equipped with a Frac30 fraction collector (both Cytiva, Marlborough, MA). The vesicle containing fractions were collected and pooled for subsequent characterization and lyophilization. Each SEC run included a 120 mL washing step to ensure the removal of all non-encapsulated glucuronidase, before the next sample was injected.

5.2.6 Beta glucuronidase assay

Glucuronidase activity was measured as described previously [36]. Free enzyme potentially present from EV leakage during storage was removed by SEC after reconstitution of lyophilized samples. For this purpose, a 1.0 cm diameter column filled with 10 mL of sepharose Cl-2b was used with 10 mM Na-phosphate buffer at pH 7.4 as the mobile phase and a flow rate of 1 mL/min. Fractions of 0.5 mL were collected. Glucuronidase activity was measured after mixing samples with fluorescein-di-β-D-glucuronide to a final concentration of 8.3 µg/mL in a total volume of 150 µL. Directly after mixing, the fluorescence was measured using a plate reader (Infinite 200Pro, Tecan, Männedorf, CH), with an excitation wavelength of 480 nm and an emission wavelength of 516 nm. After 18 h incubation at 37 °C, the fluorescence was measured again. The difference between $t_{18\,h}$ and $t_{0\,h}$ indicated the enzyme activity found in the respective sample. PBS treated in the same way as EV-containing samples was measured as a control and subtracted from samples values.

5.2.7 Cryo-TEM

Cryo-TEM pictures of EV-samples both directly after ultracentrifugation and after SEC purification were acquired as previously described [83]. Briefly, a drop of 3 µL of EV suspension was placed on a holey carbon film (type S147-4, Plano, Wetzlar, D), blotted for 2 s, then plunged into liquid ethane at T=108 K with a Gatan cryoplunger model CP3 (Pleasanton, CA). After transferring the frozen samples to a Gatan model 914 cryo-TEM sample holder, they were imaged in brightfield TEM at T=100 K with a JEOL JEM-2100 LaB6 (Tokyo, JP).

5.2.8 Formulation preparation

After isolation and SEC purification, EVs were dialyzed with 20 mM Na- or K-phosphate buffer in Slide-A-Lyzer™ MINI dialysis devices or cassettes (20K MWCO; Thermo Fisher Scientific, Waltham, MA). After dialysis, EVs were filtered through a 0.2 µm PES membrane syringe filter (VWR International, Ismaning, D) and mixed 1:1 with stabilizer stock solutions to match the respective final buffer and stabilizer concentration (see Table S-5). Unloaded and β-Glu loaded RO EVs were investigated from different batches.

5.2.9 Freeze-thawing cycle

Formulations (200 µL in 2R vials) were freeze-thawed three times on a pilot scale freeze-drier (FTS LyoStar™ 3, SP Scientific, Stone Ridge, NY) at –1 °C/min to –50 °C followed by a 30 min hold at –50 °C and thawing at 1 °C/min to 10 °C followed by a 30 min hold. Before freeze-thawing, EV concentrations were determined by TRPS and denoted as 'before FT'.

5.2.10 Freeze-drying cycle

A lyophilization process stability study was conducted using unloaded RO EVs and SBCy050 OMVs (same batches as for freeze-thawing studies) formulated in 10 mM Na-phosphate buffer pH 7.4 in combination with 0.02% P188 and 5% sucrose. Selected formulations of β-Glu loaded RO EVs were used for long-term stability studies (Table 2), including placebos consisting of identical formulations without EVs. The samples were lyophilized in 2R vials with 200 µL fill volume. Before lyophilization, EV concentrations were determined by TRPS and denoted as 'before FD'. Lyophilization was performed on a pilot-scale freeze-dryer (LyoStar™ 3). After an equilibration step at –5 °C for 15 min, the samples were frozen at –1 °C/min to –50 °C and held for 120 min. Primary drying was performed at –20 °C and 40 mTorr with manometric end point determination. The product temperature, monitored with thermocouples, was kept below the glass transition temperature of the maximally frozen concentrate (T_g') which was determined by DSC. Secondary drying was performed at 20 °C and 40 mTorr. Samples were stoppered under slight vacuum at 450 Torr nitrogen, and vials were crimped with aluminum seals. The lyophilizates were reconstituted by adding 190 µL of HPW. The reconstitution volume was calculated based on the solid content. The vials were shaken gently to ensure wetting of the complete lyophilizate.

Table 2: Formulations for freeze-drying experiments.

Formulation#	Buffer	Cryoprotectant	Surfactant
1	10 mM Na-phosphate pH 7.4	5% Suc	0.02% P188
2	10 mM K-phosphate pH 7.4	5% Suc	0.02% P188
3	10 mM Na-phosphate pH 7.4	5% Suc	0.02% PVP
4	10 mM Na-phosphate pH 7.4	5% PVP	0.02% P188

5.2.11 Long-term stability testing of lyophilized samples

For long-term stability testing, sealed lyophilizates were stored at 2-8 °C, 25 °C, and 40 °C over a period of 1 month and 6 months.

5.2.12 Dynamic light scattering

Mean particle sizes and respective polydispersity indices (PDI) were measured using a DLS platereader (DynaPro III, Wyatt Technology, D). 20 µL sample (n=3) per well of a 384 UV-well plate (Costar™, Corning, Tewksbury, MA) was analyzed at 25 °C using 10 acquisitions with 5 s each. The corresponding preset refractive index parameters were used for all samples. Viscosities of sucrose and PVP formulations required for DLS measurements were determined via an AMVn Automated Micro Viscometer (Anton Paar, Graz, A).

5.2.13 Tunable resistive pulse sensing

Concentration-based particle size distributions and zeta potentials were analyzed by TRPS (qNano, Izon Science Europe, UK). Adjustment of nanopore stretch and voltage were optimized according to manufacturer recommendations. In order to provide sufficient conductivity, 27 µL of each sample containing 10 mM phosphate (not PBS) was mixed with 3 µL of a 1.4 M NaCl solution resulting in 140 mM NaCl and 9 mM phosphate. Samples were measured in triplicate with a minimum of 500 particles per analysis. In case of fewer particles a maximum measurement time of 10 min was performed. Calibration of the nanopores NP100 (measurement size range: 50-330 nm) and NP600 (measurement size range: 275-1570 nm) was conducted using carboxylated polystyrene particle standards CPC100 and CPC1000 respectively. Calibration particles were prepared in 10 mM phosphate buffer and mixed with a NaCl solution as described before for sample particles. Zeta potential analysis was conducted according to IZON's instruction 'V3.1 Charge Analysis' using NP100 and CPC100 particles. The calibration particles were measured at three applied voltages; particles measured at the highest voltage were measured at two external pressures. Data obtained

from measured samples and calibration particles were evaluated using the template 'Zeta Template V3.1a' provided by IZON.

5.2.14 Subvisible particles

Subvisible particles were analyzed by flow cytometry imaging (FlowCam® 8100, Fluid Imaging Technologies, Inc., Scarborough, ME). A 10x magnification cell was used for the measurements. After 1:10 dilution, 160 µL sample solution was measured with a flow rate of 0.15 mL/min, an auto image frame rate of 28 frames per second, and a run time of 60 s. After each measurement, the flow cell was flushed with HPW. Particle identification was set with a distance to the nearest neighbor of 3 µm, and a segmentation threshold of 13 and 10 for the dark and light pixels respectively. The software VisualSpreadsheet® 4.7.6 was used for measurements and evaluation.

5.2.15 Nanoparticle tracking analysis

Nanoparticle tracking analysis was performed using a Nanosight LM-10 (Malvern Instruments, UK) equipped with a green laser measurement cell. Three videos of 30 s were recorded using a camera level of 14–15 and detection threshold 10 and analyzed using NTA software (NTA 3.1 Software).

5.2.16 Karl-Fischer Titration

The RM of placebo lyophilizates was determined in triplicates by Karl-Fischer titration after lyophilization and after storage. Measurements were performed using an Aqua 40.00 titrator (Analytik Jena AG, Halle, D) equipped with a headspace oven set at 100 °C. Samples of 10 to 20 mg crushed lyophilizates were analyzed in stoppered 2R vials.

5.2.17 Differential scanning calorimetry

DSC measurements were performed in 40 µL aluminum crucibles using a Mettler Toledo DSC 822e (Mettler-Toledo GmbH, Giessen, D). In order to determine the glass transition temperature of the maximally freeze-concentrated solution (T_g'), 20 µL of the liquid samples were cooled at –10 °C/min from 25 °C to –60 °C, held at –60 °C for 1 min, and reheated at 10 °C/min to 25 °C. For the determination of the glass transition temperature of the lyophilized samples (T_g), approximately 10 mg were weighed into the aluminum crucibles. Samples were preheated from 0 °C to 70 °C, cooled to 0 °C and heated to 150 °C at a scanning rate of 10 °C/min. T_g and T_g' were defined as the inflection point of the glass transition in the heating

scan of the DSC experiment. All analyses were performed in triplicate with placebo formulations.

5.2.18 Statistical analysis

Unless otherwise stated, results are given as mean value ± standard deviation (SD). Statistically significant differences were determined via one-way or two-way ANOVA followed by a post-hoc test or via a two-tailed student t-test using Origin 2019b Software (OriginLab Corporation, Northampton, MA). Mean values having p-values < 0.05 were judged to be significantly different.

6 Supporting Information

Table S-1: Hydrodynamic particle size and PDI values of SBCy050 OMVs and RO EVs before dialysis and filtration measured by DLS (mean ± SD; n=3).

Vesicle type	Particle size [nm]	PDI
SBCy050 OMVs	130.0 ± 3.5	multimodal (> 0.56)
RO EVs	186.8 ± 6.5	multimodal (> 0.56)

Table S-2: Zeta potential values of SBCy050 OMVs and RO EVs in different formulations before and after FT or FD measured by TRPS (mean ± SD, n=3). Za/Zb represents the ratio of the zeta potential after and before FT or FD.

Formulation	**Zeta potential [mV]**					
	SBCy050 OMVs			**RO EVs**		
	before	**after**	Z_a/Z_b	**before**	**after**	Z_a/Z_b
Na-Ph. pH 6.5	-23.3 ± 0.3	-36.1 ± 0.5	*1.6*	-30.4 ± 1.0	-41.7 ± 9.3	*1.4*
Na-Ph. pH 7.4	-22.5 ± 2.9	-36.4 ± 2.8	*1.6*	-29.6 ± 1.0	-39.6 ± 1.7	*1.3*
Na-Ph. pH 8.5	-23.9 ± 0.3	-40.4 ± 0.4	*1.7*	-31.2 ± 2.5	-54.4 ± 2.7	*1.7*
Na-Ph. pH 7.4 + 5% Suc	-24.0 ± 0.9	-38.0 ± 0.5	*1.6*	-32.6 ± 2.1	-49.4 ± 5.8	*1.5*
K-Ph. pH 6.0	-25.3 ± 0.4	-33.1 ± 0.8	*1.3*	-29.5 ± 0.5	-28.3 ± 1.4	*1.0*
K-Ph. pH 7.4	-26.1 ± 0.2	-33.8 ± 1.0	*1.3*	-32.2 ± 3.3	-29.6 ± 6.6	*0.9*
PBS	-22.0 ± 0.3	-38.5 ± 0.2	*1.7*	-28.0 ± 1.7	n.d.	-
PBS + 5% Suc	-29.4 ± 1.8	-40.3 ± 0.2	*1.4*	-27.4 ± 2.7	-49.0 ± 4.9	*1.8*
0.02% P188	-21.9 ± 0.4	-28.5 ± 0.5	*1.3*	-29.7 ± 1.7	-27.8 ± 1.0	*0.9*
0.02% P188 + 5% Suc	-25.0 ± 0.4	-32.2 ± 0.6	*1.3*	-30.0 ± 0.8	-26.2 ± 1.5	*0.9*
0.02% PS20 + 5% Suc	-25.5 ± 0.2	-30.6 ± 0.2	*1.2*	-27.9 ± 2.2	-32.9 ± 2.8	*1.2*
0.02% P188 + 5% Suc (**FD**)	-25.6 ± 0.5	-32.3 ± 0.8	*1.3*	-30.9 ± 0.9	-27.5 ± 3.3	*0.9*

n.d.: not detectable (insufficient particle count)

Table S-3: Zeta potential values of beta glucuronidase encapsulated RO EVs before lyophilization, after lyophilization, and after storage for 1 month and 6 months at 2-8 °C, 25 °C, and 40 °C measured by TRPS (mean ± SD; n=3).

Formulation	**Zeta potential [mV]**							
	before FD	**after FD**	**1m 2-8°C**	**1m 25°C**	**1m 40°C**	**6m 2-8°C**	**6m 25°C**	**6m 40°C**
Na-Ph. + 0.02% P188 + 5% Suc	-24.4 ± 0.2	-24.2 ± 1.1	-27.2 ±1.3	-24.5 ± 0.7	-22.5 ± 0.4	-23.4 ± 1.8	-25.0 ± 0.4	-26.1 ± 1.1
K-Ph. + 0.02% P188 + 5% Suc	-23.5 ± 0.4	-24.4 ± 0.1	-24.1 ± 0.4	-24.5 ± 0.5	-23.9 ± 0.2	-25.5 ± 0.7	-27.3 ± 1.0	-29.1 ± 0.7
Na-Ph. + 0.02% PVP + 5% Suc	-24.3 ± 0.4	-24.6 ± 1.1	-25.7 ± 0.2	-25.8 ± 0.3	-25.8 ± 0.1	-26.7 ± 0.4	-25.6 ± 0.5	-27.6 ± 0.5
Na-Ph. + 0.02% P188 + 5% PVP	-24.1 ± 0.2	-24.4 ± 0.5	-26.6 ± 0.5	-26.6 ± 0.1	-26.2 ± 0.4	-28.8 ± 0.1	-27.9 ± 1.1	-29.0 ± 0.4

Table S-4: Information on FITC-labeled antibodies.

Supplier	Description	Article number
Biozol	FITC anti-human CD9, Mouse IgG1, kappa, Clone: HI9a 25	BLD-312103
Biozol	FITC anti-human CD63, Mouse IgG1, kappa, Clone: H5C6	BLD-353005
Biozol	FITC Mouse IgG1, kappa Isotype Ctrl (FC), Clone: MOPC-21	BLD-400109
Novus Biologicals	FITC calnexin antibody, Mouse IgG2b kappa, Clone: 1C2.2D11	NBP2-36570F
Novus Biologicals	FITC isotyoe control, Mouse IgG2b, Clone: MPC-11	NBP2-37229

Table S-5: Formulation preparation; EVs were dialyzed in Component 1 and mixed with Component 2 (1:1).

Formulation	Component 1	Component 2
10 mM Na-ph. pH 6.5	20 mM Na-ph. pH 6.5	HPW
10 mM Na-ph. pH 8.5	20 mM Na-ph. pH 8.5	HPW
10 mM K-ph. pH 6.0	20 mM K-ph. pH 6.0	HPW
10 mM K-ph. pH 7.4	20 mM K-ph. pH 7.4	HPW
10 mM Na-ph. pH 7.4	20 mM Na-ph. pH 7.4	HPW
PBS		274 mmol NaCl + 5.4 mmol KCl
10 mM Na-ph. pH 7.4 + 5% Suc		10% Suc
PBS + 5% Suc		274 mmol NaCl + 5.4 mmol KCl + 10% Suc
10 mM Na-ph. pH 7.4 + 0.02% P188		0.04% P188
10 mM Na-ph. pH 7.4 + 0.02% P188 + 5% Suc		0.04% P188 + 10% Suc
10 mM Na-ph. pH 7.4 + 0.02% PS20 + 5% Suc		0.04% PS20 + 10% Suc
10 mM Na-ph. pH 7.4 + 0.02% PVP + 5% Suc		0.04% PVP + 10% Suc
10 mM Na-ph. pH 7.4 + 0.02% P188 + 5% PVP		0.04% P188 + 10% PVP

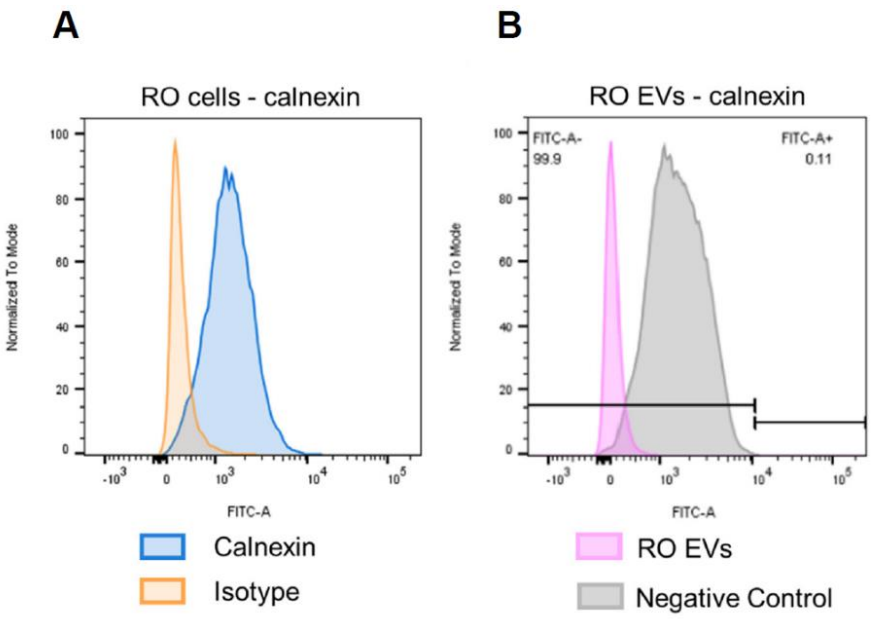

Figure S-1: Detection of calnexin as a negative EV marker. Calnexin detected in RO cells with the isotype control (A) and calnexin detected in RO EVs with a 1% BSA solution as a negative control (B).

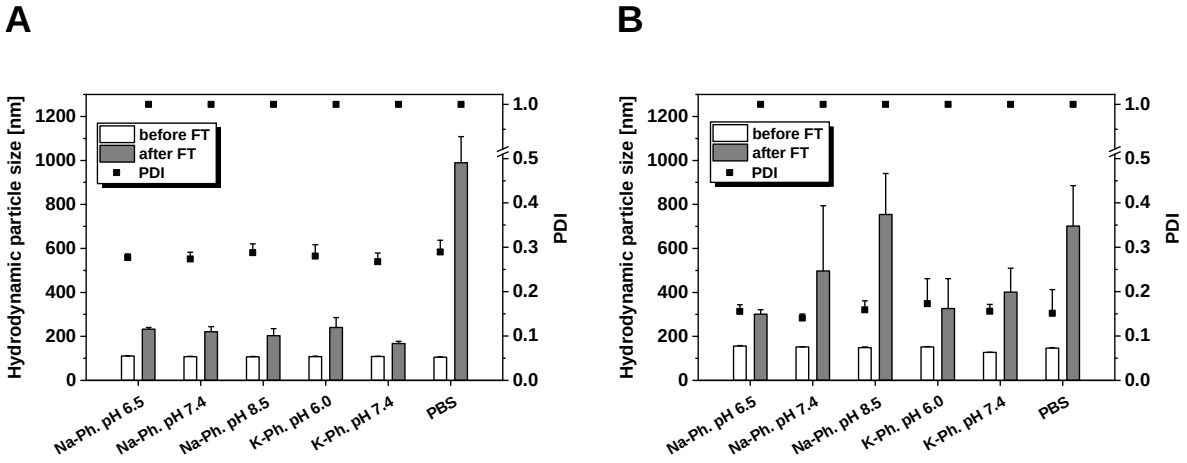

Figure S-2: Hydrodynamic particle size and PDI from DLS of freshly prepared (before FT) or three times freeze-thaw stressed SBCy050 OMVs (A) and RO EVs (B) formulated in 10 mM Na- or K-phosphate buffer at different pH values, and in PBS. PDI values >0.56 represent a multimodal size distribution and are therefore stated as '1.0'. Each data point represents mean ± SD, n=3. Statistical analysis was Student's t-test. PDI values were not evaluated statistically. After FT, all samples were significantly different ($p<0.05$) compared to the corresponding samples before FT.

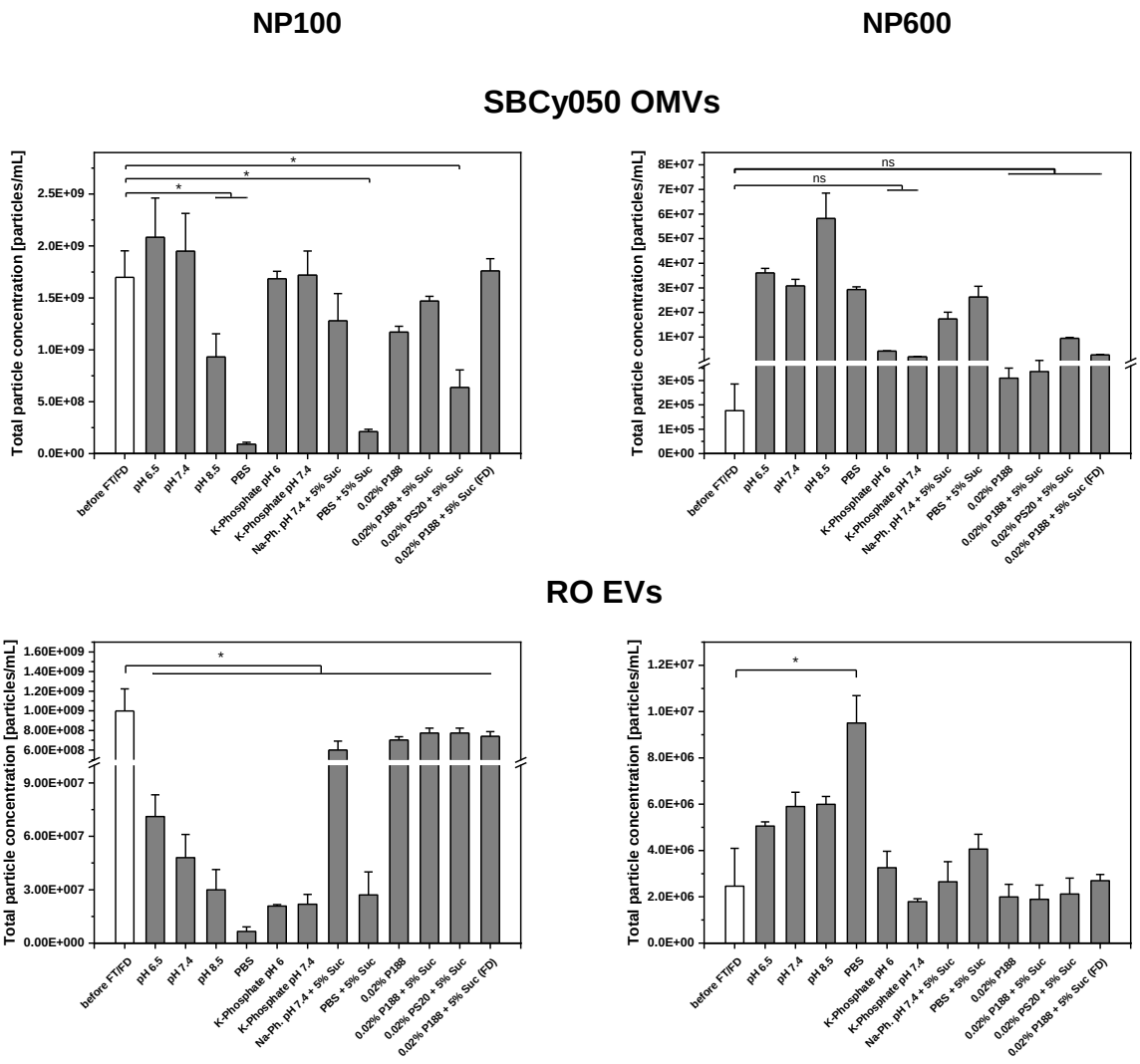

Figure S-3: Total particle concentration of EVs before FT/FD (mean), three times freeze-thaw stressed, and freeze-dried (FD) measured by TRPS NP100 and NP600. Each data point represents mean ± SD, n=3. One-way ANOVA, Bonferroni post-hoc test, *p<0.05, ns=non-significant.

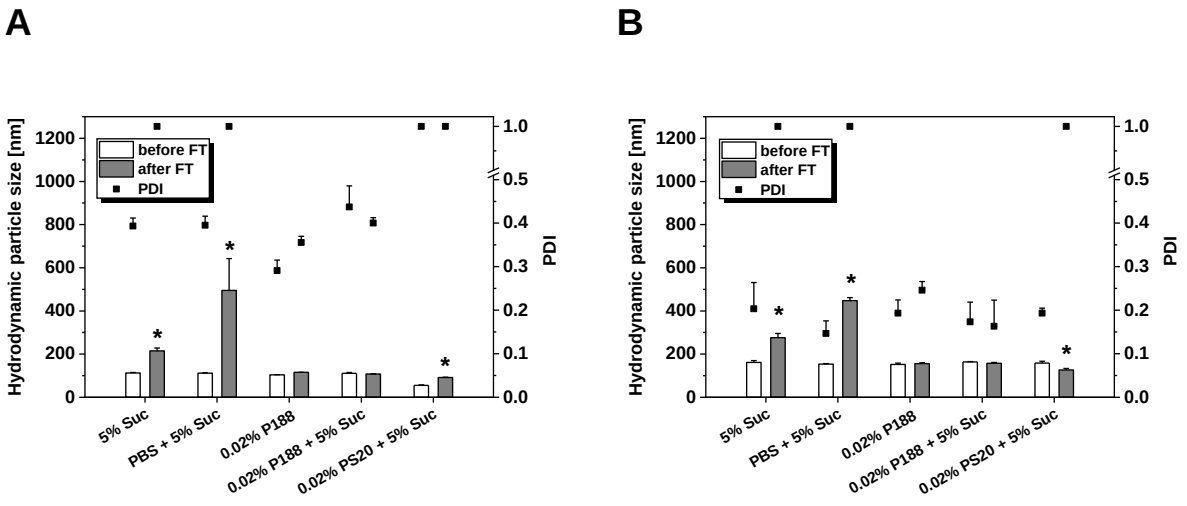

Figure S-4: Hydrodynamic particle size and PDI from DLS of freshly prepared (before FT) or three times freeze-thaw stressed SBCy050 OMVs (A) and RO EVs (B) formulated in 10 mM Na-phosphate pH 7.4 or PBS with addition of sucrose and/or surfactant. PDI values >0.56 represent a multimodal size distribution and are therefore stated as '1.0'. Each data point represents mean ± SD, n=3. Statistical analysis was Student's t-test. PDI values were not evaluated statistically. *p<0.05: samples are significantly different compared to the corresponding samples before FT.

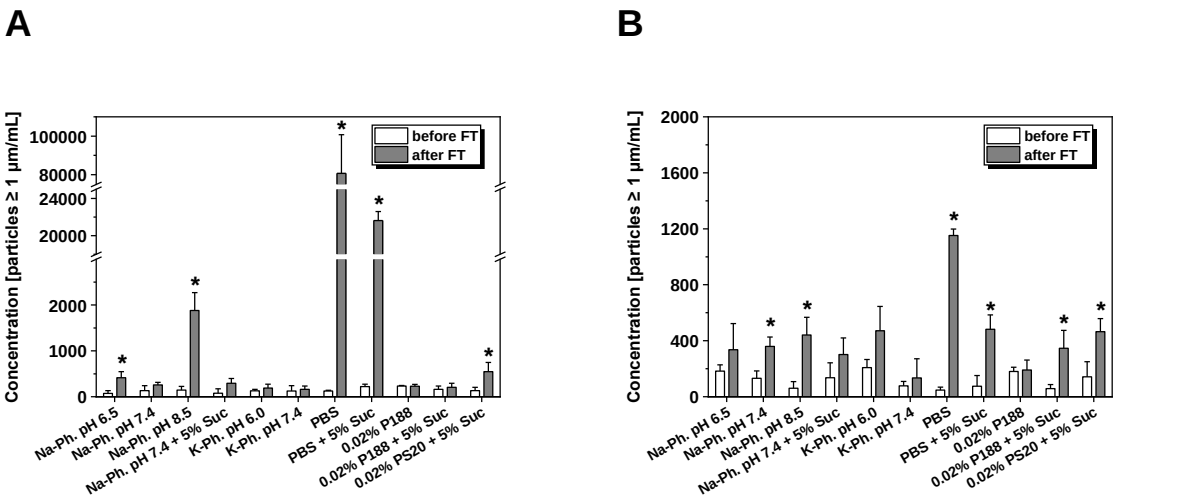

Figure S-5: Number of subvisible particles ≥1 µm of three times freeze-thaw stressed SBCy050 OMVs (A) and RO EVs (B) formulated in in 10 mM Na- or K-phosphate buffer at different pH values or PBS w/o or with addition of sucrose and/or surfactant (n=3). Samples were diluted 1:10 before measurement. Each data point represents mean ± SD, n=3. Statistical analysis was Student's t-test. PDI values were not evaluated statistically. *p<0.05: samples are significantly different compared to the corresponding samples before FT.

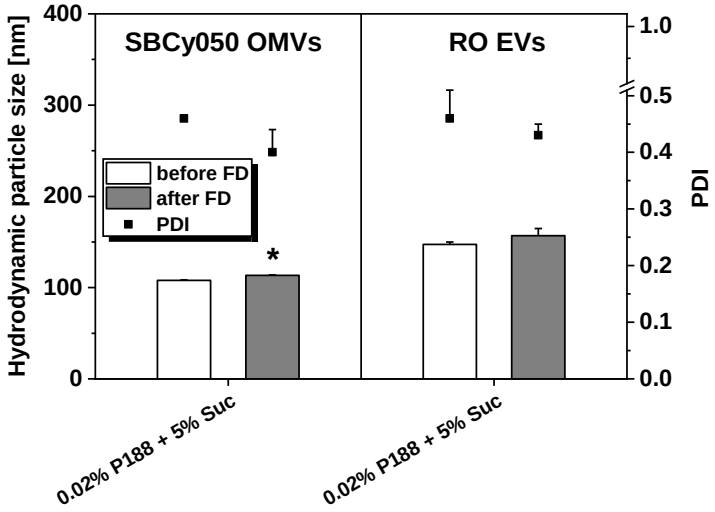

Figure S-6: Hydrodynamic particle size and PDI from DLS of SBCy050 OMVs and RO EVs formulated in 10 mM Na phosphate pH 7.4 + 0.02% P188 + 5% Suc, before and after FD. Each data point represents mean ± SD, n=3. Statistical analysis was Student's t-test. PDI values were not evaluated statistically. *p<0.05: samples are significantly different compared to the corresponding samples before FD.

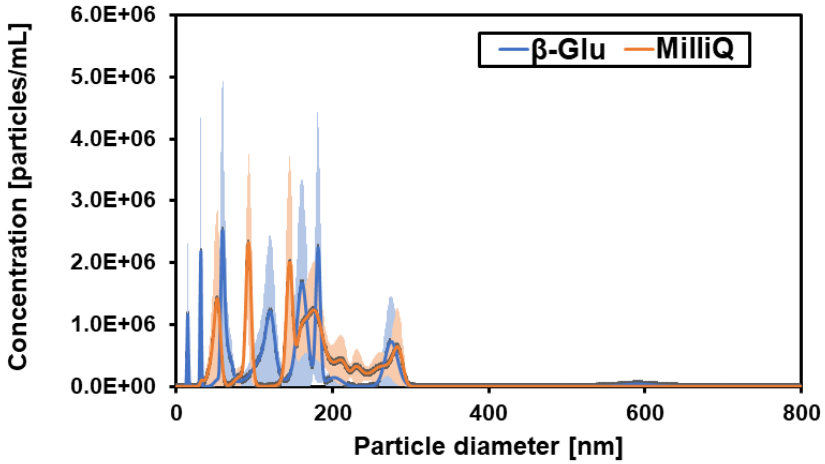

Figure S-7: Nanoparticle tracking analysis after lyophilization and reconstitution of non-encapsulated β-Glu formulated in phosphate buffer, 0.02% P188, and 5% sucrose in comparison to highly purified water.

7 References

[1] W. Wang, Lyophilization and development of solid protein pharmaceuticals, Int. J. Pharm. 203 (2000) 1–60.

[2] J.C. Kasper, G. Winter, W. Friess, Recent advances and further challenges in lyophilization, Eur. J. Pharm. Biopharm. 85 (2013) 162–169.

[3] E. Woith, G. Fuhrmann, M.F. Melzig, Extracellular Vesicles-Connecting Kingdoms, Int. J. Mol. Sci. 20 (2019).

[4] G. van Niel, G. D'Angelo, G. Raposo, Shedding light on the cell biology of extracellular vesicles, Nat. Rev. Mol. Cell Biol. 19 (2018) 213–228.

[5] C. Schwechheimer, M.J. Kuehn, Outer-membrane vesicles from Gram-negative bacteria: biogenesis and functions, Nat. Rev. Microbiol. 13 (2015) 605–619.

[6] M. Yáñez-Mó, P.R.-M. Siljander, Z. Andreu, A.B. Zavec, F.E. Borràs, E.I. Buzas, K. Buzas, E. Casal, F. Cappello, J. Carvalho, E. Colás, A. Cordeiro-da Silva, S. Fais, J.M. Falcon-Perez, I.M. Ghobrial, B. Giebel, M. Gimona, M. Graner, I. Gursel, M. Gursel, N.H.H. Heegaard, an Hendrix, P. Kierulf, K. Kokubun, M. Kosanovic, V. Kralj-Iglic, E.-M. Krämer-Albers, S. Laitinen, C. Lässer, T. Lener, E. Ligeti, A. Linē, G. Lipps, A. Llorente, J. Lötvall, M. Manček-Keber, A. Marcilla, M. Mittelbrunn, I. Nazarenko, E.N.M. Nolte-'t Hoen, T.A. Nyman, L. O'Driscoll, M. Olivan, C. Oliveira, É. Pállinger, H.A. Del Portillo, J. Reventós, M. Rigau, E. Rohde, M. Sammar, F. Sánchez-Madrid, N. Santarém, K. Schallmoser, M.S. Ostenfeld, W. Stoorvogel, R. Stukelj, S.G. van der Grein, M.H. Vasconcelos, M.H.M. Wauben, O. de Wever, Biological properties of extracellular vesicles and their physiological functions, J. Extracell. Vesicles 4 (2015) 27066.

[7] T. Kuhn, M. Koch, G. Fuhrmann, Probiomimetics-Novel Lactobacillus-Mimicking Microparticles Show Anti-Inflammatory and Barrier-Protecting Effects in Gastrointestinal Models, Small 16 (2020) e2003158.

[8] O.P.B. Wiklander, M.Á. Brennan, J. Lötvall, X.O. Breakefield, S. El Andaloussi, Advances in therapeutic applications of extracellular vesicles, Sci. Transl. Med. 11 (2019).

[9] O.M. Elsharkasy, J.Z. Nordin, D.W. Hagey, O.G. de Jong, R.M. Schiffelers, S.E. Andaloussi, P. Vader, Extracellular vesicles as drug delivery systems: Why and how?, Adv. Drug Deliv. Rev. (2020).

[10] G. Szabo, F. Momen-Heravi, Extracellular vesicles in liver disease and potential as biomarkers and therapeutic targets, Nat. Rev. Gastroenterol. Hepatol. 14 (2017) 455–466.

[11] T. Katsuda, N. Kosaka, T. Ochiya, The roles of extracellular vesicles in cancer biology: toward the development of novel cancer biomarkers, Proteomics 14 (2014) 412–425.

[12] L.J. Vella, A.F. Hill, L. Cheng, Focus on Extracellular Vesicles: Exosomes and Their Role in Protein Trafficking and Biomarker Potential in Alzheimer's and Parkinson's Disease, Int. J. Mol. Sci. 17 (2016) 173.

[13] M. Gimona, K. Pachler, S. Laner-Plamberger, K. Schallmoser, E. Rohde, Manufacturing of Human Extracellular Vesicle-Based Therapeutics for Clinical Use, Int. J. Mol. Sci. 18 (2017).

[14] T. Lener, M. Gimona, L. Aigner, V. Börger, E. Buzas, G. Camussi, N. Chaput, D. Chatterjee, F.A. Court, H.A. Del Portillo, L. O'Driscoll, S. Fais, J.M. Falcon-Perez, U. Felderhoff-Mueser, L. Fraile, Y.S. Gho, A. Görgens, R.C. Gupta, an Hendrix, D.M. Hermann, A.F. Hill, F. Hochberg, P.A. Horn, D. de Kleijn, L. Kordelas, B.W. Kramer, E.-M. Krämer-Albers, S. Laner-Plamberger, S. Laitinen, T. Leonardi, M.J. Lorenowicz, S.K. Lim, J. Lötvall, C.A. Maguire, A. Marcilla, I. Nazarenko, T. Ochiya, T. Patel, S. Pedersen, G. Pocsfalvi, S. Pluchino, P. Quesenberry, I.G. Reischl, F.J. Rivera, R. Sanzenbacher, K. Schallmoser, I. Slaper-Cortenbach, D. Strunk, T. Tonn, P. Vader, B.W.M. van Balkom, M. Wauben, S.E. Andaloussi, C. Théry, E. Rohde, B. Giebel, Applying extracellular vesicles based therapeutics in clinical trials - an ISEV position paper, J. Extracell. Vesicles 4 (2015) 30087.

[15] G.D. Kusuma, M. Barabadi, J.L. Tan, D.A.V. Morton, J.E. Frith, R. Lim, To Protect and to Preserve: Novel Preservation Strategies for Extracellular Vesicles, Front. Pharmacol. 9 (2018) 1199.

[16] D. Ingato, J.U. Lee, S.J. Sim, Y.J. Kwon, Good things come in small packages: Overcoming challenges to harness extracellular vesicles for therapeutic delivery, J. Control. Release 241 (2016) 174–185.

[17] S. Deville, P. Berckmans, R. van Hoof, I. Lambrichts, A. Salvati, I. Nelissen, Comparison of extracellular vesicle isolation and storage methods using high-sensitivity flow cytometry, PLoS One 16 (2021) e0245835.

[18] A. Jeyaram, S.M. Jay, Preservation and Storage Stability of Extracellular Vesicles for Therapeutic Applications, AAPS J. 20 (2017) 1.

[19] K.W. Witwer, E.I. Buzás, L.T. Bemis, A. Bora, C. Lässer, J. Lötvall, E.N. Nolte-'t Hoen, M.G. Piper, S. Sivaraman, J. Skog, C. Théry, M.H. Wauben, F. Hochberg, Standardization of sample collection, isolation and analysis methods in extracellular vesicle research, J. Extracell. Vesicles 2 (2013).

[20] R. Szatanek, J. Baran, M. Siedlar, M. Baj-Krzyworzeka, Isolation of extracellular vesicles: Determining the correct approach (Review), Int. J. Mol. Med. 36 (2015) 11–17.

[21] L. Ayers, M. Kohler, P. Harrison, I. Sargent, R. Dragovic, M. Schaap, R. Nieuwland, S.A. Brooks, B. Ferry, Measurement of circulating cell-derived microparticles by flow cytometry: sources of variability within the assay, Thromb. Res. 127 (2011) 370–377.

[22] J.C. Akers, V. Ramakrishnan, I. Yang, W. Hua, Y. Mao, B.S. Carter, C.C. Chen, Optimizing preservation of extracellular vesicular miRNAs derived from clinical cerebrospinal fluid, Cancer Biomark. 17 (2016) 125–132.

[23] Á.M. Lőrincz, C.I. Timár, K.A. Marosvári, D.S. Veres, L. Otrokocsi, Á. Kittel, E. Ligeti, Effect of storage on physical and functional properties of extracellular vesicles derived from neutrophilic granulocytes, J. Extracell. Vesicles 3 (2014) 25465.

[24] R. Maroto, Y. Zhao, M. Jamaluddin, V.L. Popov, H. Wang, M. Kalubowilage, Y. Zhang, J. Luisi, H. Sun, C.T. Culbertson, S.H. Bossmann, M. Motamedi, A.R. Brasier, Effects of storage temperature on airway exosome integrity for diagnostic and functional analyses, J. Extracell. Vesicles 6 (2017) 1359478.

[25] B. György, M.E. Hung, X.O. Breakefield, J.N. Leonard, Therapeutic applications of extracellular vesicles: clinical promise and open questions, Annu. Rev. Pharmacol. Toxicol. 55 (2015) 439–464.

[26] Y. Jin, K. Chen, Z. Wang, Y. Wang, J. Liu, L. Lin, Y. Shao, L. Gao, H. Yin, C. Cui, Z. Tan, L. Liu, C. Zhao, G. Zhang, R. Jia, L. Du, Y. Chen, R. Liu, J. Xu, X. Hu, Y. Wang, DNA in serum extracellular vesicles is stable under different storage conditions, BMC Cancer 16 (2016) 753.

[27] V. Sokolova, A.-K. Ludwig, S. Hornung, O. Rotan, P.A. Horn, M. Epple, B. Giebel, Characterisation of exosomes derived from human cells by nanoparticle tracking analysis and scanning electron microscopy, Colloids Surf. B Biointerfaces 87 (2011) 146–150.

[28] M. Jayachandran, V.M. Miller, J.A. Heit, W.G. Owen, Methodology for isolation, identification and characterization of microvesicles in peripheral blood, J. Immunol. Methods 375 (2012) 207–214.

[29] B.C.H. Pieters, O.J. Arntz, M.B. Bennink, M.G.A. Broeren, A.P.M. van Caam, M.I. Koenders, P.L.E.M. van Lent, W.B. van den Berg, M. de Vries, P.M. van der Kraan, F.A.J. van de Loo, Commercial cow milk contains physically stable extracellular vesicles expressing immunoregulatory TGF-β, PLoS One 10 (2015) e0121123.

[30] W. Abdelwahed, G. Degobert, S. Stainmesse, H. Fessi, Freeze-drying of nanoparticles: formulation, process and storage considerations, Adv. Drug Deliv. Rev. 58 (2006) 1688–1713.

[31] X. Tang, M.J. Pikal, Design of freeze-drying processes for pharmaceuticals: practical advice, Pharm. Res. 21 (2004) 191–200.

[32] L. van den Berg, D. Rose, Effect of freezing on the pH and composition of sodium and potassium phosphate solutions: the reciprocal system KH2PO4 • Na2HPO4 • H2O, Arch. Biochem. Biophys. 81 (1959) 319–329.

[33] K.A. Pikal-Cleland, N. Rodríguez-Hornedo, G.L. Amidon, J.F. Carpenter, Protein denaturation during freezing and thawing in phosphate buffer systems: monomeric and tetrameric beta-galactosidase, Arch. Biochem. Biophys. 384 (2000) 398–406.

[34] P. Kolhe, E. Amend, S.K. Singh, Impact of freezing on pH of buffered solutions and consequences for monoclonal antibody aggregation, Biotechnol. Prog. 26 (2010) 727–733.

[35] F. Franks, Freeze-drying of bioproducts: putting principles into practice, Eur. J. Pharm. Biopharm. 45 (1998) 221–229.

[36] J. Frank, M. Richter, C. de Rossi, C.-M. Lehr, K. Fuhrmann, G. Fuhrmann, Extracellular vesicles protect glucuronidase model enzymes during freeze-drying, Sci. Rep. 8 (2018) 12377.

[37] S. Bosch, L. de Beaurepaire, M. Allard, M. Mosser, C. Heichette, D. Chrétien, D. Jegou, J.-M. Bach, Trehalose prevents aggregation of exosomes and cryodamage, Sci. Rep. 6 (2016) 36162.

[38] C. Charoenviriyakul, Y. Takahashi, M. Nishikawa, Y. Takakura, Preservation of exosomes at room temperature using lyophilization, Int. J. Pharm. 553 (2018) 1–7.

[39] G. Midekessa, K. Godakumara, J. Ord, J. Viil, F. Lättekivi, K. Dissanayake, S. Kopanchuk, A. Rinken, A. Andronowska, S. Bhattacharjee, T. Rinken, A. Fazeli, Zeta Potential of Extracellular Vesicles: Toward Understanding the Attributes that Determine Colloidal Stability, ACS omega 5 (2020) 16701–16710.

[40] C. de Préval, M.R. Hadam, B. Mach, Regulation of genes for HLA class II antigens in cell lines from patients with severe combined immunodeficiency, N. Engl. J. Med. 318 (1988) 1295–1300.

[41] M.A. Ayala García, B. González Yebra, A.L. López Flores, E. Guaní Guerra, The major histocompatibility complex in transplantation, J. Transplant. 2012 (2012) 842141.

[42] E. Schulz, A. Karagianni, M. Koch, G. Fuhrmann, Hot EVs - How temperature affects extracellular vesicles, Eur. J. Pharm. Biopharm. 146 (2020) 55–63.

[43] J.-L. Tian, Y.-Z. Zhao, Z. Jin, C.-T. Lu, Q.-Q. Tang, Q. Xiang, C.-Z. Sun, L. Zhang, Y.-Y. Xu, H.-S. Gao, Z.-C. Zhou, X.-K. Li, Y. Zhang, Synthesis and characterization of Poloxamer 188-grafted heparin copolymer, Drug Dev. Ind. Pharm. 36 (2010) 832–838.

[44] C. Haeuser, P. Goldbach, J. Huwyler, W. Friess, A. Allmendinger, Excipients for Room Temperature Stable Freeze-Dried Monoclonal Antibody Formulations, J. Pharm. Sci. 109 (2020) 807–817.

[45] A. Schoug, D. Mahlin, M. Jonson, S. Håkansson, Differential effects of polymers PVP90 and Ficoll400 on storage stability and viability of Lactobacillus coryniformis Si3 freeze-dried in sucrose, J. Appl. Microbiol. 108 (2010) 1032–1040.

[46] J.C. Kasper, D. Schaffert, M. Ogris, E. Wagner, W. Friess, Development of a lyophilized plasmid/LPEI polyplex formulation with long-term stability—A step closer from promising technology to application, J. Control. Release 151 (2011) 246–255.

[47] P. Cizmar, Y. Yuana, Detection and Characterization of Extracellular Vesicles by Transmission and Cryo-Transmission Electron Microscopy, Methods Mol. Biol. 1660 (2017) 221–232.

[48] N.J. Bitto, M. Kaparakis-Liaskos, The Therapeutic Benefit of Bacterial Membrane Vesicles, Int. J. Mol. Sci. 18 (2017).

[49] M. Ruzicka, F. Xiao, H. Abujrad, Y. Al-Rewashdy, V.A. Tang, M.-A. Langlois, A. Sorisky, T.C. Ooi, D. Burger, Effect of hemodialysis on extracellular vesicles and circulating submicron particles, BMC Nephrol. 20 (2019) 294.

[50] R. Vogel, F.A.W. Coumans, R.G. Maltesen, A.N. Böing, K.E. Bonnington, M.L. Broekman, M.F. Broom, E.I. Buzás, G. Christiansen, N. Hajji, S.R. Kristensen, M.J. Kuehn, S.M. Lund, S.L.N. Maas, R. Nieuwland,

X. Osteikoetxea, R. Schnoor, B.J. Scicluna, M. Shambrook, J. de Vrij, S.I. Mann, A.F. Hill, S. Pedersen, A standardized method to determine the concentration of extracellular vesicles using tunable resistive pulse sensing, J. Extracell. Vesicles 5 (2016) 31242.

[51] S.L.N. Maas, J. de Vrij, E.J. van der Vlist, B. Geragousian, L. van Bloois, E. Mastrobattista, R.M. Schiffelers, M.H.M. Wauben, M.L.D. Broekman, E.N.M. Nolte-'t Hoen, Possibilities and limitations of current technologies for quantification of biological extracellular vesicles and synthetic mimics, J. Control. Release 200 (2015) 87–96.

[52] P.V. Date, A. Samad, P.V. Devarajan, Freeze thaw: a simple approach for prediction of optimal cryoprotectant for freeze drying, AAPS PharmSciTech 11 (2010) 304–313.

[53] Y. Cheng, Q. Zeng, Q. Han, W. Xia, Effect of pH, temperature and freezing-thawing on quantity changes and cellular uptake of exosomes, Protein Cell 10 (2019) 295–299.

[54] M.J. Haney, N.L. Klyachko, Y. Zhao, R. Gupta, E.G. Plotnikova, Z. He, T. Patel, A. Piroyan, M. Sokolsky, A.V. Kabanov, E.V. Batrakova, Exosomes as drug delivery vehicles for Parkinson's disease therapy, J. Control. Release 207 (2015) 18–30.

[55] S. Mathonet, H.-C. Mahler, S.T. Esswein, M. Mazaheri, P.W. Cash, K. Wuchner, G. Kallmeyer, T.K. Das, C. Finkler, A. Lennard, A Biopharmaceutical Industry Perspective on the Control of Visible Particles in Biotechnology-Derived Injectable Drug Products, PDA J. Pharm. Sci. Technol. 70 (2016) 392–408.

[56] V. Gervasi, R. Dall Agnol, S. Cullen, T. McCoy, S. Vucen, A. Crean, Parenteral protein formulations: An overview of approved products within the European Union, Eur. J. Pharm. Biopharm. 131 (2018) 8–24.

[57] C. Chen, D. Han, C. Cai, X. Tang, An overview of liposome lyophilization and its future potential, J. Control. Release 142 (2010) 299–311.

[58] E.Y. Chi, S. Krishnan, T.W. Randolph, J.F. Carpenter, Physical stability of proteins in aqueous solution: mechanism and driving forces in nonnative protein aggregation, Pharm. Res. 20 (2003) 1325–1336.

[59] Y. Ishikawa, Y. Katoh, H. Ohshima, Colloidal stability of aqueous polymeric dispersions: effect of pH and salt concentration, Colloids Surf. B Biointerfaces 42 (2005) 53–58.

[60] K. Muldrew, L.E. McGann, The osmotic rupture hypothesis of intracellular freezing injury, Biophys. J. 66 (1994) 532–541.

[61] H.D. Andersen, C. Wang, L. Arleth, G.H. Peters, P. Westh, Reconciliation of opposing views on membrane-sugar interactions, PNAS 108 (2011) 1874–1878.

[62] J.C. Kasper, M.J. Pikal, W. Friess, Investigations on polyplex stability during the freezing step of lyophilization using controlled ice nucleation—the importance of residence time in the low-viscosity fluid state, J. Pharm. Sci. 102 (2013) 929–946.

[63] X. Osteikoetxea, B. Sódar, A. Németh, K. Szabó-Taylor, K. Pálóczi, K.V. Vukman, V. Tamási, A. Balogh, Á. Kittel, É. Pállinger, E.I. Buzás, Differential detergent sensitivity of extracellular vesicle subpopulations, Org. Biomol. Chem. 13 (2015) 9775–9782.

[64] J. Yu, T.J. Anchordoquy, Synergistic effects of surfactants and sugars on lipoplex stability during freeze-drying and rehydration, J Pharm Sci 98 (2009) 3319–3328.

[65] V. Sharma, K. Stebe, J.C. Murphy, L. Tung, Poloxamer 188 decreases susceptibility of artificial lipid membranes to electroporation, Biophys. J. 71 (1996) 3229–3241.

[66] S.A. Maskarinec, J. Hannig, R.C. Lee, K.Y.C. Lee, Direct Observation of Poloxamer 188 Insertion into Lipid Monolayers, Biophys. J. 82 (2002) 1453–1459.

[67] U. Adhikari, A. Goliaei, L. Tsereteli, M.L. Berkowitz, Properties of Poloxamer Molecules and Poloxamer Micelles Dissolved in Water and Next to Lipid Bilayers: Results from Computer Simulations, J. Phys. Chem. B 120 (2016) 5823–5830.

[68] S.-L. Law, T.-C. Chuang, M.-C. Kao, Y.-S. Lin, K.-J. Huang, Gene transfer mediated by sphingosine/ dioleoylphosphatidylethanolamine liposomes in the presence of poloxamer 188, Drug. Deliv. 13 (2006) 61–67.

[69] W. Zhang, G. Wang, E. See, J.P. Shaw, B.C. Baguley, J. Liu, S. Amirapu, Z. Wu, Post-insertion of poloxamer 188 strengthened liposomal membrane and reduced drug irritancy and in vivo precipitation, superior to PEGylation, J. Control. Release 203 (2015) 161–169.

[70] W. Wang, C.J. Roberts, Protein aggregation - Mechanisms, detection, and control, Int. J. Pharm. 550 (2018) 251–268.

[71] G. Fuhrmann, A. Serio, M. Mazo, R. Nair, M.M. Stevens, Active loading into extracellular vesicles significantly improves the cellular uptake and photodynamic effect of porphyrins, J. Control. Release 205 (2015) 35–44.

[72] C. Théry, K.W. Witwer, E. Aikawa, M.J. Alcaraz, J.D. Anderson, R. Andriantsitohaina, A. Antoniou, T. Arab, F. Archer, G.K. Atkin-Smith, D.C. Ayre, J.-M. Bach, D. Bachurski, H. Baharvand, L. Balaj, S. Baldacchino, N.N. Bauer, A.A. Baxter, M. Bebawy, C. Beckham, A. Bedina Zavec, A. Benmoussa, A.C. Berardi, P. Bergese, E. Bielska, C. Blenkiron, S. Bobis-Wozowicz, E. Boilard, W. Boireau, A. Bongiovanni, F.E. Borràs, S. Bosch, C.M. Boulanger, X. Breakefield, A.M. Breglio, M.Á. Brennan, D.R. Brigstock, A. Brisson, M.L. Broekman, J.F. Bromberg, P. Bryl-Górecka, S. Buch, A.H. Buck, D. Burger, S. Busatto, D. Buschmann, B. Bussolati, E.I. Buzás, J.B. Byrd, G. Camussi, D.R. Carter, S. Caruso, L.W. Chamley, Y.-T. Chang, C. Chen, S. Chen, L. Cheng, A.R. Chin, A. Clayton, S.P. Clerici, A. Cocks, E. Cocucci, R.J. Coffey, A. Cordeiro-da-Silva, Y. Couch, F.A. Coumans, B. Coyle, R. Crescitelli, M.F. Criado, C. D'Souza-Schorey, S. Das, A. Datta Chaudhuri, P. de Candia, E.F. de Santana, O. de Wever, H.A. Del Portillo, T. Demaret, S. Deville, A. Devitt, B. Dhondt, D. Di Vizio, L.C. Dieterich, V. Dolo, A.P. Dominguez Rubio, M. Dominici, M.R. Dourado, T.A. Driedonks, F.V. Duarte, H.M. Duncan, R.M. Eichenberger, K. Ekström, S. El Andaloussi, C. Elie-Caille, U. Erdbrügger, J.M. Falcón-Pérez, F. Fatima, J.E. Fish, M. Flores-Bellver, A. Försönits, A. Frelet-Barrand, F. Fricke, G. Fuhrmann, S. Gabrielsson, A. Gámez-Valero, C. Gardiner, K. Gärtner, R. Gaudin, Y.S. Gho, B. Giebel, C. Gilbert, M. Gimona, I. Giusti, D.C. Goberdhan, A. Görgens, S.M. Gorski, D.W. Greening, J.C. Gross, A. Gualerzi, G.N. Gupta, D. Gustafson, A. Handberg, R.A. Haraszti, P. Harrison, H. Hegyesi, an Hendrix, A.F. Hill, F.H. Hochberg, K.F. Hoffmann, B. Holder, H. Holthofer, B. Hosseinkhani, G. Hu, Y. Huang, V. Huber, S. Hunt, A.G.-E. Ibrahim, T. Ikezu, J.M. Inal, M. Isin, A. Ivanova, H.K. Jackson, S. Jacobsen, S.M. Jay, M. Jayachandran, G. Jenster, L. Jiang, S.M. Johnson, J.C. Jones, A. Jong, T. Jovanovic-Talisman, S. Jung, R. Kalluri, S.-I. Kano, S. Kaur, Y. Kawamura, E.T. Keller, D. Khamari, E. Khomyakova, A. Khvorova, P. Kierulf, K.P. Kim, T. Kislinger, M. Klingeborn, D.J. Klinke, M. Kornek, M.M. Kosanović, Á.F. Kovács, E.-M. Krämer-Albers, S. Krasemann, M. Krause, I.V. Kurochkin, G.D. Kusuma, S. Kuypers, S. Laitinen, S.M. Langevin, L.R. Languino, J. Lannigan, C. Lässer, L.C. Laurent, G. Lavieu, E. Lázaro-Ibáñez, S. Le Lay, M.-S. Lee, Y.X.F. Lee, D.S. Lemos, M. Lenassi, A. Leszczynska, I.T. Li, K. Liao, S.F. Libregts, E. Ligeti, R. Lim, S.K. Lim, A. Linē, K. Linnemannstöns, A. Llorente, C.A. Lombard, M.J. Lorenowicz, Á.M. Lörincz, J. Lötvall, J. Lovett, M.C. Lowry, X. Loyer, Q. Lu, B. Lukomska, T.R. Lunavat, S.L. Maas, H. Malhi, A. Marcilla, J. Mariani, J. Mariscal, E.S. Martens-Uzunova, L. Martin-Jaular, M.C. Martinez, V.R. Martins, M. Mathieu, S. Mathivanan, M. Maugeri, L.K. McGinnis, M.J. McVey, D.G. Meckes, K.L. Meehan, I. Mertens, V.R. Minciacchi, A. Möller, M. Møller Jørgensen, A. Morales-Kastresana, J. Morhayim, F. Mullier, M. Muraca, L. Musante, V. Mussack, D.C. Muth, K.H. Myburgh, T. Najrana, M. Nawaz, I. Nazarenko, P. Nejsum, C. Neri, T. Neri, R. Nieuwland, L. Nimrichter, J.P. Nolan, E.N. Nolte-'t Hoen, N. Noren Hooten, L. O'Driscoll, T. O'Grady, A. O'Loghlen, T. Ochiya, M. Olivier, A. Ortiz, L.A. Ortiz, X. Osteikoetxea, O. Østergaard, M. Ostrowski, J. Park, D.M. Pegtel, H. Peinado, F. Perut, M.W. Pfaffl, D.G. Phinney, B.C. Pieters, R.C. Pink,

D.S. Pisetsky, E. Pogge von Strandmann, I. Polakovicova, I.K. Poon, B.H. Powell, I. Prada, L. Pulliam, P. Quesenberry, A. Radeghieri, R.L. Raffai, S. Raimondo, J. Rak, M.I. Ramirez, G. Raposo, M.S. Rayyan, N. Regev-Rudzki, F.L. Ricklefs, P.D. Robbins, D.D. Roberts, S.C. Rodrigues, E. Rohde, S. Rome, K.M. Rouschop, A. Rughetti, A.E. Russell, P. Saá, S. Sahoo, E. Salas-Huenuleo, C. Sánchez, J.A. Saugstad, M.J. Saul, R.M. Schiffelers, R. Schneider, T.H. Schøyen, A. Scott, E. Shahaj, S. Sharma, O. Shatnyeva, F. Shekari, G.V. Shelke, A.K. Shetty, K. Shiba, P.R.-M. Siljander, A.M. Silva, A. Skowronek, O.L. Snyder, R.P. Soares, B.W. Sódar, C. Soekmadji, J. Sotillo, P.D. Stahl, W. Stoorvogel, S.L. Stott, E.F. Strasser, S. Swift, H. Tahara, M. Tewari, K. Timms, S. Tiwari, R. Tixeira, M. Tkach, W.S. Toh, R. Tomasini, A.C. Torrecilhas, J.P. Tosar, V. Toxavidis, L. Urbanelli, P. Vader, B.W. van Balkom, S.G. van der Grein, J. van Deun, M.J. van Herwijnen, K. van Keuren-Jensen, G. van Niel, M.E. van Royen, A.J. van Wijnen, M.H. Vasconcelos, I.J. Vechetti, T.D. Veit, L.J. Vella, É. Velot, F.J. Verweij, B. Vestad, J.L. Viñas, T. Visnovitz, K.V. Vukman, J. Wahlgren, D.C. Watson, M.H. Wauben, A. Weaver, J.P. Webber, V. Weber, A.M. Wehman, D.J. Weiss, J.A. Welsh, S. Wendt, A.M. Wheelock, Z. Wiener, L. Witte, J. Wolfram, A. Xagorari, P. Xander, J. Xu, X. Yan, M. Yáñez-Mó, H. Yin, Y. Yuana, V. Zappulli, J. Zarubova, V. Žėkas, J.-Y. Zhang, Z. Zhao, L. Zheng, A.R. Zheutlin, A.M. Zickler, P. Zimmermann, A.M. Zivkovic, D. Zocco, E.K. Zuba-Surma, Minimal information for studies of extracellular vesicles 2018 (MISEV2018): a position statement of the International Society for Extracellular Vesicles and update of the MISEV2014 guidelines, J. Extracell. Vesicles 7 (2018) 1535750.

[73] K.B.Y. El Baradie, M. Nouh, F. O'Brien Iii, Y. Liu, S. Fulzele, A. Eroglu, M.W. Hamrick, Freeze-Dried Extracellular Vesicles From Adipose-Derived Stem Cells Prevent Hypoxia-Induced Muscle Cell Injury, Front. Cell Dev. Biol. 8 (2020) 181.

[74] M.A. Mensink, P.-J. van Bockstal, S. Pieters, L. de Meyer, H.W. Frijlink, K. van der Voort Maarschalk, W.L.J. Hinrichs, T. de Beer, In-line near infrared spectroscopy during freeze-drying as a tool to measure efficiency of hydrogen bond formation between protein and sugar, predictive of protein storage stability, Int. J. Pharm. 496 (2015) 792–800.

[75] F. Franks, Long-term stabilization of biologicals, Biotechnology 12 (1994) 253–256.

[76] S. Piszkiewicz, G.J. Pielak, Protecting Enzymes from Stress-Induced Inactivation, Biochemistry 58 (2019) 3825–3833.

[77] A. Montoya, J. Castell, Long-term storage of peroxidase-labelled immunoglobulins for use in enzyme immunoassay, J. Immunol. Methods 99 (1987) 13–20.

[78] M.T. Cicerone, M.J. Pikal, K.K. Qian, Stabilization of proteins in solid form, Adv. Drug Deliv. Rev. 93 (2015) 14–24.

[79] L.L. Chang, M.J. Pikal, Mechanisms of protein stabilization in the solid state, J. Pharm. Sci. 98 (2009) 2886–2908.

[80] K.A. Pikal-Cleland, J.F. Carpenter, Lyophilization-induced protein denaturation in phosphate buffer systems: monomeric and tetrameric beta-galactosidase, J. Pharm. Sci. 90 (2001) 1255–1268.

[81] V. Kannan, P. Balabathula, L.A. Thoma, G.C. Wood, Effect of sucrose as a lyoprotectant on the integrity of paclitaxel-loaded liposomes during lyophilization, J. Liposome Res. 25 (2015) 270–278.

[82] B. Giebel, L. Kordelas, V. Börger, Clinical potential of mesenchymal stem/stromal cell-derived extracellular vesicles, Stem Cell Investig. 4 (2017) 84.

[83] E. Schulz, A. Goes, R. Garcia, F. Panter, M. Koch, R. Müller, K. Fuhrmann, G. Fuhrmann, Biocompatible bacteria-derived vesicles show inherent antimicrobial activity, J. Control. Release 290 (2018) 46–55.

[84] M.-J. Fábrega, A. Rodríguez-Nogales, J. Garrido-Mesa, F. Algieri, J. Badía, R. Giménez, J. Gálvez, L. Baldomà, Intestinal Anti-inflammatory Effects of Outer Membrane Vesicles from Escherichia coli Nissle 1917 in DSS-Experimental Colitis in Mice, Front. Microbiol. 8 (2017) 1274.

[85] J. Hoppstädter, A. Dembek, R. Linnenberger, C. Dahlem, A. Barghash, C. Fecher-Trost, G. Fuhrmann, M. Koch, A. Kraegeloh, H. Huwer, A.K. Kiemer, Toll-Like Receptor 2 Release by Macrophages: An Anti-inflammatory Program Induced by Glucocorticoids and Lipopolysaccharide, Front. Immunol. 10 (2019) 1634.

[86] M. Richter, K. Fuhrmann, G. Fuhrmann, Evaluation of the Storage Stability of Extracellular Vesicles, J. Vis. Exp. (2019).

Chapter 6

Final summary and outlook

Many pharmaceutical nanoparticles (NPs) suffer from poor storage stability hampering research and limiting drug developability. Therefore, the present thesis focused on the lyophilization of NPs for parenteral application with the main colloidal stability. This colloidal stability is highly dependent on the properties of the NPs which are highly divers. Thus, there is a need for individual strategies in order to preserve NP properties upon freeze-drying. Still we were aiming to arrive at a fundamental understanding of the behavior of NPs during the freezing phase and the drying phase of the lyophilization process itself as well as upon subsequent storage of the lyophilizates. Chapter 1 summarizes the state of the art on this subject, bringing order into rather unstructured literature and giving practical advice on formulation and process development for lyophilization of nanoparticulate systems. The experimental part of this thesis focused on the investigation of four different NP types: i) inorganic NPs; ii) drug nanosuspensions; iii) solid lipid nanoparticles (SLNs); and iv) extracellular vesicles (EVs).

α-Al_2O_3 NPs served as a chemically, mechanically and thermally stable, non-hydrophobic model readily available at larger quantities. The studies with this NP type revealed that initial particle stabilization in liquid state may already be a hurdle and depends strongly on the buffer type and pH (Chapter 3). Citrate buffer was superior to sodium and potassium phosphate buffers both for initial stabilization and during freezing and thawing which is attributed to electrostatic interactions. The pH shift of sodium phosphate during freezing caused marked NP aggregation which can be avoided by the use of potassium phosphate buffer. The addition of further additives can improve freezing and thawing performance; especially gelatin, sucrose, and mannitol showed a high cryoprotective potential.

Lipophilic and therefore surfactant stabilized NPs of paliperidone palmitate and SLNs manufactured from trimyristin were investigated in Chapter 4. Initial particle stabilization in liquid state requires high amounts of non-ionic surfactants. Because of this surface coverage buffer type and pH did not affect FT stability. FT stability was poor in presence of mannitol which crystallizes and could be drastically improved by using sucrose which is known to form an amorphous matrix during freezing. The higher the sucrose concentration, the less aggregation was observed. The freezing step during lyophilization was of minor importance compared to the surfactant type used for NP stabilization. Nevertheless, the addition of an annealing step or freezing under controlled nucleation was beneficial, reducing the formation

of subvisible particles. DSC measurements of surfactant containing sucrose formulations revealed two glass transition events during freezing indicating a phase separation into a surfactant rich and a surfactant poor phase. Consequently, the lyophilizates also exhibited two glass transitions, one already at ~50 °C. Accelerated storage stability studies confirmed that these formulations suffer from poor stability at 40 °C. HP-β-CD can be added to the surfactant/sucrose solution to overcome the limited stability by raising this first glass transition temperature.

In Chapter 5 different formulations aspects were evaluated to improve the freeze-thaw and lyophilization stability of EVs. These biological NPs represent a highly fragile particle type due to their lipid bilayer membrane which is decorated with proteins. In FT studies, EVs were less stable at acidic pH, and in presence of NaCl resulting in marked aggregation which is in sharp contrast to the lipophilic NPs of paliperidone palmitate and SLNs. Without further excipients, EVs showed less aggregation in potassium phosphate compared to sodium phosphate, similarly to α-Al_2O_3 NPs. The addition of the surfactants polysorbate 20 and poloxamer 188 (P188) was evaluated subsequently showing complete preservation of particle size and concentration after FT in presence of P188.

In summary, the investigation of four fundamentally different NP types in this thesis provides a deeper understanding of crucial particle attributes impacting colloidal stability during freezing and lyophilization. The buffer type and ionic strength strongly affect the stability of charged particles such as α-Al_2O_3 NPs and EVs. But the impact is less important in case of the lipophilic drug nanosuspensions and SLNs which are protected from electrostatic interactions by high non-ionic surfactant concentrations. This effect is especially pronounced in presence of high sucrose concentrations. While several surfactants could not improve FT stability of α-Al_2O_3 NPs, surfactants such as polysorbate 20 and poloxamer 188 were highly important for successful preservation of lipophilic NPs and EVs. Moreover, the lyophilization scientist should be aware of the plasticizing effect of surfactants on the final lyophilizate potentially limiting storage stability. As reported in literature and also shown in this thesis, formulation aspects rather than process parameters have to be considered for successful NP lyophilization. Thus, future studies should further assess critical particle and formulation attributes of various NP types. An overall better understanding of these mutually dependent aspects will accelerate development of tailor-made formulations and successful freeze-drying of NP systems.

Curriculum vitae

Personal Details

Name:	Eduard Trenkenschuh
Date of birth:	26.05.1989
Place of birth:	Sadowoe, Kazakhstan
Nationality:	German

Work experience

02/2021 – present	Post Doc Boehringer-Ingelheim, Biberach, Germany Early Development NCE
02/2017 – 09/2020	PhD Student Ludwig-Maximilians-Universität München, Munich, Germany Department of pharmaceutical technology Supervisor: Prof. Dr. Wolfgang Frieß
05/2016 – 10/2016	Pharmacist Trainee Hirsch Apotheke, Ulm, Germany
11/2015 – 04/2016	Pharmacist Trainee F. Hoffmann-La Roche Ltd, Basel, Switzerland Formulation Research & Development (Solid dosage forms)

Education

12/2016	Pharmacist License
02/2017 – 09/2020	PhD Studies Ludwig-Maximilians-Universität München, Munich, Germany Department of pharmaceutical technology Supervisor: Prof. Dr. Wolfgang Frieß
11/2015 – 04/2016	Diploma Thesis Martin-Luther-University Halle-Wittenberg Supervisors: Dr. Susanne Page (Roche) & Prof. Dr. Peter Kleinebudde (HHU Düsseldorf)
10/2011 – 10/2015	Pharmacy studies University of Regensburg, Germany
07/2009	General qualification for university entrance (Abitur) Simpert-Kraemer-Gymnasium Krumbach, Germany